An investigation into the effects of dystrophin on the lateral mobility of muscle membrane components.

Anna Louise Dutton

An investigation into the effects of dystrophin on the lateral mobility of muscle membrane components.

Anna Louise Dutton.

University of Durham, Department of Biological Sciences
South Road, Durham, DH1 3LE.

A thesis submitted to the Department of Biological Sciences, University of Durham in accordance with the requirements for the degree of Doctor of Philosophy.

1999.

An investigation into the effects of dystrophin on the lateral mobility of muscle membrane components.

Anna L. Dutton

University of Durham, Department of Biological Sciences,
South Road, Durham, DH1 3LE, U.K.

Abstract.

Dystrophin is the product of the Duchenne Muscular Dystrophy gene locus, whose absence results in progressive skeletal muscle breakdown. Despite considerable work on the localisation of dystrophin and its associated complex, its role in muscle function remains unclear. In the light of the structural and mechanical instability of the dystrophic membrane, the idea was tested that dystrophin might impart membrane integrity and strength by anchoring membrane proteins and/or delineating the surface into specialised subcellular functional domains. Specifically, because dystrophin shows high sequence, structural and spatial similarities to the cytoskeletal protein spectrin; and because spectrin is proven to sterically restrict protein lateral diffusion through a subplasmalemmal network; the capacity of dystrophin to act as a 'molecular fence' to membrane diffusion was studied by comparing lateral mobility of membrane glycoproteins by fluorescence photobleach recovery in mdx and normal tissue. Secondly, as dystrophin has been proven to interact directly with proteins of the dystrophin associated glycoprotein complex *in vivo*, experiments addressed whether specific binding and immobilisation of the complex by dystrophin at the membrane was essential for function. Finally, given the homology of dystrophin and spectrin, the presence of dystrophin at the neuromuscular junction, and the importance of spectrins in immobilisation of voltage gated sodium channels in the nervous system, the role of dystrophin in regulating voltage gated sodium channel distribution at the neuromuscular junction was investigated. The results show that membrane glycoproteins were immobile in the presence and absence of dystrophin, suggesting dystrophin is not an essential molecular fence component. Alternatively, viability may have been the major influence on protein and lipid diffusion in these fibres and suggestions are made as to how this may be recognised and overcome for subsequent investigation. Three novel exon specific anti-dystrophin peptide antibodies were generated during the work that will be useful for studies into Duchenne muscular dystrophy in general, and dystrophin revertant fibres in particular.

Key words:

dystrophin, molecular fence, FPR, membrane, mdx revertant.

CONTENTS

Chapter 2. Materials and Methods.

Chapter 3. Generation of Anti-dystrophin Antibodies.

Chapter 6. Discussion.

List of figures.

Chapter 1. Introduction.

Chapter 2. Materials and Methods.

Chapter 3. Generation of anti-dystrophin antibodies.

Chapter 4. The role of dystrophin as a 'molecular fence'- a non-specific regulator of membrane protein distribution.

Chapter 5. Synthesis of specific fluorescent probes for FPR.

Declaration.

No part of this thesis has been submitted previously for a degree at this or any other institution. All the material is my own original work unless otherwise stated.

Abbreviations.

A_{260}	Absorbance at 260nm
A_{514}	Absorbance at 514nm
α-bgtx	α-bungarotoxin
Ach R	acetylcholine receptor
BODIPY (Fl)SE	4,4-difluoro-5,7-dimethyl-4-bora-3a,4a-diaza-s-indacene-3-propionic acid, succinimidyl ester
BSA	bovine serum albumin
cps	counts per second
D	lateral diffusion coefficient
DAG	dystrophin associated glycoprotein
Di-I	1,1'-dioctadecyl-3,3,3',3'-tetramethylindocarbocyanine perchlorate
DMD	Duchenne Muscular Dystrophy
DMSO	dimethyl sulphoxide
DNA	deoxyribonucleic acid
ECM	extracellular matrix
EDTA	ethylenediaminetetraacetic acid
FPR	fluorescence photobleach recovery
FITC	fluorescein isothiocyanate
HPLC	high performance liquid chromatography
Ig	immunoglobulin
kDa	kilodaltons
MAP	multiple antigen presenting
mdx	muscular dystrophy, x-chromosome linked
NaCh	voltage gated sodium channel
NMJ	neuromuscular junction
ODAF	5-(N-octa-decanoyl) aminofluorescein
PBS	phosphate buffered saline
PCR	polymerase chain reaction
PMSF	phenyl methyl sulphonyl fluoride
PMT	photomultiplier tube
RCA_{120}	Lectin from Ricinus Communis I
RTP	room temperature and pressure
S Con A	Succinyl concanavalin A
SDS	sodium dodecyl sulphate

SDS PAGE	sodium dodecyl sulphate polyacrylamide gel electrophoresis
s.e.m.	standard error of the mean
SPT	single particle tracking
TCA	trichloroacetic acid
TEMED	N,N,N',N'-tetramethylethylenediamine
Tris	tri (hydroxymethyl) aminomethane
TmRh	tetramethylrhodamine isothiocyanate
μ-cgtx	μ-conotoxin GIIIB
v/v	volume to volume ratio
w/v	weight to volume ratio

Chapter 1.

Introduction.

Chapter 1.

Introduction.

The objective of this thesis was to study the effects of the disorder Duchenne Muscular Dystrophy on the structure and organisation of the muscle fibre membrane. In this introduction to the experimental work I aim to explain the rationale behind the experiments that follow. In the first part I shall provide a brief overview of the diseased system that formed the basis of the study- Duchenne Muscular Dystrophy (DMD). Discussion will then move on to the more specific area of the domain structure and organisation of cell membranes- including why cells are divided into domains; how domains are formed and the experimental approaches that have provided this knowledge; and finally, why this thesis tested the idea that dystrophin could be involved in the formation of membrane domains and regulation of lateral mobility of membrane constituents.

1.1 Duchenne muscular dystrophy.

Duchenne Muscular Dystrophy is an X-linked genetic disorder affecting 1 in 3500 male births. The disease is characterised by progressive wasting of the skeletal muscles. Patients find walking increasingly difficult, leaving many wheelchair bound by the age of eleven. The disorder has been traced to deficiency of a single cytoskeletal protein, named dystrophin (Hoffman *et al*, 1987), which localises to the cytoplasmic face of the plasma membrane in normal skeletal muscle (Watkins *et al*, 1988).

1.1.2 Mdx mice.

Much of the experimental work on Duchenne Muscular Dystrophy has been performed using tissue from the mdx (muscular dystrophy, x-linked) mouse (Bulfield *et al*, 1984). This mouse possesses the same primary biochemical defect as DMD patients, namely a lack of detectable dystrophin protein in the sarcolemma (Hoffman, 1987). As in the human disease, elevated levels of muscle cytosolic proteins are found circulating in the serum indicative of muscle instability. Internally the skeletal muscle tissue shows evidence of rounds of regeneration within 3 weeks of birth, including atrophy of some fibres, variation in fibre size, degeneration of some fibres, centrally located nuclei and disruption of the plasmalemma and basal lamina (Bulfield *et al*, 1984). However, in contrast to humans, the mouse only begins to show outward signs of muscle weakness at 12 months of age, believed to reflect the greater capacity of mouse muscle for regeneration over human muscle.

The experiments investigating the function of dystrophin that are outlined in this thesis were performed on tissue from male mdx mice (gift of Prof T. Partridge, Hammersmith Hospital, London) and normal control tissue from the C57/BL 10 parental strain. As described by Bulfield *et al* (1984), these mdx mice showed no outward signs of muscle weakness until about 12 months after birth. However, mice born with a particularly severe phenotype (figure 1.1) have a lifespan of just a couple of months.

1.1.2 Histology and Pathology of DMD.

Pathologically DMD presents a classic pattern of muscle degeneration, regeneration and fibrosis (Dubowitz, 1985). Elevated serum levels of muscle proteins such as creatine kinase (CK) can be detected at an early stage (Hoffman *et al*, 1987). If observed motor difficulties suggest a patient may possess DMD, serum CK concentration is used as an early diagnostic tool. However, elevated CK levels could also signify a metabolic disorder, therefore muscle biopsies are necessary to confirm a suspected DMD diagnosis.

The appearance of dystrophic tissue at biopsy provides evidence for rounds of muscle degeneration and regeneration (reviewed in Turner *et al*, 1997, Partridge, 1997). Pathological muscle fibres possess centrally located nuclei, compared with peripherally located nuclei in fibres of normal tissue. This suggests a high level of satellite cell activity to rebuild damaged muscle fibres- following division of the satellite cell the immature myoblast nuclei have yet to migrate towards the outside of the fibre. Myofibres are regularly sized in normal muscle but irregular in dystrophic tissue. This follows replacement of necrotic mature fibres by smaller new fibres. Extensive connective tissue proliferates between fibres in dystrophic muscle. In contrast connective tissue is found in just a narrow band around bundles of fibres in normal muscle. Dystrophic muscle has extensive fibrosis, with connective tissue proliferation between the individual fibres. As the disease progresses almost all the muscle fibres will be replaced by connective tissue and fat deposits. The deposition of connective tissue is understood to be a wound response. Disruptions to the integrity of the myofibre plasma membrane lead to the presence of myotube cytoplasmic components within the extracellular matrix. The ensuing damage repair cascade ultimately leads to connective tissue formation (Partridge, 1997). As the disease worsens and myofibres become fewer in number the tissue becomes weaker, damage becomes more frequent and connective tissue growth becomes more extensive. DMD is invariably fatal by the end of the third decade of life, usually following failure of the muscles in the respiratory system.

a)

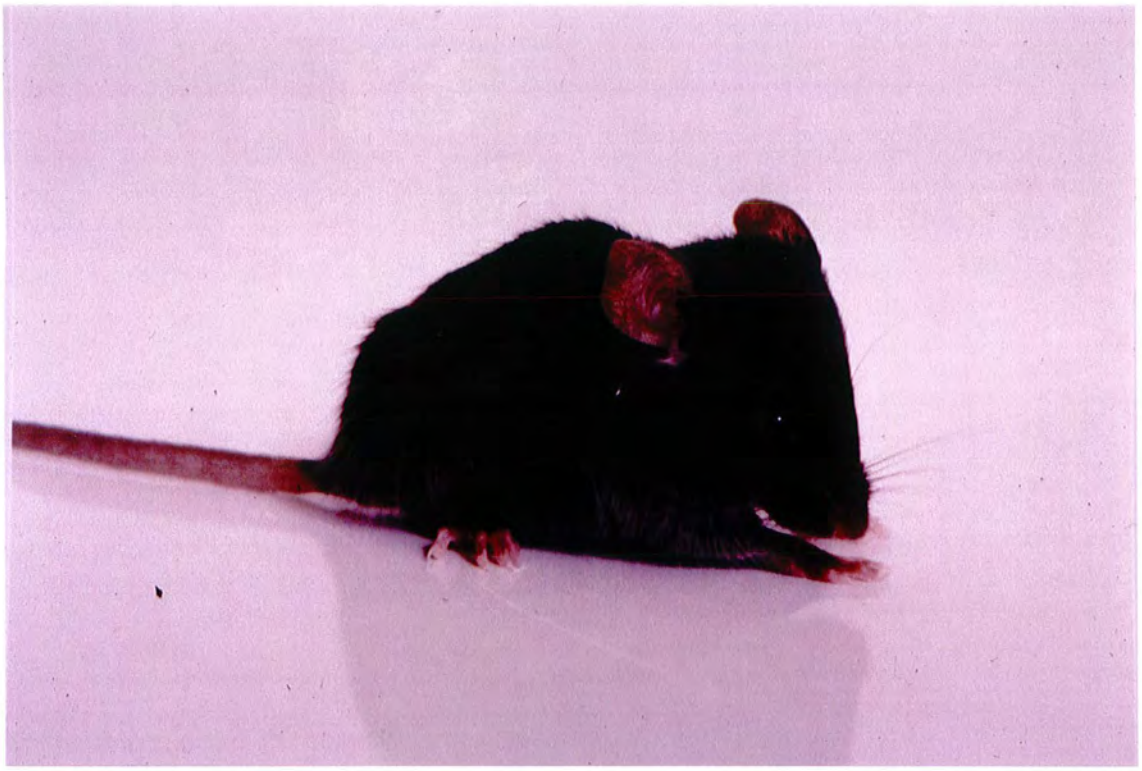

b)

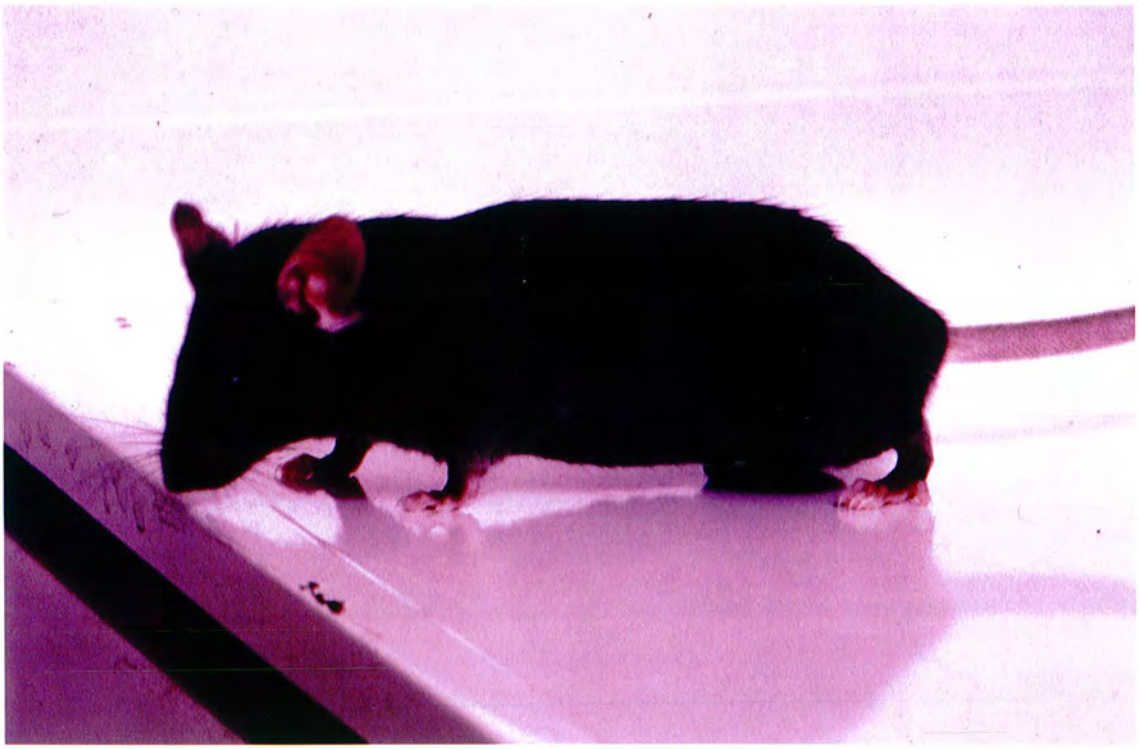

1.1.3 The dystrophin gene.

The observed pathological defects of DMD are the result of mutations in the dystrophin gene. The gene is found as a single copy located on the X-chromosome. The dystrophin gene was the first gene to be identified by chromosomal linkage analysis of affected families (Hoffman *et al*, 1987). The dystrophin gene locus is presently the largest known gene in the human genome- spanning at least 2.4Mb (compared with 30kb average gene size). The gene is not only big but also complex, with at least 85 exons (which are highly conserved throughout evolution). 98% of the locus is composed of introns which are also highly conserved and number at least 84 (reviewed in Amalfitano *et al*, 1997).

The 5' end and central portion of the dystrophin gene show high sequence homology to spectrin. The 3' end is homologous to dystrobrevin- a postsynaptic protein found in the electric organ of the ray Torpedo (Hoffman *et al*, 1988). The entire dystrophin gene is homologous to only one other known protein- Utrophin [also called Dystrophin Related Protein or DRP] (Love *et al*, 1989). Utrophin is so called because it is ubiquitously expressed within the tissues of the body (Love *et al*, 1991).

Expression of the dystrophin gene is highly tissue specific. The size and complexity of the gene is reflected in the promoter region, where at least seven different promoters control expression of differentially spliced transcripts according to cell type. The M promoter, for example, controls expression of the 14kb dystrophin transcript in skeletal muscle and at low levels in glial cells. The C (cortical), G (glial cell) and P (Purkinje cell) promoters drive formation of different transcripts within the central nervous system. Furthermore, the transcripts undergo alternative splicing at the 3' end. The transcripts fall into at least 5 different classifications of mRNA isoforms according to size. These vary from full length skeletal dystrophin, to the 4.6kb Dp71 C-terminal transcript (for a summary of the different transcripts, see Brown and Lucy, 1997, page 164).

The size and complexity of the dystrophin gene contributes to the highest spontaneous mutation rate ever reported for a human gene. The mutations are predominantly point mutations, arising by chance within the large transcript. Single spontaneous point mutations which shift the reading frame of the gene result in a phenotype far more severe than larger in frame deletions. The statistical likelihood of such an event in a large transcript may explain why half of all DMD cases are due to new mutations.

1.1.4 The dystrophin protein.

In normal healthy tissue dystrophin makes up approximately 0.002% of skeletal muscle protein (Hoffman *et al*, 1987) and is located towards the periphery of skeletal muscle fibres. Immunolocalisation clearly shows a continuous band of dystrophin protein at the cytoplasmic face of the plasma membrane (Watkins *et al*, 1988, see also figure 3.2). This localisation pattern is

characteristic of cytoskeletal proteins such as spectrin, indicating dystrophin may have a cytoskeletal function. In the tissue of DMD patients there is no detectable dystrophin protein, suggesting the mutated gene product is unstable at either the mRNA or protein level (Hoffman *et al*, 1987).

Dystrophin protein was isolated following the successful cloning of the gene. A bacterial fusion protein was generated using a fragment of the cloned cDNA, antibodies raised to the fusion peptide and the antibodies used to isolate dystrophin protein from human tissue (Hoffman *et al*, 1987). The full length skeletal dystrophin protein is big- 427 kD (Hoffman *et al*, 1987).

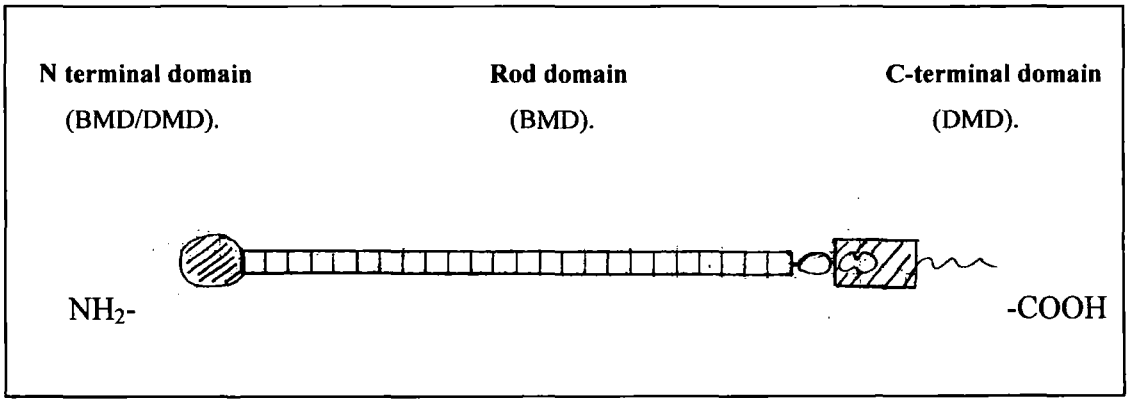

Figure 1.2 Schematic diagram of dystrophin protein.
The three distinctive regional domains, together with the common disease phenotype arising from mutations in each region are written above. (DMD, Duchenne muscular dystrophy. BMD, Becker muscular dystrophy).

From N to C terminus: Hatched circle, N-terminal actin binding domain. Boxes, 24 spectrin-like coiled-coil repeats. Open circle, WW domain. Shaded rectangle, C-terminal cysteine rich domain, Dumbell, calcium binding EF hand. Diagram modified from Winder *et al*, 1997.

The protein may be divided into three major functional domains, figure 1.2. The first domain lies at the amino terminus and shows high homology at both the DNA and amino acid level to actin binding proteins such as β-spectrin and α-actinin (reviewed in Ahn and Kunkel, 1993). 2D NMR studies confirmed the actin binding nature of the amino terminus (Levine *et al*, 1992) as did kinetic binding studies (e.g. Ervatsi and Campbell, 1993a). Deletions within the N-terminus result in the lesser Becker Muscular Dystrophy (BMD) phenotype. Similarly, insertion of an N-terminally deleted dystrophin transgene into an mdx mouse rescues the Duchenne mouse to a Becker phenotype (Rafael *et al*, 1996).

The second major domain is the central rod domain, containing 24 spectrin rod domain like repeats. This regular repeating unit has been crystallised for dystrophin and shown to fold into an anti-parallel

triple helical repeat, as found in spectrin (Winder *et al*, 1997). The rod domain has 4 hinge regions believed to confer flexibility on the molecule. The C-terminal end of the rod domain contains an EF hand homologous to that in calmodulin, α actinin and β spectrin (see Ahn and Kunkel, 1993 for review of structure). This could suggest a possible calcium binding role for dystrophin. However, the EF hand is not believed to bind calcium at physiological calcium levels (Dubreuil *et al*, 1991). The physiological significance of the different portions of the rod domain is seen in clinical data- mutations within the proximal rod domain are rarely severe, resulting in a mild phenotype. Mutations at the distal end of the rod domain result in a classic Becker phenotype.

The third region of the dystrophin protein is the C terminal domain. This domain is cysteine rich and contains a leucine zipper dimerisation motif. The function of the C-terminal domain is to interact with the dystrophin associated glycoprotein (DAG) complex.

1.1.5 Dystrophin associated glycoprotein complex.

If dystrophin, is considered to be analogous to the submembranous cytoskeletal protein spectrin, then the DAG complex may be thought of as the transmembrane spanning ankryin/band 3. Together dystrophin and DAG complex link the underlying myofibrillar actin cytoskeleton to the extracellular matrix.

A mixture of co-immunoprecipitation and protein crosslinking experiments lead to the current description of the components and associations within the DAG complex (Campbell and Kahl, 1989, Ervasti *et al*, 1990, Matsumura *et al*, 1992, Reviewed in Tinsley *et al*, 1994 and 1997, Ervasti and Campbell, 1991, Michalak and Opas, 1997), shown diagrammatically in figure 1.3. The DAG complex can be split into three subcomplexes of transmembrane and membrane associated proteins and glycoproteins according to their co-purification upon separation and hence binding affinities to each other.

The first complex- the dystroglycan complex of α and β dystroglycan- links dystrophin to the extracellular matrix. αdystroglycan is a peripheral surface proteoglycan that binds the G domain of merosin, a component of the extracellular matrix. (Merosin is also called laminin 2). β dystroglycan is a transmembrane protein, shown to bind the C-terminal domain of dystrophin (see later) and α dystroglycan.

The second complex is the sarcoglycan complex of α (also known as adhalin, the term used throughout this text), β, γ and δ sarcoglycans. These do not bind dystrophin directly, but indirectly through the DAG complex.

Finally the syntrophin complex, composed of the three similarly sized homologous proteins α1, β1 and β2 syntrophin, binds the C-terminal domain of dystrophin and forms associations with other members of the DAG complex. Expression of the syntrophins is both spatially and temporally regulated. β2 syntrophin, for example is found predominantly in utrophin-DAG complexes at the early stages of neuromuscular junction development.

The significance of the DAG complex is clinically observed. Mutations within components of the complex give rise to forms of muscular dystrophy with varying clinical severity. For example, Limb Girdle Muscular Dystrophy type-2D is caused by mutations in adhalin. (For further examples see table 7.2 Dystrophin; Gene, Protein and Cell Biology. p167)

The DAG complex is absent in DMD patients as assessed immunohistochemically (Ohlendieck and Campbell, 1991 a), Ohlendieck *et al*, 1993, Cullen *et al*, 1996). However, the genes for the DAG components are fully functional. In mdx mice, the insertion of a full length dystrophin transgene restores the DAG complex in dystrophic muscle (Rafael *et al*, 1996). The absence of dystrophin appears to render the complex unstable.

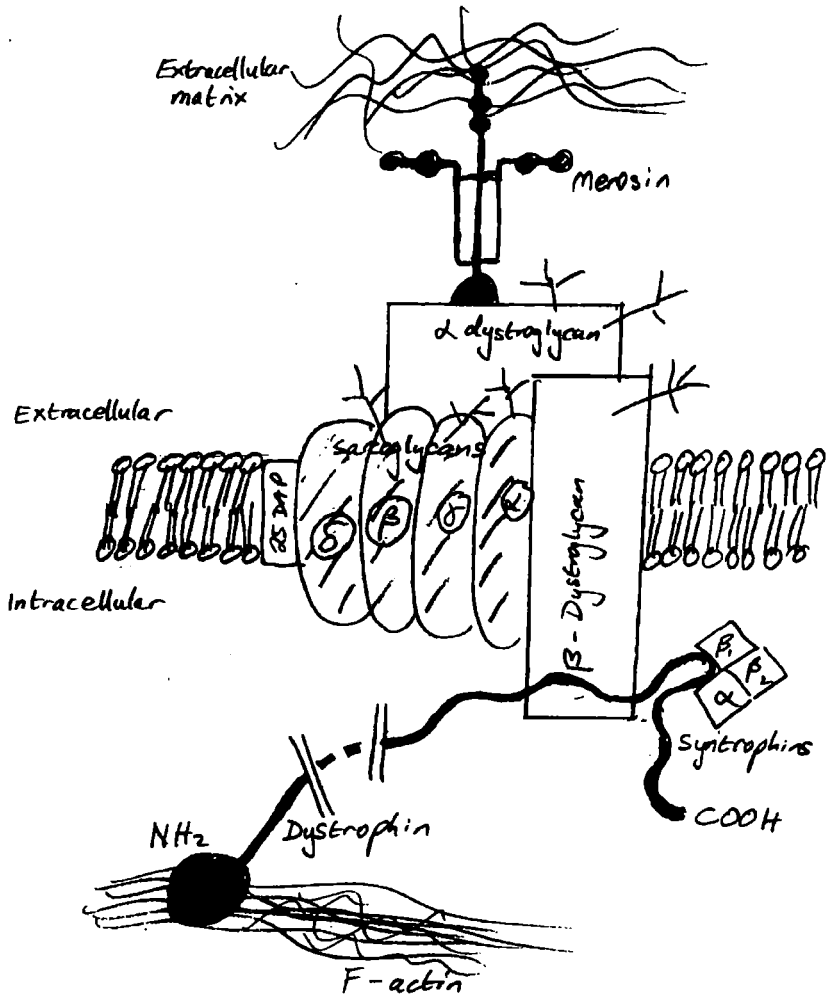

Figure 1.3 Dystrophin and the dystrophin associated glycoprotein complex.

Dystrophin covalently binds F-actin via its N-terminus and the DAG complex at the C-terminus. The DAG complex, in turn binds the extracellular matrix via the dystroglycans and merosin (laminin 2). The dystrophin / DAG complex therefore links the intracellular contractile apparatus of the muscle with the extracellular matrix. Dystrophin rod domain is shown truncated for simplicity.

Figure modified from Tinsley *et al*, 1997, Campbell, 1995, and the Novocastra Catalogue 1999, p65 (Novocastra Laboratories, Newcastle, UK).

1.1.6 Dystrophin/DAG associations and muscle function.

Binding of dystrophin's C-terminus to the DAG complex is critical for muscle function. To determine exactly which regions of the dystrophin molecule interacted with the DAG complex, Rafael *et al* (1996) generated a series of transgenic mdx mice. The mice contained a series of dystrophin constructs with deletions of the carboxyl end of the protein. All transgenes were under the activity of the muscle creatine kinase promoter, thus ensuring tissue specific expression. The ability of the transgene to rescue the phenotype of the mdx mouse (including restoration of the DAG complex) indicated the functional importance of the deleted protein region.

Deletion of two thirds of the central rod domain gave an almost fully functional dystrophin protein, whilst deletion of the N-terminal actin binding domain converted the mouse to a Becker phenotype. C-terminal mutations of dystrophin were shown to block interaction with the DAG complex and lead to the most severe dystrophic phenotype. Deletion of the C-terminal cysteine rich domain gave loss of the β-dystroglycan binding site with subsequent loss of β-dystroglycan and the sarcoglycan complex from the sarcolemma and a severe DMD phenotype. Loss of the alternatively spliced and extreme C-terminal domains had no effect on dystrophin function. These constructs successfully restored the DAG complex and gave a normal tissue phenotype, as did a construct lacking the leucine zipper dimerisation motif. *In vitro,* α1 syntrophin binds exons 73-74 of dystrophin. However, the deletion of this region in a transgenic mouse had no effect on syntrophin/DAG complex localisation *in vivo.* Expression of a C-terminal domain construct (Dp71) is sufficient to restore the DAG complex to the plasma membrane, but not sufficient to rescue the DMD phenotype.

From these experiments it may be concluded the critical function of dystrophin is binding of the DAG complex via β-dystroglycan, as disruption of this link gave the most severe phenotype in the mice. In contrast, a direct link between dystrophin and the syntrophin complex was not critical for preventing a DMD phenotype. C-terminal deletions lead to instability at either the protein or mRNA level, and a severe DMD phenotype. These experimental results mirror clinical observations. There is very little data available from patients with truncated C-terminal dystrophin, probably because such patients do not survive to the testing stage. In those cases where data is available, the DMD is invariably severe.

1.1.7. Functions of dystrophin.

1.1.7 a) Maintenance of intracellular Ca^{2+}

It has been suggested that dystrophin regulates and maintains intracellular calcium levels in muscle fibres (Reviewed in Brown and Lucy, 1997, Ahn and Kunkel, 1993). Experimental evidence for the suggestion was obtained by staining fibres with fluorescent calcium probes such as Fura 2. Mdx fibres are less able to regulate intracellular calcium levels following influx. Mdx fibres possess widely ranging intracellular calcium, unlike non-dystrophic fibres which have more even calcium levels. Myotubes from mdx mice expressing a full length dystrophin construct have normal calcium levels.

One hypothesis proposes the absence of dystrophin affects Ca^{2+} leak channels, leading to uncontrolled passage of calcium ions. However, it is not clear whether this is a direct consequence of a lack of dystrophin, or a secondary effect due to disruptions in the plasma membrane of dystrophic tissue. A direct link seems less likely given that, despite the absence of dystrophin, pre necrotic dystrophic tissue doesn't have a wide range of calcium levels. In addition, calcium levels do not gradually increase as the tissue dies. Calcium irregularities could arise from the absence of dystrophin retarding normal myotube differentiation with respect to calcium handling properties, and in particular the calcium leak channels. However, this does not explain the differences in calcium concentration between different fibres.

An increase in intracellular calcium gives an increased rate of muscle protein degradation. In turn increased degradation would lead to an increase in calcium permeability, perpetuating the degradation cycle. This furthers the notion that calcium level fluctuation is a secondary rather than primary consequence of dystrophin absence. As discussed above, direct regulation of calcium by binding to skeletal muscle dystrophin seems unlikely, as the dystrophin EF hand domain doesn't bind calcium at physiological levels.

1.1.7 b) Signal transduction.

The DNA and protein sequences of dystrophin reveal a putative cAMP dependant protein kinase domain within the rod section (Reviewed in Brown and Lucy, 1997). Kinase activity, together with dystrophin's submembranous location could potentially play a role in signal transduction. In addition to acting as a kinase, dystrophin can itself be phosphorylated and dephosphorylated at protein kinase C target sites in the rod domain. Dystrophinopathies have been attributed to deficiencies in signal transduction mechanisms. In particular, Limb Girdle Muscular Dystrophy (LGMD) type 2A is due to a

mutation in the muscle specific calcium activated neural protease 3 (CANP3), a known signalling molecule.

Finally, the N-terminal domain of dystrophin can be activated by calcium/calmodulin following a rise in intracellular calcium. The calmodulin bound NH_2 domain triggers polymerisation of G actin monomers to form the F actin polymer. The contraction induced rise in intracellular calcium therefore leads to formation of extra actin fibres. The muscle fibre is strengthened via the actin cytoskeleton, thus combating the stress of contraction.

1.1.7 c) Maintenance of muscle fibre structural integrity.

The observation that the absence of dystrophin leads clinically to muscle degeneration lead to the conclusion the major function of dystrophin is to maintain structural integrity of muscle fibres.

Based upon the evidence that the muscles most used in an eccentric manner (postural muscles) suffer the most rapid decline in force generation in DMD patients, and realising damage by mechanical factors could explain the muscular weakness in DMD, Karpati and Carpenter (1988) amongst others proposed that dystrophin was preventing mechanical damage in healthy tissue. More specifically, taking the subcellular localisation of dystrophin into account and it's proposed cytoskeletal structure, it was suggested dystrophin prevents disruption of the plasmalemma during eccentric contractions by anchoring the membrane to the cytoskeleton. Consequently dystrophin deficient muscle lacks this stability and is susceptible to shearing forces.

This situation appears to be true in the XMD dog (X-linked muscular dystrophy) which experiences significant exercise induced muscle damage. In DMD patients, however, similar exercise induced effects have not been seen. An equivalent picture is drawn in mdx mice- there does not appear to be any increase in the susceptibility of mdx fibres to contractile activity induced damage. On the other hand, muscle which already has substantial degeneration of fibres will be more susceptible to further damage than healthy fibres. This is due to the greater mechanical forces experienced by the reduced number of intact fibres and possibly explains the differences between XMD dogs and mdx mice- the mice having greater regenerational capacity (reviewed in Jackson, 1993). The role of the dystrophin-DAG complex may therefore be to maintain the structural integrity of the myofibre and membrane.

Ervasti and Campbell (1993 a) showed that dystrophin binds intracellular F-actin with its N-terminal domain and transmembrane spanning β-dystroglycan with the C-terminus. β-dystroglycan associated with α-dystroglycan which in turn binds merosin- a component of the extracellular matrix (figure 1.3).

The dystrophin/DAG complex consequently links the actin contractile fibres to the extracellular matrix (ECM) via the fibre plasma membrane. This intracellular link from fibre to ECM is proposed to maintain the integrity of individual fibres by modulating the shear forces generated during contraction (Petrof *et al*, 1993, Ervasti and Campbell 1993 a, reviewed in Ervasti and Campbell, 1993 b). Furthermore, adjacent bundles of fibres will be held together during contraction by binding to a common ECM. When dystrophin is absent, it is suggested the forces of contraction would shift the contractile fibres relative to the plasma membrane, shearing the membrane and disrupting its organisation. Small movements in the myofibrillar membrane could have a big effect on structure and integrity as the membrane is so well ordered. For example, ion permeability at sights of membrane lesions would dissipate action potentials, rendering the muscle less efficient at contraction- as would movement of ion channels relative to the sarcomere. The extra shear forces in dystrophic tissue and the subsequent membrane disruptions could account for the observed elevated serum creatine kinase levels and the greater susceptibility to osmotic stress. Dystrophin may therefore stabilise the muscle fibre membrane by modulating the contractile shear stress.

1.1.7 d) Stabilisation and organisation of the muscle fibre membrane.

Dystrophin may indirectly stabilise the muscle fibre membrane by restricting the shear stresses imposed on the membrane during contraction. Alternatively, dystrophin may contribute directly to membrane stabilisation by organising the constituents of the muscle cell surface.

1.2 Membrane organisation.

1.2.1 The cell membrane and subcellular domains.

The plasma membrane of a differentiated cell is a far cry from the homogeneous mixture of proteins surrounded by lipid envisaged by Singer and Nicholson (1972). Instead, membranes are complex structures, organised and compartmentalised into distinct functional domains. The classic example of this compartmentalisation is the epithelial cell, whose membranes are polarised into two functionally separate domains- the upper apical domain and the lower basolateral domain. The presence of tight junctions between adjacent cells not only holds the epithelial cells together into a tissue sheet, but also forms an impermeable barrier to diffusion between compartments. Following specific vectorial targeting of membrane constituents to one or other domain, the tight junction prevents free diffusion into the other membrane domain (reviewed by Rodriguez-Boulan and Nelson, 1989).

The membrane polarisation seen in epithelia is not just a curious side effect of cell-cell tethering. Instead, the maintenance of clearly defined subcellular domains is vitally important for celllular function. A clear example of membrane domain demarcation in a differentiated cell is seen in sperm. Though the spermatozoa is just one cell, immunostaining of the cell surface shows antigens to be present on the acrosome that are absent from the tail region and vice versa, for example the glycoprotein antigen PT-1 is confined to the posterior tail region prior to fertilisation (Myles *et al*, 1984). This subcellular regionalisation reflects essential domain functionality- enzymes needed for burrowing into the oocyte are unnecessary in the propulsion domain.

Cells may form supramolecular complexes at the membrane to perform a particular function. In excitable cells, for example, effective and efficient propagation of the action potential and neurotransmission at the synapse and neuromuscular junction requires the correct spatial distribution of the constituent parts. Transmission of an action potential along the nodes of Ranvier in a neuron is mediated by and dependent upon high density clustering of sodium channels at the nodal regions. Formation of such complexes requires the correct spatial targeting of the constituents followed by a method of localisation or immobilisation at the target site (Kaplan et al, 1997).

Regulation of the movement of membrane proteins is essential if a membrane is to contain regions with different functionalities. In the signal transduction for example, it would be disastrous if an activated receptor could diffuse throughout the membrane and trigger signal transduction cascades at random. Receptor and target may therefore be localised together on a cell. In addition to localising receptor and target together within a domain on one cell, the restriction of protein mobility can also permit direct communication between two adjacent cells. To facilitate inhibitory synaptic transmission for example, GABA receptors are localised in high density clusters on the neuronal cell body and dendrites, closely opposed to the sites of GABA release, where their mobility is restricted (Velasquez *et al*, 1989). Similar restrictions are needed to allow formation of supramolecular complexes from their constituent parts. Trapping proteins at an active site increases the local concentration of component proteins, raising the likelihood of protein-protein interactions and complex formation. Assembly of the complex also consequently occurs at the desired subcellular location.

1.2.2 Experimental methods for studying membrane domains.

In polarised cells, the localisation and segregation of proteins into functional domains is controlled in part by imposed restrictions on the diffusion capabilities of the proteins, restricting their lateral mobility within the plane of the membrane. In neurons, for example, a specialised domain at the initial segment of the axon acts as a barrier to protein diffusion (Winckler *et al*, 1999). Such barriers are highly selective- lipids are able to cross the diffusion barrier at the axon hillock but transmembrane spanning proteins are restricted (Winckler and Poo, 1996). By monitoring the movements of membrane proteins

in real time, possible mechanisms of organisation and distribution of membrane proteins and lipids are suggested, and insights are provided into associations with the underlying cytoskeleton. In order to study the diffusional behaviour of membrane species, two experimental techniques have been developed- fluorescence photobleach recovery (FPR), also known as fluorescence recovery after photobleaching or FRAP, and single particle tracking (SPT).

1.2.2 a) Fluorescence photobleach recovery.

FPR is a technique which facilitates the real time study of membrane fluidity, providing quantitative measurements of the distribution and lateral mobility of a membrane species of interest. FPR has been employed in this thesis to study mobility of proteins and lipids in the muscle fibre membrane.

To obtain mobility data, the studied molecule must first be specifically labelled *in situ* with a fluorescent marker. An argon laser is used to excite the fluorescent marker within a small region of the membrane defined by the laser beam. The intensity of fluorescence emitted is quantified by photon counting with a photomultiplier tube. The arrangement of apparatus is shown in schematic form in figure 1.4 a) and the actual experimental equipment is shown in figure 2.1. After normalising initial levels of fluorescence, the membrane patch is bleached rapidly (by 60-70%) with a 10,000 fold brighter pulse of laser light (figure 1.4 b, top centre). The attenuated monitoring beam is then used to track recovery of fluorescence (figure 1.4 b, top right).

Fluorescence recovery is attributed to the outward diffusion of bleached molecules away from the bleached region and an inward diffusion of unbleached molecules from the surrounding membrane. A stylised recovery curve is shown in figure 1.4 b, bottom. Using the diffusion equation,

$$D=w^2/4T_D$$

where, w is the e^{-2} beam radius and T_D is calculated from the half time for recovery ($t_{1/2}$), it is possible to calculate the diffusion coefficient of the molecule, D (Axelrod *et al*, 1976).

The fraction of the labelled molecules that are mobile, f, may be calculated from the recovery curve,

$$f= I (c) - I (o) / I (p) - I (o).$$

I (p), I (o) and I (c) are the fluorescence intensities at the pre-bleach, post-bleach and steady state (time = infinity) levels respectively. The level of fluorescence recovery reflects the proportion of molecules that are mobile. If all the molecules are freely mobile within the plane of the membrane, the post-bleach fluorescence intensity will return to pre-bleach levels.

a)

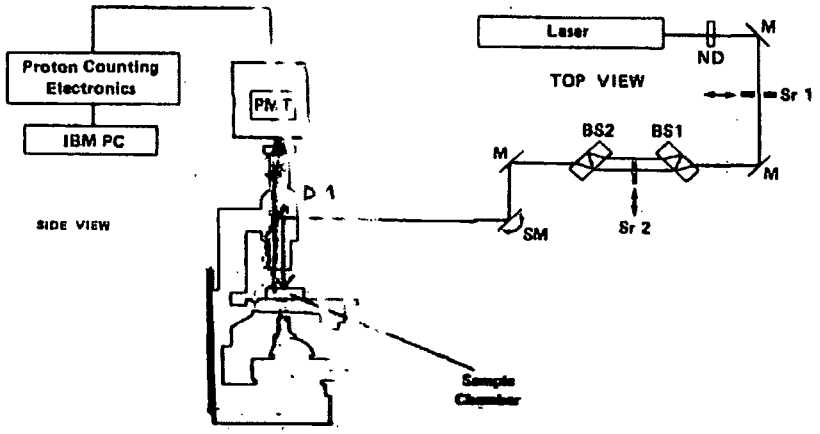

b)

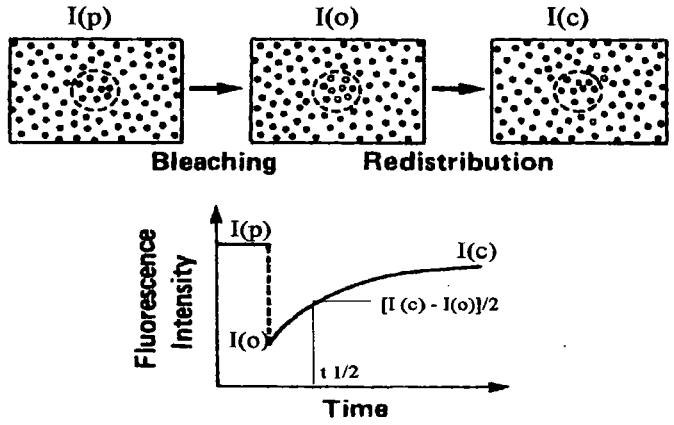

Figure 1.4 a) Diagram of FRAP apparatus FPR equipment directs either low level excitatory laser light onto a sample to monitor membrane fluorescence, or 10,000 fold brighter light through to bleach fluorescence in a small membrane region.

Mirrors and beam steerers direct the laser beam onto the sample. In monitoring mode the bleach shutter (Sr2) is closed, and only the 0.01% of laser light reflected back from the 4 prism/air interfaces is directed towards the sample. In bleach mode the shutter is opened for ~50msec under control of a computer, and the full intensity laser beam passes through to the sample. The incoming excitatory beam is focused onto the sample surface with a microscope lens. The dichroic mirror reflects excitatory light onto the sample, and allows the longer wavelength emitted fluorescence up to the photomultiplier tube where light levels are digitally quantified. Key: neutral density filters, ND; mirrors, M; dichroic mirror, DM; steering mirror, SM; shutters, Sr; beam splitters, BS, and photomultiplier tube, PMT.

1.4 b) Recovery curve for mobile species- the molecule of interest is fluorescently tagged. Initial levels of fluorescence F(I) are measured in the target area before the sample is briefly bleached F(0). If the labelled species is mobile, diffusion of fluorescent molecules into the target area will lead to recovery of fluorescence intensity over time F(t).

1.2.2 b) Typical diffusion characteristics of membrane components.

The lateral diffusion rate of a molecule within a membrane is related to its size- the smaller the species, the faster it diffuses (Saffman and Delbruck, 1975, Peters and Cherry, 1982). D determined by FPR for membrane proteins is typically of the order of ~ 10^{-10} to 10^{-11} cm^2s^{-1}. Lipids move more rapidly. D for membrane lipids is of the order of 10^{-9} cm^2s^{-1} (e.g. Jacobson *et al*, 1987).

The mobile fraction of membrane proteins and lipids is highly variable and dependant upon cell type (table 1.1). Typically, membrane lipids show 50-100% recovery in fluid membranes. Protein mobility ranges from 5 to 100% according to the mechanism of membrane/protein association (see later), with lower mobility in highly specialised differentiated cellular domains (e.g. Jacobson *et al*, 1987, Kusumi and Sako, 1996, Axelrod *et al*, 1976).

Membrane components with a mobile fraction less than 15% are deemed to be 'immobile' by FPR.

Membrane Component.	**Cell type.**	**D, diffusion coefficient (cm^2s^{-1}) (s.d.).**	**f, mobile fraction.**
NCAM (protein) [1]	C2C12 muscle cell line.	$6.9 \pm 0.2 \times 10^{-10}$	51%
Band 3 (protein) [2]	erythrocyte	4.5×10^{-11}	80%
Di I (lipid analogue) [3]	fibroblast	$1 - 1.4 \times 10^{-8}$	>90%
ODAF (lipid analogue) [4]	Bull spermatozoa (midpiece domain)	$7 - 9 \times 10^{-9}$	47 - 55%

Table 1.1 Representative diffusion data for membrane proteins and lipids.

In general, lipids show greater mobility than proteins, with faster diffusion and a greater mobile fraction. Protein diffusion is dependent upon cell type and method of protein anchoring to the membrane. (References, 1, Simson *et al*, 1998. 2, Sheets *et al*, 1980. 3, Jacobson *et al*, 1987. 4, James *et al*, 1999.)

1.2.2 c) Limitations of FPR.

There are two main limitations of FPR within these experiments. The first is timescale. The 25msec dead time between the bleach and first measurement will lead to some data loss, particularly of rapidly diffusing species. Additionally, molecules with $D<10^{-12}$ cm^2/sec will appear immobile.

Secondly the resolution of an FPR experiment is severely limited by the relative size of the bleach spot to the diffusion domain of the fluorescently marked protein- if the bleached region is larger than the area in which the labelled molecule can freely diffuse, that molecule will always appear immobile by FPR, even if it is actually diffusing freely in a small confined domain. Additionally, the size of bleached area relative to the total size of membrane will affect the magnitude of fluorescence recovery. The diffusion equations assume an infinite source of labelled molecules diffusing into the bleach area sink. In biological systems, and particularly within the confines of single cells the source of labelled molecules is finite and therefore full recovery may not be seen- even if the species is freely diffusible (see Edidin, 1993 for a full explanation of domain size and FPR data interpretation, and Angelides *et al*, 1988 for the mathematics).

1.2.2 d) Single particle tracking.

Single particle tracking (SPT) is a modification of the FPR technique that allows the mobility of a single molecule to be tracked on a cell surface (reviewed in Sheets *et al*, 1995). In SPT the protein is labelled with either colloidal gold or a fluorescent latex bead which has been covered in antibodies to the molecule of interest. Mobility of the protein-bead complex can then be followed across the cell surface with a microscope and video camera in real time. SPT is advantageous over FPR in that free diffusion within smaller scale domains can be resolved- the size of bleach spot is not limiting. Single molecular information can be obtained at nanometer resolution. FPR measurements of diffusion refer to macro scale mobility, i.e. the time it takes for a molecule to diffuse over micrometers into the bleach spot. SPT provides both micro and macroscale diffusion measurements. With SPT it is possible to measure both how quickly a protein can diffuse within a confined domain, and also how frequently that protein can cross into adjacent diffusion domains. Rotation of a fixed protein about the point of tethering can also be resolved.

A similar technique with single molecular resolution employs the use of optical tweezers (reviewed in Sheets *et al*, 1995). As with SPT the antigen of interest is labelled with latex beads. The bead may then be held in an optical trap of crossed laser beams and pulled along the surface of the cell. The forces acting upon the protein and restrictions imposed upon its lateral mobility can be studied by monitoring the distances a bead can be pulled and the forces required to cross any barriers encountered (with piconewton accuracy).

1.2.3 Micron scale domains as revealed by FPR.

Early FPR comparisons of real and artificial lipid bilayer systems showed that proteins diffused far more slowly in a cell membrane than in an artificial model. There were clearly restrictions imposed upon the Brownian diffusion of proteins in the cell (reviewed in Jacobson *et al*, 1987). The mobile fraction of fluorescent antibody labelled membrane proteins was found to relate to the size of FPR bleach spot area- the mobile fraction falling as bleach spot size increased. The same was true for the lipid analogue NBD-PC. This is contrary to expectations for a homogeneous cellular surface. In this case the same proportion of mobile proteins and lipids should be found across the membrane surface, irrespective of bleach area. This dependence of mobile fraction upon bleach spot size suggested the cell membrane is compartmentalised into regions ~2μm in diameter. When the FPR bleach region was significantly smaller than a domain, free diffusion of mobile species into the bleached area was possible. When the bleach spot size covered several domains, the membrane species- though mobile within their own domains- could not cross the domain boundaries and the apparent FPR mobile fraction went down (Yechiel and Edidin, 1987).

1.2.4 The role of the cytoskeleton in restricting protein lateral diffusion.

It is clear that in terms of functionality and physical organisation, the cell membrane is divided into micrometer scale domains. The importance of the cytoskeleton to the construction and partitioning of these subcellular domains was elegantly demonstrated in red blood cells. The biconcave structure of an erythrocyte is maintained by the cytoskeleton. Spectrin tetramers cross link into a net-like structure beneath the membrane surface, with tetramers joined together at junctional complexes. The junctional complex, including ankyrin and the transmembrane protein band 3, links the underlying spectrin network to the membrane (reviewed in Bennet, 1985). Proteins diffuse faster within blebs in the membrane, where the membrane has been pulled away from the cytoskeleton, than they do in the main body of the cell (Tank *et al*, 1982) therefore the cytoskeleton restricts protein mobility.

Spherocytic erythrocytes develop their characteristic shape because of deficiencies in the cytoskeleton. Levels of ankyrin, spectrin, band 2.1 and band 4.1 proteins are all reduced. The lateral mobility of Con A receptors in the spherocytic erythrocytes was 50 fold higher than the mobility of the same receptors in the membranes of normal erythrocytes when measured by a modified FPR technique ($D \sim 2.5 \times 10^{-9} cm^2 s^{-1}$ for spherocytic erythrocytes and $4.5 \times 10^{-11} cm^2 s^{-1}$ for normal cells) (Sheetz *et al*, 1980). The spectrin based cytoskeleton is therefore placing a restriction upon mobility of membrane proteins in normal red blood cells.

Confirmation of the role of the cytoskeleton was obtained by following the rotational and lateral diffusion of band 3 protein in the membranes of erythrocytes. Lateral mobility of free band 3 was

dependent upon the spectrin association state (spectrin dimers or tetramers), with greater lateral mobility as the spectrin dimer/tetramer equilibrium was shifted towards dimers (Tsuji and Ohnishi, 1986). The rotational mobility remained unchanged. The portion of band 3 immobilised to the cytoskeleton via ankyrin was constant throughout, so the observed changes in diffusion rates were not due to increased freely diffusing band 3. The rotation of the unbound band 3 showed it was free to diffuse, whatever the spectrin association state. The extent and rate of diffusion was determined by the cytoskeletal integrity. It was therefore proposed that spectrin and band 3 interacted physically beneath the surface of the membrane. Further evidence was provided by the 8 fold increase in lateral mobility following cleavage of the band 3 cytoplasmic domain (Tsuji *et al*, 1988).

The physical nature of the cytoskeletal interaction with diffusing membrane proteins is reflected in the correlation between diffusion rate and cytoplasmic domain size. In general, the larger the cytoplasmic region of a membrane protein, the more likely it is to encounter the cytoskeletal network. Similar evidence for a steric cytoskeleton / membrane protein interaction comes from domain swapping experiments. Restrictions imposed upon mobility correspond to the method of protein/membrane anchoring. Classical transmembrane spanning H-2 ^{b} class 1 MHC molecules are concentrated in domains within the membranes of K78-2 hepatoma cells, whilst the GPI anchored non-classical class 1 related molecules Qa-2 can pass through the domain boundaries. The mobility profile depends upon the mode of anchoring the protein to the membrane. Swapping the anchoring regions resulted in the alternative pattern of mobility (Edidin and Stroynowski, 1991). Proteins with large cytoplasmic domains are therefore held up in the cytoskeleton to a greater extent than those with smaller cytoplasmic regions. Restrictions on mobility must be conferred by the inside of the cell membrane, not the outside, as the extracellular portion of the proteins was unchanged by the domain swap.

Whether proteins are hindered by the cytoskeleton or not, interactions with other proteins in the plane of the membrane affect the rate of lateral diffusion. Rate of GPI anchored Thy-1 mobility in membrane lipid analogues is as fast as the rate of lipid diffusion. Increasing the concentration of membrane proteins reduces the rate of lateral diffusion as protein-protein interactions increase the viscosity of the membrane (Jacobson *et al*, 1987). The rate of mobility of GPI anchored proteins in the above domain swap experiment was impeded by high concentrations of membrane protein.

Lateral mobility may be constrained in that all directions of diffusion may not be equally likely. Just as bulk flow effects in a membrane may move components laterally, diffusion may be anisotropic (Jacobson *et al*, 1987).

1.3 The molecular fence model of membrane domains.

Sako and Kusumi (1994) used video enhanced contrast optical microscopy to track the mobility of individual transferrin and α_2 -macroglobulin receptors labelled with nanometer sized ligand coated colloidal gold particles on the surfaces of cultured NRK fibroblasts. The motion of the particles was consistent with confined diffusion. Rapid free Brownian diffusion occurred on a micrometer scale within confined domains ($D \approx 10^{-9} cm^2/s$). Slower long-range diffusion was seen following intercompartmental jumps (macroscopic diffusion coefficient $\approx 2.4 \times 10^{-11} cm^2/s$). The location of the boundary domains was fixed over the measuring time of the experiment, suggesting domains have hard physical barriers at their edges. Lipid domains are unlikely as the edges of adjacent domains were very close- too close for apposing lipid fields with similar viscosities. Similarly, the boundary edges were fixed in place during the measurements, but lipid domain edges would fluctuate during the measuring period. The underlying cytoskeletal network was important for the formation of the domain boundaries- disruption with cytochalasin D or vinblastin decreased the extent of confined diffusional mode and increased the simple diffusion mode (Sako and Kusumi, 1994).

The elastic nature of the boundaries was seen when laser optical tweezers were used to drag colloidal gold labelled proteins across the cell surface. The beads were released from the optical trap and sprang back into the centre of the domain at the boundaries. The barrier free path for bead motion was related to the size of protein cytoplasmic domain- 8.5μm for GPI anchored molecules c.f. 3.5μm for a transmembrane spanning receptor- as with FPR measured diffusion (Edidin *et al*, 1991). Variation in bead size from 40-210nm diameter has no effect on observed dragging rate, but disruption to the cytoskeleton does- again indicating the boundaries are cytoplasmic and cytoskeletal, not extracellular (Sako and Kusumi, 1995).

The confined diffusional modes observed, the physical nature of the boundaries and the importance of the cytoskeleton to these observations lead Sako and Kusumi (1994) to propose the 'membrane skeleton fence model' (molecular fence) of membrane organisation (later refined by Simson *et al*, 1998). This model proposes that the spectrin based cytoskeletal network beneath the cell surface restricts mobility of membrane proteins by forming a steric barrier to protein diffusion. Membrane proteins with large cytoplasmic domains are more likely to encounter the cytoskeleton and be restricted in their motion than proteins with small cytoplasmic components (figure 1.6, a). The fast micro scale diffusion rates are due to free Brownian motion within the confines of a domain boundary. The slower macroscale diffusion reflects the time taken to hop from one confined diffusion domain to the next (figure 1.5). The rate of intercompartmental transfer is predominantly influenced by the length of the cytoplasmic tail of the molecule; the integrity of the cytoskeleton (spectrin dimers are more 'open' than tetramers, so proteins can pass more easily between diffusion domains (Tsuji and Ohnishi, 1986), dissociation of the cytoskeleton by cytochalasin allows passage between domains); and the distance

between the membrane and the cytoskeletal network (hence the increased mobility in blebbed membranes).

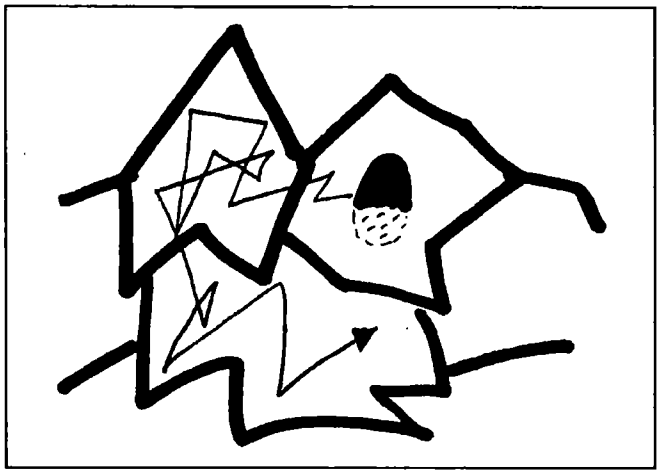

Figure 1.5 The molecular fence model of membrane organisation: mobility pattern of molecule undergoing constrained diffusion as seen by SPT.

The protein (dark spot) is free to diffuse rapidly within the confines of a cytoskeletal domain (broad lines) ($D_{microscale} \sim 10^{-9}$ cm^2s^{-1}). Intercompartmental transfer is slower ($D_{macroscale} \sim 10^{-11}$ cm^2s^{-1}) and depends upon the integrity of the cytoskeletal boundary, cytoskeleton-membrane distance, cytoplasmic domain size and kinetic energy of the diffusing molecule. Figure after Sako and Kusumi, (1994).

1.4 Other modes of restricting membrane protein mobility.

The membrane skeleton fence model is one way in which mobility of membrane proteins can be restricted, but it is not the only way to control membrane protein mobility. Five different modes of protein motion have been observed by SPT(Kusumi *et al*, 1993)- free Brownian diffusion, constrained diffusion (molecular fence), stationary phase (immobile), oscillation about a fixed point and directed motion (figure 1.6). Directed motion is believed to reflect either bulk flow, such as towards a leading edge in migrating fibroblasts, or motion along cytoskeletal motors (reviewed in Sheets *et al*, 1995). In order to explain these other variations in mobility, modes of protein confinement have been proposed that may be employed in conjunction with the cytoskeletal membrane fence model (discussed in Kusumi and Sako, 1996, Sheets *et al*, 1995).

1.4.1 Oligomerisation.

Oligomerisation of membrane proteins would not necessarily reduce their lateral mobility in a matrix of uniform viscosity, although there is some dependence of size upon lateral diffusion rates (Vaz *et al*, 1982). However, large protein complexes will be restricted in their ability to cross the boundaries between adjacent cytoskeletal domains, especially where breaks in the cytoskeleton or increased membrane/cytoskeletal distance are essential for passage (reviewed in Kusumi and Sako, 1996). Inclusion of a protein with a large cytoplasmic domain into the complex would restrict mobility of other more freely diffusing members (figure 1.6 b). The entrapment of a couple of members of a protein complex within a confined region can facilitate formation of large multimolecular assemblies on the cell surface as other members of the complex diffuse and hop between compartments into the domain, but once bound cannot diffuse out.

1.4.2 High localised concentration of proteins.

A high local concentration of proteins can restrict diffusion of a protein molecule through a region (reviewed in Sheets *et al*, 1995). Firstly, proteins increase the viscosity of the membrane lipid bilayer. Secondly, the greater the protein concentration, the greater the extent of protein-protein interactions. Such interactions could be steric, forming a physical barrier to diffusion. Specific and non-specific electrostatic interactions will influence diffusion, as will interactions with the surrounding lipid phase. Such crowding effects on diffusion are understood to account for the transient confinement of GPI anchored proteins which cannot directly interact with the cytoskeletal meshwork (figure 1.6 c).

1.4.3 Localised lipid domains.

Localised variations in the lipid bilayer could account for the differences in protein diffusion across the cell surface (figure 1.6 d). Firstly, local changes in bilayer viscosity would affect rates of protein diffusion. Secondly, specifically enriched lipid or cholesterol domains could regulate GPI anchored protein diffusion. GPI anchored proteins are found in cholesterol dependent submicron domains on the cell surface (Varma and Mayor, 1998, Friedrichson and Kurzchalia, 1998). In liposomes, GPI anchored proteins co-localise to the detergent inextractable lipid fractions. It was suggested the saturated acyl chains of the phosphatidylinositol anchor may preferentially partition into more ordered lipid domains , enriched in glycosphingolipids, sphingomyelin and cholesterol, thus localising the GPI anchored protein (Schroeder *et al*, 1994). Differences in boundary lipid composition could similarly affect diffusion rate (Jacobson *et al*, 1987).

a)

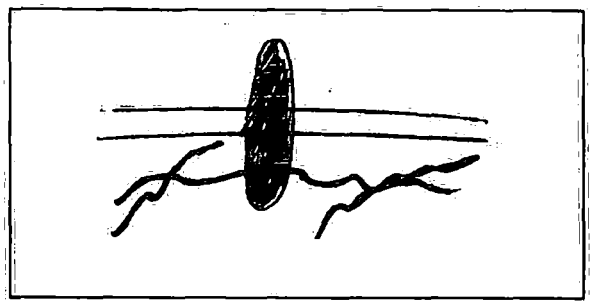

b)

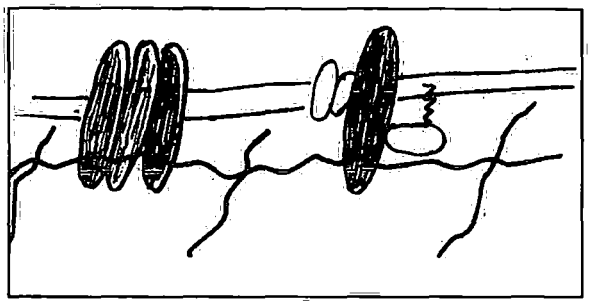

c)

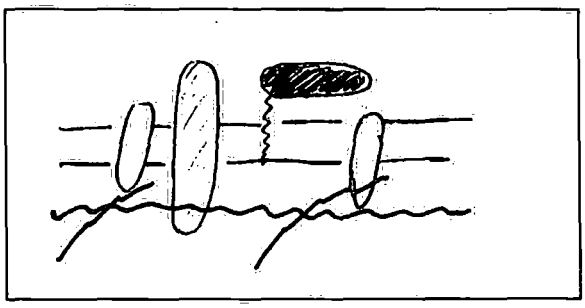

d)

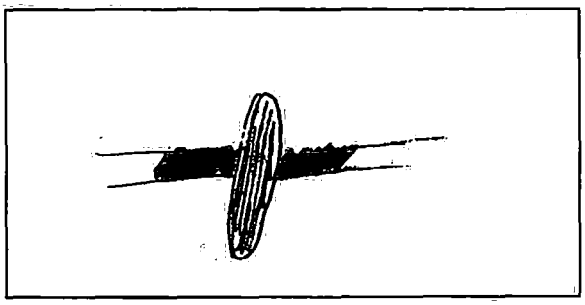

1.4.4 Protein anchoring.

FPR experiments very rarely reveal 100% mobility of membrane proteins. A portion of the proteins are invariably immobile on the timescale of the FPR measurement. Immobile proteins may be anchored in place on the membrane, usually through specific binding interactions with members of the spectrin based cytoskeleton. The portion of band 3 molecules with no rotational mobility, for example were bound to ankyrin in the cytoskeleton (Tsuiji *et al*, 1988). Single particle tracking has directly shown proteins in a stationery phase (reviewed in Sheets *et al*, 1995). Such proteins are either completely immobile, or oscillate about a fixed point. The extent of oscillation is controlled by the flexibility of the cytoskeletal linkage- rather as a dog tied to a lamppost can move, but only within a radius defined by the length of lead.

1.4.5 Membrane compartmentalisation- summary.

In summary, it has been shown that cellular plasma membranes are compartmentalised and compartmentalisation is essential for cellular function. In terms of large scale domains as found in spermatozoa or epithelial cells, the domain boundaries are clear and immutable. In addition, all cell membranes contain microscale domains. These domains may result from localised variation in membrane lipid or protein concentration. Alternatively, the underlying ankyrin and spectrin based cytoskeleton may form a steric barrier to protein diffusion by formation of a submembranous 'molecular fence'. Boundaries of the molecular fences may be crossed, depending upon the mode of anchoring of the protein to the membrane, the size of the cytoplasmic domain of the diffusing protein, the association/disassociation state of the spectrin lattice and the distance between the membrane and cytoskeleton. Aggregation of proteins into complexes can hinder diffusion across the cytoskeletal boundaries. This can localise molecules to a surface domain and facilitate macromolecular complex formation. Colocalising components of a signal transduction cascade can speed up the rate of transmission. Finally, proteins may be bound specifically and directly to the cytoskeleton. Diffusion is prevented altogether, but some oscillation about a fixed point is possible.

1.5 Dystrophin and membrane integrity.

Organisation of the protein and lipid constituents of a cell membrane is vital for proper cellular function. The evidence outlined below suggests that the structure of the muscle membrane is compromised in the muscular dystrophies and therefore indicates that a possible function of dystrophin is organisation of muscle fibre membrane constituents.

Duchenne muscular dystrophy patients possess elevated levels of muscle cytosolic proteins in their serum. Hoffman and Gorospe (1992) proposed that the serum enzyme abnormalities in Duchenne muscle arose from leakage of the muscle cytoplasmic constituents into the blood through defects in plasma membrane integrity. [At the time they hypothesised that the reverse passage of calcium into the cell could lead to death, though since then the absence of measurable calcium influx found in mdx myotubes *in vitro* (reviewed in Jackson, 1993), argues against this.] As dystrophin is the key missing protein in DMD, the leaky membranes suggested dystrophin somehow maintains muscle membrane integrity.

An absence of dystrophin affects membrane stability under applied osmotic stress. Mature muscle fibres and cultured myotubes from mdx mice show greater sensitivity to imposed hypo-osmotic stress than C57/Bl 10 strain control muscle (Menke and Jockusch, 1991). This whole cell experiment contradicts the findings of an earlier study carried out on domains the size of a few micrometers where membrane stability was measured with the application of suction through microelectrodes. No difference was found in the resistance to applied stretch between of mdx and normal fibre membranes (Franco and Lansman, 1990).

Dystrophin deficiency has also been shown to affect the mechanical stiffness/deformability of the muscle fibre membrane as measured by 'cell poking'. Prior to differentiation the stiffness of normal and mdx myotubes was comparable. Post differentiation (following induction of dystrophin expression) normal myotubes were found to be four fold stiffer than mdx myotubes. Dystrophin therefore mechanically reinforces the muscle membrane (Pasternak *et al*, 1995).

1.6. Organisation of the muscle fibre membrane at the neuromuscular junction.

The neuromuscular junction (NMJ) is the site of nerve-muscle intra-cellular communication. The junctional region of the myofibre membrane possesses a highly specialised assembly of proteins, in an arrangement directly related to function. The junction consists of three regions- the presynaptic nerve terminal, the highly convoluted postsynaptic muscle fibre membrane and the intervening basal lamina. These three regions are unique in terms of protein composition and spatial assembly. Biochemically, the muscle membrane at the NMJ has high concentrations of two particular proteins. The first, the nicotinic acetlycholine receptor (AChR), is found at the crests of the folds- juxtaposed with the presynaptic motor ending. The second protein is the voltage gated sodium channel (NaCh), responsible for the membrane depolarisation that ultimately leads to contraction. NaChs are found at the depths of the postsynaptic folds (Flucher and Daniels, 1989) (figure 1.7).

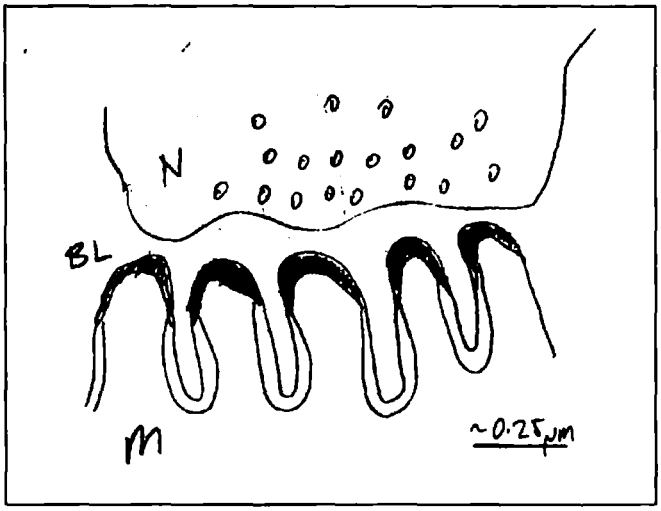

Figure 1.7 Schematic representation of the neuromuscular junction. N, synaptic ending of motor neuron. BL, basal lamina. M, muscle fibre. Regions of high acetylcholine receptor density at the tops of the postsynaptic folds are shaded, regions of high voltage gated sodium channel density at the pits of the folds are open. Diagram modified from Sealock and Froehner, 1997, p.140. Scale bar is approximate.

AChR are located at the tops of the folds of the muscle membrane, at an almost crystalline density of 10 000 molecules/μm^2 (Fertuck and Salpeter, 1976). None of the complex structure is present prior to innervation- pre-existing AChR diffuse to the site of neural contact (Anderson and Cohen, 1977) where they become immobilised. AChR must be specifically anchored in place at the NMJ crests, since the receptors are capable of free diffusion in muscle fibre membranes prior to innervation. Axelrod *et al* (1976) first showed that receptors cluster and immobilise at the NMJ by following the mobility of AChRs by FPR. The receptors fell into two classes. The first were mobile receptors undergoing apparently free diffusion. These were uniformly distributed across the muscle cell surface. The second class of receptors were immobile. These had formed dense, highly granular clusters. Clustering of AChRs therefore gave rise to immobilisation of the receptors. Further experiments looking at the re-formation of the clusters showed clustering to be a constant process. Mobile receptors from outside the NMJ diffused towards existing clusters where they are trapped and immobilised (Stya and Axelrod, 1983). It was proposed that a mechanism must exist to immobilise the AChRs clusters and this could come from a submembranous anchoring network.

The precise anchoring mechanism of receptors at the crests remains unknown. However, most of the evidence suggests involvements from cytoplasmic protein constituents of the crest membrane and possibly the basal lamina (Bloch and Pumplin, 1988; Froehner, 1991; Apel and Merlie, 1995).

A comparable situation is found with localisation of the muscle NaCh. NaCh are diffusely distributed and freely mobile within the sarcolemma of un-innervated muscle. Upon innervation of the muscle fibre, the channels become localised to the NMJ where they are immobilised (Angelides, 1986).

The mature NMJ, in common with pre and post-synaptic specialisations on all excitable cells, has ion channels localised to specific domains on the cell surface. AChRs and NaChs are able to undergo free diffusion in immature myoblasts prior to innervation. The question must be addressed of how these channels and other specialised proteins become localised as they do to specific specialised subcellular domains, rather than remaining in a state of free diffusion on the cell surface. In neurons, sodium channels become clustered at axon hillocks, initial segments and the nodes of Ranvier. In muscle fibres, AChRs and NaChs cluster at NMJs.

1.6.1 The spectrin based cytoskeleton and muscle sodium channel localisation.

Electron microscopic evidence suggests that, as in the central and peripheral nervous systems, an ankyrin/spectrin based system may immobilise NaChs in muscle. NaChs and ankyrin colocalise at the depths of the folds of neuromuscular junctions (Flucher and Daniels, 1989).

Different spectrin isoforms exhibit differential subcellular localisation in muscle tissue. Erythroid β-spectrins, for example, localise at the costameric junction between Z-lines and the sarcomere, whilst non-erythroid spectrin colocalises with the erythroid forms at the Z-lines but is also found homogeneously distributed across the membrane surface (Vybiral *et al*, 1992). This would suggest that different isoforms of spectrin perform different functions in different domains of the muscle membrane.

Just as the cytoskeletal constituents ankyrin and spectrin are proven to be necessary for localisation and immobilisation of ion channels in the brain and peripheral nervous system, and possibly involved at the NMJ, the presence of the homologous proteins dystrophin and utrophin at the NMJ is consistent with a potential involvement in regulating ion channel distribution. Considering the homology between dystrophin and β-spectrin, dystrophin may have a similar specialised function in subcellular domains to isoform specific spectrins.

1.6.2 Utrophin and the NMJ.

Utrophin exists exclusively at the NMJ of skeletal muscle (Khurana *et al*, 1991), and specifically with AChRs and rapsyn at the crests of the post-synaptic folds (Bewick *et al*, 1992). Utrophin, together with β-dystroglycan co-localises to sites of AChR clustering from early development throughout the

postnatal maturation of the NMJ (Bewick *et al*, 1996), suggesting some role in cluster formation or stabilisation.

Agrin is the signalling molecule released by the motor neuron that induces formation of the NMJ specialisations on the muscle fibre (Nitkin *et al*, 1987). The only known agrin binding molecule within muscle fibres is dystroglycan- in the case of the muscle NMJ this is α-dystroglycan (Gee *et al*, 1994 amongst others). AChRs colocalise with utrophin at the tops of the folds, therefore clustering of the AChRs could be via agrin, dystroglycan and utrophin.

Rapsyn, rather than utrophin, is believed to be the main player in AChR clustering. Rapsyn, a 43kDa peripheral membrane protein, is sufficient to induce formation of AChR clusters (Froehner *et al*, 1990) and colocalises precisely with AChRs from the earliest stages of synaptogenesis. Rapsyn knockout mice fail to assemble post-synaptic specialisations at their NMJs (including utrophin localisation, suggesting rapsyn induces the entire post-synaptic cytoskeletal apparatus) (Gautam *et al*, 1995). A stabilisation role seems most likely for utrophin since it is not essential for formation of AChR clusters. Although utrophin co-localises with AChRs, utrophin knockout mice show no major differences in NMJ structure and organisation compared to normal mice, though a reduction in the total numbers of AChRs and the extent of post-synaptic folding is observed (Deconinck *et al*, 1997). It is believed this reduction in folding leads directly to the reduction in AChRs, as there is less space for the receptors to occupy.

1.6.3 Dystrophin and the NMJ.

It is unlikely that dystrophin is involved in clustering of AChRs, especially as mdx mice possess normal AChR clusters at endplates (Lyons and Slater, 1991). Utrophin is still present in mdx muscle and could contribute to AChR clustering via DAGs (present, though down-regulated) at the crests of the folds. Instead, dystrophin, like spectrin in neurons, may have a role in the localisation of sodium channels at the depths of the junctional folds.

Dystrophin, in contrast to utrophin, can be seen throughout the muscle plasma membrane. The exception lies at the NMJ, where dystrophin is excluded from the utrophin/AChR rich domains and is found at high concentration in the membrane region immediately adjacent to the AChRs in the depths of the junctional folds (Sealock *et al*, 1991, Byers *et al*, 1991), the same region as the voltage dependent sodium channels. β-spectrin immunostaining is similarly found alongside dystrophin and NaChs at the depths of the junctional folds and outside the region of AChRs (Bewick *et al*, 1992).

Localisation of dystrophin to the folds of the junction is developmentally regulated and after AChRs have begun to aggregate. Early on in development of the NMJ, dystrophin is present but at no greater

density than elsewhere. By P14 (approximately the same time as formation of extensive junctional folding and NaCh accumulation), dystrophin concentration is enhanced at NMJs relative to the remainder of the membrane, and reduced at AChR rich regions. Similarly, β-spectrin concentration rises at the junction in parallel with development of the post-synaptic folds and accumulation of NaChs (Bewick *et al*, 1996).

All four proteins β-spectrin, utrophin, dystrophin and β-dystroglycan are found at the NMJ before the junction obtains denervation stability, therefore whilst they may all contribute to formation of the NMJ, they cannot confer total stability on the NMJ structure (Bewick *et al*, 1996).

The physiological role of dystrophin at the NMJ is not clear, especially as dystrophin is not essential for junctional formation. Mdx mice have normal NMJs, although some reduction in the extent of folding has been noticed (Lyons and Slater, 1991). Dystrophin may therefore be maintaining the complex folded nature of the motor end plate via interactions with the basal lamina. However, dystrophin is also found in specific synaptic structures in the brain, e.g. Purkinje cells of the cerebellum. Here there is no specialised basal lamina, therefore dystrophin is either redundant or it is involved in ordering the post-synaptic apparatus in a non-basal lamina dependent fashion (Lidov *et al*, 1990, 1993).

1.7 Aims and Objectives.

Given that DMD is linked to defects in muscle membrane integrity, dystrophin shows high sequence, structural and spatial similarities to the cytoskeletal protein spectrin- a proven organiser of membranes and regulator of membrane protein lateral mobility; and an absence of dystrophin affects the mechanical stability of the muscle cell membrane, the experiments presented in this thesis attempted to quantify the contribution made by dystrophin protein to membrane organisation.

1.7.1 Dystrophin as a non-specific barrier to membrane diffusion- a molecular fence.

The dystrophin gene shows high homology to the cytoskeletal proteins spectrin and α-actinin. The large central rod domain has 24-spectrin like repeats, whilst the adjacent amino terminal actin-binding domain is highly homologous to the actin binding domains of α-actinin and spectrin (Koenig *et al*, 1988). This high homology suggests a cytoskeletal role for the dystrophin protein, a suggestion reinforced by the ultrastructural observation that dystrophin possesses the distribution pattern of a cytoskeletal network protein (Porter *et al*, 1992).

The importance of spectrin and spectrin-like proteins in maintaining membrane organisation and for mechanical integration of the cell membrane is well documented. In both mice and humans an increasing number of genetic diseases are being traced to mutations in members of the erythrocyte spectrin-based cytoskeletal protein family. For example, human neurofibromatosis type 2 is caused by defects in a protein related to protein 4.1 of erythrocytes (Bianchi *et al*, 1994); whilst an ankyrin deficiency seen in the brain as well as erythrocytes of nb/nb mice (with associated reduction in spectrin levels) leads to degeneration of a population of Purkinje cell neurons, development of ataxia and signs of cerebellar dysfunction (Peters *et al*, 1991). Medical defects have correlated with a compromised 'molecular fence' in these cells- the original experiments to illustrated the role of spectrin in restricting protein lateral mobility were performed on the red blood cells of patients with spherocytic anaemia (Sheetz *et al*, 1980).

It may be considered optimistic to suggest dystrophin, like spectrin, is an essential structural component of the membrane skeleton. In terms of total protein dystrophin is a very minor component of skeletal muscle, making up just 0.002% of the protein of muscle fibres (Hoffman *et al*, 1987). On the other hand, the plasma membrane is a small fraction of the total components of a muscle fibre, the bulk of the protein residing in the contractile fibres. Dystrophin makes up 4.8±0.8% of the protein in isolated sarcolemma, a 2400 fold enrichment compared to muscle as a whole, and comparable with the density of spectrin in brain membranes (Ohlendieck and Campbell, 1991 b). Dystrophin is therefore a major component of the membrane cytoskeleton.

In the light of the apparent instability of the dystrophic membrane; the high sequence homology between dystrophin and spectrin; the similar subplasmalemmal localisation of dystrophin and spectrin; and the proven importance of spectrin to restriction of membrane protein lateral mobility, the first set of experiments presented in this thesis measured the capacity of dystrophin to regulate membrane protein mobility through formation of a submembranous 'molecular fence' (chapter 4). Such regulation is by nature non-specific- a molecular fence barrier sterically restricts protein diffusion according to size but not by functionality. Additionally, the membrane molecular fence is not impermeable. Though the physical barrier may restrict protein diffusion, variations in distance from the membrane to the cytoskeleton together with breaks in the cytoskeletal lattice can allow the occasional passage of otherwise hindered proteins through the membrane. Restriction of proteins is therefore subject to some fluctuation.

To monitor the role of dystrophin as a steric and non-specific regulator of membrane protein lateral diffusion as part of a cytoskeletal 'molecular fence' the lateral mobility of membrane surface glycoproteins was compared in both normal and dystrophic muscle tissue. Mobility measurements were obtained by FPR, using fluorescent lectins as non-specific markers of membrane surface glycoproteins.

1.7.2 Dystrophin as an organiser/anchor of specific membrane proteins.

The final part of this study investigated the ability of dystrophin to regulate distribution of two membrane proteins which dystrophin is known to either bind to or closely associate with *in vivo*- i.e. to specifically regulate lateral mobility of membrane glycoproteins by tethering or crowding mechanisms.

As outlined above, as an alternative to the indirect mode of segregation by a membrane skeleton fence, proteins may be held in place by direct binding to underlying cytoskeletal constituents. Binding of band 3 protein to the spectrin binding protein ankyrin links band 3 to the spectrin cytoskeleton. Once bound to ankyrin/spectrin the band 3 is unable to diffuse laterally in the plane of the membrane or undergo rotational movement (Tsuiji *et al*, 1988). Proteins undergoing confined diffusion may slowly traverse the membrane by intercompartmental hopping. Tethered proteins on the other hand are bound at their tethered site (unless the binding affinity for protein and cytoskeletal tether is weak enough to permit dissociation). The tethering mechanism is therefore particularly important for cell- cell communication, where localisation of receptors at the site of signal transduction is essential for effective information transfer.

Direct binding and anchoring of proteins to the spectrin based cytoskeleton is required for efficient action potential propagation in the central and peripheral nervous systems. Localisation of neuronal sodium channels involves both ankyrin and spectrin. An Ankyrin $_G$ isoform is found at the nodes of Ranvier in the central nervous system, suggesting it could interact with NaChs and spectrin to immobilise the channels at the node (Kordeli *et al*, 1995). Brain ankyrin immobilises sodium channels by binding directly to their cytoplasmic domain and linking the channel to the underlying spectrin cytoskeletal network (Srinivasan *et al*, 1988). The ankyrin binding is of high affinity and stoichiometric. It is also sodium channel specific, neither GABA receptors nor DHP receptors co-immunoprecipitated with anti-ankyrin antibodies. Once the NaChs were bound to ankyrin, their rotational and lateral diffusion was restricted. The linkage of sodium channels to the cytoskeleton in neuronal tissue has the potential to either stabilise the channels after assembly of the subunits and/or to place the channels at the nodes of Ranvier and axon hillock.

1.7.2 a) Dystrophin and regulation of DAG complex mobility.

As discussed in section 1.1.5, dystrophin binds the DAG complex at the plasma membrane of skeletal muscle (figure 1.3). Despite considerable work to illustrate the subcellular locations of, and associations between, dystrophin and the DAGs, the role of this complex in muscle function is unclear. Specific dystrophin mediated immobilisation of the DAGs would localise the DAG complex to a fixed site on the membrane.

Membrane immobilisation of the DAGs by dystrophin has implications for function of the complex. Immobilisation of the DAGs would preventing their internalisation, and may account for the reduction in DAG levels in DMD. Complex immobility lends weight to the modulation of shear stress theory for dystrophin function, as the relative positions of contractile apparatus and muscle membrane would be maintained following contraction. Furthermore, cross linkage of membrane proteins can give rise to an increase in cell rigidity- binding of a monoclonal antibody to glycophorin A induces immobilisation of the glycophorin in the red blood cell membrane and an increase in the rigidity of the cell surface (Knowles *et al*, 1994). Cross linking of the DAGs could therefore be important for muscle cell rigidity. Finally, given the large size of the DAG complex, restriction of DAG complex mobility would hinder lateral mobility of other membrane proteins through crowding effects.

In order to quantify the ability of dystrophin to bind directly to the DAGs and immobilise them on the muscle cell surface, mobility of the DAGs was followed by FPR. Considering the tight associations between adhalin and the other DAGs, mobility of adhalin was measured and taken to be representative of the DAG complex as a whole.

1.7.2 b) Dystrophin and regulation of sodium channel lateral mobility.

The function of dystrophin at the NMJ is presently unknown. Dystrophin is found at the depths of the folds of NMJs in skeletal muscle fibres, alongside NaChs and β-spectrin. The importance of spectrin for immobilisation of sodium channels in the central and peripheral nervous system is well established. Dystrophin shows homology to spectrin both in terms of gene/protein sequence and subcellular localisation. A direct link between dystrophin and NaCh localisation is yet to be proven, but it is possible that dystrophin is localising ion channels, directly or indirectly, by maintaining structural domains within the membrane. Domains could require binding to NaChs, or restriction of NaCh mobility through crowding effects of the DAG. Formation of the domains may stabilise the folding of the membrane at the NMJ (considering the reduced folding in mdx mice).

Since this project was started, reports suggest β-spectrin precisely co-localises with NaChs in the NMJ and dystrophin does not (Wood and Slater, 1998). Nevertheless, dystrophin may still be important for reinforcing the β-spectrin cytoskeleton and/or stabilising NaCh clusters at the NMJ, or for creating a boundary domain at the edge of the junction. Such roles may still influence sodium channel lateral mobility and organisation.

The question was therefore asked whether dystrophin specifically associates with muscle-specific voltage gated sodium channels and immobilises them in place at the NMJ, just as β-spectrin specifically immobilises the sodium channels of the nervous system.

1.7.2 c) Measuring specific dystrophin-membrane protein interactions.

The most informative method of monitoring the mode of diffusion/vibration of anchored and closely confined proteins would be SPT. The size of bleach spot in FPR is such that distinctions can be drawn between 'mobile' and 'immobile' with respect to macro scale motion in an area significantly greater than the bleached spot (i.e. over the whole cell surface), but rotation about a fixed point in an area smaller than the bleach spot cannot be resolved. SPT on the other hand would distinguish between proteins undergoing free Brownian diffusion in a small confined domain and a protein rotating around a fixed axis. For the sake of this study the FPR approach is adequate to distinguish whether specific proteins are or are not tethered/restricted in the presence of dystrophin, as untethered proteins are expected to undergo free diffusion on a macro scale.

The ability of dystrophin to maintain the structural integrity of the muscle fibre membrane by associating specifically with membrane proteins of the DAG/NMJ and anchoring the proteins in place on the membrane, was measured by comparing the lateral mobilities of the proteins in normal and dystrophic tissue by FPR. Fluorescent markers to adhalin and the muscle voltage gated NaCh are not available commercially, therefore specific FPR probes had to be generated before dystrophin-imposed restrictions on lateral mobility could be quantified (chapter 5).

Chapter 2.

Materials and Methods.

Chapter 2.

Materials and Methods.

2.1 Materials.

The anti-dystrophin antibody MANDYS-1 was a gift from Prof. G.E. Morris, MRIC, North East Wales Institute, Wrexham, UK. The anti-adhalin antibody Ad1/20A6 was a gift from Dr L.V.B. Anderson, Dept of Neurobiology, University of Newcastle Upon Tyne. Anti-rat brain spectrin antibodies were a gift of Eun-Hye Joe, Baylor College of Medicine, Houston, Texas, U.S.A.

BODIPY Fl conjugates were purchased from Molecular Probes; μ-Conotoxin GIIIB came from Alomone Labs, (Jerusalem, Israel); fluorescent polyclonal goat anti-rabbit antibodies were from Kirkegaard and Perry Laboratories (Gaithersburg, MD, USA); resin immobilised MAP peptides came from Genosys, (Cambridge, UK); Nitrocellulose membranes and Enhanced Chemiluminescence (ECL) reagents from Amersham; Tissue-Tek OCT compound from Sakura Finetek; (U.S.A.), Titremax Gold from Stratech Scientific (Bedford, UK). All other reagents were purchased from Sigma or BDH. All chemicals were of analytical or molecular biology grade.

2.2 Solutions.

Antibody dilution buffer

1mg/ml Bovine serum albumin
10% heat inactivated goat serum
0.5% TRITON-X100
in PBS/sucrose.

Coomassie blue protein gel -stain

MeOH:H_2O (1:1 v/v)
10% glacial acetic acid (v/v)
0.25% coomassie brilliant blue (w/v).

Coomassie blue protein gel -destain

MeOH:H_2O (1:1 v/v)
10% glacial acetic acid (v/v).

Gelatine slide coating solution

0.5% gelatine (w/v)

0.05% Chromium (III) potassium sulphate (w/v), in distilled water.

Krebs' buffer

119mM NaCl

25mM $NaHCO_3$

11mM glucose

4.7mM KCl

2.5mM $CaCl_2.2H_2O$

1.2mM KH_2PO_4

1.2mM $MgSO_4.7H_2O$.

PBS

137mM NaCl

8.5mM $NaH_2PO_4.12H_2O$

1.5mM KH_2PO_4

2.7mM KCl

PBS/Sucrose

PBS plus 35mM sucrose.

PBS-Tween

PBS plus 0.1% Tween 20.

2x Protein gel loading buffer

100mM Tris-Cl pH6.8

200mM dithiothreitol

4% SDS (w/v)

0.2% bromophenol blue (w/v)

20% glycerol (v/v).

5% β mercaptoethanol (v/v).

Protein extraction buffer

0.1M NaCl, 10mM

Tris-Cl pH 7.6

1mM EDTA pH8

1μg/ml aprotinin

1μg/ml pepstatin

1µg/ml leupeptin

100µg/ml PMSF.

Resolving polyacrylamide gel

4.5% or 7.5% acrylamide/bis-acrylamide (w/v)

0.1%SDS (w/v)

0.07% ammonium persulphate (w/v)

0.375M Tris HCl pH 8.8.

Stacking gel

3% or 5% acrylamide/bis-acrylamide (w/v)

0.1%SDS (w/v)

0.07% ammonium persulphate (w/v)

0.125M Tris HCl pH6.9.

Gels were polymerised with 1µl TEMED/ml gel.

Tris glycine protein gel running buffer

25mM Tris base

250mM glycine pH 8.3

0.1% SDS (w/v).

Western transfer buffer

48mM Tris base

39mM glycine

0.037% SDS (w/v)

20% MeOH (v/v).

Methods.

General molecular biological methods were performed as described in Sambrook *et al*, (1989).

2.3 Immunisation of rabbits.

New Zealand White Rabbits were immunised following a modification of Butz *et al*, (1994). One rabbit was exposed to the mid regional peptide alone (DURD M), one to just the c-terminal peptide (DURD C) and a third to an equal concentration of both the mid regional and c-terminal peptides simultaneously (DURD M/C).

For initial immunisation and intermediate boosts, 500 µg of 17mer peptide MAP beads were suspended in 300µl deionised water, briefly sonicated until cloudy[1], then emulsified with a 1:1 (vol/vol) ratio of Titremax gold. 200µl of suspension was injected intramuscularly into each hind limb, and the remainder injected subcutaneously. Boosts were at ~4 week intervals (three boosts for DURD C and two for DURD M and DURD M/C antibodies). Final boosts were as above, but with a 2:1:1 ratio of peptide/deionised water: Titremax gold: Freunds complete adjuvant[2]. Exsanguination was from a marginal ear vein, followed by cardiac puncture.

Serum isolation followed the protocol in Harlow and Lane (1988a). Briefly, blood was clotted at 37°C for 1 hour. The clot was 'ringed' with a pipette, then left at 4°C overnight to contract. Serum was removed by centrifugation at 10,000g for 10 minutes at 4°C and stored at 4°C in the presence of 0.02% sodium azide.

2.4 Immunohistochemistry.

Hind limb muscles were removed from adult animals and cryofrozen in Tissue-Tek OCT compound at -196°C. The tissue was cut into 8µm sections using a cryostat and placed onto gelatine coated slides. The sections were washed several times with PBS/sucrose and blocked for 30 minutes with 10% heat inactivated goat serum. Sections were incubated for an hour with 1/75 anti-dystrophin, and 1/50 anti-

[1] Sonication is essential to crack the resin beads and so increase the surface area of exposed immobilised peptide.

[2] Whilst the sole use of Titre-max gold is safer for the animal, this adjuvant alone failed to raise sufficient titre of antibodies. Freunds Complete Adjuvant was therefore added to the final immunisation. The short time (4 weeks) between Freunds immunisation and exsanguination prevented formation of granulomas, and no subcutaneous irritation was observed. The Titre-max gold was adequate for initial sensitisation and boosts of the animal. This procedure, using Freunds Complete adjuvant in the final immunisation, is in accordance with Home Office Guidelines and would be recommended for future production of antibodies.

rat brain spectrin (fodrin) rabbit polyclonal antibodies (Vybiral *et al*, 1992) diluted in antibody dilution buffer. All slides were washed with PBS/sucrose then stained for 1hour with 1/100 fluorescein conjugated polyclonal goat anti-rabbit antibodies. After washing, slides were visualised and photographed under a MicroRadiance confocal microscope (Bio-Rad) using a 50x oil immersion objective, 488nm excitation light and 500nm longpass filter.

2.4.1 Gelatine coating of slides.

Glass microscope slides were flamed in ethanol, then soaked in 0.5% gelatine (w/v), 0.05% Chromium (III) potassium sulphate (w/v) solution in distilled water for five minutes. Excess solution was poured off and slides dried at 37°C overnight.

2.4.2 Human muscle tissue.

Human skeletal muscle was obtained during routine hip joint replacement surgery at the Middlesborough General Hospital, Middlesborough, UK. The procedure was approved by the University of Durham Ethical Advisory Committee and the Medical Director of South Tees Acute Hospitals NHS Trust. Samples were embedded in Tissue-Tek OCT compound in dry-ice cooled isopentane immediately after removal, then stored at -80°C.

2.5 Protein analysis.

2.5.1 SDS Polyacrylamide gel electrophoresis.

SDS polyacrylamide gel separation of proteins was performed according to the method of Sambrook *et al*, (1989) in a Bio-Rad Mini Protean II apparatus. The equipment was assembled and run according to manufacturers instructions.

Resolving gels were made from either 4.5% (dystrophin gels) or 7.5% (lower molecular weight proteins) acrylamide/bis-acrylamide depending on protein size. Likewise, stacking gels were made from either 3% (dystrophin gels) or 5%(lower molecular weight proteins) acrylamide/bis-acrylamide. Gels were polymerised with 1µl TEMED/ml gel. Proteins were boiled for 5min in an equal volume of 2x protein gel loading buffer then spun at top speed in a microfuge for 2 min before loading. Gels were run in tris-glycine running buffer for 30min at 60 volts than 1-2 hours at 100 volts.

2.5.2 Dystrophin protein extraction.

Hind limb skeletal muscle was removed from adult mice and homogenised with a Polytron homogeniser in 1:1 ratio of protein extraction buffer: SDS PAGE loading buffer. 4μg of protein/lane was run on a 4% polyacrylamide gel. Proteins were transferred to a nitrocellulose membrane over 2 ½ hours in western transfer buffer at 20volts and 4°C.

2.5.3 Coomassie blue staining of proteins.

Gels were simultaneously fixed and stained by shaking overnight in a minimum 5 gel volumes methanol:water (1:1 v/v), 10% glacial acetic acid (v/v), 0.25% coomassie brilliant blue (w/v). Proteins were visualised by destaining for 4-8 hours in 3 changes of 5 volumes methanol:water (1:1 v/v), 10% glacial acetic acid (v/v).

2.5.4 Transfer of proteins to nitrocellulose filters.

Following SDS PAGE separation, proteins were transferred to nitrocellulose membrane using a Bio-Rad Trans-blot SD semi-dry transfer cell. Gel, membrane and filter paper were soaked in western transfer buffer then assembled in the apparatus. High molecular weight proteins were transferred at 20 volts for 2-3 hours at 4°C, lower molecular weight for 40 min at room temperature.

2.5.5 Ponceau S staining of proteins on Nitrocellulose filters.

To confirm adequate and even transfer of proteins, Bio-Rad Mini Protean II gel sized nitrocellulose filters were incubated for 15min in 5ml 0.2% Ponceau S in 3%TCA whilst shaking, until filters were uniformly stained red. Filters were destained in 3 changes of 30ml distilled, de-ionised water.

2.5.6 Western analysis.

Filters were blocked for an hour in 5% non-fat milk / PBS-Tween then left for two hours in primary antibodies diluted 1/35 in 5% non-fat milk / PBS-Tween. Filters were washed three times for 5 min in 5% non-fat milk / PBS-Tween, then incubated with a 1/2000 dilution of horseradish peroxidase conjugated secondary antibody in 5% non-fat milk / PBS-Tween for 1 hour. Filters were washed twice for five minutes in PBS-Tween, then three times in deionised water. Proteins were visualised using enhanced chemiluminescence (ECL) reagents.

2.5.7 Coupling of dystrophin peptides to BSA.

Peptides were coupled to BSA using a modification of Harlow and Lane (1988 b). 1mg linear peptide was added to 3mg BSA in a total volume of 2ml PBS. An equal volume of 0.1% glutaraldehyde in PBS was added slowly whilst shaking, and the reaction left shaking for 2hrs. 1M glycine, pH7.2 was added to 200mM final concentration and the pH brought to neutral with 2M NaOH. The reaction was left for one hour, then dialysed overnight at 4°C against 3 changes of PBS.

For SDS PAGE, ~2.5μg linear peptide/BSA was loaded per lane with an equal volume of SDS gel loading buffer and run on a 7.5% polyacrylamide gel. 120μg BSA was run alongside in the control lane. Proteins were transferred to a nitrocellulose filter for 45mins at room temperature.

2.6 Fluorescence recovery after photobleaching (FPR).

2.6.1 Dissection.

12-18 month old adult male mice were sacrificed by cervical dislocation according to Home Office guidelines. The calf muscle was removed and teased apart in Krebs' buffer freshly perfused with 95% oxygen/5%CO_2.

2.6.2 Tissue labelling.

2.6.2 a) Labelling of muscle membrane glycoproteins.

The fibres were washed in Krebs and incubated with 25nmol fluorescein isothiocyanate (FITC) conjugated lectin for 25 minutes in the dark.

2.6.2 b) Labelling of membrane lipids.

The fibres were washed well in oxygenated Krebs buffer and labelled for 15 minutes in the dark with a 1:1 ratio of oxygenated Krebs buffer: 3.5μM 5-(N-octa-decanoyl) aminofluorescein (ODAF) in 1% ethanol/oxygenated Krebs buffer (w/v).

The fibres were washed well after labelling, transferred to a petri dish of freshly oxygenated Krebs buffer and held in place with Blu-tack.

2.6.3 Photobleach recovery.

The mobility of fibre surface components was measured using the spot photobleaching technique. The apparatus is illustrated in figure 2.1. A Zeiss Universal fluorescence microscope was used with a 63x, 1.2 NA water immersion lens placed directly into the dish containing the fibre (Angelides *et al* 1988). The monitoring argon-ion laser (Coherent Innova 90. 488nm, 5W) was focused through the microscope to a beam radius of 0.85μm. An 80msec, 5mW laser pulse was used to bleach approximately 70% of the fluorescence, and the attenuated monitoring beam used to monitor the time course of the recovery. Photon counting was done using a photomultiplier tube (PMT). (Products for research, Inc, St Danvers, MA, USA.) and modified IBM-XT PC. Following photobleaching the fibres were photographed under a Nikon fluorescence microscope.

Non-ambient temperature data was obtained by heating the stage of the microscope by conduction. A brass heat block coupled to a 70°C circulating water bath was placed on the microscope stage at least 1 hour before data collection (figure 2.1 d). The sample was placed in a glass petri dish on a glass slide on the stage, adjacent to the heating device. Circulating water was switched off during data collection to minimise vibrations. Heat loss was reduced by surrounding the equipment in bubble wrap.

2.6.4 Analysis, terminology and interpretation of FPR data.

Diffusion coefficients (D_L) and the mobile fractions (f) were determined by curve fitting procedures (Axelrod 1983). D_L was determined in cm^2 /s from $D_L = w^2 / 4T_D$ where T_D is the half time for recovery and w is the e^{-2} beam radius. (The e^{-2} radius relates diffusion to the size of bleached circle. This value is used in preference to πr^2, as the intensity of the laser light across the circular bleached region is gaussian in distribution i.e. the laser is brighter in the middle of the spot than it is towards the edges. The e^{-2} radius is therefore smaller than the total area of the laser beam, encompasing ~95% of the total. For the 63x water immersion objective used in these experiments with a 0.85μm beam radius, the e^{-2} value corresponds to a bleached area of ~2μm^2). To reduce the significance of fibre-fibre variations a number of measurements (>10) were taken for each fluorophore. The diffusion time T_D and the degree of fluorescence recovery, *f*, were obtained for each FPR curve. Results were analysed statistically to obtain the mean values and standard deviation of *f*, D_L and T_D. Values are given in the tables, figures and text with the standard error of the mean.

The word 'significant' is applied to the FPR data with respect to changes in FPR mobility patterns and not in a statistical sense. For example, the difference between 4 ± 1 % and 7 ± 1.5% mobile fractions may be 'significantly different' statistically. However, in terms of FPR, all mobility with <15% recovery of fluorescence is classed as 'immobile'. Therefore, the difference between 4% and 7% is not 'significant' here as the molecules are immobile in both cases. A 'significant' change in mobility

patterns would be from 5/10% mobility up to 20% or higher. For example, the lateral mobility characteristics of free β_3 subunits of $GABA_A$ receptors on the surface of Cos 7 cells are: D, 18.9 ± 3 $x10^{-10}$ cm^2s^{-1}, f, $43 \pm 13\%$. When the α_1 subunit is present, there is a 'significant' reduction in mobility of the β_3 subunit: D, 1.3 ± 0.4 $x10^{-10}$ cm^2s^{-1}, f, $8 \pm 4\%$ (Peran *et al*, submitted).

In cases where the mobile fraction is low (<15%), the accuracy of curve fitting is compromised. The mathematical algorithms used during data analysis fit the observed recovery curves to the diffusion equation, $D_L = w^2 / 4T_D$. When recovery is small, the 'curves' are flat lines (e.g. figure, 4.4). The curves therefore do not accurately fit the diffusion equation ($\chi^2 > 1x10^{-4}$, and the values of D_L have large errors.

Figure 2.1 FPR equipment. (q.v. figure 1.4)

a) Water cooled argon ion laser light is reflected by mirrors towards the beam splitters.
b) Beam splitting apparatus. From left to right, diaphragm, prism 1, bleach shutter, prism 2 and mirror. The prisms and bleach shutter direct either the full intensity bleaching laser beam (shutter open) or the 10,000 fold attenuated monitoring beam (reflected light from the prism glass/air interfaces only, shutter closed) towards the sample. The mirror sends the light path towards the beam steerer (B.S.) which then directs the beam into the side of the microscope.
c) Microscope and photon counting apparatus. Light directed by the beam steerer enters the microscope optics via a focusing lens and a dichroic mirror reflects the excitatory beam down towards the sample. Emitted fluorescent light passes up through the dichroic mirror and a series of longpass light filters within the microscope, cutting out the excitatory wavelength light and allowing the emitted light through into the photomultiplier tube (PMT).
d) Modified apparatus to increase measuring temperature. Circulating water from 70°C bath passes through the insulated pipes and heats the stage by conduction. Surrounding insulating bubble wrap removed for clarity.

Light paths are shown by red arrows.

a)

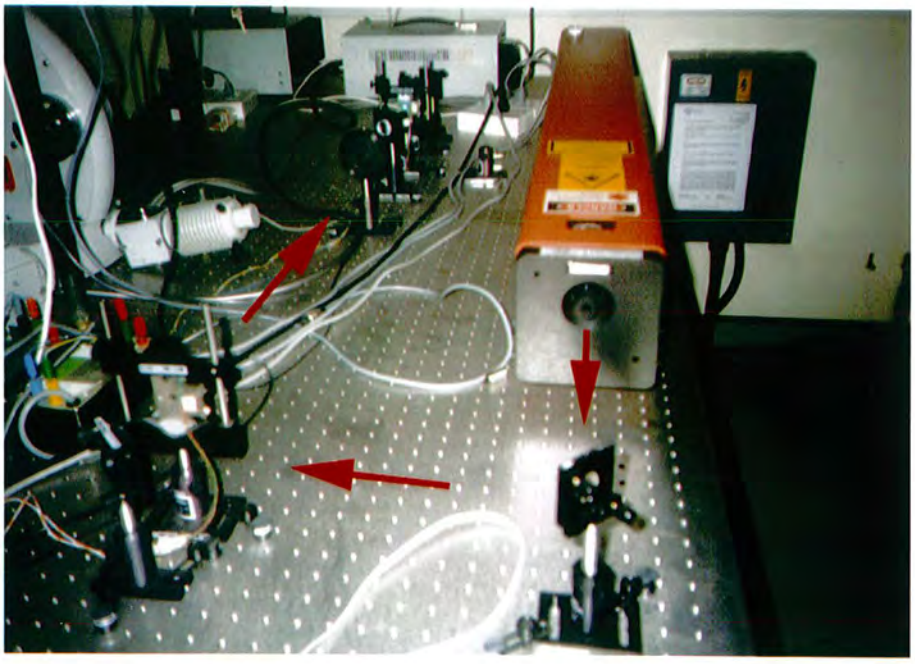

b)

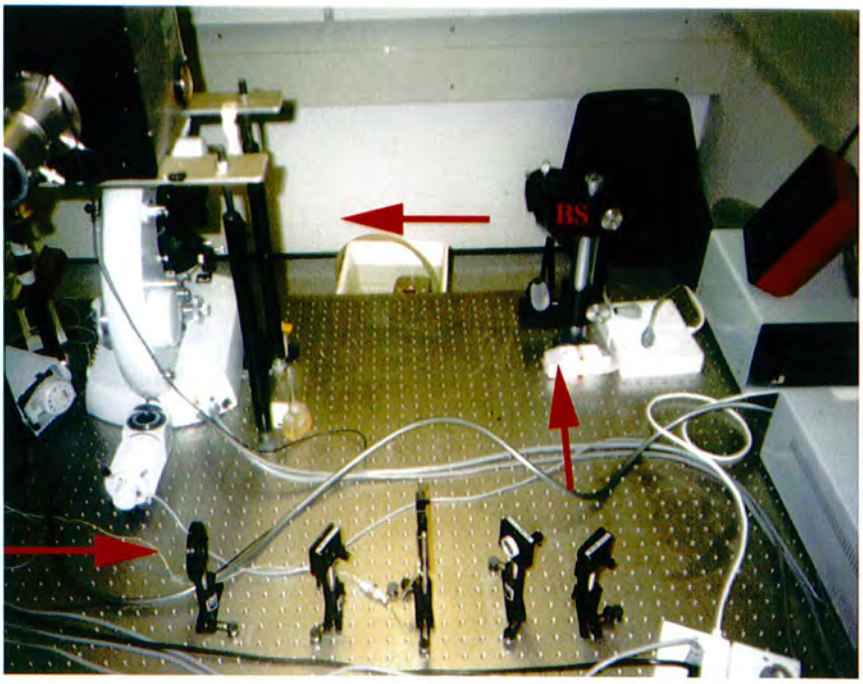

c)

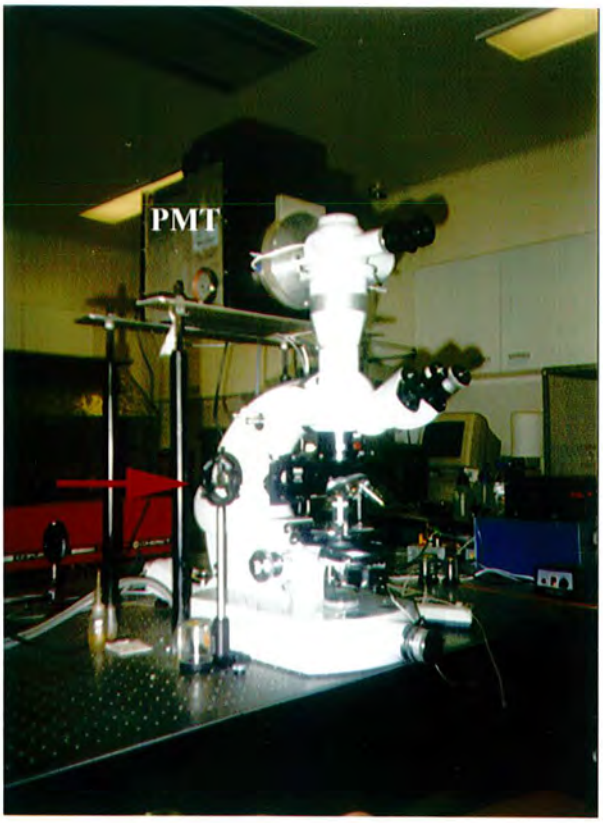

d)

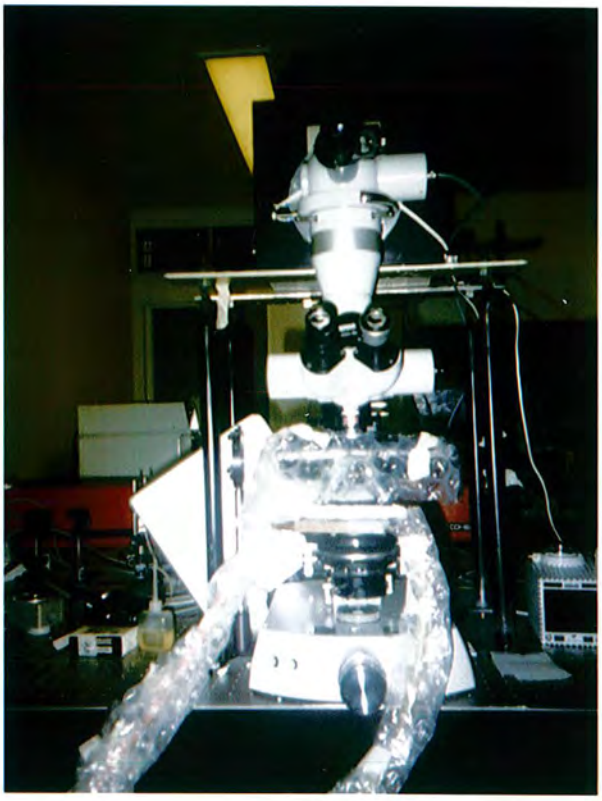

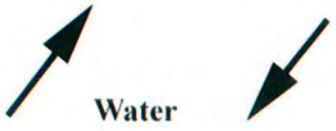

2.7 Synthesis of fluorescent probes for photobleach recovery.

2.7.1 Preparation of fluorescently labelled muscle sodium channel specific probe.

μ-conotoxin GIIIB was labelled with 4,4-difluoro-1,3,5,7-tetramethyl-4-bora-3a,4a-diaza-s-indacene-8-propionic acid, succinimidyl ester (BODIPY (Fl) -SE), using a modification of Joe and Angelides (1993) and protocol supplied on request from Molecular Probes. Reactions used a 2:1 molar ratio of amino groups to succinimidyl ester to maximise modification of the toxin.

19 nmol μ- conotoxin GIIIB was dissolved in 200μl 0.1M Na_2HCO_3 buffer, pH 9. 190 nmol BODIPY (Fl) SE was dissolved in 200μl DMSO, then added to the toxin and the reactants left for 1½-3 hours in the dark at room temperature, vortexing occasionally.

2.7.2 HPLC purification of products.

The labelled toxin was purified using C4, C18 and CN reverse-phase HPLC columns. The solvent system was solvent A: 5-95% (by volume) acetonitrile for 30 minutes, then 100% acetonitrile for 5 minutes. Solvent B: 0.1M TEAA (triethylammonium acetate) pH7. 100-200μl reaction mixture was added per HPLC run, depending upon the size of column loop. Products were monitored at 214 and 493nm using a SMART flow cell, 3mm path length, 0.7μl volume.

2.7.3 Gel purification of products.

A 1ml, 25cm long sephadex G10 column was made up in a 1ml disposable blow out plastic pipette and equilibrated prior to reactant addition with 4 column volumes of PBS. 300μl of μ-cgtx/BODIPY-SE reaction mixture was added to the top of the column. Fractions were eluted with PBS. 3 minute fractions were collected over 8 hours. Fractions were pooled into 9 minute aliquots and analysed spectroscopically at 514 and 260nm using a Pharmacia Biotech Ultrospec 2000 UV/visible spectrophotometer.

2.7.4 Fluorescent modification of anti-adhalin monoclonal antibody.

600μl of tissue culture supernatant, reconstituted from lyophilised form at 4x original concentration in mQ H_2O (equivalent to ~0.18mg IgG) was reacted with 60μg BODIPY-SE at 10mg/ml in DMSO. The pH of the mixture was adjusted to ≥ pH 8.5 and the mixture left for 4 hours at RTP in the dark.

Modified and unmodified antibody was separated from free dye by spinning the reaction mixture at 1000g for 15 seconds through a 2ml sephadex G10 column, assembled in the body of a disposable plastic syringe. The supernatant was collected and the dye (bound to the column) discarded.

Chapter 3.

Generation of Anti-dystrophin Antibodies.

Chapter 3.

Generation of anti-dystrophin antibodies.

3.1 Introduction.

In order to confirm the presence or absence of dystrophin within the experimental membranes, a reliable and unambiguous test for dystrophin was needed. Commercially available antibodies proved unsuitable for the task of immunohistochemical analysis of dystrophin protein. At present all commercially available antibodies to dystrophin are mouse monoclonal in origin. The need for anti-mouse secondary antibodies to visualise the monoclonals gave rise to high background signals on mouse tissue. The staining of the secondary antibodies appeared to be specific, forming rings around the outside of the mouse muscle fibres (data not shown). This cross reactivity may arise as a consequence of injecting crude mouse serum into a goat to generate the secondary antibody- due to the unrefined nature of the serum, the goat raises specific antibodies to a highly immunogenic serum component (possibly a fragment of extracellular matrix in origin), in addition to the mouse Ig. This component is then detected by the secondary antibody in samples of mouse tissue. Goat anti-mouse IgG $F(ab)_2$ fragment secondary antibodies were not specific enough to cut out the background. Blocking with unlabelled goat anti-mouse antibody as an alternative approach proved unreliable and non-reproducible (data not shown).

The apparent specificity of the background staining to components of the extracellular matrix, and the proximity of this staining to the site of dystrophin localisation rendered anti-mouse secondary antibody staining- and hence anti-dystrophin mouse monoclonal antibodies- uninterpretable and unsuitable for the determination of dystrophin in experimental mouse tissue. To enable a more accurate and reliable assignment of the dystrophic status of the tissue, rabbit polyclonal antibodies were generated.

The suitability of the synthesised antibodies for detection of dystrophin revertant fibres was revealed during their characterisation. This is discussed separately in part 2, following the characterisation data.

- **Part 1. Production and characterisation of anti-dystrophin peptide antibodies.**

3.1.1 Dystrophin MAP peptides.

As dystrophin protein is large, unstable and difficult to extract and purify, antibodies were raised against 17 amino acid long synthetic dystrophin peptides. To increase the surface area and secondary structural permutations of the peptides, resin-immobilised branched Multiple Antigen Presenting (MAP) peptides were synthesised. The peptides were injected in their native immobilised resin bead state to a) avoid the need for coupling to carrier peptides prior to injection and b) simplify the process of affinity purification if required- the peptide beads could be used directly in a column.

The two chosen peptides corresponded to amino acids 2371-2399 inclusive (mid-region) and 3619-3635 inclusive (at the c-terminal region) of human skeletal muscle dystrophin. This is equivalent to amino acids 2367-2392 (mid) and 3613-3629 (c-terminal) of the murine sequence, with just one amino acid change in the mouse mid regional sequence, shown in figure 3.1 below. These regions show high conservation between species, but little homology to utrophin, spectrin or other characterised proteins. Regions of the C-terminal peptide showing sequence conservation with utrophin are shown beneath the mouse peptide sequence. There was no significant dystrophin/utrophin homology for the mid region peptide. Peptides were chosen primarily on the basis of their uniqueness to dystrophin, so that any potential cross reactivity could be limited. Additionally, the presence of proline residues within the sequence was chosen to provide some secondary structure.

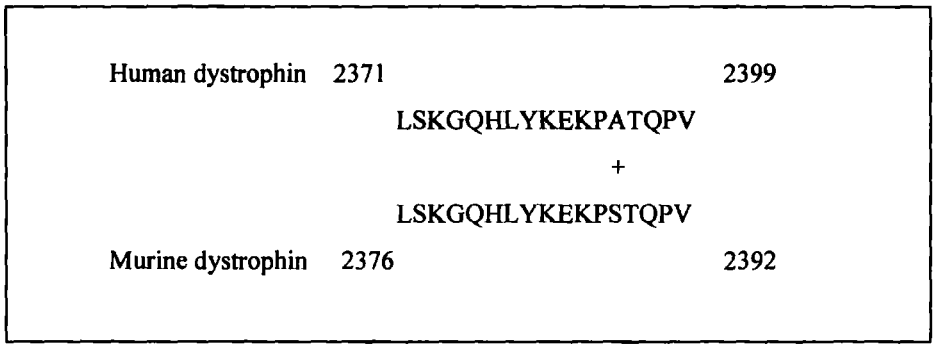

a) Dystrophin mid-region MAP peptide, DURD M.

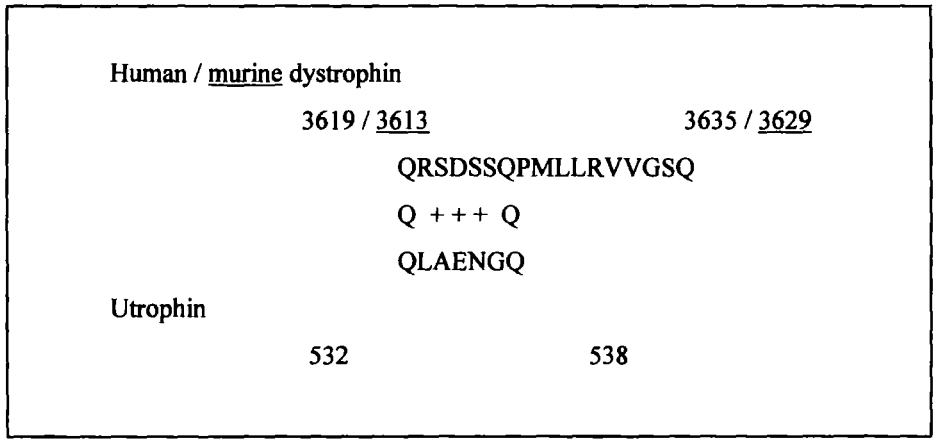

b) Dystrophin C-terminal MAP peptide, DURD C.

Figure 3.1. 17mer MAP Peptide sequences used to generate antibodies to a) the mid region, DURD M and b) the C-terminus, DURD C, of skeletal muscle dystrophin.

The extent of utrophin homology is shown for the C-terminus. There was no significant utrophin homology in the mid region. + represents like-for like amino acid substitutions. Numbers correspond to amino acid residues as designated by SwissProt. Succession numbers: Human, sp|P11532|DMD_HUMAN DYSTROPHIN. Murine, sp|P11531|DMD_MOUSE DYSTROPHIN. Utrophin, gn1|PID|e303779.

Results.

3.2 Production of anti-dystrophin antibodies.

New Zealand White rabbits were injected intramuscularly and subcutaneously with 17mer peptides corresponding to amino acids 2371-2399 (mid-region, DURD M) and 3619-3635 (C-terminal region, DURD C) inclusive of the human dystrophin sequence. Rabbits were exposed to either one or both peptides.

3.3 Characterisation of antibodies.

The presence of antibodies in the sera was tested initially by immunohistochemistry on unfixed frozen skeletal muscle sections. To illustrate the location of the sub-sarcolemmal cytoskeleton, membrane integrity, section quality, and provide a positive staining control, sections were stained in parallel with anti-spectrin antibodies. This particular antibody was raised to an isoform of rat brain spectrin, also called fodrin (Vybiral *et al*, 1992). Although the epitope was neuronal in origin, the antibody detects spectrin within muscle. Staining for the spectrin isoform is documented at locations throughout the subsarcolemmal lattice, with particularly bright staining at costameres, sarcomeres and neuromuscular junctions (Vybiral *et al*, 1992).

3.3.1 Immunohistochemistry.

The DURD M, DURD C and DURD M/C antibodies all stain sections of C57/Bl control skeletal muscle tissue, figure 3.2. The location of staining was comparable with that found for rat brain spectrin i.e. the antibodies recognised an epitope found at the plasma membrane. The bright costameric staining of the spectrin antibodies was not repeated to the same intensity with the dystrophin antisera. Pre immune sera from the rabbits did not highlight the membranes. Staining was detected at up to 1/100 dilution of crude anti-sera, although optimal staining was obtained at a 1/75 dilution. No affinity purification was necessary for this application. The staining at the plasma membrane was, generally, evenly distributed as previously reported by Arahata *et al*, (1988) for skeletal muscle dystrophin.

No equivalent staining was observed on sections of mdx muscle. Staining of serial sections from the same mdx animals with the anti- rat brain spectrin antibodies produced bright signals at the plasma membranes. The lack of signal from the dystrophin antisera was therefore due to the absence of the protein epitope, rather than due to poor integrity of the membranes in the sections. This staining of C57/Bl 10 tissue but not mdx tissue, combined with the positive spectrin stain is consistent with production of antibodies to dystrophin.

Figure 3.2 Immunohistology of anti-dystrophin peptide antibodies.

3.2a. DURDC anti-dystrophin C-terminal peptide antibody immunoreactivity.

Immunohistochemistry of 8μm transverse sections of unfixed fast frozen quadriceps muscle with DURD C antibodies against dystrophin c-terminal peptide (1/75 dilution) and antibodies to rat brain spectrin (1/40 dilution) (Vybiral *et al*, 1992).

C57/bl- C57/Bl dystrophin positive mouse tissue, DURDC antibody;

C57/bl, Pre immune serum- C57/Bl dystrophin positive mouse tissue, DURDC antibody pre-immune serum.

Mdx mouse- mdx muscle, DURDC antibody.

mdx mouse-spectrin mdx muscle, anti-rat brain spectrin antibody.

human- human muscle, DURDC antibody.

rat- rat muscle, DURDC antibody.

The anti-dystrophin antibody can be seen to stain at the plasma membrane of C57/Bl mouse, human and rat muscle, but not mdx tissue. No immunoreactivity was seen from the rabbit serum prior to sensitisation (pre-immune serum). The absence of staining in mdx tissue reflects an absence of dystrophin, rather than proteolysis or poor tissue/cytoskeleton integrity, as sections from the same muscle stained clearly for the presence of spectrin. Scale bar 100μm.

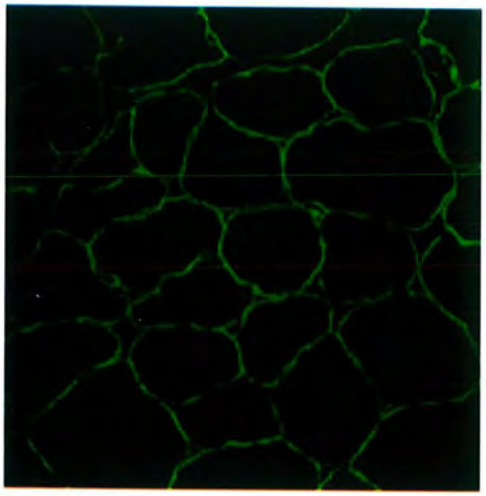

C 57/bl

C 57/bl, Pre immune serum

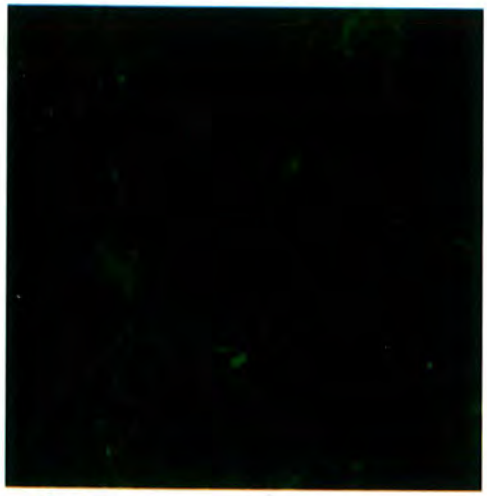

mdx mouse

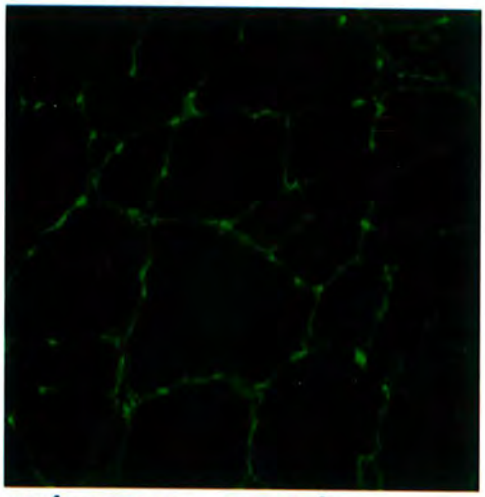

mdx mouse- spectrin

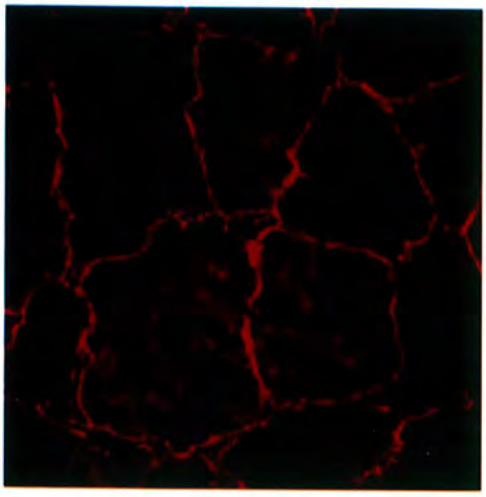

human

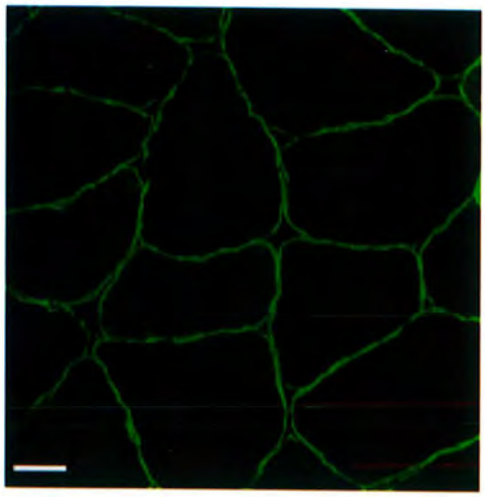

rat

Figure 3.2 b. DURD M anti-dystrophin mid regional peptide antibody immunoreactivity.

Immunohistochemistry of 8μm transverse sections of unfixed fast frozen quadriceps muscle with DURD M antibody against dystrophin mid-regional peptide (1/75 dilution) and antibody to rat brain spectrin (1/40 dilution) (Vybiral *et al*, 1992).

C57/Bl- C57/Bl dystrophin positive mouse tissue, DURDM antibody;

C57/Bl, Pre immune serum- C57/Bl dystrophin positive mouse tissue, DURDM antibody pre-immune serum.

Mdx mouse- mdx muscle, DURDM antibody.

mdx mouse-spectrin mdx muscle, anti-rat brain spectrin antibody.

human- human muscle, DURDM antibody.

rat- rat muscle, DURDM antibody.

The anti-dystrophin antibody can be seen to stain at the plasma membrane of C57/Bl mouse, human and rat muscle, but not mdx tissue. No immunoreactivity was seen from the rabbit serum prior to sensitisation (pre-immune serum). The absence of staining in mdx tissue reflects an absence of dystrophin, rather than proteolysis or poor tissue/cytoskeleton integrity, as sections from the same muscle stained clearly for the presence of spectrin. Scale bar 100μm.

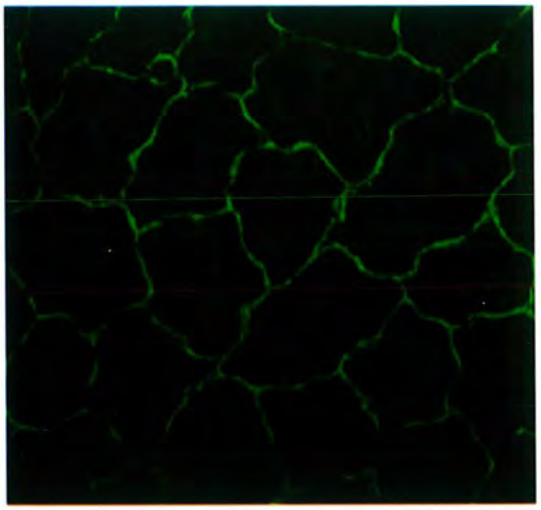

C57/B1

C57/B1, Pre-immune sera

mdx

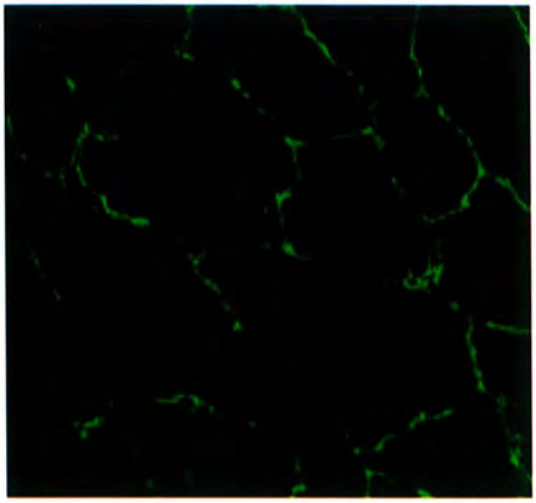

mdx- spectrin

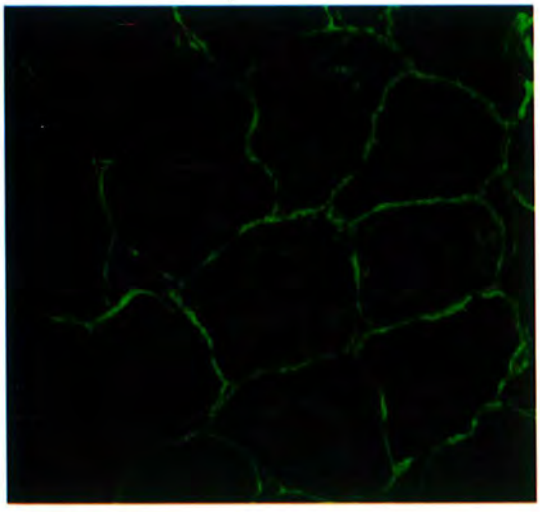

Human

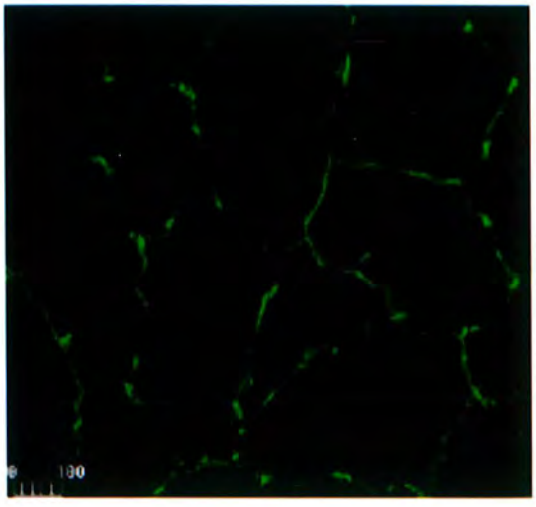

Rat

Figure 3.2 c. DURD M/C anti-dystrophin mid regional and C-terminal peptide antibody immunoreactivity.

Immunohistochemistry of 8μm transverse sections of unfixed fast frozen quadriceps muscle with DURD M/C antibody against both dystrophin mid-regional and C-terminal peptides (1/75 dilution) and antibodies to rat brain spectrin (1/40 dilution) (Vybiral *et al*, 1992).

C57/Bl- C57/Bl dystrophin positive mouse tissue, DURDM/C antibody;

C57/Bl, Pre immune serum- C57/Bl dystrophin positive mouse tissue, DURDM/C antibody pre-immune serum.

Mdx mouse- mdx muscle, DURDM/C antibody.

mdx mouse-spectrin mdx muscle, anti-rat brain spectrin antibody.

human- human muscle, DURDM/C antibody.

rat- rat muscle, DURDM/C antibody.

The anti-dystrophin antibody can be seen to stain at the plasma membrane of C57/Bl mouse, human and rat muscle, but not mdx tissue. No immunoreactivity was seen from the rabbit serum prior to sensitisation (pre-immune serum). The absence of staining in mdx tissue reflects an absence of dystrophin, rather than proteolysis or poor tissue/cytoskeleton integrity, as sections from the same muscle stained clearly for the presence of spectrin. Scale bar 100μm.

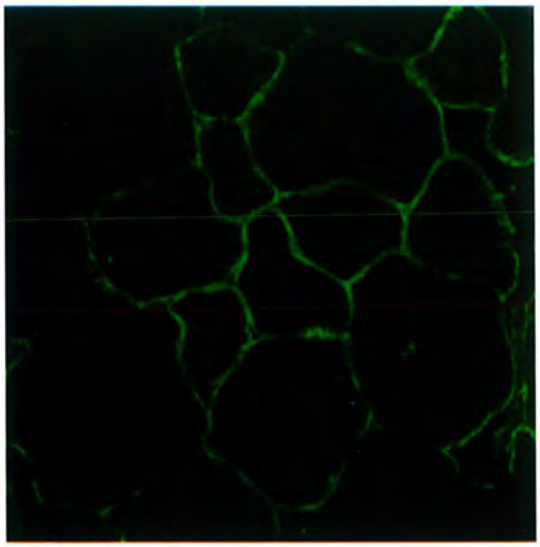

C57/Bl

C57/Bl, pre-immune serum

mdx

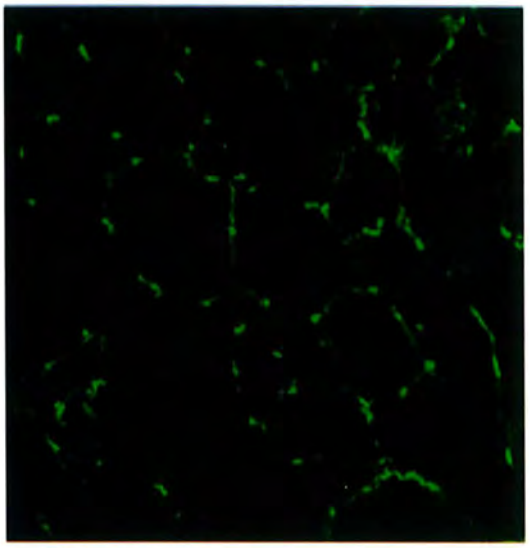

mdx, spectrin

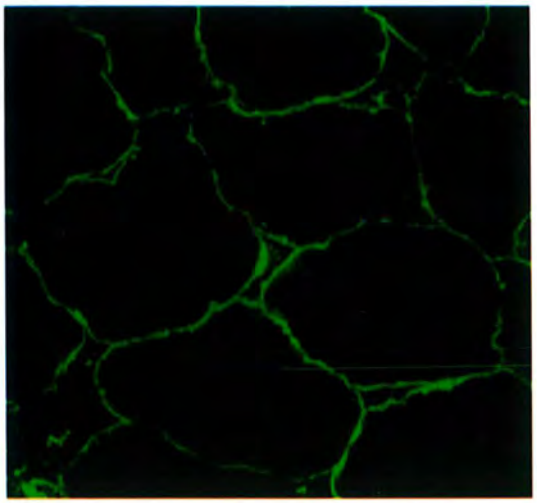

human

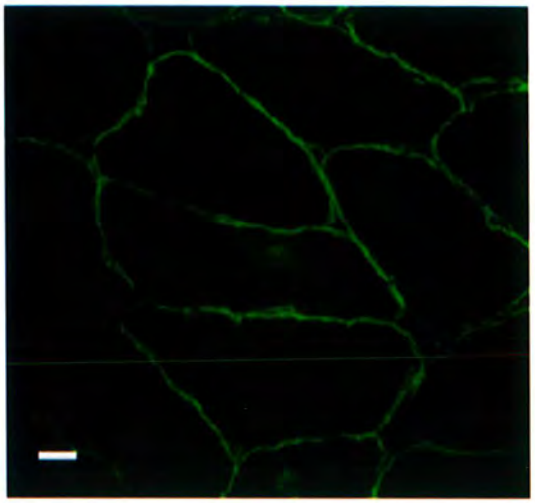

rat

In light of the highly conserved nature of dystrophin at the chosen peptide regions, the antibodies were tested for their additional ability to detect dystrophin in human and rat tissue. All three antibodies recognised a plasma membrane localised component of unfixed frozen transverse sections of human and rat skeletal muscle (figure 3.2). The subcellular site of immunoreactivity was comparable with the sub-plasmamembraenous location of spectrin staining in the same tissue (data not shown). The staining pattern was consistent with the observations of dystrophin staining in C57/Bl and mdx mice- suggesting all three antibodies are able to detect native skeletal muscle dystrophin in a range of species.

3.3.2 Skeletal muscle protein western blots.

The DURD M and DURD M/C antibodies detect a protein of ~400KDa on an immunoblot of C57/bl mouse quadriceps muscle proteins. There was no corresponding reactivity of mdx quadriceps muscle tissue. The immunogenic species appeared to have the same 427 kDa molecular weight as dystrophin, as seen by immunobloting the adjacent lanes with MANDYS-1 (gift from Prof. G.E.Morris, NEWI), a mouse monoclonal antibody to exons 31 and 32 of the dystrophin gene (Nguyen thi Man and Morris, 1993), (figure 3.3).

The DURD C antibody did not detect the same ~400kDa species as the DURD M and DURD M/C antibodies on an immunoblot. This could be a consequence of proteolysis. The epitope is at the extreme C- terminus and may therefore be particularly susceptible to proteolytic cleavage. The DURD C antibody did detect a protein of ~140kDa in C57/bl muscle tissue extracts that was absent from mdx muscle. This 140kDa species could be the proteolytically cleaved C-terminus of dystrophin. On the other hand, it could be that the C-terminal epitope is no longer recognisable in the SDS denatured form of dystrophin protein. Cytoskeletal proteins are particularly prone to this phenomenon- their native structures are susceptible to disruption by SDS, possibly reflecting the importance of polar residues in cytoskeletal constituents (H. Epstein, personal communication).

The immunohistochemical data and skeletal muscle extract immunoblot show the antibodies to recognise a species present in C57/bl control mouse but not mdx mouse skeletal muscle tissue. Furthermore, the immunoblot data suggests the detected molecule is of approximately 427kDa molecular weight- the accepted size of dystrophin (Hoffman *et al*, 1987). These data together support the assertion that the antibodies recognise dystrophin protein.

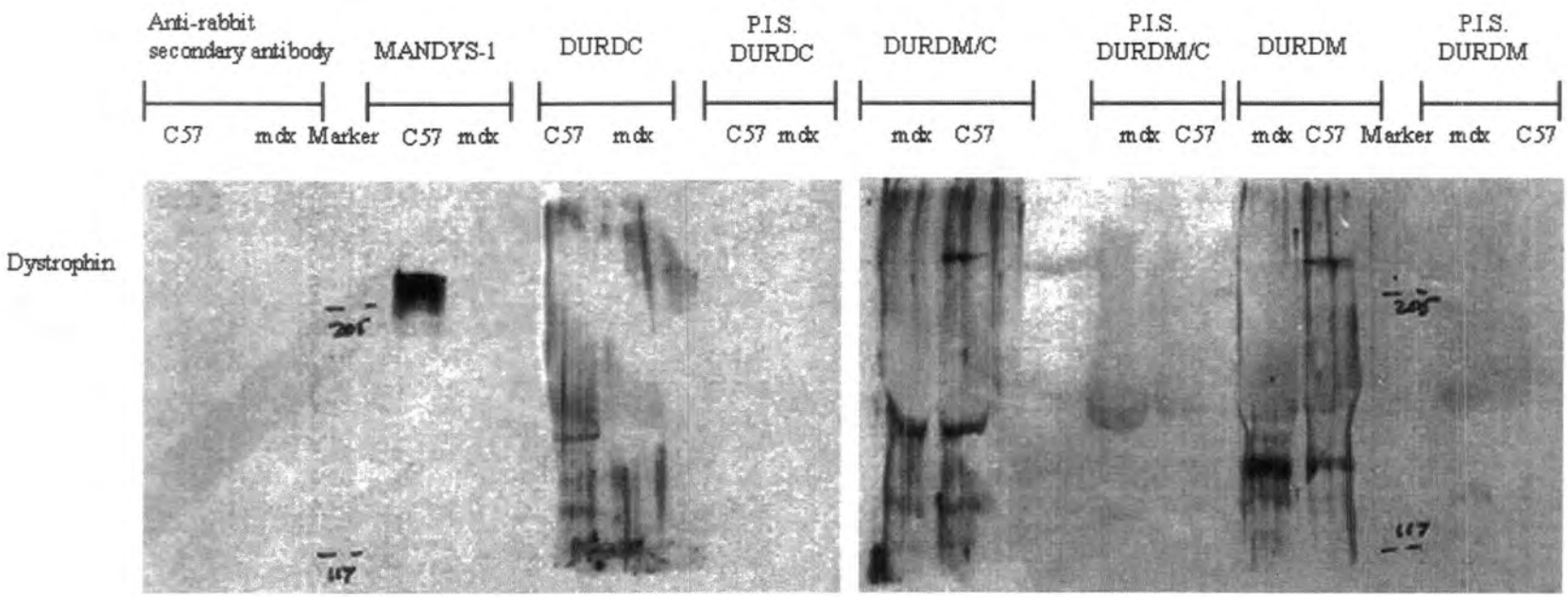
Anti-rabbit
secondary antibody
MANDYS-1
DURDC
P.I.S.
DURDC
DURDM/C
P.I.S.
DURDM/C
DURDM
P.I.S.
DURDM
C57 mdx Marker C57 mdx C57 mdx C57 mdx mdx C57 mdx C57 mdx C57 Marker mdx C57
Dystrophin
205
117
205
117

3.3.3 Anti-dystrophin peptide western blots

To confirm the epitope specificity of the antibodies, 2.5μg of linear dystrophin peptide coupled to BSA was run per lane on a 7.5% polyacrylamide gel. Each peptide was subjected to western analysis with the three anti-peptide antibodies. 120μg of BSA alone was run alongside to confirm that any observed immunoreactivity was due to the peptide component and not the BSA carrier molecule.

The DURD C peptide antibody recognises the 66kDa C-terminal peptide-BSA construct at a $1/60^{3}$dilution. There was no immunoreactivity to the mid-regional peptide-BSA construct. Immunoreactive species at 120, 180 and 240kDa are dystrophin C-terminal peptide coupled to two, three or four crosslinked BSA molecules, figure 3.4.

The DURD M antibody detected the mid-regional peptide-BSA construct at 1/60 dilution, but did not detect the dystrophin C-terminal peptide-BSA construct.

The DURD M/C antibody raised by co-injection of both the mid regional and C-terminal peptides recognised both BSA coupled peptides on a western blot. The immunoreactivity observed from this antibody on tissue sections is therefore a reflection of antibody binding to both regions of the dystrophin molecule. There was some observed difference in intensity between the chemiluminescence signals from the two peptide lanes. However, ponceau S staining of the filter suggested uneven loading of the different peptides was the primary cause of the discrepancies, rather than significant differences in epitope immunoreactivity (data not shown).

The three antibodies therefore bind exclusively to the peptide they were raised against and do not cross react with the other epitope.

---

3. In the cases of all three antibodies, the sensitivity of detection of native peptide is such that the antibodies could be used at far greater dilution than the 1/60 of this experiment. The film in figure 3.4 was exposed to the filter for just 3 seconds and was still over exposed.

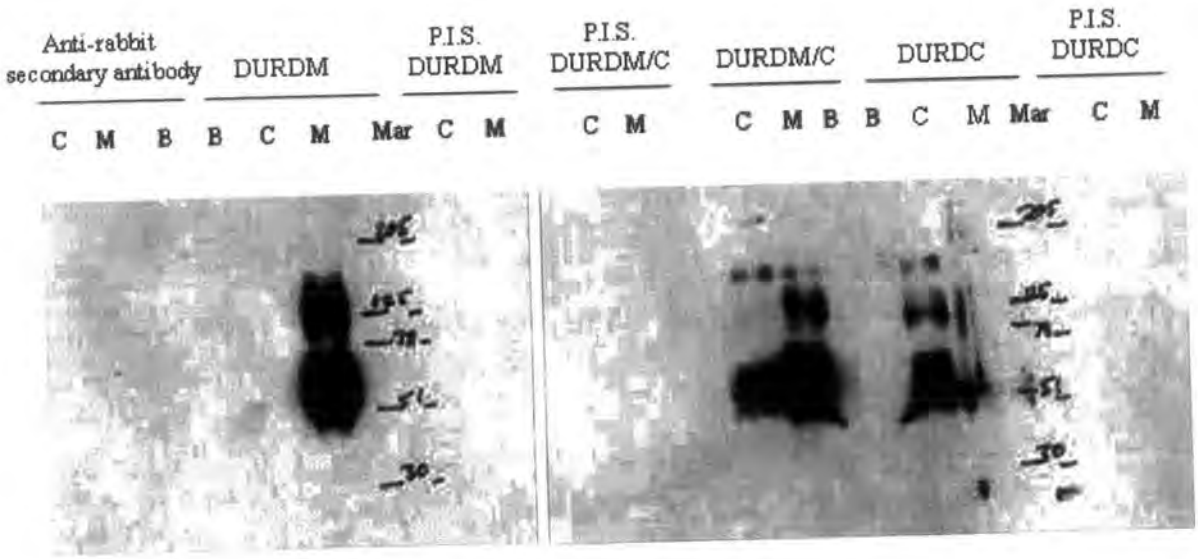

Figure 3.4. Immunoblot analysis of anti-dystrophin antibody epitope specificity.
7.5% SDS polyacrylamide gels of linear 17mer dystrophin peptides coupled to BSA carrier protein, western blotted and probed with 1/60 dilution of anti-dystrophin polyclonal antibodies. Mar, molecular weight markers in kDa, C, dystrophin c-terminal peptide, M, dystrophin mid-regional peptide, B, bovine serum albumin (BSA). For full sequence of peptides, q.v. figure 3.1

The DURD M antibody detects the mid regional peptide-BSA construct but shows no immunoreactivity towards either the c-terminal peptide construct or BSA alone. The antibody raised against the anti-dystrophin c-terminal peptide, DURD C, demonstrates immunoreactivity towards the c-terminal peptide alone, whilst the DURD M/C antibody recognises both epitopes. Note bands are observed at 66, 132, 198 and 264 kDa, corresponding to oligomers of BSA cross linked to the peptides. Pre-immune sera (P.I.S.) from the rabbits has no significant immunoreactivity at the same sera concentration; and no reactivity is observed from the horse radish peroxidase conjugated anti-rabbit secondary antibody alone.

3.4 Discussion, Part 1.

Generation of anti-dystrophin antibodies.

It has been shown by both immunohistochemistry and western blotting that three different rabbit polyclonal antibodies have been generated. The subsarcolemmal distribution, absence of immunoreactivity in mdx mice, and molecular weight of the detected species in skeletal muscle all suggest the antibodies recognise 427kDa skeletal muscle dystrophin. The antibodies specifically recognise the region of dystrophin that they were raised against- they do not cross react. Furthermore, the DURD M/C antibody raised against both the mid regional and c-terminal peptides recognises both epitopes equally, rather than one epitope preferentially.

The high affinity of the unpurified antibodies for dystrophin protein in mouse tissue, together with their rabbit polyclonal origin makes them a suitable tool for detection of dystrophin in mdx and C57/Bl experimental mouse tissue. The additional reactivity with human dystrophin may make them suitable for diagnostic as well as research use. Ideally to enable successful detection and analysis of dystrophin, antibodies should detect dystrophin protein in both the native and SDS denatured states. Both detection methods are currently used in the clinical diagnosis of DMD. The ability of the DURD C antibody to fulfil this function may therefore be limited. It is not uncommon for small peptide specific antibodies to be capable of detecting either native or SDS denatured protein, but not both forms e.g. as reported by Nguyen thi Man *et al*, (1992). This reflects the lack of sufficient secondary structural recognition that arises from using peptides.

3.5 Summary

The aim of this experiment was to generate anti-dystrophin polyclonal antibodies that could be used to determine the presence or absence of dystrophin in the experimental tissue from FPR mobility studies.

Three such antibodies have been raised, characterised and found to be dystrophin specific.

• Part 2. Dystrophin revertant fibres.

3.6 Immunoreactivity of anti-dystrophin peptide antibodies with revertant fibres.

In order to test the specificity of the anti-dystrophin peptide antibodies, transverse sections of mouse quadriceps muscle fibres were stained with the antisera. Negative staining was expected in mdx tissue, consistent with the accepted absence of dystrophin. It was observed firstly with DURD M/C that in some animals, fibres within the mdx background were staining strongly with the antisera. Initially this was attributed to an incomplete blocking step prior to primary antibody addition. Multiple repetitions with extended blocking steps made no detectable difference to the intensity of staining in these fibres and staining was observed with too great a frequency to be coincidental. The pre-immune sera from the same rabbits gave no signal, nor did secondary antibody alone. This suggested firstly that blocking had been successful and secondly the staining was a specific event following epitope recognition by the primary antibodies. The antibody was binding dystrophin or a related protein in the mdx tissue.

The pattern of positively stained fibres in the tissue was distinctive. The fibres were either isolated single fibres (figure 3.5a) or patches of adjoining positive fibres (figure 3.5b). Where patches of fibres were found, they varied in size from 2 to ~20 myotubes. In all cases every fibre in the patch stained positively- there were no negative fibres within the patches and no clusters of mixed positive and negative fibres. This pattern suggested the clusters of positive fibres arose by means of clonal expansion.

3.7 Somatic reversion in mdx mice/DMD.

The fibres detected by the DURD M/C antibody are mdx revertant fibres. Strongly staining dystrophin positive fibres have been reported in both mdx mice and DMD patients (Hoffman *et al*, 1990, Nicholson *et al*, 1989). For example, antibodies to the C-terminal region of dystrophin showed a small proportion of dystrophin positive fibres are found in >50% of DMD patients (Nicholson *et al*, 1989). These fibres arise by a somatic mechanism which restores the original reading frame of the dystrophin gene, overriding the effects of the original mutation.

Commonly the initial mutation in DMD gives rise to a shift in the dystrophin reading frame (reviewed in Amalfitano *et al*, 1997). This results in premature termination of transcription, and either no dystrophin or production of an N-terminally truncated dysfunctional protein. Generally the exon boundaries in dystrophin do not correspond with the ends of helicies or of automonously folding units, so the sequence surrounding the site of mutation is likely to become disrupted too (Koenig and Kunkel, 1990). The sites of these deletions are not evenly distributed throughout the genome. Instead, there are two main deletion prone areas. The first is around exon 45 and the second towards the 5'end of the

gene (Worton and Thompson, 1988). In revertant fibres these genetic mutations are removed by a differential pattern of exon splicing. Splicing of additional exons produces a truncated mRNA. As the boundaries of the exons do not necessarily align with the start of a codon, the differentially spliced truncated mRNA may revert back to in-frame mRNA and so functionally correct the frameshift mutation. Regions of the genome flanking the genomic mutation can be missing in revertant fibres (Klein *et al*, 1992). Revertant fibres therefore produce a functional dystrophin protein which lacks the regions of the molecule encoded by the original genetic mutation.

The reversion of the fibres could be due to a somatic deletion mutation- removing extra exons from the dystrophin gene, or it could be a splice site mutation- splicing out extra exons from the mRNA. To establish which of these options is the case would require sequencing the genome of the revertant fibres. This is difficult due to the low frequency of the fibres. However, as the age of a DMD patient increases, the proportion of revertant fibres increases (Fanin *et al*, 1992). This is consistent with the notion of a stable but infrequent somatic mutation giving rise to dystrophin positive fibres. These positive fibres are stronger than their dystrophic counterparts and are therefore preferentially selected for over time (dystrophin negative fibres succumbing to greater shearing forces and dying off).

Such a mechanism of dystrophin restoration was reported by Thiet Thanh *et al* (1995 a) as having occurred in the muscle tissue of a patient with DMD. The patient possessed a frameshift deletion within exon 45 of the dystrophin gene which gave rise to the initial dystrophic phenotype. Immunostaining muscle tissue from the patient with exon specific monoclonal antibodies, together with RT-PCR across the exons demonstrated that deletion of exon 44 and/or exon 46 was sufficient to override the mutation. In order to remove the additional exons and restore dystrophin expression, satellite cell nuclei in the revertant fibres had undergone somatic mutation.

Figure 3.5 Mdx revertant fibres.

Transverse serial sections of quadriceps muscle from mdx mouse, immunostained with DURD M/C antibody. Dystrophin positive fibres are found a) singly and b) in patches. Scale bar represents 100μm.

Figure 3.6 Exon specificity of anti-dystrophin antibodies.

Revertant dystrophin positive fibres from serial sections of mdx quadriceps muscle, immunostained with a) DURD C, b) DURD M and c) DURD M/C. Positive staining of the tissue with antibodies to both exons 49 (M) and 76 (C) indicates expression of both exons was restored by the somatic mutation in these fibres. Scale bar represents 100μm.

a)

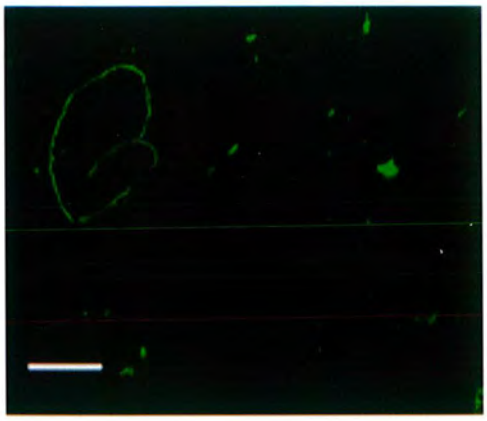

b)

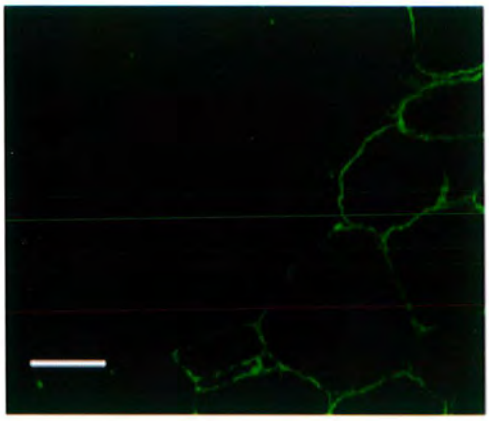

DURD C

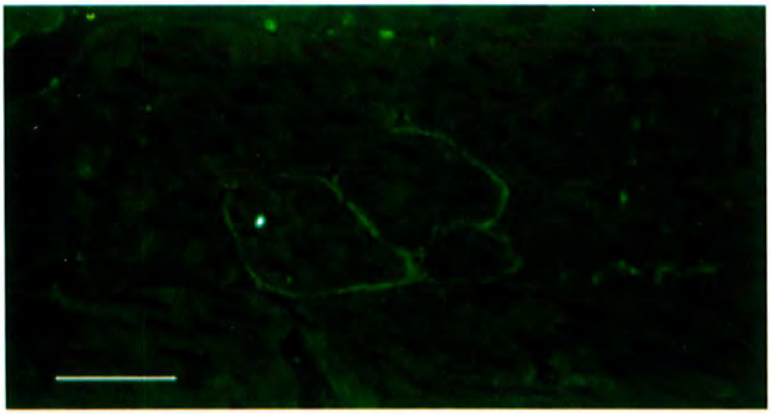

DURD M

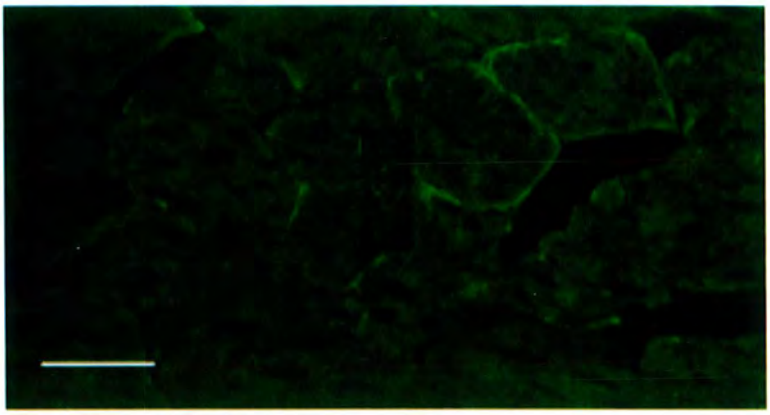

DURD M/C

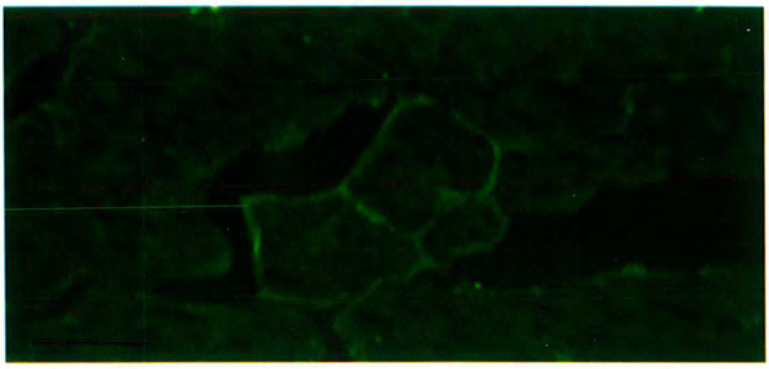

3.8 Exon specificity of anti-dystrophin peptide antibodies.

The primary mutation in mdx mice is a C to T base change at position 3185 in exon 23. This mutation causes premature termination (Sicinski *et al*, 1989). Given that the DURD M/C antibody had detected the presence of revertant dystrophin, the question was asked which epitopes had the antibody recognised, and therefore, which exons were transcribed in the revertant fibres. The DURD M peptide corresponds to a region of exon 49 in the human dystrophin gene and the DURD C peptide is transcribed from exon 76 (Roberts *et al*, 1993). In particular, it was asked whether one or other exon had been spliced out during the reversion process.

To enable dissection of the exon specificity of the dystrophin expression in revertant fibres, transverse serial sections of mdx muscle were immunostained with antibodies DURD C and DURD M, and the presence or absence of revertant fibres investigated. In this particular experimental animal, just one small patch of revertant fibres was found in the muscle. From the location of the fibres in the serial sections, it was clear that the same fibres were expressing both exons 49 and 76 (figure 3.6). Neither exon was spliced out in order to correct the original mutation. The somatic event must therefore have occurred elsewhere in the dystrophin gene.

3.9 Discussion, Part 2-

Mdx reversion.

It is clear that the exon splicing event in the fibres of this particular animal was outside the two exon regions analysed in this study. It is also apparent that such an event, wherever it may have been, successfully restored the reading frame in these two regions of the protein.

3.9.1 Significance of revertant patch size.

The number of fibres in the revertant patch reflects the stage of development in which the mutation arose. The revertant mutation must first arise in a single satellite cell nucleus. If that satellite cell mutates early on in the development of the fibre, the cell will undergo many further rounds of cell division, forming a whole cluster of dystrophin positive myofibres. Hoffman *et al* (1990) reported that it's possible to observe dystrophin expression at the level of each individual revertant nucleus. The relatively large dystrophin mRNA undergoes restricted diffusion. Expression of dystrophin is therefore patchy along the length of the myotube, with strongest expression near to revertant nuclei. In the case of the patch observed here the mutation occurred at a late developmental stage, so far fewer nuclei contain the revertant molecule and the patch is small.

3.9.2 Uses for exon specific antibodies.

In DMD patients the expression of revertant fibres in skeletal muscle can reduce the severity of the DMD phenotype (Nicholson *et al*, 1993). As these antibodies can detect the presence of revertant fibres, they could be used to predict the severity of DMD in a patient and therefore assist with planning an appropriate clinical strategy.

The ability to detect revertant fibres may also be of use to quantify the success of induced somatic reversion. Given that revertant fibres are reported to reduce the severity of DMD, investigations are underway to see if natural dystrophin reversion has potential therapeutic benefits (T. Partridge, personal communication) In mdx mice, the numbers of revertant fibres increases following irradiation of the muscle tissue. This is believed to reflect an increase in the rate of somatic mutation induced by the irradiation (Hoffman *et al*, 1990). Whilst irradiation carries its own risks, the results are encouraging.

The negative staining of C-terminal antibodies in the muscle tissue of DMD patients (who may possess some N-terminally truncated dystrophin) allows for simple immunohistochemical diagnosis. In the case of Becker MD, dystrophin protein is present in skeletal muscle tissue. The protein is truncated and therefore functionally compromised, with severity corresponding to the site and extent of deletion. A crude test for the presence or absence of dystrophin will not indicate the underlying cause of myopathy in BMD. Furthermore, the moderatly reduced levels of dystrophin protein are easily confused with a limb girdle MD phenotype. Southern blotting and PCR are the preferred techniques for BMD analysis at present. Large deletions are detectable on a western blot if the deletion produces an observable difference in molecular weight. Exon specific monoclonal and polyclonal antibodies such as these are preferential to antibodies directed against large bacterial fusion proteins when characterising the site of deletion in BMD. Small deletions can be detected by studying which epitopes are recognised from a large panel of highly specific antibodies (Thiet Thanh *et al*, 1995 b). The site of mutation and the deletion boundaries can be narrowed down specifically.

On the other hand, the potential for these antibodies is limited when tracing the transplantation success of dystrophin positive myoblasts into dystrophic tissue (e.g. Beauchamp *et al*, 1999). In this case it is desired that the transplanted fibres can be detected in the host tissue and their viability traced. It would be preferable if revertant fibres were not detected too, and therefore antibodies specific to the spliced out exons are desired.

3.9.3 Future potential.

Full elucidation of the site of somatic rearrangement within dystrophin revertant tissue requires a far greater selection of exon specific antibodies than were generated for this FPR study. Ideally a whole

panel of exon specific antibodies is needed to narrow down the exact nature of the mutations and pattern of exon splicing. To this end these antibodies have been made available to Profs G.E. Morris and T.A. Partridge, to compliment their own collections of antibodies for the study of dystrophin revertant fibres.

Chapter 4

The role of dystrophin as a 'molecular fence'- a non-specific regulator of membrane protein distribution.

Chapter 4

The role of dystrophin as a 'molecular fence'- a non-specific regulator of membrane protein distribution.

4.1 Introduction.

The subplasmamembranous cytoskeleton forms a regular latticework beneath the plasma membrane of a cell. This lattice work may restrict and confine mobility of integral and peripheral membrane proteins by forming a steric barrier to their diffusion- the so called 'molecular fence' proposed by Kusumi *et al*, (1994) (Simson *et al*, 1998), discussed in detail in section 1.3. Such regulation of protein distribution is essential for delineation of the cell surface into specialised functional domains.

The cytoskeletal constituent spectrin is a proven regulator of membrane protein mobility within many cell types including red blood cells and neurons (Tsuji and Ohnishi, 1988, Joe and Angelides, 1993). Dystrophin, the protein produced by the Duchenne Muscular Dystrophy locus, is a cytoskeletal component with a high level of sequence and structural homology to spectrin, including 24 spectrin-like repeats and an amino terminus capable of actin binding (Koenig *et al*, 1988). Dystrophin, like spectrin, has been localised to beneath the plasma membrane (Porter *et al*, 1992).

Immunolocalisation studies in muscle fibres have shown the organisation of membrane glycoproteins to be severely affected by an absence of dystrophin, specifically the glycoproteins of the DAG complex (Ohlendieck and Campbell, 1991). Clinical findings of muscle cytosolic constituents free within the serum of DMD patients and the evidence for extensive wound healing activity (*q.v.* section 1.1.2) suggest the absence of a functioning dystrophin/DAG complex results in sarcolemmal membrane instability. The rigidity and deformability of the membrane are also affected (Pasternak *et al*, 1995).

As stability of the dystrophic membrane is compromised, dystrophin has sub-plasmalemmal distribution; is homologous to spectrin and is known to interact with glycoproteins of the DAG complex; this study addressed whether dystrophin could organise membrane structure by regulating lateral mobility of membrane glycoproteins; either by forming a 'molecular fence' to membrane protein diffusion or as a direct linker of surface glycoproteins. To examine the role of dystrophin in organisation of the muscle cell membrane and illustrate the interactions between the membrane constituents and cytoskeleton, fluorescence photobleach recovery (FPR) studies were conducted into the mobility of general classes of membrane glycoproteins in *mdx* and normal mouse muscle fibres.

- **Part 1. The effects of dystrophin deficiency on glycoprotein mobility.**

In order to quantify the true physiological contribution of dystrophin to restriction of membrane protein mobility, fluorescence photobleach recovery experiments were performed on the surface of live teased muscle fibres. Fluorescently coupled lectins were used as probes to label general classes of surface glycoproteins. Lectins are not believed to perturb the membrane or affect the mobility of the labelled proteins (Axelrod *et al*, 1976), so the photobleaching approach should provide a good indication of real-time protein diffusional behaviour.

All the lateral mobility data presented in the tables, graphs and figures of this chapter was compiled from multiple individual photobleach curves. Data from the individual curves is contained in the appendix, together with the means, standard deviations and standard errors of the mean for the compiled data sets. The diffusion coefficient (D) and mobile fraction (f) values given here are the mean ± standard error of the mean (s.e.m.).

4.2 Results.

4.2.1 Tissue buffer and fibre viability pilot study.

From early studies of live muscle tissue labelled with lectin and bathed in PBS, during the FPR experiments marked and characteristic shifts in glycoprotein behaviour were observed during the later stages of data acquisition (approximately 1hour to 1hour 20 min after tissue removal- equivalent to around 30min into data collection). These changes were reproducible. Following early signs of glycoprotein immobility, a sudden rapid recovery was observed. The rapid phase made way within minutes for slow but complete recovery behaviour, which slowed in its rate of recovery as acquisition time progressed (figure 4.1). The initial stage pattern of mobility was stabilised and lengthened by changing to oxygenated Krebs buffer. The rapid recovery shift was therefore taken as a sign of fibre necrosis and care was taken to obtain all glycoprotein FPR data prior to any sudden irregular shifts in protein mobility patterns.

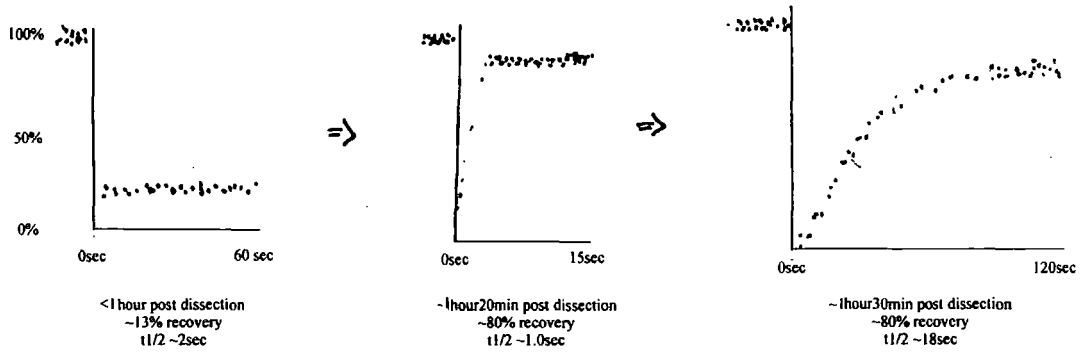

Figure 4.1 Changing pattern of fluorescence recovery with increasing experimental time.

Stylised FPR recovery curves obtained from muscle fibres labelled with FITC conjugated lectins in PBS buffer system. y-axis represents fluorescence intensity as a percentage of normalised pre-bleach levels. x-axis, time post-bleach in seconds. t1/2, half time for recovery in seconds. Time scales at which the curves were obtained are approximate.

4.2.2 *Lens culinaris* receptor mobility.

Mobility of the terminal α-D-mannosylated and α-D-glucosylated classes of glycoproteins was monitored by labelling live, teased soleus muscle fibres with fluorescein isothiocyanate (FITC) coupled lectin from *Lens culinaris* and following the pattern of fluorescence recovery after photobleaching (Figure 4.2). The appearance of post-bleach fibres suggested that tissue integrity had been maintained throughout the experiments (Figure 4.2 a,b).

Lens culinaris binding glycoproteins were found to be immobile in the sarcolemma of both mdx and control C57/BL 10 (C57/Bl) mouse calf muscle fibres within the time frame limitations of the experiment ($D_{immobile}<10^{-12}cm^2/sec$), figures 4.2, 4.3, and table 4 1. A small mobile fraction of *Lens culinaris* binding glycoproteins (f≈8%) was detected in both mdx and normal C57/Bl tissue systems. Whilst there was inevitably some fibre-fibre and tissue-tissue variation, this was smoothed out by the large sample size. For each lectin, data was collected from a minimum of two different animals of each genotype, >10 measurements taken per animal.

The large errors in the data are a feature of the curve fitting equations rather than the quality of data itself. The smaller the recovery, the less the data mirrors free diffusion into a uniform circular area from an infinite sink and therefore the harder the curves are to fit to the data and the greater the errors.

Were the recovery larger, the errors would be smaller. The magnitude of the errors should not detract from the consistent observation that there was no mobility in the systems.

After conducting the photobleach experiments, the presence or absence of dystrophin within the tissue was confirmed by immunostaining fast frozen unfixed quadriceps muscle sections from the animal with anti-dystrophin polyclonal antibodies (figure 4.2 e,f). To confirm that genetic absence of dystrophin was the cause of negative tissue staining and not insufficient secondary antibody, poor section integrity or degradation of cytoskeletal proteins, serial sections were stained in parallel with anti-rat brain spectrin polyclonal antibody as a positive control (figure 4.2 g and h) (gift of E-H Joe. Vybiral *et al*, 1993).

4.2.3 S Con A receptor mobility.

Succinyl-concanavalin A (S Con A), like *Lens culinaris*, binds to terminal α-D-mannosylated and α-D-glucosylated residues on glycoproteins. S Con A data therefore acted as an internal control for instrument sensitivity. As for *Lens culinaris*, S Con A-FITC binding glycoproteins are largely immobile on the timescale of the experiment, table 4.1, figure 4.3. There is no significant[4] difference in mobility between mdx and normal sarcolemmal glycoproteins, the mobile fraction of glycoproteins being ~10% in each case. These mobile species possessed diffusion coefficients of the order of $5x10^{-10}cm^2/sec$, comparable with published data for the free Brownian diffusion of large proteins within a phospholipid bilayer [for example, $D=3.7x10^{-10}cm^2/sec$ for free Brownian diffusing NCAM isoforms expressed in C2C12 muscle and NIH 3T3 cells (Simson *et al*, 1998)].

[4] 'significant' is used here in an FPR sense, not a statistical sense. For details, q.v. section 2.6.4.

Figure 4.2 . Representative data set from the recovery of glycoproteins on normal and dystrophic muscle.

a) b) Fluorescence photobleach recovery curves from live C57/Bl (left hand column) and live mdx (right hand column) soleus muscle fibres labelled with 25mM *Lens culinaris*-FITC. Vertical line represents the point of photobleaching; y-axis, light intensity as a percentage of normalised pre-bleach levels; x-axis, time pre- and post bleach (s). The fibres appeared intact following completion of photobleach experiment, c) d) . The presence or absence of dystrophin in the fibres was confirmed by staining transverse sections of quadriceps muscle from the same animal with DURD C anti-dystrophin C-terminal antibody e) f); whilst staining with anti- spectrin antibodies indicated sarcolemmal cytoskeletal proteins were intact in the sections h) g).

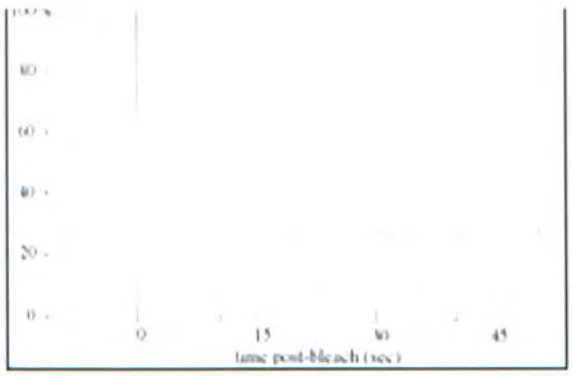
0
15
30
45
time post-bleach (secs)

a)

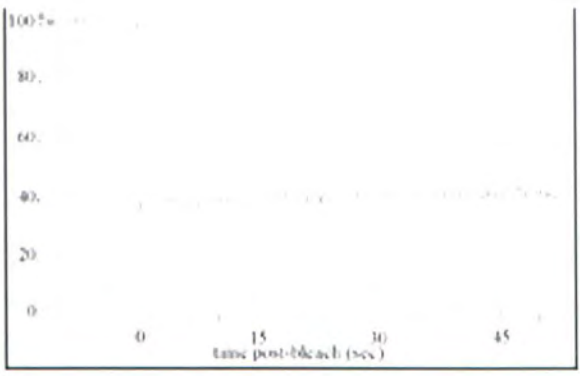
0
15
30
45
time post-bleach (secs)

b)

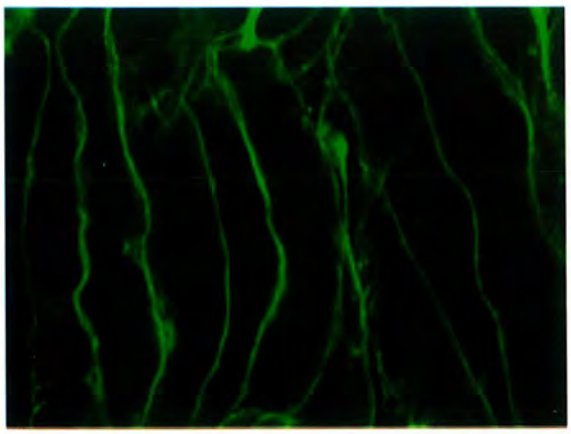

c)

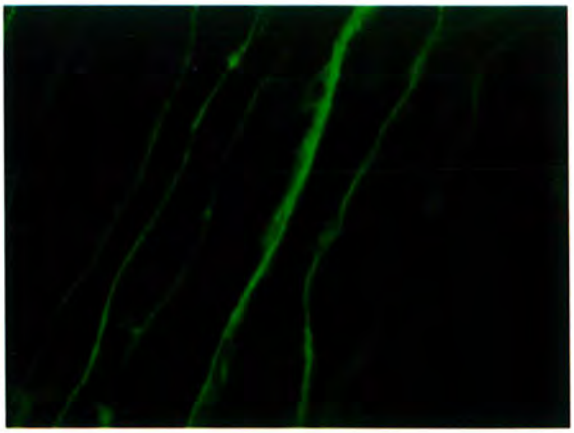

d)

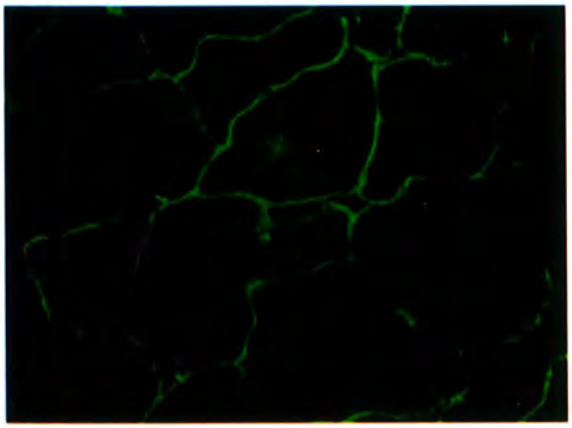

e)

f)

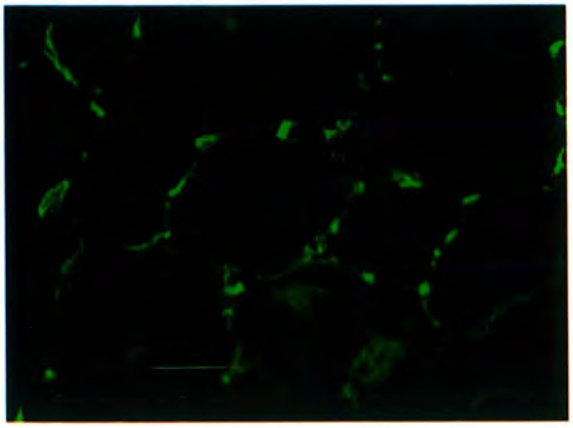

g)

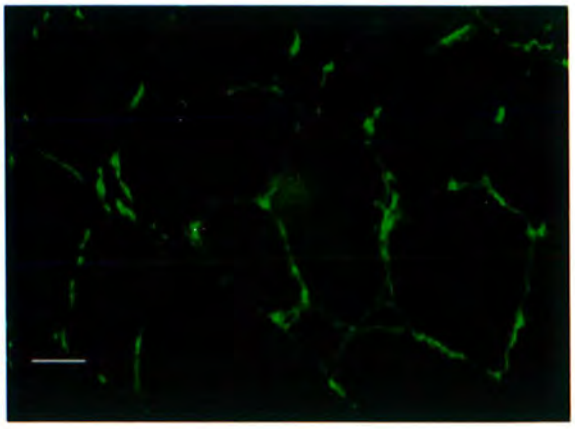

h)

4.2.4 *Ricinus communis* agglutinin receptor mobility.

Ricinus communis agglutinin 120 (RCA120) is known to bind to a 370kDa component of the DAG complex (Voit *et al*, 1989), amongst other N-acetly-glucosamine containing glycoproteins. The FPR data in table 4.1 indicates the RCA120 lectin binding glycoproteins are largely immobile in the sarcolemma of mdx and control mouse muscle (recovery ~11%), with no significant difference in mobility between the two systems

Lectin.	**Mouse Genotype.**	**n sample size**	**f, Fluorescence recovery (%).**	**T_D, recovery (sec).**	**D_L, Diffusion coefficient $x10^{-10}cm^2/sec.$**
S-Con A.	C57 normal	28	10.50 ± 2.32	4.39 ± 1.34	4.13 ± 1.21
	mdx	38	9.03 ± 1.87	4.18 ± 2.02	5.68 ± 3.00
Lens culinaris.	C57 normal	28	8.11 ± 1.63	3.79 ± 1.82	10.6 ± 10.4
	mdx	36	7.69 ± 2.13	2.69 ± 1.19	8.77 ± 5.22
RCA_{120}	C57 normal	31	10.38 ± 2.46	3.30 ± 1.19	6.03 ± 2.29
	mdx	21	11.71 ± 1.82	4.31 ± 1.73	4.13 ± 1.89

Table 4.1. Summary of glycoprotein mobility. There was no significant differences in mobility of the glycoprotein classes in mdx and C57/Bl muscle fibres.

Diffusional behaviour of fluorescently labelled glycoproteins on the surface of C57/BL 10 and mdx dystrophic mouse muscle fibres, as determined by FPR. Fluorescence recovery is given as a % of normalised pre-bleach levels. Values are mean ±s.e.m. for all pooled data curves.

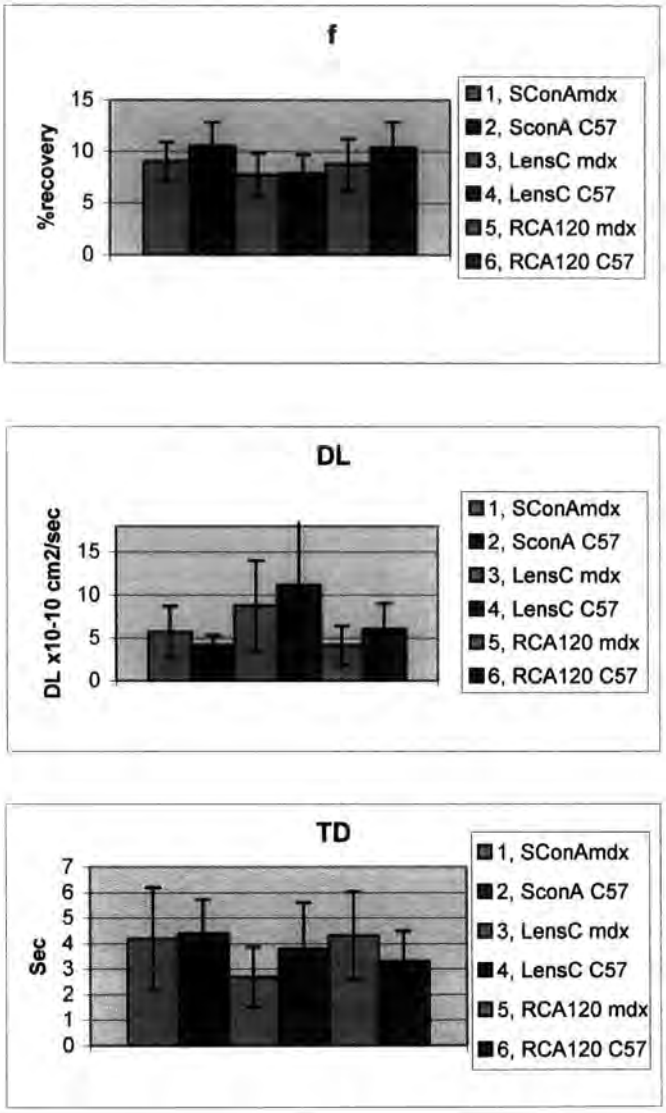

Figure 4.3 Comparison of glycoprotein mobility in C57/BL 10 and mdx muscle fibre membranes.

There was no significant difference in mobility of any of the investigated classes of glycoproteins as measured by FPR. Live fibres were labelled with 25nM FITC conjugated lectins S Con A, *Lens culinaris* and RCA $_{120}$, and the mobility of labelled glycoproteins tracked by fluorescence recovery after photobleaching. Sarcolemmal glycoproteins were immobile in both tissues, f <11% within the limitations of detection ($D_L \geq 1x10^{-12}cm^2/s$) ['immobile' c.f. f~80% for free band 3 protein in erythrocytes (Tsuji *et al*, 1988)]. f, fluorescence recovery as a % of normalised pre-bleach levels; D_L, diffusion coefficient (cm^2/s) and T_D, half time for recovery (s). All values are mean ± s.e.m. Column numbering runs from left to right.

4.3 Discussion, Part 1.

The experiments here addressed the notion that dystrophin, with its structural and sequence homology to cytoskeletal proteins, was acting as a constituent of the membrane skeleton fence in accordance with the "membrane skeleton fence model" of Kusumi *et al*, (1993) . This model proposed that 'the membrane associated cytoskeleton (membrane skeleton) provides a barrier to free diffusion of membrane proteins due to steric hindrance, thus compartmentalising the membrane into many small domains for diffusion of membrane proteins'.

4.3.1 Dystrophin and regulation of glycoprotein lateral mobility.

It has been seen that there is little appreciable difference in the mobility of sarcolemmal glycoproteins in dystrophic and normal tissue. This suggests that dystrophin is not vital for the setting up of sarcolemmal membrane domains or the restriction of sarcolemmal glycoprotein diffusion. This observation does not unequivocally rule out a fencing action of dystrophin in healthy tissue. Immunohistochemistry of the mdx fibres showed the underlying spectrin network to be present and apparently intact within dystrophic tissue, and so the spectrin network could be retaining proteins regardless of the presence of dystrophin. Although it would have been possible to add cytochalasin or brefeldin A to the fibres to remove the spectrin cytoskeleton, their effects on protein mobility is well documented (e.g. Sako and Kusumi, 1994) and the dystrophin network may also be disrupted. It is possible that dystrophin may complement the existing cytoskeletal network in healthy fibres. Extra rigidity will be imparted to the network in the presence of dystrophin through a more dense, more highly cross linked array of cytoskeletal proteins. Given the proximity of dystrophin to the sarcolemmal membrane and the sizes of the dystrophin molecule and DAG complex, it is likely that dystrophin will form a steric barrier to the diffusion of some membrane species. All these actions would reinforce an existing cytoskeletal system, but due to the presence of the remaining cytoskeleton, would not necessarily give rise to an altered mobility phenotype if that reinforcement were removed. The results do suggest, however, that a membrane fence role is not a primary function of skeletal muscle dystrophin.

4.3.2 Redundancy within the membrane skeleton.

On the other hand, the observed similarities in glycoprotein mobility in the presence and absence of dystrophin could reflect the high levels of redundancy found within cytoskeletal and extracellular matrix protein complexes (discussed in Gorski and Olsen, 1998). The presence of cytoskeletal and ECM proteins with some regional sequence and structural homology to dystrophin/DAG complex

components may be sufficient to compensate for the lack of dystrophin/DAGs in MD tissue in the non-contractile resting state. Such homologous constituents could maintain sarcolemmal glycoprotein distribution and restrict membrane diffusion through similar (though lower affinity) protein-protein interactions. Under the resting conditions of an FPR experiment such a system would seem correctly organised with imposed restrictions on protein mobility. However, under conditions of shear stress the failings of this pseudo complex could then become apparent. The protein-protein links of homologous proteins, though adequate for protein immobilisation and diffusion restriction, may then prove inadequate to prevent stress induced destruction of the tissue and a diseased state would follow.

The extracellular matrix (ECM) remained in place throughout the acquisition of recovery data. Considering the interrelationship of the membrane surface glycoproteins and the ECM components, the effect of the ECM on surface glycoprotein immobility must be considered. A densely packed, highly cross linked matrix on the surface of a muscle fibre could corral membrane surface proteins as effectively as a submembranous barrier. If this is the case in muscle fibres, removal of cytoskeletal components such as dystrophin will have a limited impact on the mobility of membrane components, even though structural integrity of the fibre has been compromised.

The contribution of the ECM to restriction of cell surface protein mobility was investigated by FPR in Rous sarcoma virus transformed chick embryo fibroblasts by Boullier *et al* (1992). Transformation with the virus induces breakdown of the cellular exoskeleton. To investigate the effects of such ECM decomposition, cells were treated with trypsin to remove their exoskeleton (primarily composed of fibronectin in this cell line), resulting in rounded non-adherent cells. The fluidity of the lipid phase was unchanged by this procedure as shown by Di-I mobility. The diffusion rate of S Con A receptors by contrast was $3x10^{-10}cm^2s^{-1}$, approximately 2 to 4 times faster than in untreated cells. The fibronectin based ECM was consequently proposed to make a significant contribution to restriction of surface glycoprotein mobility, and therefore viral induced fibronectin loss contributed to the increased surface protein mobility observed in the cell line following viral transformation. (Although the authors did acknowledge break down of other ECM and surface proteins in addition to fibronectin is possible by trypsin).

It would be possible to treat these muscle fibres with trypsin to remove the ECM and see if the ECM had the main influence on surface glycoprotein immobility in this system. The danger with this approach is that the membrane glycoproteins themselves could also be affected by the degradation. Disruption of specific protein-protein linkages on the surface would affect mobility of the surface proteins involved, perhaps freeing them of their true constraints. Similarly disaggregation of large complexes could increase rates of diffusion of the constituent parts. Stripping away all but the submembranous cytoskeleton would show what role the cytoskeleton can play- and perhaps how dystrophin is essential in such a role- but the physiological significance of such an experiment must then be questioned.

4.4 Experimental artefacts.

There was one further possible explanation for the apparent lack of protein mobility in the fibres studied- that the observed data was artefactual, rather than a true representation of membrane glycoprotein behaviour. Previous reports of muscle glycoprotein mobility have described recovery of fluorescence. For example Schlessinger *et al*, (1976) observed approximately 66% recovery of Con A labelled glycoproteins on myoblasts. Whilst several of the curves published in earlier papers show moving tissue samples rather than true recovery (the published recovery curves possessing kinks instead of smooth increases in % fluorescence e.g. Axelrod *et al*, 1976), the probability that something was amiss in the collection of the data in this study- and that therefore a proportion of the glycoproteins are mobile in the tissue could not be ruled out. Instrumentation failure or sensitivity was not believed to be a problem. The replacement of labelled tissue with slides of free fluorescein dye diluted in 100% glycerol gave detectable and complete fluorescence recovery. Additionally, once the glycerol was replaced by 80% glycerol / 20% water the rate of recovery increased, suggesting the bleach shutters and detector was functioning and that all optical beams were in line.

The simplest method to determine whether fluorescence recovery behaviour of the labelled probe was a true reflection of membrane glycoprotein diffusion or actually artefactual was to increase the experimental temperature and look for an effect on mobility of membrane constituents.

• Part 2. The effects of temperature upon glycoprotein mobility in this study.

4.5 Introduction.

FPR measurements of glycoprotein mobility showed three different classes of glycoprotein were immobile in normal and dystrophic mouse muscle membranes. The immobilisation of membrane glycoproteins could be representative of physiological behaviour in mouse muscle. Alternatively, the data may have been influenced by experimental conditions and therefore not reflect the physiological situation.

It was possible that the lack of glycoprotein mobility in the two systems was a consequence of the experimental temperature affecting membrane fluidity and behaviour, rather than the tethering or constraining action of the cytoskeleton and/or extracellular matrix. The lectin based glycoprotein study

was conducted at an ambient temperature range of 18-22°C. In most cases the mdx/C57 Bl comparisons were performed on the same or consecutive days, so temperature variation between experiments was kept to 1 or 2°C. Data was pooled from several animals in each case, so effects of any minor temperature fluctuations on diffusional behaviour will have been smoothed out in the analysis.

20±2°C is not physiological temperature for the tissue in this system. This was not believed to compromise the study or hinder comparison of mobility as many FPR experiments have been conducted at either non-regulated ambient temperature or with no reference to temperature at all, with no reported difficulties or unexplained membrane rigidity. For example Edidin and Stroynowski (1991) successfully compared mobility of conventional and inositol phospholipid-anchored membrane proteins in K78-2 hepatoma cells by FPR at 20°C.

4.5.1 Effects of temperature on diffusion.

For molecules undergoing free Brownian diffusion, the rate of translational diffusion is related directly to temperature according to the linear diffusion equation:

$$D_T = k_B T b_T$$

Where D_T is the translational diffusion coefficient, k_B is Boltzmann's constant, T the absolute temperature and b_T translational velocity under unit force.

4.5.2 Gel/fluid phase transitions in biological membranes.

In complex matrices such as cell membranes, the linear relationship of diffusion with temperature no longer holds over comparatively large distances. Membranes constitute a panoply of co-existing phases. Depending upon the temperature and protein/lipid/cholesterol constituents of the system there may be a mixture of gel and fluid phases of differing melting points. Proteins may be in a free moving fluid environment at one end of the cell and in a semi-rigid gel phase just micrometers away.

Hydrodynamic theory predicts that the diffusion coefficient for a membrane constituent, D, should increase with increasing membrane temperature. The membrane fluidity of all cells is directly affected by temperature to a greater or lesser extent. In some specialised plant cells, however, the magnitude of temperature effects are significantly restricted compared with animal cells and reconstituted bilayer systems.

4.5.2 a) Gel and fluid phases in plant membranes at low temperature.

At low temperatures the membranes of plants and many heterotherms consist of a melee of co-existent gel and fluid phases. Metcalf *et al* (1986), suggested the plasma membranes of soybean cells may be a composite of stable immiscible domains of fluid and gel-like lipids after measuring the lateral mobility of phospholipid and lipid probes in the protoplast membrane by FPR. At 18°C the membrane probes possessed two parallel and independent patterns of recovery. The fluorescent markers either partitioned into a slow moving phase of D~5x10^{-10}cm^{2}s^{-1} (~30% of total membrane fraction)- representing a gel phase- or into a fast diffusing fluid phase of D~3 x10^{-9}cm^{2}s^{-1} (40% of membrane labelled fraction). At 37°C the gel phase had melted and a single mobile lipid phase was found (D~ x10^{-8}cm^{2}s^{-1}, recovery ~60%). Changes in temperature of the system produced large irregular changes in the diffusion coefficients of membrane lipids. The magnitude of changes in D with temperature was significantly greater then the smooth gradual increase in fluidity expected for decreasing lipid phase viscosity with increasing temperature (46 fold increase in $D_{di\text{-}l}$ from 18 to 37°C, compared with 2 fold increase expected from of fluid viscosity), providing further evidence for a series of co-existing gel and fluid membrane domains at low temperature. Functionally, this adaptation is believed to ensure constant provision of active fluid phase membrane in the protoplast without sharp phase transitions and irrespective of external temperature.

Similarly, in chill-sensitive maize roots the plasma membrane contains a variety of gel and fluid domains which stabilise membrane fluidity over a range of temperatures- the diffusion coefficient of phospholipid probes within the membrane underwent no significant change with varying temperature, and the temperature sensitive plant membranes remained fluid at low temperature (Kloster *et al*, 1994). Non-chill sensitive protoplasts did undergo significant changes in lipid diffusion rate at temperatures below 10°C. Protein diffusion on the other hand showed only slight changes from 2 to 21°C in both cell types, suggesting the different phase lipid domains regulate protein fluidity over a range of temperatures. The corresponding membrane lipid mobile fraction showed slight increase over that range but was consistently less than 100%, therefore gel and fluid phases existed throughout.

As many proteins favour a fluid lipid environment, it was proposed the decreased mobile fraction of proteins at lower temperature (albeit with similar D values) occurred as fewer of the membrane lipids were in a fluid state, thus allowing less of the protein to diffuse. Alternatively, aggregation of membrane proteins at lower temperatures could also have reduced the mobile protein fraction. The increasing mobile fraction of lipids with temperature pointed to progressive gel phase melting as temperature increased.

Some specialised plant membranes are therefore a mixture of gel and fluid domains across a range of temperatures. This adaptation is important to regulate membrane fluidity and function under fluctuating environmental conditions.

4.5.2 b) Gel and fluid phases in animal cell membranes.

This situation of gel and fluid phases is not seen as commonly in animal cells, particularly those of homoeothermic organisms. In general, the cells of mammals do not need to maintain fluidity over such a wide range of temperatures as plant cells therefore in the majority of mammalian cells, the requirement of complex multiple phases within membranes is avoided. The comparatively lower levels of negatively charged phospholipid and reduced sterol levels in animals give rise to more uniform and greater overall membrane fluidity at RTP. At lower temperatures the increased cholesterol concentration keeps the membranes fluid.

There are some temperature dependent phase transitions in mammalian cells. The mobility of Di-I in the membranes of human fibroblasts undergoes a sharp shift in mobility at 10°C corresponding to a phase transition. Mobility then increases smoothly with temperature, apart from at 25°C when a kink is observed in the curve (Jacobson *et al*, 1981). The extracted and reconstituted plasma membrane lipid systems from the same cell lines are more complex. Here, above the 10°C discontinuity one component diffusion was observed, but below 10°C two component diffusion was seen- in accordance with a lateral phase separation of the membrane lipids as the membrane cools to form a multi phase equilibrium. In the true cell membrane, the presence of cholesterol smoothed out the two phases such that a simple one phase system was observed, increasing membrane fluidity with increasing temperature.

4.5.2 c) Membrane composition and fluidity.

The presence of cholesterol within animal cell membranes restricts the extent of rapid temperature dependent shifts in fluidity and maintains fluidity at lower temperatures. The consequences of cholesterol depletion on membrane lipid fluidity was highlighted by Thompson and Axelrod (1980). At low temperatures (-5 to 5°C), the diffusion of a fluorescent lipid probe was 50% slower in the membranes of cholesterol depleted human erythrocytes than in the membranes of non-depleted erythrocytes. Above the phase transition temperature of the membrane lipids, the presence or absence of cholesterol made no difference to fluidity (though fluidity was still temperature dependent).

The ratio of lipid to protein (L:P ratio) in a membrane has significant impact on the fluidity. At temperatures above the phase transition temperature of the lipid matrix, both protein and lipid diffusion

coefficients decrease as the L:P ratio decreases. It is argued that at high L:P ratios this is probably controlled by the temperature dependent viscosity of the membrane whilst at low L:P ratios steric crowding and protein-protein interactions slow diffusion. Below the transition temperature of the membrane the opposite occurs. The presence of high levels of protein maintains the fluidity of the membrane and removes the large abrupt change in diffusion coefficients at the transition temperature (Peters and Cherry, 1982).

Though animal cell membranes generally have just one fluid phase, there are exceptions. Sperm cells have a fraction of non-diffusing lipid in their membranes as a result of lipid-lipid interactions, providing an equivalent to co-existent gel and fluid domains. Differential scanning colorimetry revealed the anterior region of the sperm plasma membrane undergoes two major endothermic phase transitions at ~26 and ~60°C, consistent with the models of gel/fluid transitions and in accordance with a partially melted bilayer at physiological temperature (Wolf *et al*, 1990). It was suggested such ability to maintain fluidity over a range of temperatures was necessary as sperm pass through a range of temperature environments during maturation and fertilisation.

4.6 Temperature and muscle membrane fluidity.

In plant and animal cells adapted for temperature fluctuations the cell membranes may retain fluidity over a range of temperatures via a co-existent mix of gel and fluid phases. In general, temperature phase transitions in animal cells are less complex and more linear, following the basic trend of lower temperature, lower fluidity. It is possible that the immobility of muscle membrane glycoproteins at 20°C is a consequence of reduced membrane fluidity at sub-physiological temperatures. To investigate whether temperature was limiting mobility in the glycoprotein FPR study, experiments were repeated at a higher temperature.

Whilst it has been proven that membrane lipids may undergo a series of complex temperature dependent gel/fluid changes, the characterisation of such phase transitions in muscle fibres was unnecessary to demonstrate whether temperature was limiting. A simple increase in protein mobility at greater temperature would be sufficient to indicate lack of fluidity in the cold is the main explanation for immobility of glycoproteins at ambient conditions, rather than cytoskeletal or other imposed restrictions.

4.7 Results.

It is well accepted from both experiment and casual day to day observations that the fluidity of lipid/cholesterol rich environments is subject to temperature fluctuations. To investigate whether

surface glycoproteins were immobile in the ambient temperature muscle plasma membranes studied by FPR because of the presence of a semi-solid gel matrix, or whether it was a result of cytoskeletal effects, the mobility of the glycoproteins was re-measured at the higher temperature of 30°C, and the results compared with the ambient data.

4.7.1 Equipment temperature modifications and limitations.

Increasing the measuring temperature required modification of the traditional FPR apparatus. In the absence of a heated microscope stage, a crude but adequate heated water bath arrangement was assembled (figure 2.1 d). A circulating water bath at 75°C provided the heat. The water passed through a brass block placed on top of the stage to heat the apparatus by conduction. The sample sat in a glass (rather than tissue culture grade plastic to improve conduction) petri dish placed on a glass slide on the stage and was likewise heated by conduction. The block was too tall to fit underneath the sample directly under the microscope objectives. Positioning the sample adjacent to the brass heating block rather than directly on it allowed the sample to be viewed under phase before photobleaching. The apparatus was insulated with polystyrene and bubble wrap.

The equipment modification gave adequate heating up to 29±1°C. Due to heat loss and the multiple heat transfer steps this equipment will go no higher. Ladha *et al* (1997) extrapolated mobility of a fluorescent lipid analogue in the plasma membrane of bull spermatozoa at 30°C to be approximately twice that at 20°C, but still about one fifth the diffusion rate at 37°C. 29°C was therefore not expected to heat the membranes to a position of full fluidity, but should induce measurable differences over the 20°C situation. Additional difficulties with the heating apparatus came from vibrations of the circulating water. The flow of water through the block caused the tissue sample to vibrate, preventing the acquisition of interpretable recovery data. To overcome this the waterbath was switched off during data collection and on between experiments. This gave a stable sample temperature for up to 20 minutes. Sample temperature was monitored at intervals with a digital thermometer.

4.7.2 The effects of temperature on mobility of membrane glycoproteins.

The effects of temperature on the mobility of terminal α-D-mannosylated and α-D-glucosylated glycoproteins on the surface of experimental muscle fibres was measured by FPR of S Con A-FITC labelled mouse muscle fibres at 29±1°C. It was assumed that the behaviour of S Con A labelled glycoproteins was representative of protein behaviour and hence membrane fluidity as a whole, and therefore experiments were not repeated using other fluorescent lectin probes. To see if a contribution from dystrophin to regulation of membrane glycoprotein mobility could be detected at the greater temperature, all experiments were conducted in parallel with tissue from C57/BL and mdx mice.

Due to the small levels of fluorescence recovery obtained during many of the individual experiments, the recovery data could not be fitted to the diffusion equation within the limits of statistical tolerance (q.v. section 2.4.4). In these cases the % recovery was determined by eye from the experimental curves. Diffusion coefficients could not be calculated where this was a problem, therefore $n_{DL}<n_{total}$ and the diffusion coefficients given in table 4.2 have large errors.

4.7.2 a) Temperature and dystrophic muscle membranes.

~90% of S Con A-FITC labelled membrane surface glycoproteins were found to be immobile in the sarcolemma of mdx mouse muscle fibres at 29±1 °C, as summarised in table 4.2 and figures 4.4, and 4.6. The small portion of proteins that were mobile (~9.%) had diffusion coefficients of the order of $\sim 3 \times 10^{-10} cm^2 s^{-1}$, as expected for freely mobile proteins.

The 9% recovery of fluorescence / 91% immobility of proteins at 30 °C was equivalent to the membrane state at ambient temperature for mdx fibres labelled with S Con A-FITC. At ambient temperature 90% of the labelled membrane glycoproteins were immobile in mdx tissue. Therefore heating the fibres had no effect on the portion of mobile proteins in the membranes. Similarly within the margins of experimental error the rates of diffusion for the small percentage of mobile species was comparable in mdx tissue at both temperatures.

4.7.2 b) Temperature and normal muscle glycoproteins.

The pattern of glycoprotein mobility at 30 °C in C57/Bl muscle fibres is shown in figure 4.5. The effects of temperature on surface glycoprotein mobility in C57/Bl tissue were similar to mdx fibres. An increase in temperature of ~9 °C produced no significant increase in either the proportion of mobile membrane glycoproteins (f~10% in both cases) or the rate of diffusion of the mobile fraction ($D_{L29} \sim 2.95 \times 10^{-10} cm^2 s^{-1}$ c.f. $D_{L20} \sim 4.13 \times 10^{-10} cm^2 s^{-1}$) when compared with 20 °C values for both S Con A and *Lens culinaris*-FITC conjugated lectins (table 4.2 and figures 4.2, 4.5 and 4.6).

a)

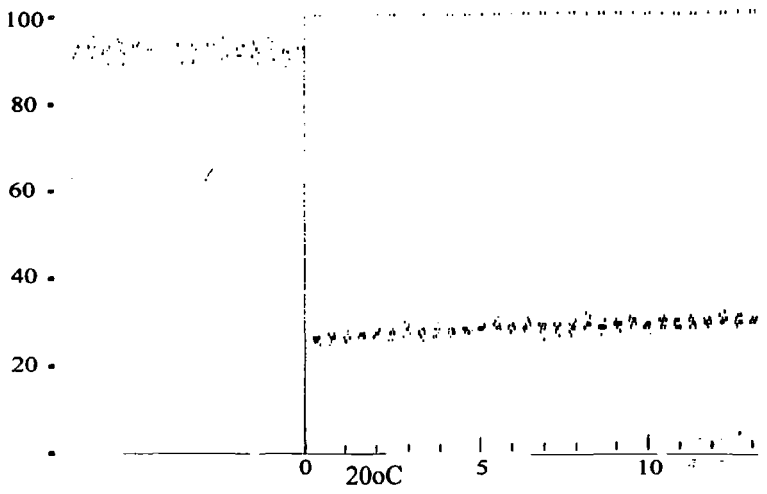

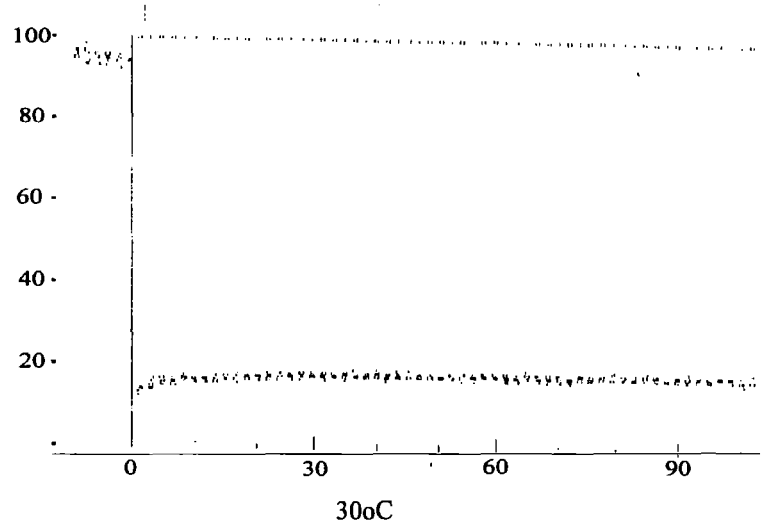

b)

Figure 4.4 Effects of increased temperature on glycoprotein mobility.

Increasing experimental temperature had no significant effect on the mobility of surface membrane glycoproteins in mdx mouse muscle.

Above. FPR recovery curves from live mdx muscle fibres labelled with 25mM S Con A-FITC and photobleached a) at 20°C and b) at 29°C. The point of photobleach is represented by the vertical line. y-axis, fluorescence recovery as a percentage of normalised pre-bleach levels. x-axis, time post-bleach in seconds.
Right. Live- The teased live muscle fibres photographed by fluorescence microscopy following the photobleach experiment.
Dys. Confirmation of the dystrophic nature of the tissue. Transverse sections of unfixed frozen quadriceps muscle from the experimental animals immunostained with 1/75 dilution of DURDC anti-dystrophin c-terminal peptide antisera and anti-rabbit-FITC secondary antibody.
Spec. Control stain for cytoskeletal integrity in the tissue sections. 1/40 anti-rat brain spectrin antibody. Scale bar represents 100μm.

Live

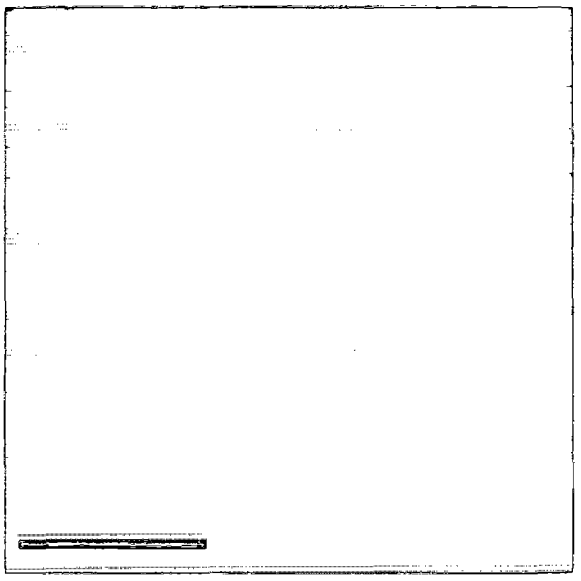

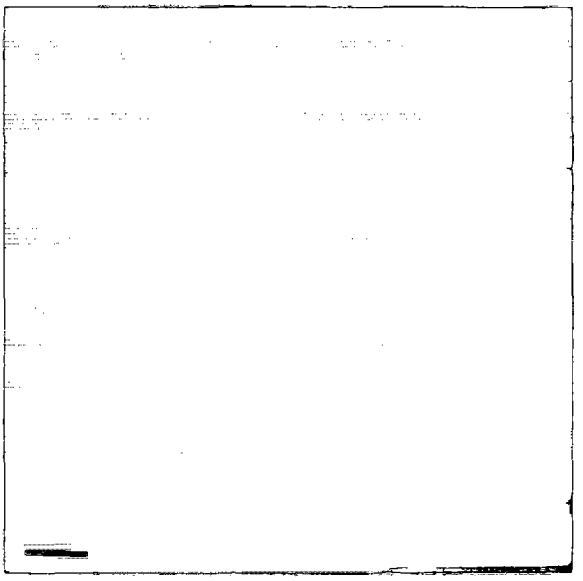

Dys

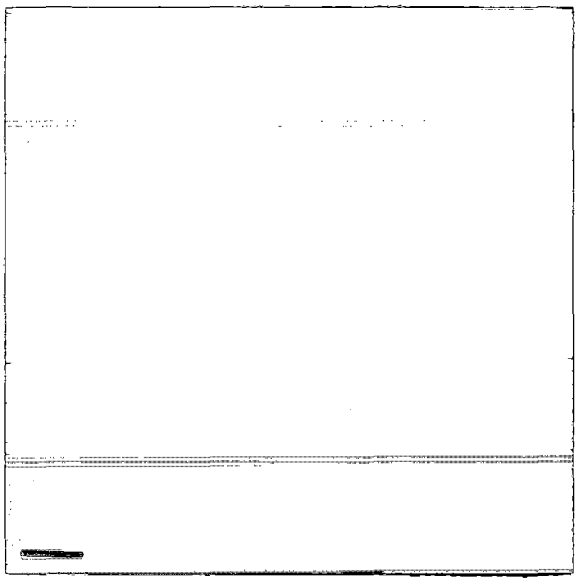

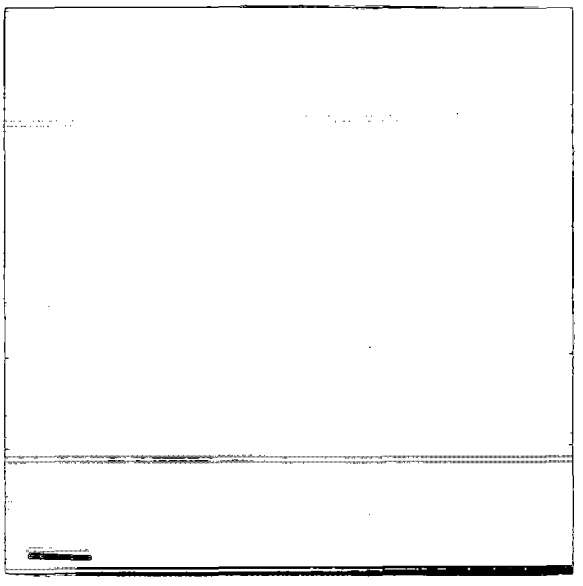

Spec

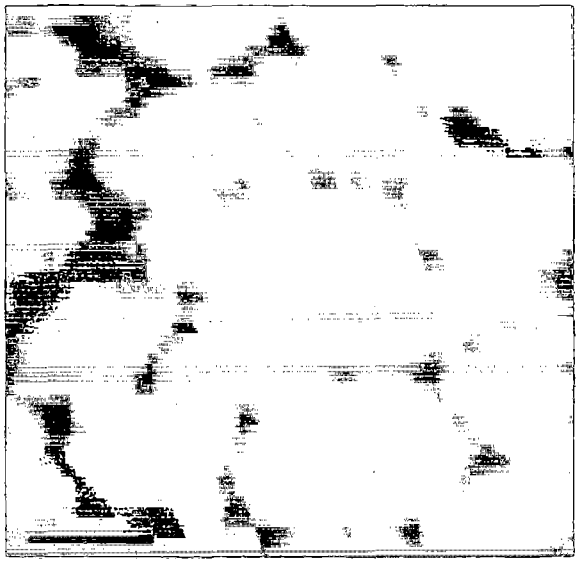

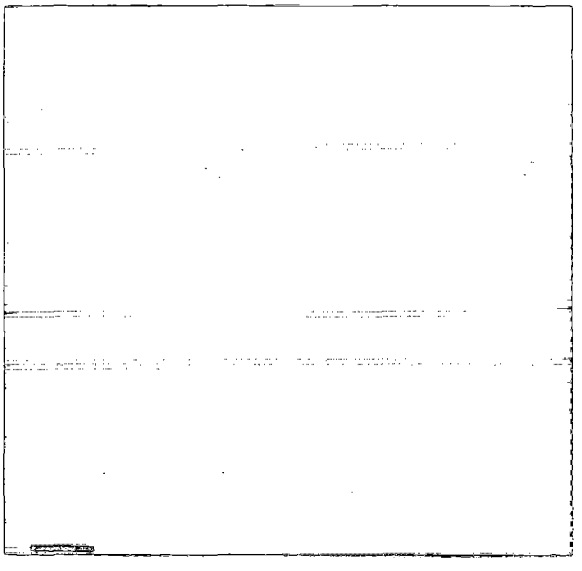

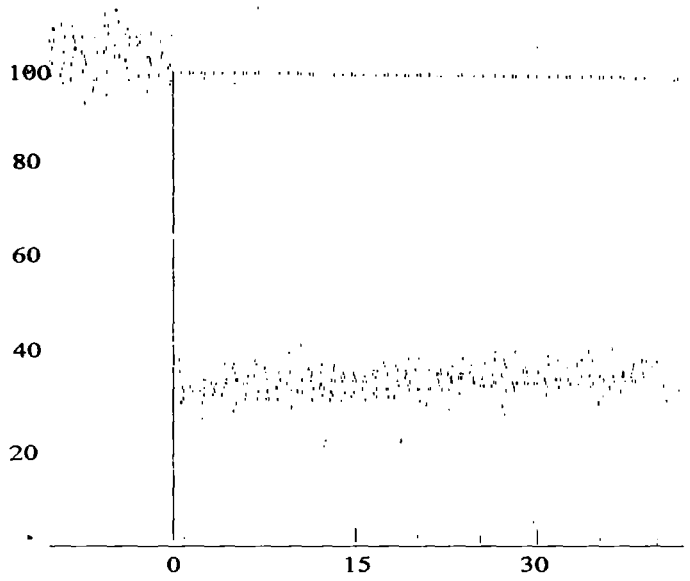

Figure 4.5 Mobility of S Con A receptors in normal muscle at 30°C.

S Con A binding glycoproteins were immobile on the surface of C57/BL 10 muscle tissue at 29±1°C.

Above. FPR recovery curve from live C57/BL 10 muscle fibre labelled with 25mM S Con A-FITC and photobleached at 29±1°C. The point of photobleach is represented by the vertical line. y-axis, fluorescence recovery as a percentage of normalised pre-bleach levels. x-axis, time post-bleach in seconds.

Right. Live S Con A -FITC. The photobleached tissue, photographed under fluorescence illumination at completion of the photobleach experiment.

Dystrophin. Confirmation of the presence of dystrophin in the tissue. Transverse sections of quadriceps muscle from the experimental animal, immunostained with 1/75 dilution of DURDC anti-dystrophin c-terminal peptide antisera and anti-rabbit-FITC secondary antibody.

Spectrin. Control stain for cytoskeletal integrity in the tissue sections. 1/40 anti-rat brain spectrin antibody. Scale bar represents 100μm, all photographs to the same scale.

Live
S ConA-FITC

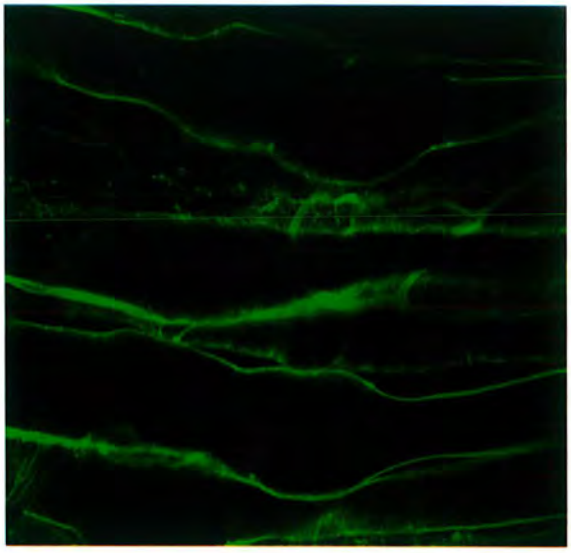

Dystrophin

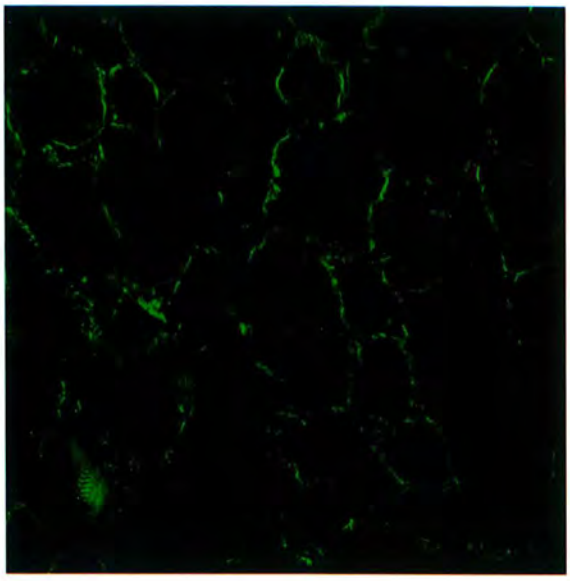

Spectrin

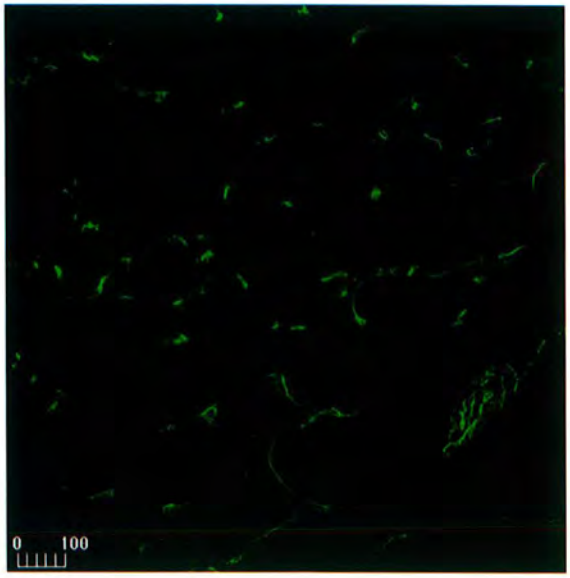

Temperature	Mouse Genotype.	n sample size	f, Fluorescence recovery (%).	T_D, recovery (sec).	D_L, Diffusion coefficient $x10^{-10}cm^2/sec.$
20±2°C	C57/BL 10	28	10.50 ± 2.32	4.39 ± 1.34	4.13 ± 1.21
	mdx	38	9.03 ± 1.87	4.18 ± 2.02	5.68 ± 3.00
29±1°C	C57/BL 10 (immobile)	7	10.1 ± 3.84	9.85 ± 6.15	2.95 ± 1.96
	(mobile)	17	68.4 ± 6.79	0.97 ± 0.42	24.8 ± 14.8
	mdx	24	10.58 ± 3.84	7.42 ± 3.59	3.00 ±1.20

Table 4.2 Effects of temperature on glycoprotein mobility as measured by FPR. Comparison of mobility of S Con A labelled surface glycoproteins at 20±2°C and 29±1°C. Values are mean ± s.e.m. of all pooled experiments. 20°C data reproduced from table 4.1.

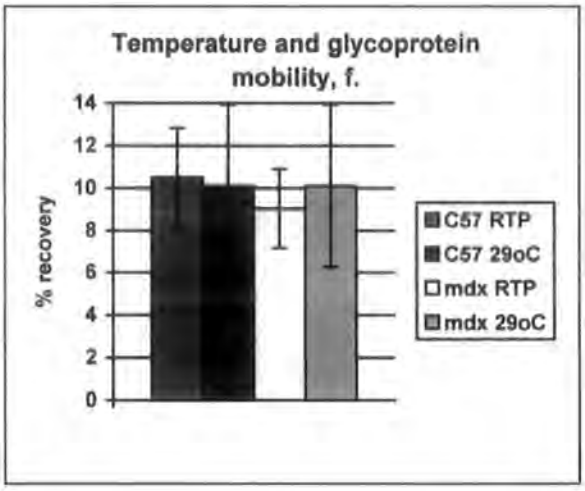

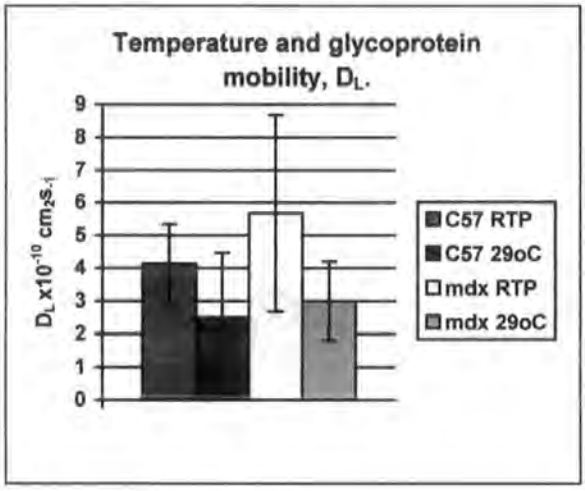

Figure 4.6 Comparison of temperature dependent glycoprotein mobility in C57/BL 10 and mdx muscle fibre membranes.

There was no significant difference in mobility of glycoproteins at ambient temperature and 29°C as determined by FPR.

Live fibres were labelled with 25nM S Con A- FITC and the mobility of labelled glycoproteins tracked by fluorescence recovery after photobleaching at ambient and 29°C. Sarcolemmal glycoproteins were immobile on the surface of mdx and C57BL 10 muscle fibres at both temperatures, f <12% within the limitations of detection ($D_L \geq 1x10^{-12}cm^2/s$) f, fluorescence recovery as a % of normalised pre-bleach levels; D_L, diffusion coefficient (cm^2/s^{-1}). Values are mean ± s.e.m. for all pooled data curves.

4.7.3 Mobile S Con A receptors.

A consistent fraction of mobile S Con A receptors were observed in the fibres of C57/Bl tissue (table 4.2, figure 4.7) at 30°C. This observation could illustrate diffusion of a population of mobile receptors within the membrane. However, several further lines of observation suggest this is not a mobile fluid phase in the surrounding gel phase. Firstly, the shape of mobile curves changes with time according to a characteristic pattern- a pattern that mirrored the mobility of glycoproteins on the surface of experimental fibres in the PBS system and which was interpreted as fibre breakdown (c.f. figure 4.1). Secondly, the mobile phases were never observed at the start of an experiment, only after around 15 minutes or longer. Additionally, once the receptors appeared mobile, it was rare for an immobile curve to be observed. If the fibres contained simultaneous gel and fluid phases, both mobile and immobile recovery curves should have been obtained at all stages in the data collection- the patterning should not have been time dependent. Thirdly, quality of fit of the diffusion equation curves during analysis of these later stage mobile experiments was variable, suggesting recovery was possibly artefactual rather than true diffusion based recovery in some cases.

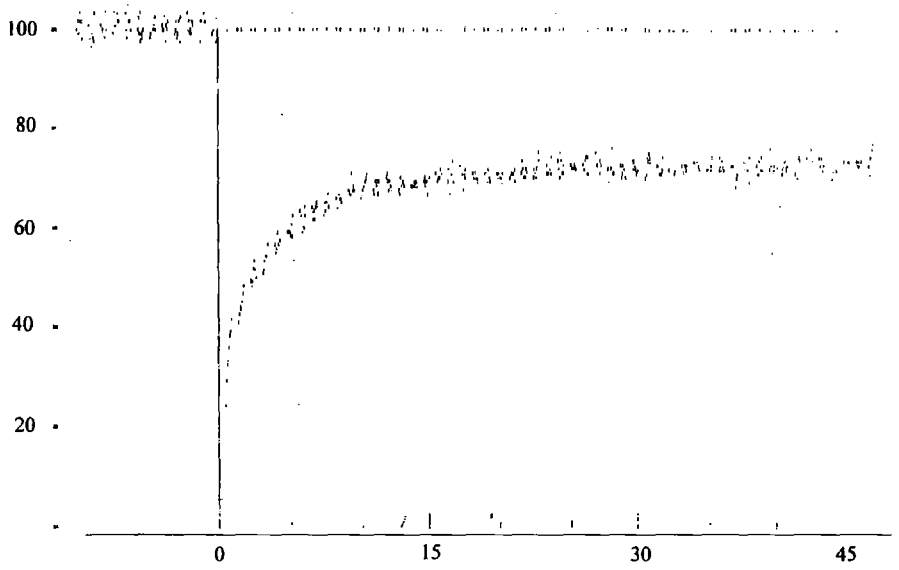

Figure 4.7 S Con A binding surface glycoproteins were mobile in some C57/BL muscle fibres at 29±1°C.

FPR recovery curve from live C57/BL muscle fibre labelled with 25mM S Con A-FITC and photobleached at 29±1°C. The point of photobleach is represented by the vertical line. y-axis, fluorescence recovery as a percentage of normalised pre-bleach levels. x-axis, time post-bleach in seconds.

4.7.3 a) Cytoskeletal breakdown.

One explanation for these curves is fibre movement in the dish. If the fibre is touched by the water immersion lens during focusing it can become detached from the blu-tack holding it in the petri-dish and start to move. Movement of the bleached area away from the monitoring region can give the false impression of fluorescence recovery. However, the shape of curve following fibre movement is distinctive, and didn't always match up to the observed data. A possible alternative explanation is cytoskeletal degradation in the fibres. In PBS the fibres were assumed to have broken down when the sudden transition to mobile glycoprotein behaviour was observed (*q.v.* section 4.2.1). This was no longer observed under ambient conditions once Krebs buffer was substituted. The increased experimental temperature may be accelerating the onset of fibre breakdown in these cases.

Evidence for the effects of cytoskeletal breakdown on membrane protein mobility has come from FPR experiments on Rous Sarcoma virus (RSV) infected chick embryo fibroblast cells (Boullier *et al*, 1992). Diffusion constants for S Con A-TmRh receptors were 2 to 3 times faster in RSV transformed cells than in normal chick embryo fibroblasts. In transformation-defective temperature-sensitive virus transformed cells, the increase in mobility occurred between 6 and 12 hours after induction of the virus. This corresponded temporally with the observed morphological changes in these cells (rounding up) that took place as the virus induced cytoskeletal breakdown and /or loss of extracellular fibronectin. The diffusion coefficient for Di-I was relatively consistent in these cells, indicating lipid fluidity was unchanged. Therefore loss of cytoskeletal interactions are proposed to have caused the observed increased in surface glycoprotein mobility.

Further experiments need to be done in order to test this suggestion in the muscle tissue. The monitoring of recovery behaviour before and after addition of cytoskeletal disrupters would show if the pattern of recovery observed here matches that of cytoskeletal degradation. The addition of sodium azide would accelerate fibre death, and so induce cytoskeletal degradation. Spontaneous fibre twitching is a further possibility for the recovery. In this case, however, the observed recovery would be expected to be rapid throughout rather than rapid then slow. Boosting the Mg^{2+} concentration from 1.2 to ~2mM in the surrounding tissue buffer would be sufficient to inhibit any spontaneous activity.

Such mobility was occasionally observed in mdx tissue too. However, in this case the pattern of recovery consistently failed to fit the diffusion equations within statistical tolerance. Furthermore, there was little consistency in the shape of recovery curves. Fibre movement seems the most likely cause of the 'temperature dependent' recovery in this case.

4.8 Discussion, Part 2.

Membrane surface glycoproteins were immobile in the tissues of both C57/BL and mdx dystrophic mice, at ambient temperature and 29°C. There was no significant difference in the extent or rate of fluorescence recovery in either system under either set of conditions. This suggests that in this system the diffusion of membrane surface glycoproteins is unaffected by an increase in temperature or the presence or absence of dystrophin. The absence of significant variation in dystrophin deficient mice is in accordance with the observations at 20°C. As discussed previously, this suggests that formation of a submembranous molecular fence is not a primary role of dystrophin and that dystrophin is not essential for restriction of glycoprotein mobility in muscle fibres.

4.8.1 Cytoskeletal restrictions on temperature induced mobility.

The lack of increased glycoprotein mobility with 9°C rise in temperature suggests there was no overall increase in membrane fluidity at the greater temperature. It is possible that, as originally assumed, surface glycoproteins are greatly restricted in their ability to move in the sarcolemma. Restrictions imposed by an underlying cytoskeletal meshwork, the extracellular matrix and direct anchoring of surface proteins to the cytoskeleton would prevent movement of component proteins, irrespective of temperature and surrounding membrane lipid fluidity. Immobility would be the conclusion reached by FPR methodology if the glycoproteins were freely diffusing- and indeed diffusing faster at higher temperature- but within confined domains smaller than the size of the bleach spot.

4.8.2 Phase transitions and mobility.

On the other hand, an observable increase in protein diffusion would be expected if the proteins were held in a semi-solid gel/fluid matrix at ambient temperature. Increasing the temperature should increase the proportion of total membrane protein that is free to diffuse (assuming some membrane proteins are untethered and freely diffusible) as a fraction of total membrane protein with restricted diffusion in gel rafts at RTP become surrounded by fluid phase lipids at 29°C. If, as with the protoplast system the viscosity of the fluid phase lipid is uniform with temperature, the rate of protein diffusion may not be expected to change at 29°C (D_L ~constant), but the mobile fraction would have been expected to increase.

It was possible that the lipids in the experimental membranes exist within a mixture of gel and fluid phases over the temperature range, and the free diffusing proteins partition preferentially into the immobile gel phase [rather than equally distributed between gel and fluid phases- this would have produced two parallel patterns of protein recovery data, one fluid, one gel phase, which was not

observed]. In this case, as the temperature increases there will be limited increase in protein diffusion. However, as the proportion of gel phase lipid reaches a minimum, spatial constraints will drive proteins into the lipid phase. Theoretically, this gel saturation point may not have been reached by 29°C and so the protein could have remained predominantly in the gel phase and appeared immobile. Physical observation of the fibres post-bleach argue against this, however. The surfaces of the muscle fibres appeared uniformly stained with S Con A- FITC at both temperatures. Were the proteins partitioned preferentially into gel-phase domains, some irregularity in membrane staining might be expected- especially at the higher temperature where the proportion of total membrane in the gel phase would be smaller and therefore S Con A-FITC fluorescence would be restricted to confined domains. To unequivocally rule this out the muscle fibres would have had to be warmed to greater temperature and the experiment repeated. Unfortunately, the heating apparatus on the FPR equipment was unable to facilitate this.

4.9 Temperature conclusions.

It seems from these experiments that temperature was not the main influence upon membrane surface glycoprotein behaviour in the original experimental system. Either the cytoskeleton is tethering or restricting protein diffusion in the membrane or some other as yet unidentified factor is having the same effect. However, the possibility remains that lipid phase fluidity could also be affecting the mobility of the glycoproteins.

The only way to firmly establish whether the membrane fluidity was compromised in the experimental fibres and whether or not temperature was the main influence on surface glycoprotein mobility was to look at mobility of the membrane lipids under the same experimental conditions at 20 and 29°C. If two categories of membrane lipid behaviour were observed- one gel, one fluid- then temperature dependent protein partitioning could be an explanation for the glycoprotein data. Similarly, if the lipid matrix is more viscous at room temperature (or possibly in a gel state) and more fluid at 29°C, then a) protein diffusion could be limited by (gel/fluid) lipid viscosity, b) preferential partitioning of proteins into the gel phase is a possible theory and c) cytoskeletal / ECM influences could be regulating surface glycoprotein immobility.

- **Part 3- Effects of temperature on lipid fluidity in the experimental system.**

4.10 Introduction.

Increasing the experimental temperature had little appreciable effect on the mobility of surface glycoproteins in plasma membranes of both mdx and C57 muscle. This could be a reflection of imposed restrictions upon membrane glycoprotein mobility in the system. Direct anchoring of membrane proteins to the cytoskeleton would render them immobile, irrespective of the measuring temperature. Similarly if the proteins were confined to micrometer scale domains smaller then the bleach spot, they would appear immobile by FPR - even though they may be diffusing faster within their small domains at the greater temperature. As discussed earlier, in plant protoplasts the melting of a mixture of co-existent gel and fluid domains ensures the mobile proteins diffuse at constant rate, regardless of external temperature constraints. It is theoretically possible that such a system is in place here, though such systems are rare in mammalian cells and have not previously been described for muscle.

To fully differentiate between solid gel/lipid phases in the membrane restricting protein mobility and the effects of tethering or the cytoskeleton it was necessary to measure mobility of membrane lipids in the two systems at different temperatures. Lipid mobility in the muscle fibres was monitored using the fluorescent lipid analogue 5-(N-octa-decanoyl) aminofluorescein (ODAF). Whilst 1,1'-dihexadecyl-3,3,3',3'-tetramethylindocarbocyanine (Di-I) is commonly used as a lipid reporter, Ladha *et al* (1997) found that Di-I only stained the membranes of dead or permeabilised cells. ODAF in contrast stained both live and dead cells, with differential staining patterning between the two cell types. Additionally, ODAF analysis can be performed using a fluorescein optical filter set and was therefore more suited to this experimental system.

4.10.1 Lipid mobility in sperm plasma membranes.

An indication of the expected results came from studies of ODAF lipid analogue mobility in the membranes of spermatozoa (Ladha *et al*, 1997). In live sperm from several different species, increasing membrane temperature increases lipid phase fluidity as measured by FPR (figure 4.8). The magnitude of fluidity increase is non-linear with temperature, with ~4 times greater increase in rates of lipid analogue diffusion over the sperm head domain between 20 and 37°C than between 5 and 20°C. The different cellular membrane domains demonstrated differing sensitivity to temperature suggesting that, in addition to proteins, the membrane lipids are arranged into specialised domains in these cell types. % recovery of fluorescence was high across all regions of the sperm at all temperatures (>90%).

4.10.2 Lipid mobility in muscle plasma membranes.

It would therefore be expected that the fluidity of membrane lipids in this experimental muscle membrane system would show similar regulation by temperature. The extrajunctional muscle membrane is currently believed to be homogeneous with respect to lipid composition therefore regionalised domain variations in temperature would not be expected, but some overall rise in fluidity would be expected. The 29°C limit on measuring temperature imposed by the apparatus would not give rise to complete membrane fluidity, but should produce some measurable increase over fluidity at ambient temperature if temperature is a limiting factor. Given that, despite regionalisation of the sperm membrane the lipids showed high levels of recovery throughout, it would be expected that lipid diffusion would be unhindered by cytoskeletal barriers under the muscle surface and so the levels of fluorescence recovery from the lipid analogue would be significant (>50%).

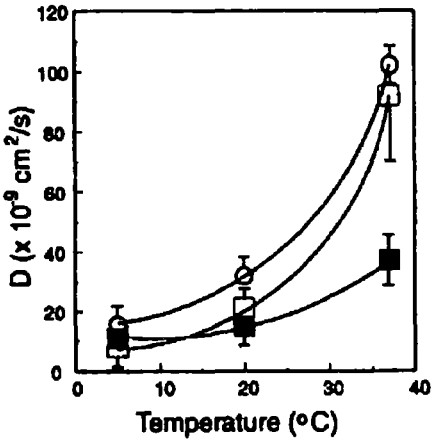

Figure 4.8 Effects of temperature on lateral diffusion coefficients of ODAF in live-pattern bull spermatozoa. ODAF diffusion was more temperature-responsive on the acrosome (circles) and postacrosome (hollow squares) cellular regions than on the midpiece (black circles). Values are means ± s.e.m. of 3 separate experiments. Figure reproduced from Ladha *et al*, (1997).

4.11 Results.

To measure lipid phase dynamics in the experimental system, muscle fibres from C57 and mdx mice were extracted as for the glycoprotein studies. Fibres were labelled with a 1:1 ratio of oxygenated Krebs buffer: 3.5μM ODAF in 1% ethanol/oxygenated Krebs buffer for 15 minutes at monitoring temperature, then subjected to photobleach analysis. Levels of fluorescence reporter were kept to the minimum necessary to generate a signal for FPR so as to minimise the perturbing effects of the dye intercalating into the membrane.

4.11.1 Mobility of membrane lipids.

The results of the experiments are shown in figure 4.9 and table 4.3.

Incorporation of the lipid label appeared uniform across the fibres (figure 4.9 Live). Bright patches of unincorporated dye were minimal. There was no indication of unincorporated crystalline dye on the surface of the fibres- as is often found with Di-I fluorescent lipid marker- therefore measurement of dye crystal mobility was avoided.

As with the 29°C glycoprotein experiments, the small levels of fluorescence recovery obtained during many of the individual experiments prevented fitting of the recovery data to the diffusion equation within the limits of statistical tolerance. In these cases the % recovery was determined by eye from the experimental curves. Diffusion coefficients could not be calculated for curves where this was a problem, therefore $n_{DL}<n_{total}$ and the diffusion coefficients given in table 4.3 have large errors. For two of the sets of data the proportion of non-analysable curves was considerably greater than those which could be fitted. In these cases, the diffusion coefficient and/or half time of recovery for the remaining data may not be a true representation of the whole and the value of D_L is given as 'immobile' in table 4.3.

Temperature	**Mouse Genotype.**	**n sample size**	**f, Fluorescence recovery (%).**	**T_D, recovery (sec).**	**D_L, Diffusion coefficient x10^{-10}cm^2/sec.**
22±1°C	C57/BL 10	21	8.43 ± 3.86	8.01 ± 6.01-	immobile
23±1°C	mdx	25	19.2 ± 7.5	18.00 ± 8.26	1.44 ± 0.91
29±1°C	C57/BL 10	20	10.3 ± 3.70	7.74 ± 4.07	3.58 ± 1.96
29±1°C	mdx	22	10.3 ± 4.86	10.9 ± 6.6	immobile

Table 4.3. Effects of temperature on lipid mobility as measured by FPR. Comparison of mobility of ODAF fluorescent lipid analogue at ambient and 29±1°C. Values are the mean ± s.e.m. of all pooled data curves.

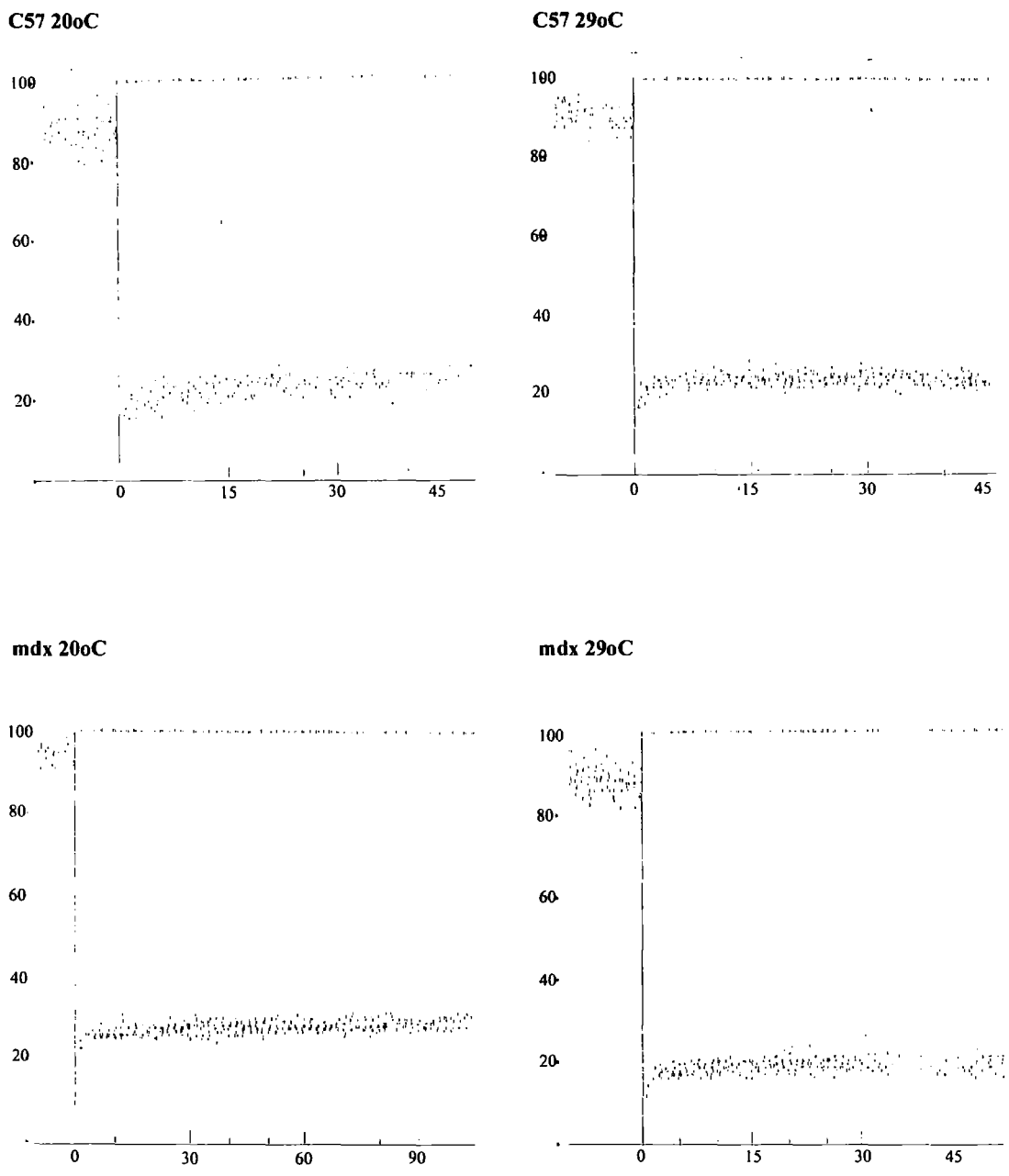

Figure 4.9 Effects of temperature on ODAF lipid analogue mobility.
The membrane lipid analogue ODAF appeared immobile in the membranes of mouse muscle tissue at both 20 and 29°C as determined by FPR. a) C57/BL10, 20°C. b) C57/BL10, 29°C. c) mdx, 20°C and d) mdx, 29°C.

Above. FPR recovery curves from live C57/BL 10 and mdx muscle fibres labelled with 1.75μM ODAF fluorescent lipid analogue and photobleached at 20±1°C and 29±1°C. The point of photobleach is represented by the vertical line. y-axis, fluorescence recovery as a percentage of normalised pre-bleach levels. x-axis, time post-bleach in seconds.

Right. Live- The same live ODAF stained muscle fibres photographed under fluorescence illumination post-photobleach.
Dys- Confirmation of the presence of dystrophin in the tissue. Transverse sections of quadriceps muscle from the experimental animal, immunostained with 1/75 dilution of DURDC anti-dystrophin c-terminal peptide antisera and anti-rabbit-FITC secondary antibody.
Spec- Control stain for cytoskeletal integrity in the tissue sections. 1/40 anti-rat brain spectrin antibody. Scale bar represents 100μm, all pictures to same scale.

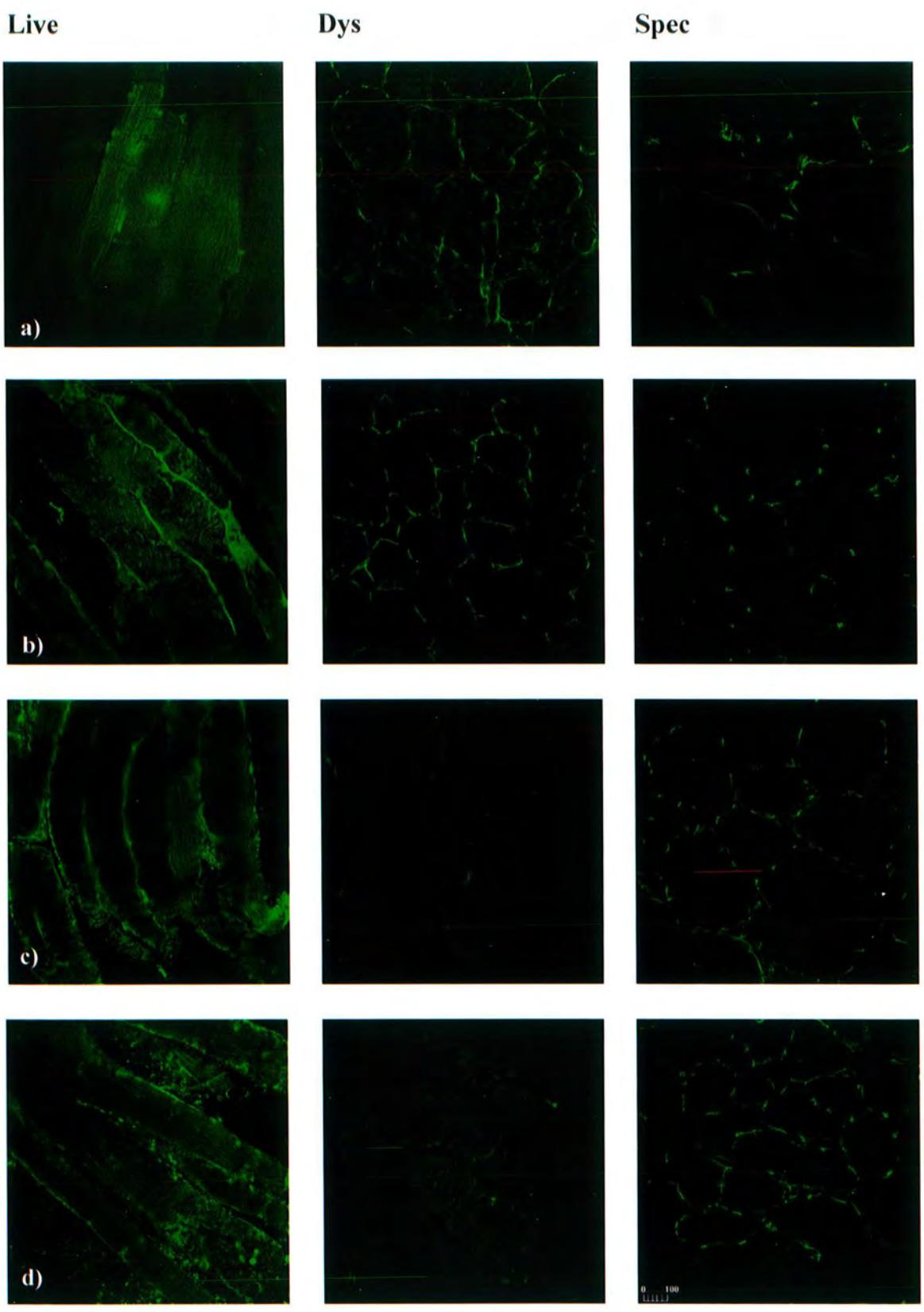
Live
Dys
Spec
a)
b)
c)
d)
0
100

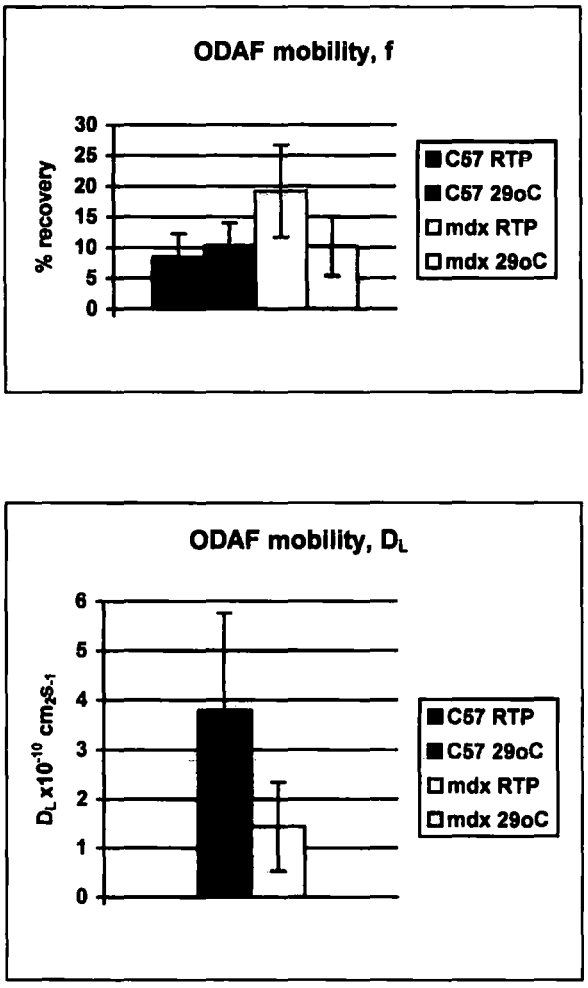

Figure 4.10 The fluorescent lipid analogue ODAF is immobile in the plasma membrane of experimental muscle fibres at ambient temperature and 29°C as measured by FPR.

Comparison of lipid phase fluidity in C57/BL 10 and mdx muscle fibre membranes. Live fibre membranes were labelled with 1.75μM ODAF and the mobility of the fluorescent lipid analogue tracked by fluorescence recovery after photobleaching at ambient and 29°C. The ODAF marker was immobile on the surface of mdx and C57BL 10 muscle fibres at both temperatures within the limitations of detection ($D_L \geq 1x10^{-12}cm^2/s$) f, fluorescence recovery as a % of normalised pre-bleach levels; D_L, diffusion coefficient (cm^2/s^{-1}). Values represent mean ± s.e.m. of all pooled data curves.

The ODAF labelled muscle membranes of C57 and mdx mice showed little recovery of fluorescence when subjected to FPR analysis at ambient temperature. (table 4.3, figure 4.9, figure 4.10). The lipid phase was therefore immobile in the membranes of these tissues (recovery ~10% for C57 and 18% for

mdx muscle). The rate of diffusion of the lipid phase was significantly slower than that expected for membrane lipids (in the region of ~$2x10^{-10}$ cm^2s^{-1} , c.f. expected values of ~10^{-9} cm^2s^{-1}). Though care must be taken in interpreting rates of diffusion given such low levels of recovery, this suggests the lipid phase that was free to move was hindered in its passage- perhaps by the large regions of immobile phase. Increasing the labelling and photobleaching temperature to ~29°C similarly had little effect on the mobility of the lipid phase- either upon the fraction of mobile species (lipid phase on the whole remaining immobile) or on the rate of diffusion for the small mobile fraction where this could be calculated. Mobility of the ODAF lipid analogue therefore indicated the lipid phase was immobile in the experimental membranes at 20 and 29°C.

4.11.2 Effects of dystrophin on lipid mobility.

The presence or absence of dystrophin made no significant difference to the mobility of the membrane lipid phase within the measuring errors of the experiment, (table 4.3, figure 4.9, figure 4.10). ODAF fluorescence showed only 10% recovery at 29°C, regardless of whether dystrophin was present or not, suggesting that dystrophin does not have a major influence upon lipid phase mobility in this particular system.

4.11.3 Immobile lipid phases.

The failure of the membrane constituents to show any sensitivity to external temperature was a matter of concern. Though membrane proteins could conceivably be anchored in place by an underlying matrix, direct binding to the cytoskeleton or ECM interactions, the immobility of the membrane lipid phase is harder to rationalise. Membrane lipids would have been expected to show considerably greater than 10% recovery at room temperature. Had lipids been immobilised in gel phase states under ambient conditions, an increased mobile fraction and an increased diffusion rate would have been expected at 29°C. However, this was not observed. Errors of membrane labelling, e.g. failure of probe to intercalate into the membrane or FPR measurement of the ECM constituents would lead to spurious results and misinterpretation of membrane lipid behaviour. An alternative explanation pertains to the membrane itself- perhaps the probe immobility is indicative of the membrane fluidity, and the proteins and lipids have become immobilised in the experimental fibres.

Such an immobilised state has been reported for spermatozoon membranes labelled with ODAF and subjected to FPR (Wolfe *et al*, 1998). It was found that lipid diffusion in the plasma membrane of live spermatozoa varied significantly between surface domains, because of either compositional heterogeneity, or differences in bilayer disposition, or the presence of intramembranous barriers that impede free exchange between domains. This diffusion was temperature sensitive as would be

expected for intercalation of the reporter probe into the lipid phase. In dead or permeabilised cells on the other hand, the position was completely different. The dead cells (illustrated by differential patterning of ODAF staining and permeability to propidium iodide vital dye) contained large immobile phases of lipid as measured by ODAF FPR. These immobile phases were virtually insensitive to experimental temperature.

4.11.4 Viability of experimental muscle.

Mdx muscle fibres from the completion of a 29°C ODAF experiment were vital stained with 0.1% trypan blue to see if the fibres were viable at the end of an experimental run. This was 1hour 15 minutes after the initial dissection from the animal (figure 4.11). The vast majority of muscle fibres took up the blue dye into both their nuclei and cytosol. By the end of the experiment, therefore, the majority of muscle fibres were no longer viable.

Repeating the vital stain with freshly dissected and teased muscle showed that ~50% of the fibres had taken up the blue dye. These were therefore compromised in integrity during preparation. Over the duration of the FPR experiment, the remainder of the fibres had died off. Deterioration of the tissue during mobility measurements was noted particularly for glycoproteins, as the pattern of recovery changed towards the ends of experiments - a sign taken to indicate fibre breakdown. As a consequence of this, care was always taken to collect data within 1hr 20 min of dissection, and to place more emphasis on the data from early FPR experiments than those later on in a run.

The fibres that remained viable were randomly distributed throughout the tissue sample. It would not therefore be possible to knowingly select a viable fibre from the mass under the microscope. This observation that 50% of the fibres had taken up the dye therefore fails to match the experimental data from FPR. It would be expected that 50% of the fibres would possess freely diffusing lipids concomitant with live healthy fibres and a fluid lipid phase. The remaining 50% might be expected to show immobile lipid rafts. Instead almost all fibres failed to recover fluorescence after photobleaching. Those fibres that did show some recovery appeared to have moved in the dish and their curves failed to fit the diffusion equation. The immobility data would match up to viability observations if the fibres were only damaged sufficiently to take up the dye at a late stage in fibre death, but the immobile lipid phases developed sooner.

Figure 4.11 Integrity of muscle fibres was compromised during experimental preparation.
Dissected and teased muscle fibres vital stained with 0.5% Trypan blue, 1hr 15 minutes after dissection. Permeabilised fibres take up the stain. Scale bar represents 100μm.

Figure 4.12 Surface of live C57/Bl muscle fibres stained with fluorescent lectin.
The fluorescent S Con A lectin marker stains the glycoproteins of neurons and the extracellular matrix, in addition to the surface of the muscle fibre membrane. Scale bar represents 100μm.

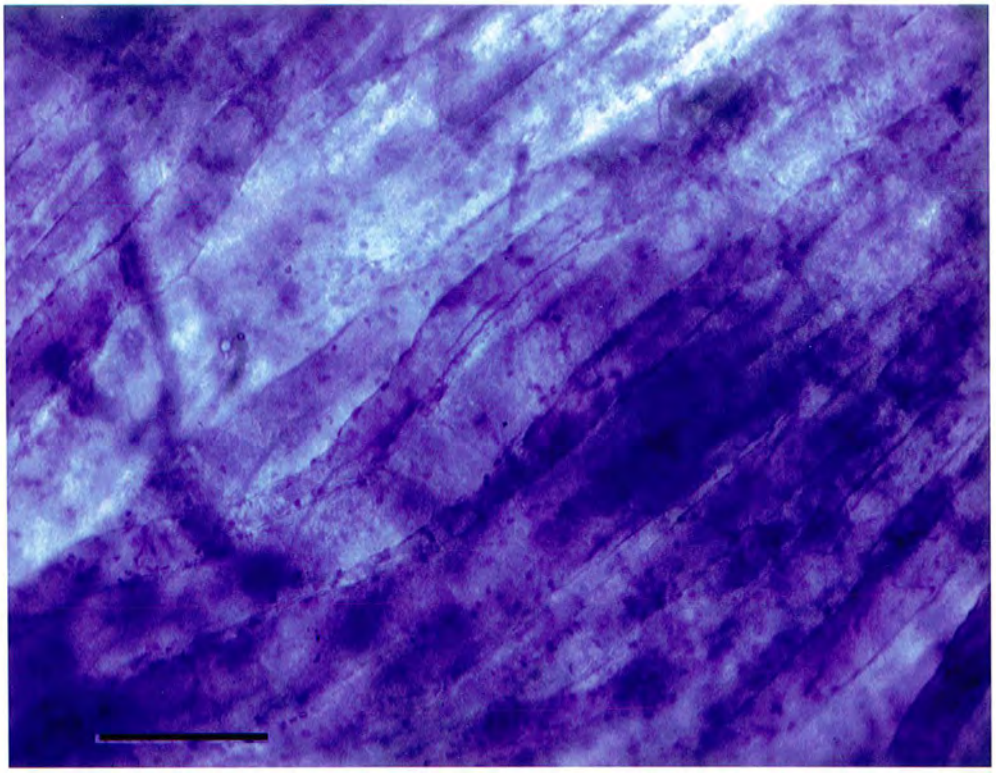

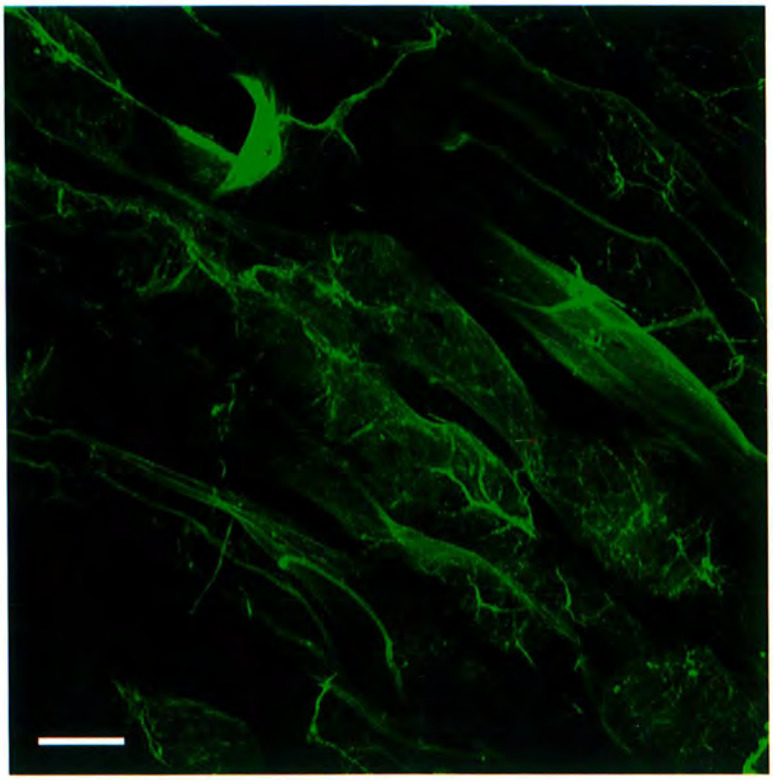

4.12 Discussion Part 3, effects of temperature on lipid mobility.

This study set out to quantify the contribution dystrophin makes to non-specific regulation and restriction of muscle membrane components through formation of a submembranous 'molecular fence'. Dystrophin shows high sequence and structural homology to the cytoskeletal protein spectrin and is found beneath the plasma membrane in muscle fibres. These characteristics suggested dystrophin, like spectrin, could be involved in organisation of the muscle membrane- acting as a direct anchor of specific membrane proteins or through steric restrictions on mobility.

The experiments presented here found both glycoproteins and lipids were in a temperature-insensitive phase in the muscle membranes. This was the case in the presence and absence of dystrophin. Whilst it is theoretically possible that 90% of the surface glycoproteins of mouse muscle are held rigidly in place by a specific tethering complex or by the underlying cytoskeleton, it seems unlikely that the lipid phases are also solid in the true physiological state. It was expected that membrane lipids would show at least some degree of mobility in the muscle fibre membranes. Instead, the ODAF experiment revealed the experimental membrane system to be rigid.

4.13 Experimental shortcomings.

It is highly unlikely that this FPR data truly reflects the physiological behaviour of live muscle membranes. It is more likely indicative of shortcomings in the experimental set up.

4.13.1 FPR labelling procedure.

It is possible that the lack of recovery observed results from failure of the fluorescent markers to incorporate into the membranes. In the case of the S Con A-FITC, extracellular regions and particularly regions of the ECM were seen by confocal microscopy to have taken up the probe. Extracellular staining was invariably several fold brighter than membranous staining as seen by FPR photon counts and fluorescence microscopy. Care was taken during data collection to avoid experiments in abnormally bright regions, so ECM measurements should not have unduly contributed to immobility. Similarly the myelin sheaths of neurons readily incorporated the dyes, but visualisation of the fibre before photobleaching prevented data acquisition from nerves.

4.13.2 Probe cross linking.

Cross linkage of membrane proteins by the lectin could have lead to the observed glycoprotein immobility. Multivalent lectins have the potential to bind proteins together into large immobile rafts if added to the cells at high enough concentrations. 50μg/ml Con A was sufficient to completely immobilise the fluorescent components of spherocytic red blood cell membranes as measured by FPR (Sheetz *et al*, 1980). Whilst this could provide an explanation for the immobility of glycoproteins in the system, the observed immobility of the lipid phase cannot be rationalised this way. The ODAF reporter probe does not cross link membrane proteins or lipids. Cross linking could have contributed to protein immobility, but is unlikely to be the main cause.

4.13.3 Non specific FPR probe-membrane interactions.

Electrostatic binding of the probes to the surface, rather than incorporation into the bilayers may have given rise to the observed data. Labels were added to fibres at concentrations and in carrier solvents previously reported to give successful membrane incorporation (e.g. Wolfe *et al*, 1998) and visualisation of the fibres post-bleach suggested the membranes were labelled, but such a close electrostatic association cannot be ruled out completely.

Electrostatic binding of probe to membrane could be proposed for the ODAF lipid analogue. The effects of temperature on ODAF mobility is used as a control for probe intercalation in FPR experiments- membrane inserted probe would be expected to show temperature dependent changes in mobility whereas non-specifically associated probe held in place by ionic interactions at the cell surface would be less temperature regulated (Ladha *et al*, 1997, Wolfe *et al*, 1998). However, the methodology used here for staining the tissue fibre membranes was applied successfully to lipid domains in other tissues which did show temperature dependent regulation (Ladha *et al*, 1997). Whilst there is invariably some tissue-tissue variation in biological systems, it seems strange that this muscle system should be so unique that neither the glycoprotein probes nor the lipid marker associated specifically with membrane species under conditions that have labelled successfully in many other systems. Though lack of specific labelling cannot be ruled out, it is possible that other factors are contributing to the observed immobility.

4.13.4 The FPR experimental focal plane and ECM measurements.

The differentiation between the plane of the membrane and the ECM is less clearly defined during photobleaching than under a fluorescent microscope as a visual check of the focal plane is not possible. The photobleach focal plane was selected as the plane with the greatest photon counts- believed to

correspond to the plane of the membrane, as the probes are supposedly membrane markers. All fibres were checked under phase contrast to confirm approximate alignment with the membranes (the plane of focus with fluorescence and phase were marginally different therefore this could only be approximated). But, given the intimate relationship between membrane and ECM and the spatial resolution of the FPR optics, ECM photobleaching cannot be ruled out completely. If experiments were in fact on the extracellular matrix rather than the membrane, then perhaps the immobility is less surprising. The ECM is a highly cross linked latticework of proteins, glycoproteins, glycolipids and proteoglycans. The stability of the cross linkages imparts the structural integrity and rigidity to the ECM and surrounding cells. The constituents of this matrix would be expected to be fixed as a consequence of function, rather than freely diffusing. Immobility of matrix components as seen by FPR would be expected.

If it is the case that ECM components have been studied here instead of muscle fibre membranes, it is interesting to note that the absence of dystrophin had no effect on the organisation of the matrix as determined by FPR. Dystrophin is associated with merosin (M-laminin) in the ECM of the muscle fibres, via α- and β-dystroglycan in the DAG complex (*q.v.* figure 1.3). This association, linking the integral actin contractile fibres of the muscle fibre with the surrounding extracellular matrix is understood to impart structural rigidity to the muscle fibre and prevent stress induced damage. Indeed, this is presently thought to be the primary function of dystrophin (section 1.1.7 c, Petrof *et al*, 1993). Merosin deficiency produces congenital muscular dystrophy (reviewed in Campbell, 1995). However, if this data pertains to the ECM, it suggests disruption of the contractile fibre-ECM link does not compromise the structural integrity of the ECM itself. Whilst DAG proteins are down regulated in mdx mice, this may not significantly affect the cross linking of the matrix. If the ECM has been studied here, it suggests the bridging function of the dystrophin/DAG complex is important for giving structural strength to muscle fibres, but not for organisation or function of the ECM components.

Confirmation of the ECM nature of the results could come by stripping the ECM from the fibres and repeating the FPR experiments. If the patterns of lipid and protein mobility shift dramatically from the observations thus far, then it is possible that the ECM has been studied. However, confusion is then possible between this interpretation and the suggestion the ECM is anchoring membrane proteins in place. Acquisition of fluorescent ECM component probes and repetition of the photobleach experiments would provide definitive data on the behaviour of the ECM in the fibres, and illustrate any significant effects of dystrophin deficiency and indicate whether this study parallels ECM behaviour.

4.13.5 Role of the ECM in protein immobilisation.

As discussed earlier, the extracellular matrix could be immobilising membrane components in this system. It is unlikely that the ECM would contribute directly to restriction of membrane lipids, but if

the ECM could significantly reduce protein lateral mobility, movement of lipids through the dense immobile proteins would be sterically hindered.

High levels of extracellular matrix constituents can hinder measurement of mobile surface glycoproteins. For example the high levels of fibronectin on Rous sarcoma virus transformed chick embryo fibroblasts masked mobility of the free membrane proteins as measured by FPR (Boullier *et al*, 1992). To overcome this problem the same spot was bleached four times on the membrane surface. The initial bleach gave an indication of the total portion of immobile proteins (understood to be ECM proteins such as fibronectin), about 60% for normal chick embryo fibroblast cells. Subsequent bleaches traced the mobility of just the freely diffusing proteins in the membrane (as the immobile proteins had been bleached irreversibly in the first round). By the fourth bleach 83% of the total fluorescence was recovering. The diffusion coefficients of the mobile fractions remained constant throughout and therefore behaviour of the same mobile protein species was studied in each case.

As dystrophin is believed to interact directly with the extracellular matrix, the effects of dystrophin deficiency on the mobilities of ECM proteins is of interest. However, given the lack of observed differences, the complex ECM surrounding muscle fibres and the high levels of immobile proteins found in the glycoprotein study, this repeat bleach methodology is worthy of consideration for further experiments to measure mobility of the mobile fraction.

4.13.6 Non-viability of experimental fibres.

The most important finding of this study was that tissue integrity could have been compromised during excision and preparation of the fibres, and was undoubtedly compromised by the end of data collection. In vitro muscle systems are notoriously difficult to sustain over time- particularly due to incomplete oxygenation of central fibres. The large shifts in membrane glycoprotein mobility, from immobile to rapid and then slow mobility were taken to indicate fibre death in a PBS buffer system. When this was no longer observed in oxygenated Krebs buffer the fibres were believed to be intact. The reappearance of this behaviour at 29°C was thought to reflect an accelerated rate of tissue breakdown at the greater temperature, and therefore data was only analysed before this point. Unfortunately it may be this observed shift in mobility was either artefactual (maybe as a result of fibre motion), or indicative of a later stage in fibre breakdown, possibly cytoskeletal degradation. Cytoskeletal breakdown is a characteristic feature of cell death- dying cells in culture are often seen to round up shortly before they detach from the substratum , and as discussed earlier, will give rise to increased protein mobility.

4.13.7 Lipid phase immobility and cell death.

Likewise, the suggested presence of large areas of an immobile lipid phase points towards dead fibres. Immobile phase lipids are found in some specialised cells and organelles (Metcalf *et al*, 1986), particularly those that function over a range of temperatures. Though immobility in the muscle fibres could be interpreted as low temperature partitioning between gel and fluid phases at ambient temperature, the vital staining and failure of the system to respond to temperature argues against this.

Equivalent findings are apparent in dead or permeabilised spermatozoa. Upon cell death a large immobile lipid phase (recovery <15%) develops across the plasma membrane domains, in contrast to >90% lipid phase recovery in healthy motile sperm. (Ladha *et al*, 1997, Wolfe *et al*, 1998). It was impossible to calculate values of diffusion coefficients for the dead sperm as, like here, the small levels of recovery gave wide ranging values of D. The sperm membrane rigidity was found to be completely temperature insensitive in the dead cells, even up to 50°C (R. Jones, personal communication). The membrane lipid phase in this study was also immobile and not reversed by increased temperature (although it was not possible to test at temperatures>30°C), indicative of fibre death. The immobility was not a feature of the ODAF probe in sperm membranes as fluorescein phosphatidyl-ethanolamine gave the same results in permeabilised sperm.

Why lipids form immobile rafts in dead cells still remains to be answered. Possible explanations for the formation of the immobile fractions are reviewed in Ladha *et al* (1997) and Wolfe *et al* (1998). They include 1. Formation of stable non-bilayer lipid structures such as hexagonal II-type lipids- formation of such structures is acyl chain length, pH and salt concentration dependent. The stability of the structures could account for their persistence over time. 2. Interaction of lipids with the submembranous actin cytoskeleton via transmembrane proteins. 3. Localised variations in cholesterol composition- cholesterol interacts with unsaturated fattyacyl chains and will consequently affect rates of lipid diffusion. 4. Loss of transmembrane asymmetry following depletion of ATP and inactivation of ATP dependent flippases. 5. Fatty acyl chain shortening, cross linking and decomposition induced by oxygen free radicals- cross linking of unsaturated acyl chains will give rigidification of the membrane. Finally, 6. Ca^{2+} mediated crosslinking has been suggested- Ca^{2+} ions can cross link negatively charged phospholipids and sulphogalactosylglycerolipids by forming salt bridges with the polar head groups. This leads to microaggregation into 'lipid blocks'. Leakage of calcium from damaged sarcoplasmic reticulum or the 25mM Ca^{2+} ions in the Krebs buffer could induce crosslinkage in the muscle. However, lipid blocks are temperature sensitive, unlike the immobile fraction here.

4.13.8 Potential causes of muscle fibre breakdown.

4.13.8 a) Damage during dissection.

Tissue viability could be compromised at several different points in the study. Firstly, fibres can become damaged during excision of the muscle. Care was taken to remove muscle by the tendon and minimise fibre cutting. Whilst this was a simple procedure at the achilles tendon it was more complex near the knee joint and some fibre damage was unavoidable. It may be best if future photobleach experiments concentrate exclusively at the regions of muscle near intact tendons where fibres are more likely to be whole.

4.13.8 b) Buffer system.

Secondly, the oxygenated Kreb's buffer may be unable to sustain the tissue for any length of time. As stated above, it was believed the absence of sudden time dependent shifts in glycoprotein mobility in the Krebs buffer system compared with a PBS/sucrose buffer indicated extended tissue life in the Krebs buffer. The composition of Krebs buffer, though more complex in metal ion constituents than PBS, may be inadequate for long time scales. Replacement with a tissue culture media/aminoacid/salt type buffer may be more appropriate for future experiments. The levels of Ca^{2+}, O_2 and pH of the buffer could be problematic too. The Ca^{2+} only dissolves in the Krebs once the buffer is adequately oxygenated with $95\%O_2/5\%CO_2$. During the measuring stage, some Ca^{2+} ions did come out of solution. The pH of the buffer could have shifted and/or the oxygen been depleted by half an hour into the experiment. Re-oxygenation of the buffer, or replacement with fresh buffer mid-experiment is theoretically possible, but in practice tended to detach the tissue from the petri dish so that no more FPR data could be collected.

4.13.8 c) Buffer system and calcium.

The concentration of Ca^{2+} ions in the Krebs (25mM) may be too high. If the tissue is already compromised, e.g. following damage during dissection, taking up elevated extracellular calcium may trigger cell death.

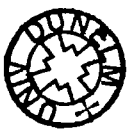

It is now well established that uptake of abnormally high levels of extracellular calcium damages muscle fibres, and influx of calcium down an extra to intracelluar concentration gradient was proposed as a potential cause of DMD (reviewed in Jackson, 1993). A minor change in plasma membrane permeability could allow a relatively large amount of calcium to enter the cell. High external calcium concentrations of the order of 3-10mM increase cytosolic creatine kinase release from isolated animal and human muscle and are therefore sufficient to cause fibre damage. Within the muscle fibre calcium

causes ultrastructural damage to mitochondria, activates calcium dependent proteases in the cytoplasm and may damage the cytoskeleton. Additionally, calcium overload could trigger free radical mediated damage. (reviewed in Jackson, (1993).

4.13.8 d) Fibre teasing.

Thirdly, the method of physically teasing the fibres apart may be the main contributor to tissue damage. During the teasing the fibres are sheared relative to each other, squashed by the forceps and in some cases stretched. No matter how carefully this procedure is conducted some damage is inevitable. Vital staining showed which fibres had been damaged post-photobleach, but is not a feasible technique prior to data collection- any levels of fluorescence from the vital dye will increase the background signals during FPR analysis. Though only dead fibres should take up the dye to any significant extent, it is still a potential problem. Vital dyes are toxic to cells if left on for any length of time and the effects of such dyes on membrane structure are unknown.

The use of diaphragm muscle was substituted for hind limb tissue in the hope that the thinness of the muscle would prevent the need for teasing the fibres apart. The overlying membrane still had to be removed before labelling to ensure labelling of muscle surface, not tissue partition. This, like teasing pulled the fibres to some extent. The main problem, however, arose during excision of the tissue. Vital staining showed 50% of the diaphragm fibres became permeabilised during dissection. Unlike the calf muscle, the dead fibres were adjacently situated in quadrant-like distributions rather than randomly distributed- but without a suitable stain for live of dead tissue, the FPR measurements could not be preferentially conducted on live fibres.

Enzymatic separation of the fibres could be employed instead of physical separation. Muscle fibres could be pre-treated with collagenase to separate the fibres before photobleaching. In this case enormous care must be taken to keep enzymatic degradation to a minimum. Permeabilisation of the fibres must be avoided. Additionally, as stated above the ECM may contribute to regulation of surface protein distribution in muscle fibres. Removal of the inter-fibre collagen matrix may affect the basal lamina around the fibres and lead to increased glycoprotein mobility, as found following trypsinisation of chick embryo fibroblasts (Boullier *et al*, 1992). This could affect not only the mobility of surface glycoproteins in general, but also affect the distribution, function or potential of the dystrophin/DAG complex to restrict protein mobility.

4.13.9 Alternative experimental system for future work.

Separating muscle fibres from their bundles seems difficult without damaging them unnecessarily. An alternative approach would be to use live cultured fibres. Primary cultures from neonatal mouse muscle failed to grow in preliminary experiments. However, Terry Partridge has developed a method of growing myofibres in culture that may prove useful for comparative photobleaching in future studies. Live fibre explants will grow when plated on a matrigel matrix. The explanted myofibres may die, but satellite cells from the fibres proliferate, grow out of the original fibre and fuse to give new myotubes. It is possible that the new fibres may have less well developed basal lamina than the original mature muscle, but thus far they appear to retain the all the characteristics of mature fibres (T.Partridge, personal communication, Beauchamp *et al*,1999).

These fibres in culture would be advantageous over dissected teased fibres in that the fibres can be maintained in a live state during the experiments. Fixed fibres on a culture matrix are less likely to vibrate than teased stuck down fibres so data collection should be a simpler procedure with fewer ambiguous curves that may or may not show recovery, depending upon whether the fibre is slowly moving or not. Autofluorescence from tissue culture plastic is always a problem with FPR of cultured cells, as is fluorescence from phenol red in the culture medium. These difficulties should be surmountable by growing the cells on glass coverslips and transferring the coverslips to glass dishes for experimentation; and growing cells in phenol-red free media.

Hopefully it will then be possible to further investigate the contribution of dystrophin to immobilisation and organisation of muscle fibre membrane constituents.

4.13.10 FPR conclusions.

Muscle membrane lipids and glycoproteins were immobile and temperature insensitive in dystrophic and normal muscle tissue as measured by FPR. Membranes may theoretically contain immobile lipid rafts in the physiological state. However, the data is more likely indicative of experimental artefacts- either of the labelling procedure, FPR equipment or tissue viability.

Lipid mobility data was consistent with observations in dead sperm cells, suggesting the muscle fibres were damaged during dissection and teasing, and were not sustained by the chosen buffer. This severely limited the capacity of this experimental system to study dystrophin's effects on restraining muscle glycoprotein mobility. The contribution of dystrophin to the subplasmamembranous cytoskeletal 'molecular fence' could therefore not be measured.

As discussed previously, the amino acid sequence and cellular location of dystrophin suggest a cytoskeletal function for the protein. It would therefore be interesting to pursue studies into dystrophin's role in organising and stabilising the muscle membrane. A viable tissue system is required to facilitate further work.

Chapter 5

Synthesis of specific fluorescent probes for FPR.

Chapter 5

Synthesis of specific fluorescent probes for FPR.

5.1 Introduction.

Dystrophin and other cytoskeletal proteins may regulate the structure and organisation of the muscle fibre membrane in two ways, as discussed in detail in section 1.4. Firstly, dystrophin could act non-specifically. In this hypothesis dystrophin would adopt a general 'molecular fence' role. By forming a physical barrier to protein diffusion, the dystrophin fence would restrict free movement of integral and peripheral membrane proteins. Secondly dystrophin could directly binding and tether membrane proteins. A protein bound either directly to dystrophin or indirectly via a complex of proteins, would be restricted in its ability to move within the membrane.

To investigate how dystrophin could regulate the distribution, behaviour and function of particular integral membrane proteins, this work looked at the capacity of dystrophin to bind specifically to two such proteins, tethering them at the membrane and restricting their lateral mobility. In the light of the reported direct binding interactions between dystrophin and the members of the dystrophin associated glycoprotein complex, the first study addressed the ability of dystrophin to regulate mobility of adhalin (α-sarcoglycan / 50 DAG), known from co-immunoprecipitation experiments to bind dystrophin via β-dystroglycan (figure 1.3).

5.1.1 Dystrophin and adhalin localisation.

The absence of dystrophin protein in DMD leads to a reduction of all the DAGs from the sarcolemma of affected individuals (Ohlendieck *et al*, 1992). The DAG chosen for the study was adhalin, a member of the sarcoglycan complex, figure 1.3. Adhalin is a 50kDa novel transmembrane spanning protein (Roberds *et al*, 1993). Together with β, γ and δ sarcoglycans it makes up the sarcoglycan complex of the DAG (complex reviewed in Duggan and Hoffman, 1996). Adhalin does not bind directly to dystrophin, but co-immunoprecipitates with anti-dystrophin antibodies (and the reverse is also true- anti-adhalin antibodies pull down dystrophin) and is therefore in tight association (Ervasti *et al*, 1990).

Adhalin deficiency is the primary cause of severe childhood autosomal recessive muscular dystrophy (also called limb girdle muscular dystrophy type 2D). Adhalin levels are reduced in the sarcolemma of affected patients, despite normal levels of dystrophin (Matsumara *et al*, 1992).

Measurements of adhalin protein mobility were chosen to illustrate mobility of the whole DAG complex. This was because firstly, adhalin is closely associated with the other members of the DAG complex. Monoclonal antibodies against adhalin pull down the whole DAG complex (Ervatsi and Campbell, 1991). Secondly, adhalin has a large extracellular domain (Roberds *et al*, 1993). The protein should therefore be accessible on the surface of live fibres, so avoiding the need to permeabilise the tissue. Thirdly, whilst adhalin levels are reduced in dystrophic muscle, the distribution of the protein is unchanged (Cullen *et al*, 1996). Fourthly, an antibody was available to the extracellular domain of adhalin (gift of Dr L.V.B. Anderson, University of Newcastle, U.K.). This could therefore be used as the base for a specific probe for the protein in FPR studies.

Dystrophin expression affects the distribution of adhalin protein in muscle tissue. In DMD patients, the lack of dystrophin leads to reduced levels of adhalin in the plasma membrane. Though levels of adhalin protein are low, the protein is still localised to the sarcolemma (Cullen *et al*, 1996), suggesting dystrophin is not essential for DAG protein targeting. The reduced levels indicate dystrophin could be required to stabilise adhalin at the membrane. Perhaps by binding free adhalin and sequestering it at the plasma membrane, dystrophin prevents adhalin re-internalisation and degradation.

The ability of dystrophin to bind specifically to the DAG complex in the muscle fibre membrane and hold the complex in place was therefore measured by tracking the mobility of the DAG complex with FPR.

5.1.2 Dystrophin and NaCh localisation.

The parallel investigation looked at the role of dystrophin in tethering or restricting NaCh mobility at the neuromuscular junction. In this case, unlike the DAGs, no direct binding interaction between NaChs and dystrophin has yet been proven. However, as outlined in section 1.6.4, dystrophin and NaChs co-localise to the pits of the junctional folds in mature NMJs (Sealock *et al*, 1991). As NaChs become immobilised at the NMJ during maturation of the junction (Angelides, 1986); different spectrin isoforms are localised to specific subcellular locations where they could perform different functions (Vybiral *et al*, 1992); dystrophin shares high sequence homology with spectrin; dystrophin appears at the NMJ at the same developmental stage as NaChs (Bewick *et al*, 1996); and β-spectrin and ankyrin have been shown to be required for localisation of NaChs at the nodes of Ranvier in neurons (Srinivasan *et al*, 1988); dystrophin could conceivably contribute to the localisation and immobilisation of neuromuscular junctional NaChs. Immunocolocalisation studies allow potential interactions between

proteins to be inferred, but cannot give direct evidence for protein-protein interaction, nor illustrate the true physiological / functional relevance of such close proximity. Fluorescence photobleach recovery of live fibres provides a real time insight into the precise contribution of dystrophin to ion channel and DAG complex tethering.

The FPR study of glycoproteins on the muscle cell surface was conducted using fluorescently tagged lectins bound to sugar moieties on surface proteins. This methodology, whilst informative, is not specific to any one particular protein. In order to study the mobility of individual protein species, a fluorescent marker which exclusively recognises the protein of interest is required. In the cases of the NaCh and the DAG complex, no high specificity fluorescent markers were available commercially. Consequently, fluorescently tagged probes had to be synthesised *de novo* before the FRP experiments could be performed.

5.1.3 Fluorescent probe characteristics.

In order to produce an effective fluorescent molecular marker, certain characteristics were desired in the synthesised probe (reviewed in Angelides, 1989). Firstly, the probe should show similar binding characteristics to the unlabelled marker. The probe must still be able to interact with the receptor binding site, binding with high specificity to the protein of interest (>80%) to minimise levels of background signal. Spectroscopically, the fluorescent component of the molecule should have a high extinction coefficient ($\varepsilon \geq 50{,}000 M^{-1}cm^{-1}$) and a high quantum yield ($\Phi \geq 0.4$). Together these ensure maximum light output at the desired wavelength, so that small numbers of bound receptors may be detected experimentally. In addition, the absorption and emission wavelengths should exceed 480nm, so that probe signals are not lost amongst autofluorescence from the tissue. Finally, the probe should have a non-perturbing effect on the labelled cell so that observations of probe behaviour truly reflect physiological behaviour of the target molecule.

5.1.4 Voltage gated NaCh probe.

It is often difficult to visualise specific receptors on cell surfaces due to their low density. Conveniently, NaChs are clustered at high density at NMJs. They should therefore be easily detected with an effective probe.

The base for the synthesised voltage gated NaCh marker was the 22aa peptide neurotoxin μ-conotoxin GIIIB (μ-cgtx). This neurotoxin (also known by the name geographutoxin II or GTX-II) is derived from the venom of the piscivorous cone snail *Conus geographus* and is used by the snail to paralyse its more agile prey when hunting. The toxin binds specifically to the muscle isoform of the NaCh, with

essentially no binding to the neuronal form (Olivera *et al*, 1985). This high specificity makes μ-conotoxin GIIIB an ideal marker to visually label NaChs at the neuromuscular junctions of normal and dystrophic mice. The toxin binding domain is on the extracellular face of the NaCh (Olivera *et al*, 1985), so fluorescent toxin free in solution should gain unhindered access to the binding site during the labelling reaction.

5.1.5 Neurotoxins as ion channel markers.

The use of fluorescent neurotoxins as probes of ion channels is not without precedent. For example, tetramethylrhodamine (TmRh) derivatives of conotokin-G have been used to measure the mobility of neuronal N-methyl-D-aspartate receptors (Benke *et al*, 1993). In muscle tissue, NaChs on the surface of chick myotubes were labelled with TmRh- *Leiurus quinquiestriatus* toxin to investigate the effects of innervation on NaCh mobility (Angelides, 1986). Toxins are attractive for this purpose as their high receptor affinity and specificity gives high receptor and low background signals. Toxins do not cross link like antibodies and are small in size, so they are particularly well suited to mobility studies.

Toxins are considered suitable non-perturbing probes as, thought they exert an effect on their receptors, they are non-lethal to the cell. Fluorescent α-bungarotoxin for example inhibits muscle contraction. The other properties of the muscle cell are essentially unaffected by the bungarotoxin- action potentials are still generated and cell death rate is unchanged. This situation is proposed to result from the high specificity of toxins for their receptors, such that the other cellular processes remain undisturbed (Angelides, 1989).

5.1.6 Adhalin probe.

There are no neurotoxins found to date which interact with members of the dystrophin associated glycoprotein complex. To study the mobility of the DAG complex a monoclonal antibody to adhalin (α-sarcoglycan) was used as the base for a membrane protein probe. Monoclonal antibodies, like neurotoxins, bind with high specificity to the epitope they were raised against. They can therefore be used to highlight particular proteins amongst the many on a membrane surface. Antibodies, unlike neurotoxins, can be cross linked together- by secondary antibodies in particular. Cross linking restricts mobility of the bound species and give rise to anomalous diffusion data. To restrict the extent of cross linking, the monoclonal antibody was fluorescently modified directly- as with the neurotoxin- rather than using a secondary antibody visualisation step.

Adhalin is a transmembrane spanning component of the DAG complex,. The chosen monoclonal antibody [clone Ad1/20A6, a gift from Dr L.V.B.Anderson, University of Newcastle] binds an epitope

on the extracellular domain of adhalin, between amino acids 217 and 289. The epitope should therefore be accessible by the antibody when added to the surface of live fibres, making this a suitable starting reagent for a membrane probe.

5.1.7 Probe synthesis strategy.

Fluorescent modification of molecular probes may be done either indirectly, via a reactive probe intermediate, or directly in one step. For the indirect approach, the molecular probe has a reactive group added during the initial step (such as a thiol group). This is then reacted further to produce the final product (e.g. with a fluorescent maleimide). This method is advantageous as more than one derivative can be added to the thiol intermediate for different purposes if desired (such as biotinylation/ fluorescein/ rhodamine) and the thiol group can be used to separate intermediate from native toxin on a column. The net positive charge on the molecule (often needed for activity) is retained. On the other hand, the increased steps can lead to reduced yield of final product.

In order to generate the fluorescent markers as simply, cheaply and efficiently as possible a one-step modification strategy was adopted. Amino groups on lysine residues and at the N-terminus of the peptide/antibody were reacted with a fluorescent succinimidyl ester according to the mechanism below, figure 5.1. There are 5 potential reactive sites in μ conotoxin GIIIB- lys 8,9,11 and 16 plus the N-terminal amino group (Olivera *et al,* 1985). The NMR structure of GIIIB shows the lys residues to be arranged radially around the exterior of the toxin, projecting into the solvent and forming potential sites of interaction with anionic sites on the NaCh (Hill *et al*, 1996). All five sites are therefore theoretically accessible for modification by the succinimidyl ester. The immediate environments of the amino groups affects their pKs and hence relative reactivities. This, combined with steric constraints dictates the final nature of the reaction products.

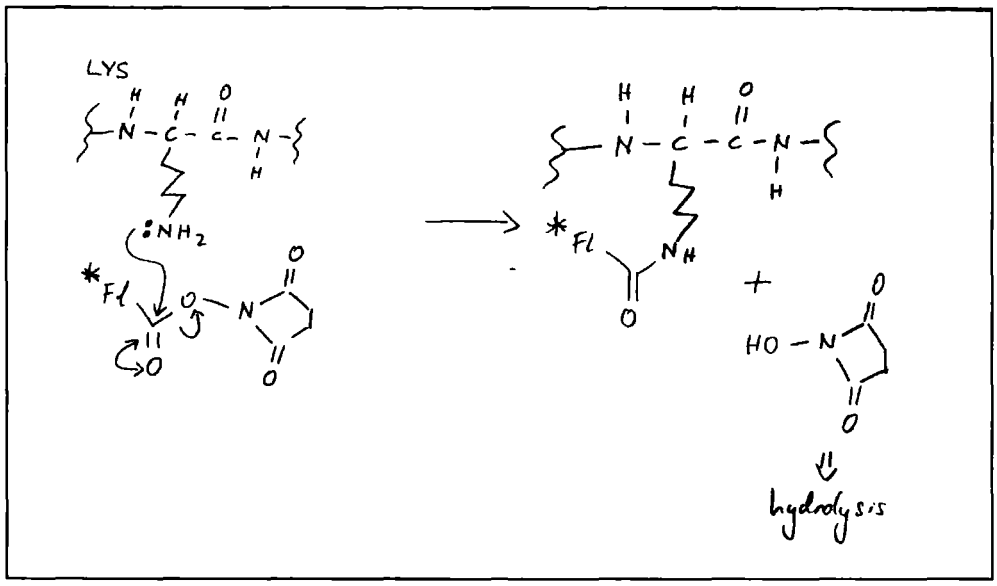

Figure 5.1 Reaction mechanism of peptides with succinimidyl esters.
Lysine side chain and N-terminal amino groups react by addition-elimination with the fluorescent succinimidyl ester, leaving the fluorophore coupled to the peptide. Fl* represents the fluorophore.

5.1.6 BODIPY fluorophore.

The use of fluorescent succinimidyl esters to couple fluorescent species to proteins, and in particular toxins, has been previously reported. For example, Joe and Angelides (1993) generated fluorescent tityus toxin γ to label neuronal NaChs. The fluorescent molecule of choice in these previous experiments has been carboxytetramethylrhodamine- Succinimidyl ester (TAMRA-SE). For this study the novel fluorescent reagent 4,4-difluoro-1,3,5,7-tetramethyl-4-bora-3a,4a-diaza-s-indacene-8-propionic acid, succinimidyl ester (BODIPY (Fl) -SE) (figure 5.2) was chosen.

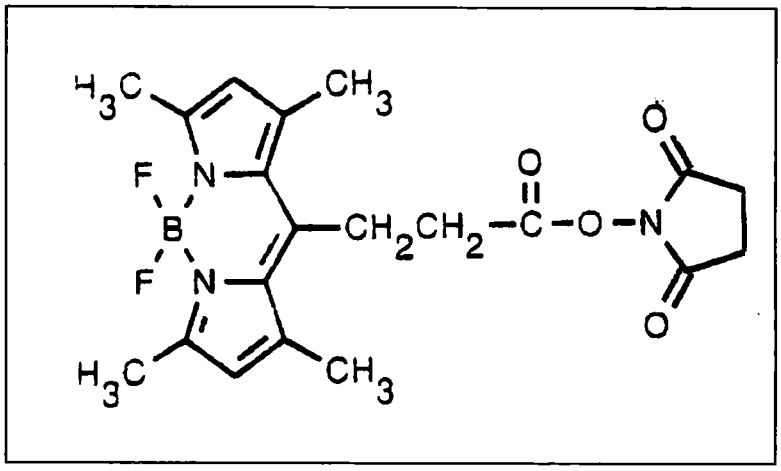

a)

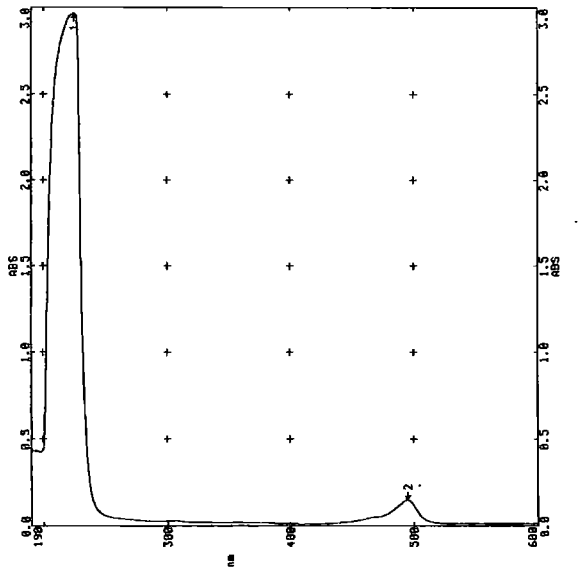

b)

	BODIPY (Fl)	Fluorescein
Absorption maxima	503nm	494nm
Emission maxima	512nm	520nm
ε $cm^{-1}M^{-1}$	>80,000	73,000

c)

Figure 5.2 4,4-difluoro-1,3,5,7-tetramethyl-4-bora-3a,4a-diaza-s-indacene-8-propionic acid succinimidyl ester [BODIPY(Fl)- SE].

a) Structure, b) absorption spectra and c) spectral characteristics of BODIPY (Fl). Absorption spectral peaks are 1: 2.968 A.U. @ 224.8nm, and 2: 0.152 A.U. @ 495.3nm at 5μg/ml in 0.1M NaHCO3 buffer pH 8.5. Structure a) and data for figure c) obtained from Molecular Probes handbook of fluorescent probes and research chemicals.

BODIPY (Fl) is an analogue of fluorescein, absorbing the 488nm blue line from an argon laser and emitting in the green range. Fluorescein is photochemically unstable, being susceptible to photobleaching even in room light. This is undesirable in an FPR probe as fading during recovery observation can mask the true extent of diffusion. BODIPY shows greater photostability than fluorescein. Additionally, BODIPY's emission bandwidth is narrower. This leads to higher emission peak intensity therefore BODIPY probes should give off sufficient photon counts, even at low concentrations of receptors.

TAMRA is also photostable in comparison to fluorescein, and has been the fluorophore of choice for several toxin molecular probes (e.g. Joe and Angelides, 1993). However, during TAMRA synthesis, two isomers , (5) and (6)- carboxytetramethylrhodamine are formed. Consequently during fluorescent modification of peptides, both the (5) and (6) fluorescent isomers of modified peptides are produced. For a peptide such as μ-cgtx with multiple lysine residues and hence many potential sites of esterification, the number of different reaction products (in this case, 10) becomes too numerous for effective separation and characterisation. BODIPY-SE has just one isoform. The potential number of reaction products is therefore halved by using BODIPY. (Note- for the adhalin antibody, where the number of potentially modifiable sites is too large to practicably separate the different modified isoforms, the choice of BODIPY over TAMRA was less critical. BODIPY was used to prevent reconfiguring the laser between experiments).

Results.

5.2 Production of fluorescent anti-adhalin monoclonal antibody.

5.2.1 Verification of unmodified antibody specificity.

To visualise adhalin molecules on the surface of muscle fibres for FPR experiments the anti-adhalin monoclonal antibody clone Ad1/20A6 was used as a specific marker of adhalin protein. The antibody was tested to confirm its specific activity prior to modification by western blotting skeletal muscle protein extracts. The monoclonal antibody recognises a 50kDa protein consistent with recognition of 50kDa adhalin on a western blot of muscle protein extract from Balb C dystrophin positive mice (figure 5.3). The recognition pattern is in accord with the presence of 50kDa adhalin in muscle tissue of Balb C control mice. The staining is not due to the anti-mouse secondary antibody, but instead is specific to adhalin.

The intensity of staining of Balb C muscle is significantly greater than that observed for mdx muscle. Adhalin is detectable in tissues of mdx mice, but is significantly reduced relative to the control. Given the similar intensity of secondary antibody bands in the two lanes, it may be assumed this difference is not due to differences in protein loading, but instead reflects the down regulation of DAGs in dystrophic tissue.

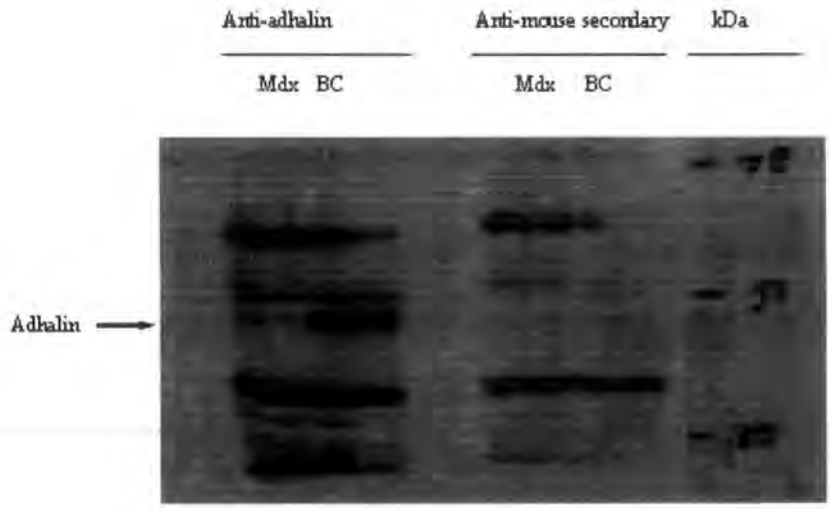

Figure 5.3 Skeletal muscle tissue immunoblot to verify activity of anti-adhalin monoclonal antibody.

Nitrocellulose blot of total skeletal muscle protein from Balb C (BC) dystrophin positive control and mdx dystrophic mouse. 7.5% polyacrylamide gel / 10mg protein per lane. Skeletal muscle blot was immunostained with 1/400 dilution of anti-adhalin monoclonal antibody clone Ad1/20A6 and visualised with 1/3000 anti-mouse -horseradish peroxidase conjugated secondary antibody. Anti-mouse secondary blot was immunostained with 1/3000 secondary antibody alone.

5.2.2 Synthesis and purification of adhalin probe.

Following verification of the anti-adhalin specificity of the monoclonal antibody, the anti-adhalin antibody was fluorescently modified by reacting at 1:10 molar ratio with BODIPY-SE under alkaline conditions.

To minimise the background signal from the adhalin marker, the probe was purified from the reaction mixture post-modification. The antibody supernatant/BODIPY mixture was passed through a G10 column to separate the high MW antibody from unreacted low MW free dye. The mixture was spun rapidly through the column, rather than eluted through under gravity to prevent undue dilution of the antibody. To restrict contamination by free BODIPY dye, the column was not washed after the spin, thus ensuring the majority of free dye remained within the column.

To test that the antibody had been successfully modified and purified from free dye, and also to give a crude indication of the yield of the reaction, the modified antibody fraction from the column was run on a 7.5% polyacrylamide gel. To allow identification of the gel components the unmodified adhalin monoclonal culture supernatant and free hydrolysed BODIPY dye were run alongside the reaction products. Coomassie blue staining of the gel showed the column spun reaction mixture contained many of the protein fractions present in the original culture supernatant including IgG anti-adhalin monoclonal antibody (figure 5.4 a).

To illustrate the presence of the BODIPY fluorophore, the same SDS gel was visualised under uv light (figure 5.4 b). The unmodified monoclonal culture supernatant did not fluoresce under uv illumination (figure 5.4 b, unmod.). Strong uv excitation was observed from the column spun reaction mixture (figure 5.4 b, mod.). The larger molecular weight fluorescent species co-migrated with the tissue culture supernatant protein. This, together with the molecular weight, indicates the antibody had been fluorescently tagged by the BODIPY SE. Serum in the culture media contributes significantly to the total protein as co-migration with BSA illustrates.

The lower molecular weight band at the leading edge of the gel front in the modified lane co-migrated with free hydrolysed BODIPY dye (though clear to see on the gel, the band was too faint to pick up on the photograph). This is therefore unreacted dye remaining after purification. The proportion of unreacted dye was less than that in the reaction mixture prior to column spinning, therefore the G10 column removed a significant percentage of free hydrolysed BODIPY.

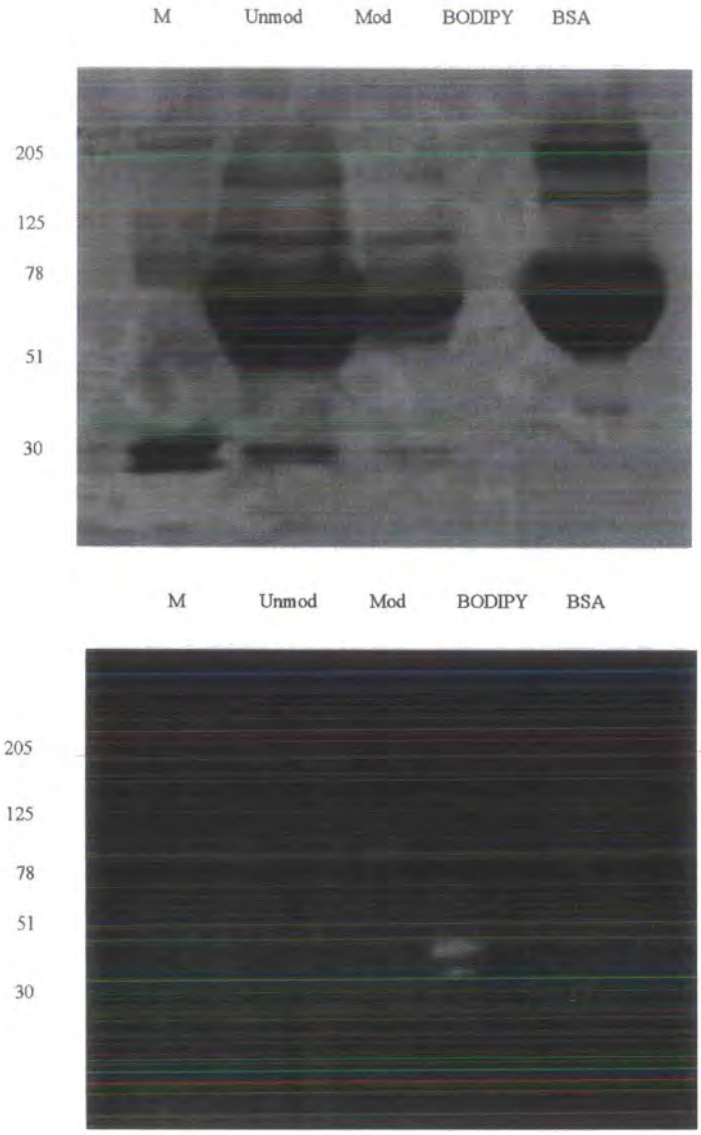

Figure 5.4 Fluorescent modification and purification of anti-adhalin monoclonal antibody.
The modified antibody can be seen to fluoresce under uv light. The fluorescent band co-migrates with unmodified antibody and not free BODIPY dye.

a) Coomassie blue stained 7.5% SDS gel of adhalin monoclonal antibody tissue culture supernatant before reaction with BODIPY-SE (Unmod), after modification and G10 column purification (mod), free hydrolysed BODIPY-SE alone (BODIPY) and BSA. Molecular weight markers (M) are in kDa.

b) The same 7.5%SDS gel visualised under uv light to illustrate the presence of the BODIPY fluorophore in the modified fractions.

5.3 Use of anti-adhalin-BODIPY antibody for FPR.

An absence of detectable dystrophin protein in DMD and mdx mice leads to down regulation of DAGs in the sarcolemma. In order to measure the effects of dystrophin deficiency on DAG tethering and hence the ability of dystrophin to restrict the movement of specific membrane proteins, live fibres from C57/Bl 10 and mdx mice were teased and labelled with 1/30 dilution of column purified adhalin-BODIPY construct. The labelled fibres were then subjected to FPR analysis to measure adhalin lateral mobility.

Detectable photon counts from the tissue were low- of the order of ~2,000-5,000 counts per second (cps), compared with >25,000 counts for glycoprotein studies. 2000 cps is only ~1500 counts above background PMT dark levels. In order to test whether the low level counts were due to specific fluorescence of the μ-cgtx-BODIPY probe, or down to background fluorescence from the experimental set-up, live fibres from mdx and C57/Bl 10 mice were teased, held down with Blu-tak in a glass petri dish and immersed in oxygenated Krebs buffer as for the NaCh labelling experiments. Autofluorescent laser counts from the experimental system were of the order of 2,000-3,500 cps, as for the adhalin antibody-BODIPY labelled tissue. The detected photon counts from probe labelled tissue were therefore autofluorescence, rather than specific labelling by the fluorescent antibody.

5.4 Immunohistochemical analysis of adhalin probe activity.

To investigate why the adhalin marker failed to give a high fluorescent signal under the FPR apparatus, the labelled fibres were observed under a fluorescence microscope (fluorescein optical filter set 488nm excitation, 520nm emission). The fibres appeared green, consistent with adhalin detection, but the signal was low (figure 5.5 a). The green staining could have been in the extracellular matrix of the muscle fibres, or specifically located at the plasma membrane. To see if the probe staining was at the level of the plasma membrane, as expected for visualisation of adhalin, transverse sections of muscle fibres were stained at 1/20 dilution with the anti-adhalin-BODIPY construct.

Adhalin, with its plasma membrane localisation, is seen around the edges of immunostained muscle fibres in normal tissue. This staining is observed successfully in transverse sections of rat[5] quadriceps muscle stained with unmodified adhalin antibody and anti-mouse rhodamine secondary antibody (figure 5.5 b). The monoclonal antibody can therefore detect native adhalin. However, the anti-adhalin-BODIPY mixture failed to show comparable staining when placed directly on mdx tissue sections at 1/10 dilution (figure 5.5 c). The negative stain was not due to the down regulation of adhalin protein in mdx tissue - the same lack of distinctive, bright adhalin rings was observed with C57/Bl mouse sections

[5] Rat muscle was stained in preference to mouse muscle to avoid the high background staining of anti-mouse antibodies on mouse muscle sections.

too (figure 5.5 d) suggesting the probe was inactive. Increasing the concentration and incubation time of adhalin probe made no difference to the staining pattern.

To test if the anti-adhalin antibody supernatant was still active following the modification procedure, the column spun modified supernatant was added to rat muscle sections at 1/20 dilution and visualised with anti-mouse rhodamine secondary antibody. Bright rings of adhalin detection were seen in the muscle tissue (figure 5.5 e). The modified anti-adhalin antibody supernatant is therefore capable of binding specifically to native adhalin in tissue sections. However, from the intensity of BODIPY fluorescence on tissue sections it appears the extent of fluorescent modification is low. Fluorescent signal intensity from the anti-adhalin antibody marker is too weak for this preparation to be an effective FPR molecular probe.

Figure 5.5 Anti-adhalin antibody-BODIPY probe activity.

Live fibres stain weakly with the anti-adhalin -BODIPY construct. The modified probe supernatant retains anti-adhalin antibody activity, but levels of BODIPY fluorescence are too weak for FPR experiments.

a) Live fibres stained with adhalin-BODIPY probe.

Transverse quadriceps muscle sections, b) from rat, immunostained with unmodified anti-adhalin antibody and anti-mouse-rhodamine secondary antibody. c) from mdx and d) C57/Bl mice, stained with 1/10 adhalin-BODIPY probe. e) from rat, immunostained with 1/10 adhalin-BODIPY probe and anti-mouse-rhodamine secondary antibody.

Scale bars represent 200μm.

a)

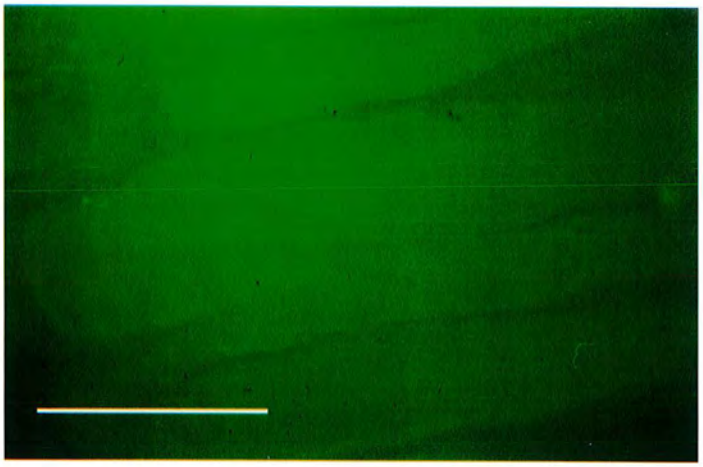

b)

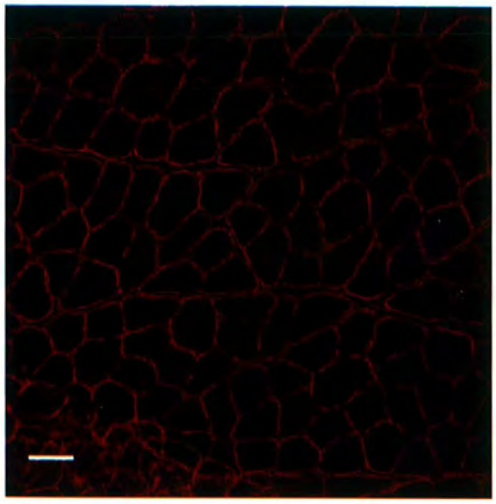

c)

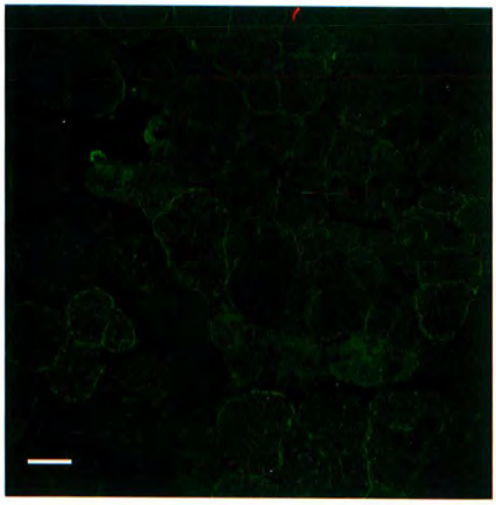

d)

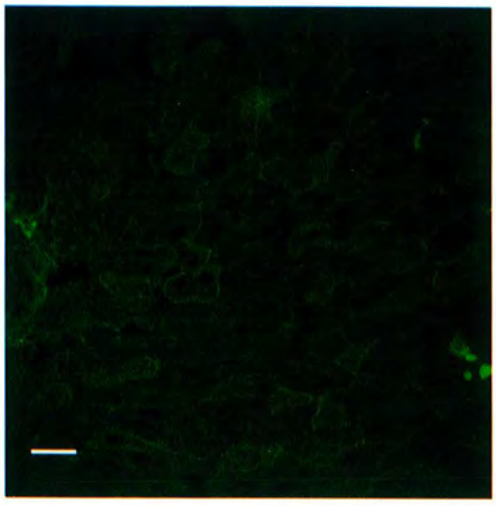

e)

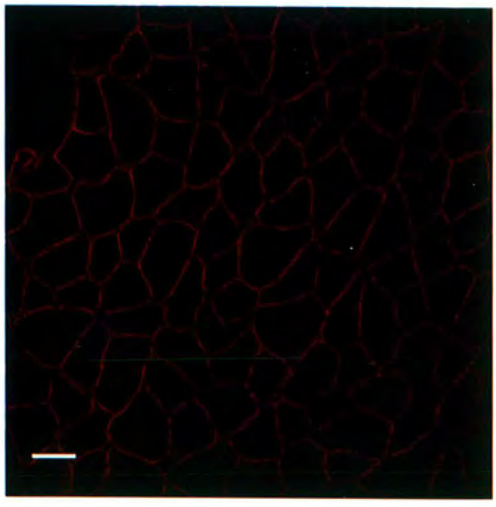

5.5 Production of fluorescent NaCh marker.

To generate the NaCh marker, μ-cgtx GIIIB was reacted at 2:1 ratio of BODIPY-SE to lysine side chains (10:1 molar ratio) using a modification of Joe and Angelides (1993)[6] and protocol supplied on request from Molecular Probes. A large excess of BODIPY was avoided to prevent multiple modification of the toxin. Multiple modification increases steric bulk and reduces likelihood of a biologically active product. The reaction was carried out in 0.1M $NaHCO_3$ buffer at alkaline pH to catalyse the esterification reaction.

5.5.1 Purification of μ-cgtx GIIIB-BODIPY by HPLC.

Following the fluorescent modification reaction, efficient separation of modified from unmodified toxin was needed. Native toxins bind with high specificity to their target receptors and are typically active at low concentrations. Residual unmodified toxin may bind preferably to the receptor molecule, blocking entry of the fluorescent derivative and so preventing the fluorescent signal. Traditionally HPLC has been employed to separate reactants from products (e.g. Benke *et al*, 1993) as this allows not only removal of unreacted starting materials, but also resolution of the different individual modified isoforms. The different species can be determined spectroscopically due to their differing absorption properties. BODIPY absorbs strongly in the 480-550nm range, but poorly at 240/260nm. The alkyl chain backbone and side chain carbon-carbon bonds of the peptide absorb strongly at 214nm. The lack of extended π conjugation in the peptide leads to poor absorption at higher (~500nm) wavelengths. It is therefore simple to resolve toxin, modified toxin and free BODIPY from their relative absorptions at 214 (or 260/280nm) and 500nm.

The usual solvent system for toxin / TmRh HPLC is 5-95% acetonitrile (AcCN) in 0.1% trifluroacetic acid. This was found to be inappropriate in this instance. The BODIPY dye hydrolysed under acidic conditions, forming an insoluble red precipitate. 0.1M triethylammoniumacetate (TEAA) was therefore substituted for 0.1% trifluroacetic acid.

5.5.1 a) Reverse phase HPLC purification.

Traditional reverse-phase HPLC, whilst proven for rhodamine coupled toxin resolution was unsuitable for resolution of the toxin and BODIPY starting materials. The small (2,640MW) peptide toxin could be clearly resolved on a C_{18} column, 5-95% AcCN, 0.1M TEAA at 260nm detection (figure 5.6 a).

---

[6] This protocol describes fluorescent modification of a scorpion toxin with a tetramethylrhodamine - succinimidyl ester to produce a specific neuronal voltage gated NaCh marker for FPR. This is in no way connected to the disputed production of antibodies against the NaCh, and no such connections should be made.

However, the BODIPY fluorophore is extremely hydrophobic. The dye bound irreversibly to a C_{18} column, making it unsuitable for separation of free dye and toxin-dye conjugates.

A less hydrophobic C_4 reverse phase column was substituted for the C_{18} (5-95% AcCN, 0.1M TEAA). The C_4 gave excellent resolution of the BODIPY fluorophore at 500nm detection wavelength (figure 5.6 b). Unfortunately, the peptide μ-conotoxin failed to adhere to the short C_4 alkyl chains. The peptide was carried through in the void volume at the start of the HPLC run and could not be detected amongst the initial surge from the column. Although the peptide protonation state could be altered by changing the pH of the TEAA, the extent of incompatibility is such that the peptide would still fail to stick. The well established reverse-phase alkyl chain column method is thus unsuitable for purification and resolution of BODIPY modified toxins.

a)

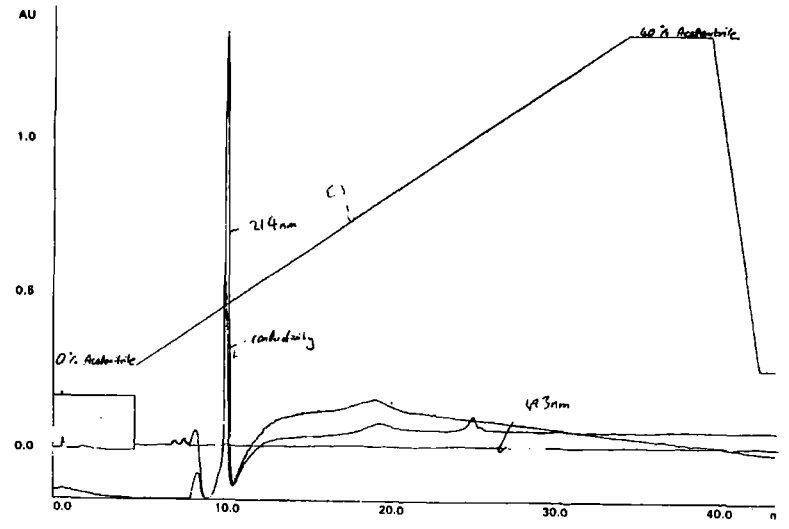

b)

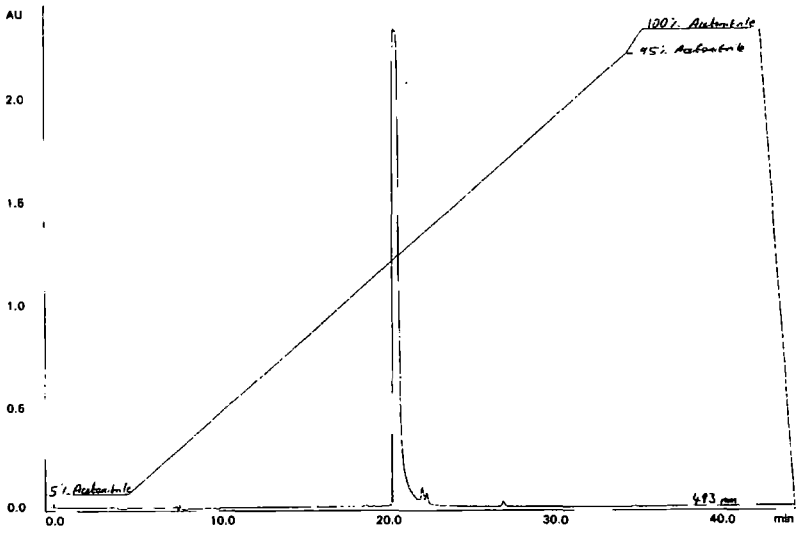

Figure 5.6 Reverse phase HLPC profiles for starting reagents of NaCh probe synthesis.

a) 214 and 493 nm HPLC profile of μ-conotoxin GIIIB. C18 reverse phase column. Solvent A, 0-40% acetonitrile over 35min. Solvent B, 0.1% TFA. x-axis, retention time (min). y-axis, absorption.

b) HPLC profile of BODIPY (Fl) SE. C_4 reverse phase column. Solvent A, 0-100% acetonitrile. Solvent B, 0.1M TEAA pH7. x-axis, retention time (min). y-axis, absorption. Monitoring wavelength, 493nm.

5.5.1 b) CN column purification.

Taking into account the incompatible hydrophobicity characters of the modification starting reagents, either the HPLC column could have been changed for something more compatible, or the fluorophore could have been altered to a more hydrophilic reagent. BODIPY was retained over the less hydrophobic TmRh-SE to restrict the number of fluorescent derivatives. Instead the HPLC column was switched from an alkyl to a cyano (CN) column. Resolution of both native toxin and BODIPY dye was possible with the cyano column. Native toxin eluted after 6.1 minutes on a 30 minute gradient of 0-95% AcCN (figure 5.7 a). The BODIPY dye and hydrolysed derivatives eluted after 9.1 minutes, (figure 5.7 b). The difference in retention times was large enough to separate the two starting reagents by this method. Though the column detector was unable to monitor at both 260 and ~500nm, the appearance of a peak over and above the starting reagents in the modified reaction mixture profile, at either wavelength would indicate toxin-BODIPY conjugate.

The initial analytical run of reaction product mixture indicated the toxin had been modified successfully by BODIPY-SE in the coupling reaction. At 514nm an extra peak was detected after 8.57 minutes when compared to the dye hydrolysis profile (figure 5.7 c). CN columns are therefore more suited than alkyl reverse phase columns for separation of hydrophobic BODIPY coupled peptides by HPLC.

The gradient did not resolve different modified peptide isoforms. It could be that just one fluorescent derivative of the toxin was generated during the esterification reaction because of thermodynamic or steric constraints. Alternatively, the solvent gradient and column system in this first trial separation may have been too harsh or too insensitive to differentiate between the isoforms. Before a preparative run could be conducted on the reaction products, however, the HPLC detector broke down. Column time could not be obtained again on a reasonable timescale and so a different method of reagent separation had to be adopted.

5.5.2 Gel column purification.

Following the difficulties with HPLC separation of reactants and products, a cruder gel column purification method was adopted. Whilst gel columns are less sensitive, time consuming and lead to dilution of the sample, the likelihood of obtaining some workable probe was higher than persisting with HPLC. The labelled toxin was purified by passing through a 1ml, 25cm sephadex G10 column, eluting with PBS. To detect the presence of products and reactants in the fractions, 9 minute eluents were pooled and analysed spectroscopically at 514nm for BODIPY absorbance and 260nm for toxin absorption.

Figure 5.7 CN column HPLC profiles for starting reagents and products of NaCh probe synthesis. Solvent A, 0-95% acetonitrile over 30min. Solvent B, 0.1M TEAA pH7. x-axis, retention time (min). y-axis, absorption. Numerical values indicate retention times.

a) 220 nm HPLC profile of μ-conotoxin GIIIB. b) 514 nm HPLC profile of BODIPY (Fl)-SE. c) 514 nm HPLC profile of μ-conotoxin GIIIB/ BODIPY (Fl)-SE mixture, post-coupling reaction. Additional peak corresponding to BODIPY tagged μ-cgtx marked with asterisk.

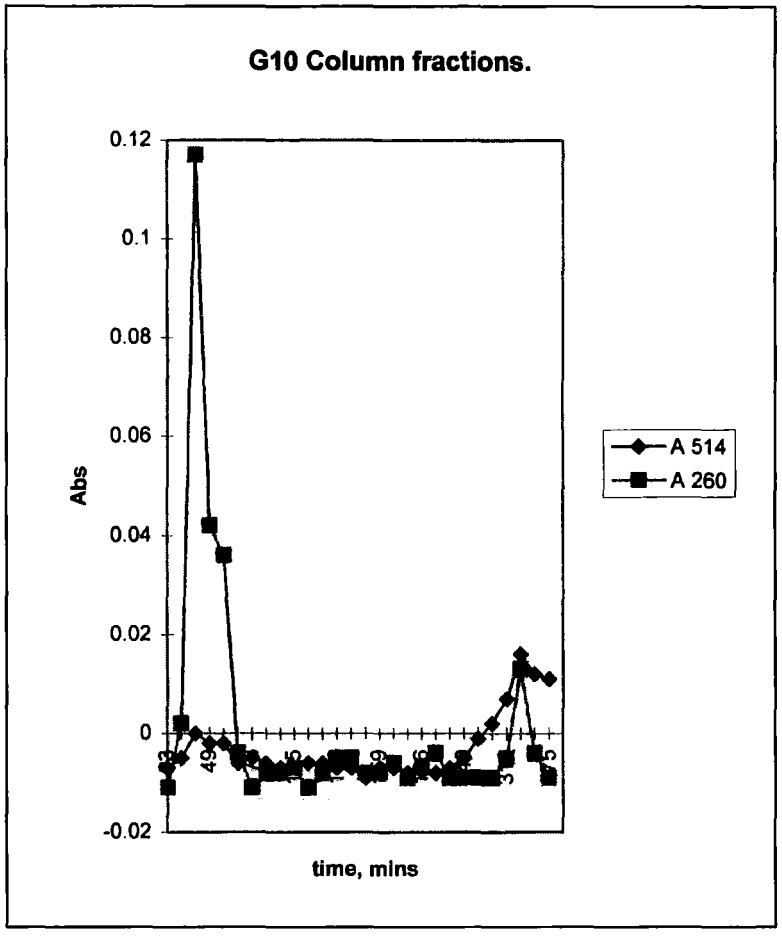

Figure 5.8 Sephadex G10 column elution profile of BODIPY-SE/ μ-cgtx GIIIB modification reaction mixture.

514 and 280nm spectroscopic analysis of 1/6 diluted column fractions, collected and pooled every 9 minutes. Unreacted toxin and toxin-BODIPY conjugates passed through the column in under an hour. Small molecular weight unreacted BODIPY fluorophore and free dye were restricted in their passage through the column and eluted 3-4 hours later.

From the HPLC profiles of unreacted and modified toxin it can be seen that native toxin had little detectable 514nm absorption but high 214→280nm absorption. The absorption spectra of the G10 gel column fractions shows high A_{260} absorbance, in accordance with the presence of μ-cgtx, after approximately 45 minutes (figure 5.8). This was the same time as the void volume takes to clear through the column, therefore the toxin passed straight through with little resistance. The high A_{260} absorbance toxin fraction also possessed a significant 514nm peak. This suggested the BODIPY

fluorophore had conjugated to some proportion of the toxin. This peak fraction was therefore kept as a potential fluorescent NaCh marker.

The free hydrolysed and unreacted BODIPY (relatively high A_{514}: A_{260} ratio) took over 4 times as long to pass through the column, (figure 5.8). The smaller molecular weight dye was retained by the pores of the gel matrix whilst the larger toxin conjugated dye variants carried straight through. The fluorescent species with longer retention time were deemed to be free dye and discarded.

5.6 NaCh mobility measurements.

The aim of the μ-cgtx modification reaction was to generate a fluorescent marker of muscle NaChs, so that NaCh mobility could be measured and compared by FPR. From the elution profile of the G10 column it could be concluded that: a) at least a proportion of the μ-cgtx had been successfully conjugated to the BODIPY succinimidyl ester to make a fluorescent NaCh FPR probe, and b) The majority of the free BODIPY dye had been separated from the toxin-BODIPY conjugate by the gel filtration column purification. Following this successful isolation of the modified μ-cgtx from the sephadex column, the 45 minute G10 column fraction μ-cgtx-BODIPY construct was added to teased live muscle fibres of C57/Bl 10 mice at 1/35 dilution in oxygenated Krebs buffer. The live fibres were transferred to the FPR instrument for NaCh mobility measurements.

Under the laser the photon counts from the labelled tissue were of the order of ~2,000-5,000 c.p.s, as found with the adhalin probe. Additionally, the levels of counts were uniform across the tissue. This was contrary to expectations for a NaCh marker. Though low counts across the body of the fibre is not unusual, regions of higher counts would be anticipated when scanning across the tissue, corresponding to increased probe binding at areas of high NaCh density such as NMJs. It consequently seemed that autofluorescence was once more the main source of photon counts.

5.7 Fluorescent histological tests for μ-cgtx-BODIPY activity.

5.7.1 μ-cgtx-BODIPY staining of live fibres.

In order to ascertain whether the lack of photon counts reflected too little label on the tissue, or an absence of effective high intensity NMJ staining by the probe, teased live fibres stained with 1/35 μ-cgtx-BODIPY were observed under a fluorescence microscope. Neuromuscular junctions can be seen in live fibres by staining nicotinic acetylcholine receptors with fluorescently coupled α-bungarotoxin (α-bgtx). Under the fluorescence microscope these stained NMJs take the form of bright rounded spots on the surface of the plasma membrane - often in a line, corresponding to multiple points of innervation

at adjacent sites along the fibres (figure 5.9 a). The pattern of α-bgtx-FITC staining on live fibres was compared with that of μ-cgtx-BODIPY to reveal whether the probe successfully highlights neuromuscular junctional NaChs.

The observed pattern of live fibre staining from the μ-cgtx-BODIPY differed from the α-bgtx-FITC. Many conotoxin stained fibres possessed a uniform green stain along their length. The expected clear, rounded NMJ spots were not apparent. Instead, diffuse patches of staining were observed on the fibre surfaces. These brighter patches were clustered, as would be expected for a NaCh marker. The staining colour on the other hand was yellow, rather than fluorescein green. The colour hinted that the patches could be non-specific background in nature. (figure 5.9 b). These patches were also visible with a red 514/560nm filter set, but true BODIPY-FL derived fluorescence should give minimal signal intensity with red emission filters. Increasing the concentration of probe increased the intensity of the uniform green stain along the fibre lengths. Clear bright rounded NMJ spots were still undetectable, but could have been lost amongst the brighter background stain. The diffuse green/yellow patches remained.

It was possible that the diffuse patches of staining were NaChs at neuromuscular junctions. Their diffuse appearance could have been a consequence of compromised fibre integrity/ breakdown. NaChs could have been present throughout the plasma membrane, hence the uniform green staining. Alternatively, the toxin could have lost biological activity during the modification procedure and so be unable to bind muscle NaChs.

Figure 5.9 μ-conotoxin-BODIPY probe on live fibres.

Fibres of C57/Bl mouse muscle, stained with a) α-bungarotoxin-FITC for acetylcholine receptors at NMJs, and b) μ-conotoxin-BODIPY for equivalent staining of NaChs. μ-conotoxin stains diffusely, rather than at clearly defined NMJ sites. Outlines of individual fibres may just be made out. Scale bar, 100μm.

Figure 5.10 μ-conotoxin-BODIPY probe on mouse muscle sections.

Transverse sections of a) C57/Bl and b) mdx mouse muscle, stained with 1/20 μ-conotoxin-BODIPY construct. The construct does not specifically stain NMJs. Scale bar in μm.

a)

b)

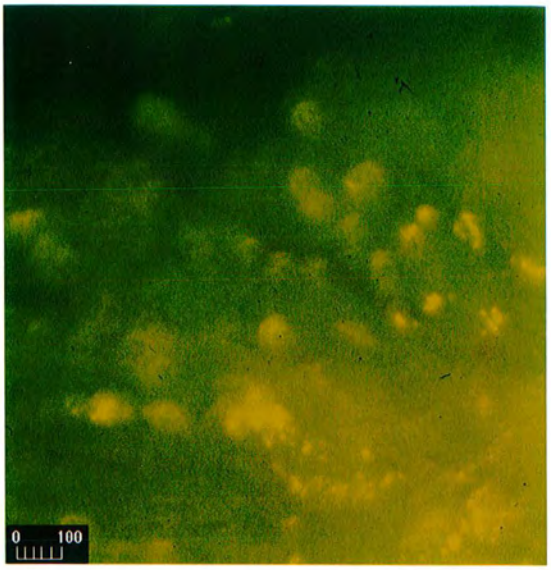

a)

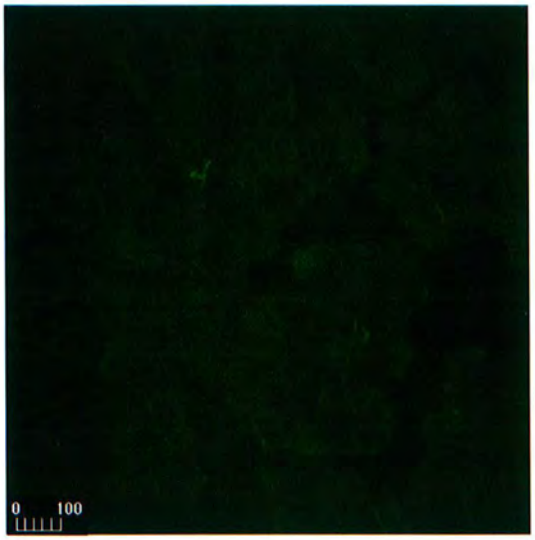

b)

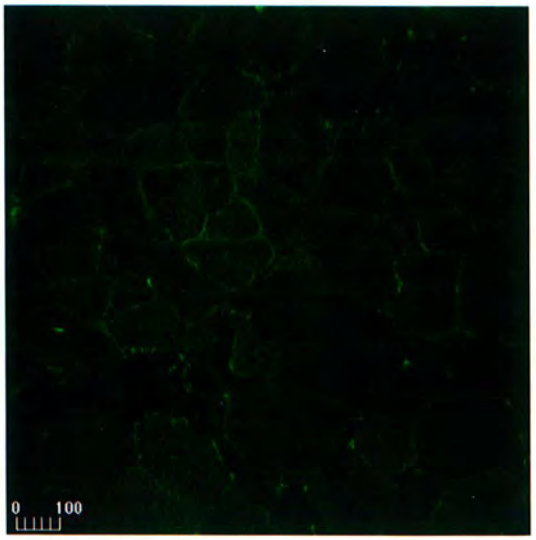

Figure 5.11 Failure of μ-cgtx-BODIPY to bind neuromuscular junctional NaChs.

Transverse sections of unfixed C57/Bl quadriceps muscle, co-stained with μ-cgtx-BODIPY and α-bgtx-rhodamine. NMJs are stained by α-bgtx-Rh, but not μ-cgtx-BODIPY. a) red channel, b) green channel, c) both channels. μ-cgtx-BODIPY stains outside NMJ regions. d) green channel, e) red channel, f) both channels.

Scale bar represents 100μm.

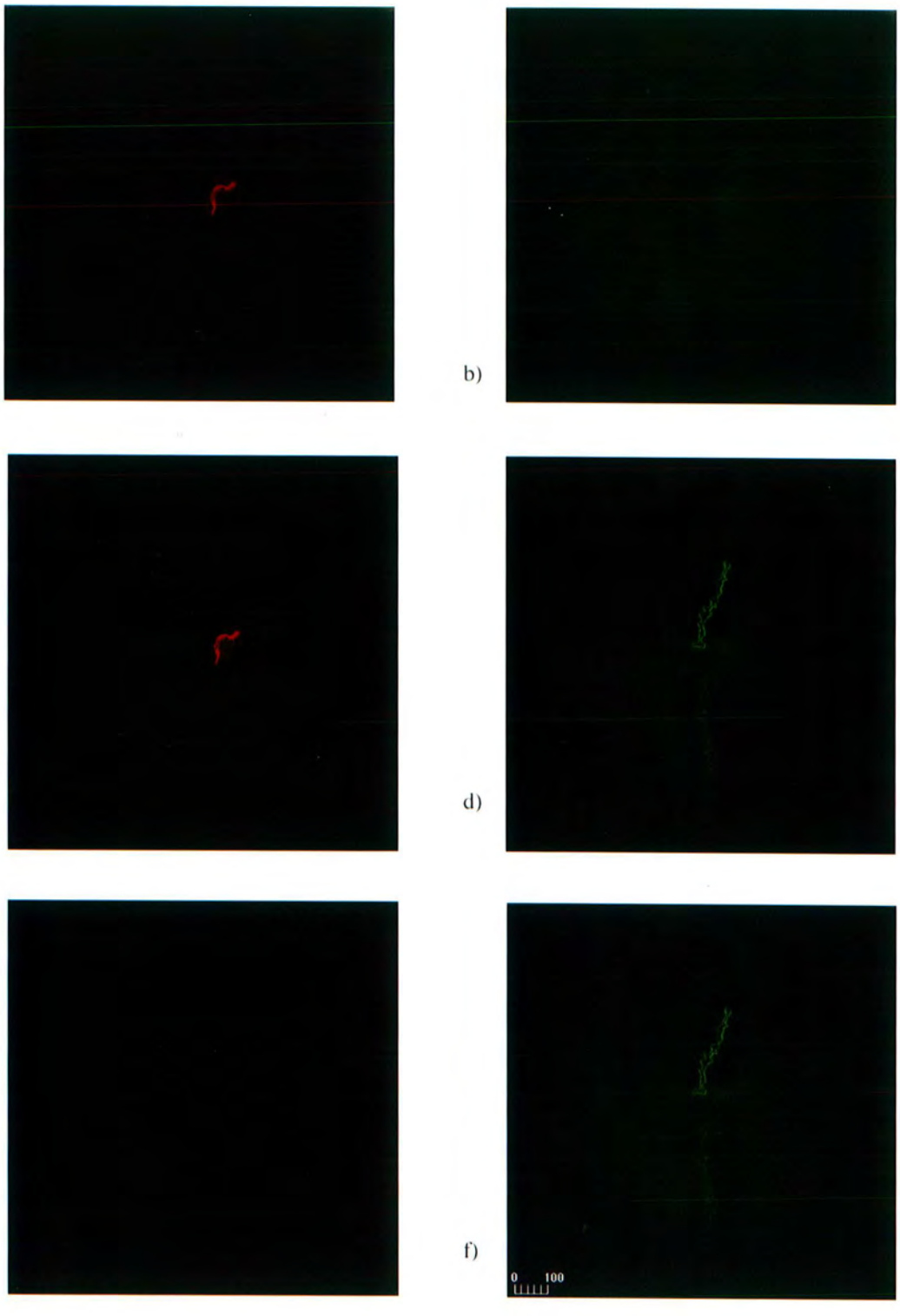
a)
b)
c)
d)
e)
f)
0
100

5.7.2 μ-cgtx-BODIPY staining of tissue sections.

To confirm if the observed staining was actually NaCh in nature, 10μm transverse sections of mdx and C57 BL quadriceps muscle were labelled singly with μ-cgtx-BODIPY (Fl), and double labelled with μ-cgtx-BODIPY (Fl) and rhodamine α-bgtx. Colocalisation of red and green fluorescence was analysed by confocal microscopy. μ-cgtx-BODIPY alone labelled unevenly across the tissue (figure 5.10). Particularly bright staining was found around the edges of some muscle fibres, with isolated fibres staining more brightly in their interior than others. Similar patterns were seen in both C57/BL and mdx mouse sections. The diffuse yellow patches of staining observed on live fibres did not localise specifically to the membranes of sectioned fibres. This, together with the yellow colour and the red channel detection, indicates the diffuse staining is not a result of μ-cgtx-BODIPY binding NMJ NaChs. It is more likely to be non-specific background staining.

α-bgtx -Rh clearly labelled acetylcholine receptors at NMJs within the tissue of mdx and C57/Bl mice (figure 5.11 a). No colocalised green μ-cgtx -BODIPY staining was found at the same NMJ. This co-staining would have been expected had the μ-cgtx bound specifically to NaChs (figure 5.11 b and c). μ-cgtx -BODIPY therefore does not bind with high affinity to NMJ NaChs.

μ-cgtx -BODIPY did stain some regions of the tissue sections with high specificity (figure 5.11 d). Although this appeared to be signs of NaCh detection and binding, no corresponding α-bgtx-Rh staining was present (figure 5.11 e and f) therefore it is unlikely to be NMJ specific. It seems, given the morphology of the BODIPY stained regions, that the dye is taken up by blood vessels and the lipid rich myelin sheaths of neurons, but not by NMJs.

μ-cgtx GIIIB binds slowly and reversibly to NaChs. The final possibility remained that the absence of staining reflected the short incubation period of tissue and label (15 minute (live) and 30 minute (sections)). To study this, sections were labelled overnight with the μ-cgtx -BODIPY. This increased the extent of non-specific binding by the BODIPY dye. Levels of stain increased at the fibre membranes and interiors, but NMJ staining did not increase. Short labelling time was therefore not the cause.

5.8 μ-cgtx-BODIPY synthesis - summary.

The spectroscopic data from the sephadex column implied that the μ-cgtx GIIIB had been successfully coupled to the BODIPY flurophore, and the modified toxin separated from the free unmodified dye (dye alone eluting at a later time). However, the modified toxin failed to highlight NaChs in teased live fibres and transverse muscle sections. NMJs were present in the tissue, as seen with the α-bgtx, but the

μ-cgtx-BODIPY was unable to bind strongly and specifically to junctional NaChs. The lack of probe-NaCh binding resulted in insufficient photon counts for FPR analysis of NaCh mobility in normal and dystrophic muscle.

Discussion.

5.9 Synthesis of fluorescent anti-adhalin antibody.

The level of direct BODIPY signal from the modified anti-adhalin culture supernatant was too low for successful application as an FPR probe. The immunohistochemical analysis suggests the lack of fluorescent signal obtained during FPR studies on adhalin protein mobility was due to insufficient fluorescent modification of the anti-adhalin antibody, but not due to loss of adhalin-binding affinity during the modification. The lack of direct adhalin-BODIPY signal in tissues could arise because the anti-adhalin antibody was not modified at all, or because it was modified but not at sufficiently high levels. The presence of the fluorophore may compromise the ability of the antibody to recognise and bind the antigen, reducing the binding affinity of the modified antibody. If modified antibody is not present at high enough levels relative to unmodified, the unmodified antibody, with its greater binding affinity, will bind to adhalin molecules. Unmodified antibody will thus prevent binding of the fluorescent form and therefore prevent detectable fluorescence. It was not clear whether the adhalin antibody was inactivated completely by the modification process as the levels of modification were too low to tell.

The column spinning purification process by itself was adequate for separation of free dye from antibody- levels of dye post-spin were significantly reduced compared to reaction mix levels, and from the immunohistochemistry results the spun fraction specifically recognised adhalin protein. Some free dye was carried through the column in the spin procedure. Given the 'sticky' nature of BODIPY (both hydrophobicity- BODIPY bound with great affinity to eppendorf tubes- and reactivity of the SE group), free dye would bind to surface residues on the muscle fibre. As adhalin distribution is even across the sarcolemma, it would be difficult to distinguish between adhalin signal and that from bound dye. However, as the autofluorescence from the tissue was of similar magnitude to the adhalin probe labelled tissue, the levels of free dye carried through in the spun culture supernatant must not call for great concern.

5.9.1 Cross reactivity.

From the uv visualised gel of modified antibody supernatant it is clear that the antibody was not the only protein modified in the esterification reaction. The serum proteins have reacted with the fluorophore too. This will generate high levels of background signal from free modified proteins in the antibody labelling solution (though many of these unbound fluorescent proteins should be removed during the post-labelling washing of the tissue). In addition, and more significantly, reaction of the BODIPY-SE with proteins other than the IgG in the supernatant, will titrate out the reactive BODIPY from the reaction mix- lowering the concentration of BODIPY-SE available for esterification of the antibody. Boosting starting levels of BODIPY-SE would increase the final level of modified antibody. Difficulties may arise in separating the increased levels of free BODIPY dye from the antibody post-reaction, but several extra column spinning steps should reduce this. Similarly, the levels of non-specific protein modification would rise if the concentration of BODIPY -SE were increased. Enrichment of the antibody fraction, e.g. with protein A beads, would reduce non-specific protein levels and hence the extent of BODIPY-SE titration from the reaction mix, although some antibody would be lost during the purification.

5.9.2 Suitability of a monoclonal antibody as a DAG probe for FPR.

The possibility remains that the lack of fluorescent signal reflected an inability of the fluorescently tagged probe to access the protein epitope on live fibres. The anti-adhalin antibody recognises an epitope in the extracellular domain of the protein. It is possible that the adhalin molecule is surrounded by ECM proteins when *in situ* on the muscle membrane. Bulky ECM matrices may block access of the antibody to the epitope and therefore prevent specific binding of probe to target molecule. If this were to be the case, smaller Fab' antibody fragments may be able to squeeze through the matrix and access the adhalin molecule where complete antibodies are hindered. Fluorescently modified Fab' antibody fragments have been used successfully to measure the mobility of GABA A receptors on the surface of cerebellar granule cells. In these cells the mobility of fluorescent Fab' labelled receptors was comparable to fluorescent drug labelled receptors (Peran et al, 1999, submitted). Fab' fragments are advantageous over full antibodies in that they are less susceptible to antibody- antibody cross linking. Additionally, they are smaller in size. The mass and bulk of an Fab' fragment is therefore less likely to slow diffusion of the receptor than the complete antibody molecule.

The assertion that the adhalin molecules were inaccessible on live fibres conflicts with the tissue section observations. If adhalin was closely associated with other proteins around the antibody binding site, then the same should be true in sections (although the ECM would not form such a tight seal). The secondary antibody experiments revealed the epitope was accessible in sections. Given that identical concentration of labelled probe gave no fluorescent signal on the same sections, insufficient fluorescent

modification is more likely the cause of inadequate adhalin probe fluorescence than epitope inaccessibility.

5.10 Synthesis of fluorescent NaCh marker.

5.10.1 Effects of modification on biological activity.

Whilst the NaCh probe has been synthesised, it appears to be biologically inactive. Perhaps this is not surprising given the small size of the toxin- just 22aa, 2640.2 mol.wt. The addition of a 350mol. wt. fluorophore will have a significant impact on the size, structure and behaviour of the peptide. In particular, the steric hindrance of the dye could restrict entry of the toxin to the binding site on the NaCh, or active site modification could prevent recognition altogether. The binding activity of μ-conotoxins has been reported to be susceptible to modification. For the GIIIA form of the toxin, the replacement of amino acid residues with alanine affects activity as shown in the following table (Sato *et al*, 1991).

Residue modified→Ala.	**Effect on ED_{50}.**
Arg 13	↓ 200 fold
Arg 19	↓ 25 fold
Lys 16	↓ 6 fold
Hyp 17	↓ 6 fold
Arg 1	↓ 5 fold
Lys 11	↓ 4 fold
Lys 8	↓ 2 fold

Table 5.1 Effects of chemical modification on biological activity for μ-conotoxin GIIIA. Amino acid residues were chemically replaced with alanine during *de novo* synthesis of the synthetic toxin, and the effects on the ED50 values for rat diaphragm twitch contraction inhibition compared. (Adapted from Sato *et al*, 1991.)

No equivalent chemical modification study has yet been performed on μ-cgtx GIIIB. However, from sequence comparisons and the 3 dimensional structure of the GIIIB molecule, the critical residues for receptor interaction are believed to be Arg 13, Lys 16, Hyp 17 and Arg 19, whilst Arg 8 and Lys 9 are

proposed to make the first lose interaction with the NaCh. Had either BODIPY- modified Lys 16 or Lys 9 been major products of the fluorescent coupling reaction, the biological activity of the fluorescent toxin would be severely compromised.

5.10.2 Purification of modified toxins.

The sephadex column purification method employed is unable to resolve the different modified toxin isoforms. Consequently, active fluorescent species could not be separated from inactive ones. During muscle labelling, non-specific binding of inactive isoforms could override the signal from active toxin, preventing visualisation of the NMJs. Likewise, unmodified toxin carried through from the column will compete with modified toxin for the NaCh binding site. If, as postulated, modified toxin binds with lesser affinity, the unmodified toxin will occupy the receptors and block access by the fluorescent forms.

HPLC remains theoretically the best prospect for resolution and separation of the different modified isoforms. Had more time and the equipment been available, the use of the cyano-column could have been pursued further for BODIPY resolution. Alternatively, carboxytetramethylrhodamine-succinimidyl ester modification could have been tried, with C18 reverse-phase columns to separate the extra modified isoforms. On the other hand, if toxin modification results in lack of NaCh recognition (regardless of the fluorophore), HPLC resolution of the isoforms will merely give rise to several inactive products rather than one inactive mixture.

The uniform green staining along the lengths of live fibres is most probably caused by residual BODIPY dye carried through with the toxin during column purification. Any unhydrolysed BODIPY-SE will cross react with amino groups of molecules on the surface of the muscle fibre. However, cross reacting ester is unlikely to be the major cause of the staining. The succinimidyl ester is highly reactive. It would be expected that ester groups which didn't react with lysine residues would have been hydrolysed by water- catalysed by the alkaline environment of the $NaHCO_3$ buffer. As has been stated above, BODIPY is extremely hydrophobic. Free dye from the reaction mixture could intercalate in to the hydrophobic lipid bilayer and colour the membrane green. Thermodynamically, this membrane solubilisation of the dye is favourable to remaining free in aqueous solution. It is therefore most likely that free hydrolysed BODIPY dye is the source of the live membrane staining.

Similarly, the specific bright green staining of nerves and blood vessels in muscle sections is probably a result of hydrophobic free hydrolysed BODIPY dye incorporating into the lipid rich domains of the tissue.

5.11 Implications for further studies.

The aim of these experiments was to generate fluorescent probes for monitoring the mobility of specific classes of membrane proteins in the presence and absence of dystrophin. The hydrophobic nature of the novel BODIPY fluorophore enforced changes to the traditional modification protocols, but in both the case of the anti-adhalin antibody and the μ-conotoxin, the probes appeared to have been synthesised by reacting with the novel fluorophore BODIPY-SE. Unfortunately, neither probe proved effective once placed on the tissue.

Levels of modification were too low to tell whether the adhalin antibody was inactivated by the modification process and therefore whether the antibody is still a potential marker of adhalin on live muscle tissue. Purification of the IgG fraction prior to modification may lead to better labelling. These experiments have not shown direct need for Fab' fragments thus far, but papain digestion of the antibodies may yet be important if a fluorescent antibody proves unable to break through the ECM or hinders protein diffusion with its large size.

5.12 Dystrophin as a direct anchor of membrane proteins.

The overwhelming technical difficulties of this study have left unanswered the question of how dystrophin contributes directly to organisation of the muscle fibre membrane through specific associations with membrane proteins. If adhalin is inaccessible to antibodies in live fibres, the modification and membrane labelling techniques used here can be applied to antibodies directed against other extracellular members of the DAG complex so that the contribution of dystrophin to DAG anchoring may still be studied.

As it appears fluorescent modification of μ-conotoxin renders the toxin inactive, the problem of how to study the mobility of NaChs on the surface of muscle fibres persists. Previous reports have described the successful fluorescent modification of tetrododoxin (TTX), saxitoxin (STX),and Toxin V from *Leiurus quinquiestriatus* (Lqq V) (e.g. Joe and Angelides, 1993) all of which bind NaChs in both muscles and nerves. (5) and (6) carboxytetramethylrhodamine coupled Toxin V from *Leiurus quinquiestriatus* (TmRhd-Lqq V) was used successfully to illustrate by FPR the immobilisation of NaChs on muscle fibres upon innervation (Angelides, 1986). Whilst the use of a muscle-specific μ-conotoxin is preferable, fluorescent Lqq V, TTX or STX could be used to measure the mobility of muscle NaChs. The use of epi-fluorescence illumination prior to photobleach should ensure muscle rather than neuronal NaChs are aligned under the bleach spot.

Chapter 6.

Discussion.

Chapter 6.

Discussion.

6.1 Aims.

The experiments in this thesis addressed the notion that dystrophin, with its structural and sequence homology to cytoskeletal proteins, imparted structural integrity and mechanical strength to muscle membranes by acting as a either a specific linker of DAG/NMJ membrane proteins and/or as a constituent of the membrane skeleton fence in accordance with the "membrane skeleton fence model" (Kusumi *et al*, 1993, Simson *et al*, 1998). This model proposed 'the membrane associated cytoskeleton (membrane skeleton) provides a barrier to free diffusion of membrane proteins due to steric hindrance, thus compartmentalising the membrane into many small domains for diffusion of membrane proteins' (Kusumi *et al*, 1993).

It has been demonstrated by FPR that there is little appreciable difference in the mobility of sarcolemmal glycoproteins in the dystrophic and normal muscle tissue of the experimental system. Both glycoproteins and lipids were immobile in the membranes studied. Unfortunately, due to the potential non-viability of the photobleached fibres shown by lipid immobility and vital staining, care must be taken in interpreting the data.

6.2 Suitability and limitations of the FPR approach.

FPR remains a suitable method for testing the hypothesis that dystrophin organises and stabilises membranes, as it allows real-time analysis of membrane fluidity on a micrometer scale. There are however, serious limitations with the experiments.

6.2.1 Fluorescent labels

Firstly the FPR technique is only as good as the fluorescent label. The ratio of mobile to immobile species measured is greatly affected by the strength of specific label signal compared with non-specifically bound label, background room light levels and tissue/ dish /culture media autofluorescence. If the specific signal is too small, low level mobility of labelled molecules will be lost amongst the background (which will not recover after bleaching). When monitoring the direct effects of dystrophin

mobility on specific classes of membrane proteins, it was proven that the specific membrane protein probes had been synthesised (figures 5.4, 5.6, 5.8). However, due to either loss of biological activity during modification, or high levels of reactants carried through to the labelling mixture, the specific level of fluorescence signal was too low to facilitate the FPR measurements.

If the labels bind outside the desired region e.g. to the ECM instead of the membrane, or if access of the label to the target site is blocked, mobility characteristics of an undesired region will be measured and the data misinterpreted. As discussed earlier, the equipment cannot finely resolve the plane of photobleach as the focal plane alignment of the laser beam was not identical to that seen by phase microscopy. The plane of highest photon counts was taken as that of the labelled membrane surface, but measuring of extracellular matrix cannot be ruled out. Electrostatically bound probes can be differentiated from specifically bound probes in terms of behaviour- often with minimal recovery- but if the expected behaviour is unknown confusion can result.

Similarly, photostability of the label influences the magnitude of measured recovery. Fluorescein is susceptible to photolysis. During pre-bleach this is seen as falling photon counts. Bleaching during the recovery phase masks the full extent of recovery and hence mobile fraction. In the light of the immobility of the FITC conjugated lectins and the improved photostability of ODAF and BODIPY, this shouldn't have affected this study adversely.

6.2.2 Limitations imposed by the FPR apparatus.

FPR results and the sensitivity of measurement are influenced by the FPR apparatus in addition to the membrane label. Limitations are found with the photomultiplier tube (PMT) aperture, beam alignment and the size of the bleach spot. If the aperture on the PMT is set too large, photons from tissue regions outside the bleach spot and room levels will form the bulk of the photon counts, drowning out specific signals from recovering tissue and giving the impression of immobility. The alignment of the incoming monitoring beam, bleach beam and emitted fluorescence must be checked at each experimental run. Misalignment results in non-spherical bleach spots and/or failure to measure recovery across the whole bleached area. Consequently the recovery produced is non-gaussian so fails to fit the diffusion equations.

Bleach spot size is important when data is interpreted as 'immobile'. The FPR definition of immobile is $D \leq 10^{-12} cm^2 s^{-1}$, defined by the sensitivity of the monitoring apparatus. This definition does not allow for domain size. Fluorescent molecules may be freely diffusing within a domain smaller than the size of the bleach spot. In this case the FPR interpretation will always be one of immobility, even though the molecules are unrestricted in their motion (Yechiel and Edidin, 1991, Edidin, 1993). Likewise, if the bleach spot overlaps two adjacent small domains the extent of recovery will be dependent upon the

proportion of each domain within the spot. This phenomenon was explored by Edidin and Stroynowski (1991) who were able to define membrane domains on the scale of micrometers following the observed relationship between increasing bleach spot size and decreasing percentage fluorescence recovery. A truer indication of diffusion domain scale, especially where domains are small would come from the alternative method of single particle tracking.

The 25ms dead time between bleaching and monitoring fluorescence recovery is significant, especially for lipid studies. Where recovery is rapid the dead time can cause problems, particularly as the curve fitting equations weight the initial recovery points more heavily. If the first stages of recovery are missed the fibre is interpreted as having bleached insufficiently and the software will not analyse the curve.

Whilst FPR data is often given as definitive, it is subject to personal interpretation. The decision to include a recovery curve in the final analysis or not for example is based upon experience rather than clear guidelines. In this study, data with χ^2 for curve fitting $\leq 1 \times 10^{-4}$ was included whilst the rest was discounted. The visual interpretation of fibre movement was usually confirmed by high χ^2 values.

6.2.3 Experimental tissue.

Finally, no matter how good the FPR technique or data interpretation the tissue must be viable. Modification of the tissue buffers or setting up a culture fibre system was not possible here due to time limitations. Future experiments should bear these findings in mind and include a suitable test to monitor fibre integrity. The ODAF FPR experiment is a simple way to test the general system, though for muscle it does not allow clear visual distinction between live and dead fibres. Indications of viability timescale would then have to be extrapolated to other fluorescent labels.

6.3 Dystrophin as a regulator of membrane protein lateral mobility.

Sadly, the numerous technical problems encountered during this work prevented quantification of the capacity of dystrophin to organise components of the muscle fibre membrane and set up subcellular domains.

6.3.1 The potential for dystrophin to form and reinforce molecular fences.

The FPR experiments presented in chapter 4 found no significant difference in glycoprotein and lipid mobility in mdx and normal muscle tissue. Were the data to be a true representation of muscle

membrane dynamics, the glycoprotein immobility in both the presence and absence of dystrophin could suggest that dystrophin is not vital for the setting up of sarcolemmal membrane domains or the restriction of sarcolemmal glycoprotein diffusion. This observation does not unequivocally rule out a fencing action of dystrophin when present in healthy tissue. The high levels of redundancy in the cytoskeletal and ECM systems may compensate for dystrophin loss of function with respect to restriction of protein mobility. Immunohistochemistry of the mdx fibres showed the underlying spectrin network to be present and apparently intact within dystrophic tissue (figure 4.2). Spectrin could therefore have restricted protein mobility in these experiments. It is possible that dystrophin may complement the existing cytoskeletal network in healthy fibres. Although it would have been possible to add cytochalasin or brefeldin A to the fibres to remove the spectrin cytoskeleton and therefore measure dystrophin directly, their dramatic effects on protein mobility are well documented (e.g. Sako and Kusumi, 1994) and the dystrophin network may also have been be disrupted.

Extra rigidity will be imparted to the cytoskeletal network in the presence of dystrophin, through a more dense, more highly cross linked array of proteins. Given the proximity of dystrophin to the sarcolemmal membrane and the sizes of the dystrophin molecule and DAG complex, it is likely that dystrophin will form a steric barrier to the diffusion of some membrane species. All these actions would reinforce an existing cytoskeletal system, but due to the presence of the remaining cytoskeleton, would not necessarily give rise to an altered mobility phenotype if the dystrophin reinforcement were removed. If significant, the results do suggest that a membrane fence role is not a primary function of skeletal muscle dystrophin.

On the other hand, the immobility of membrane glycoproteins and lipids can be interpreted as a sign of a non-viable experimental system. In this case it is premature to draw major conclusions from the immobile glycoprotein and lipid phases in the dystrophic and normal fibres. Further study on viable fibres may reveal that the original hypothesis stands and dystrophin may yet contribute significantly to the regulation and organisation of membrane proteins into defined functional domains.

6.3.2 Support for the molecular fence hypothesis.

Parallel studies using either completely alternative methods or variations on the FPR technique suggest there may be some truth in the molecular fence hypothesis, or at least that there's a measurable change in membrane conformation or fluidity when dystrophin is absent.

Cultured rat and mouse myotubes expressing an anti-sense dystrophin construct have significantly faster mobility of Con A receptors on the myotube surface than normal myotubes as measured by FPR. The proportion of mobile receptors seemed unchanged (Zs-Nagy *et al*, 1995). Whilst there were many errors in the design of this experiment (small size of data samples, inclusion of data from twitching

myotubes and unusually small margins of error), the results do suggest a barrier to rapid diffusion could be missing in dystrophic fibres and therefore dystrophin could be restricting protein mobility.

Similarly, membrane phospholipids show altered mobility in DMD compared to normal tissue when measured by ^{13}C NMR. In normal healthy muscle tissue, 15-23.2% of phospholipids appeared mobile, compared with 43.2-81.3% in Duchenne dystrophy patients (Barany and Venkatasubramanian, 1988).

Both observations are consistent with increased membrane fluidity in the absence of dystrophin. Whether this is indicative of a molecular fence, and whether this is a specific and essential function remains open to interpretation- proteins diffused faster when dystrophin expression was knocked out, so a restriction upon diffusion was undoubtedly removed. Dystrophin could be a submembranous barrier, holding up the passage of diffusing molecules. In this case the micro (sub domain) scale rate of diffusion would have been approximately constant in the presence or absence of dystrophin and the FPR measured rate of macro-scale diffusion would be expected to increase after knockout (assuming the detected non-mobile fraction were not completely anchored to other membrane skeleton components. If this were to be the case, removal of dystrophin barriers would not affect tethering and therefore would not increase mobile fraction). A completely impermeable dystrophin barrier does not perfectly fit the observations- in this case the mobile fraction might have increased in dystrophic cells (as diffusion domain size relative to size of bleach spot would be no longer limiting), but the mobile fraction did not increase. Instead, it seems proteins may become momentarily tangled up in the dystrophin network, but then be free to diffuse away in any direction.

6.3.3 The potential for dystrophin to organise/anchor specific membrane proteins.

The fluorescent probes synthesised to study mobility of specific membrane proteins were inactive, leaving the ability of dystrophin to regulate organisation and lateral mobility of specific membrane proteins open to question.

6.3.3 a) Dystrophin as a regulator of DAG complex mobility.

The association between dystrophin and the DAG complex is now well established, but the function of the complex remains unclear. Localisation of the subsarcolemmal domain of the dystrophin protein and the DAG complex to the membrane is insufficient for full function. Transgenic *mdx* mice expressing a cysteine rich and C-terminal domain construct of dystrophin have localisation of the DAG complex restored, but their dystrophic phenotype remains (Greenberg *et al*, 1994). Localisation of the large DAG complex to the plasmalemma in these cases may be sufficient to hinder mobility of some inter and trans- membrane proteins. However, the inevitable restrictions on diffusion imposed by the physical

bulk of dystrophin and the DAG complex are insufficient to override the dystrophic phenotype without the remainder of the dystrophin molecule. In this transgenic system and in dystrophic tissue the DAG could be anchored by the ECM. Successful formation of an active fluorescent DAG marker could illustrate by FPR whether the DAG complex is actually tethered, and hence if direct anchoring of the DAG is an essential functional requirement for dystrophin.

6.3.3 b) Dystrophin as an organiser of the NMJ.

The study into the role of dystrophin in regulating NaChs at the NMJ was based upon the co-localisation of dystrophin and NaChs, the homology of dystrophin to spectrin and the role of spectrins in anchoring NaChs in the nervous system.

During the course of these experiments reports have been published which cast doubt on an exact dystrophin/NaCh relationship. Wood and Slater (1998) used observational and quantitative immunofluorescence of muscle sections and en-face NMJs to show that there were fine differences in the patterning of dystrophin and NaChs, particularly in the peri-junctional region. The concentration and distribution of β-spectrin and ankyrin $_G$ on the other hand showed direct parallels to NaChs. They proposed that an ankyrin $_G$ / β-spectrin latticework could be essential for NaCh immobilisation- providing a universal ankyrin/spectrin mechanism for ion channel localisation across all excitable cells [c.f. ankyrin/spectrin in brain/CNS- Sirinivisan *et al*, 1988, Joe and Angelides, 1992].

If dystrophin is not binding NaChs, as these observations suggested, its function at the NMJ is unclear. Dystrophin is not essential for formation of the folds, though it may stabilise them (Lyons and Slater, 1991) nor for correct localisation of the NaChs (mdx mice possess correctly distributed NaChs (Wood and Slater, 1998)). Perhaps the function lies with the junctional DAGs, especially since the ECM at the NMJ is highly specialised. β-dystroglycan colocalises with AChR and utrophin throughout development of the NMJ and with dystrophin at the mature junction (Bewick *et al*, 1996). Given that the AChR clustering protein rapsyn co-associates with β-dystroglycan (Cohen *et al*, 1995), it has been proposed that the β-dystroglycan serves to stabilise the ion channel clusters. In the absence of dystrophin the levels of utrophin could be such that utrophin/β-dystroglycan can compensate for a lack of dystrophin and mask dystrophin's true function. If utrophin can compensate for dystrophin deficiency, FPR of fluorescently tagged DAGs should reveal little difference in mobility at the NMJ. If utrophin is truly responsible for this anchoring and lack of dystrophic phenotype, mobility measurements away from the NMJ should show a difference in mdx mice- as utrophin expression is too low outside the NMJ to compensate for dystrophin absence. Then again, neuromuscular transmission is unaffected by dystrophin deficiency, so perhaps the presence of dystrophin at NMJs is just evolutionary redundancy.

6.4 The extracellular matrix and membrane protein diffusion.

The extracellular matrix remained attached to the muscle fibres throughout the photobleach experiments. The capacity of this highly crosslinked latticework to restrict the motion of membrane proteins has not been fully elucidated, but must not be overlooked in this particular system. The DAG complex has been shown to bind the extracellular matrix protein merosin (Ervatsi, and Campbell, 1993). A fully functional dystrophin-actin contractile network- DAG link is not necessary for complex formation, and the DAG complex is fully restored by a dystrophin C-terminal construct (Rafael *et al*, 1996). Although down regulated, the DAG proteins are still free to form a multimolecular assembly in the absence of dystrophin, and associate with merosin through α-dystroglycan. Such highly specific associations must serve to restrict the lateral motion of complexed proteins. Furthermore, a consequence of the specific anchoring of large protein complexes to regions of the plasma membrane by the ECM is a steric restriction upon the mobility of neighbouring membrane components. Mutations within the extracellular macromolecular complexes that serve to anchor cells to the basal lamina continue to be identified as causative in both muscular dystrophies (for example α7 integrin chain in congenital myopathy) and junctional epidermolysis bullosa (α6 integrin chain) (reviewed in Gorski and Olsen, 1998). This must indicate that the role of intracellular and sarcolemmal proteins in maintaining the structural integrity of muscle fibres is only half the story, the extracellular matrix plays an equally important part.

6.5 Dystrophin, lipid domains and tight junctions.

Perhaps the organisational role of dystrophin and it's associated proteins will lie in setting up lipid domains, rather than directly influencing membrane proteins. The increased lipid fluidity in dystrophic fibres could account directly for the increased rates of protein diffusion seen by FPR - it would be interesting to see if the results of ODAF FPR mobility comparisons in live normal and mdx muscle fibres agree with the NMR data. Formation of cholesterol rich domains and/or regions high in charged phospholipid will influence localised viscosity and mobility within those domains, compared to diffusion over a homogeneous surface. Evidence is mounting for the role of cytoskeletal proteins in lipid domain delineation. Returning to the spermatozoon, the membrane lipid domains of these cells are determined by specialised structures such as the posterior ring between the head and mid-piece, and annulus between midpiece and principle piece (reviewed in Ladha *et al*, 1997). The posterior ring and annulus appear as electron dense regions within and below the lipid bilayer. They are thought to be analogous to tight junctions - whose capacity to prevent diffusion of proteins and lipids between the apical and basolateral surface of epithelial cells is well accepted.

Drawing further comparisons between the muscle cell and the spermatozoon, formation of the tight-junction like boundaries in the sperm cell is developmentally regulated, with greater restrictions imposed as the sperm matures (James *et al*, 1999). Diffusion of Con A receptors within muscle fibre membranes is also temporally regulated, with larger mobility restrictions in mature myofibres than immature myotubes (Zs-Nagy *et al*, 1995),

Personally, I favour the suggestion that the major role of dystrophin and its associated glycoproteins may be formation of similar tight-junctional (or adherens junctional) like complexes in the membrane (possibly within close contacts) (Michalak and Opas, 1997). In epithelial cells the tight and adherens junctions are essential for maintaining tissue integrity. Loss of plectrin from the hemidesmosome plaque, for example results in epidermolysis bullosa of the skin and an associated muscular dystrophy (Smith *et al*, 1996). In Duchenne muscular dystrophy, the connections through the intermediate basal lamina are lost between adjacent muscle fibres. In DMD applied external abrasions do not provide the disruptive force between cells. Instead, muscle contractions pull upon the fibres. Consequently, contractile shear stress disrupts the intercellular connections within the tissue and leads clinically to the observed muscle degeneration. Such a model is reliant upon a fully functioning junctional complex, not just on any individual molecule. It can therefore be seen how mutations in any constituent of the DAG complex can give rise to a diseased phenotype- with disease severity dependent upon a proteins significance within the junction.

As in epithelial cells and spermatozoa, the tight-junction like dystrophin complex may serve to delineate functional membrane domains. In excitable cells of the muscles and nervous system, this domain demarcation may be essential for function. Although neither dystrophin nor utrophin are essential for formation of specialised structures like NMJs, the junctional complex may help retain ion channels and receptors at the site of neurotransmitter release- and just as importantly, prevent dilution of receptors at the site by restricting inward diffusion of extrajunctional species into the area. The ability of tight junctions to hold two cells closely together would have structural importance at the synapse and NMJ, where close cell-cell proximity is essential for function. (Perhaps whilst rapsyn is essential for localisation of AChRs, it is utrophin that pulls the motor neuron and muscle together at the NMJ). Similarly, this structural element of the dystrophin/DAG complex and the basal lamina associations could give 3 dimensional stability to junctional folds. The presence of dystrophin outside the region of voltage gated sodium channels at the NMJ may therefore provide a rigid boundary around the junctional domain of the muscle membrane.

Such speculation can only be confirmed through further experimentation, for example to ask are NaChs fixed at the neuromuscular junction, or are extrajunctional channels able to diffuse into the postsynaptic folds? Despite its limitations and the inherent difficulties in probe synthesis, FPR remains one of the best methods available to address this type of question.

6.6 Consequences of this study for proposed functions of dystrophin.

During the timescale of this PhD study, many papers have been produced investigating the roles of dystrophin and it's associated proteins. However, despite knowing dystrophin's sequence, seeing the clinical consequences of dystrophin protein deficiency, predicting regions of protein structure, and finding further associated proteins, the question still remains unanswered- what is dystrophin doing? It seems that knowledge of protein-protein interactions and of further members of the DAG continues to grow, but the true functional significance of that knowledge remains elusive.

Whether dystrophin is or is not an essential molecular fence constituent, the results presented here do not negate any of the models of dystrophin function proposed so far. Of these models, the notion of dystrophin as a molecular 'shock absorber' is still the favoured role- modulating contractile shear stress in muscle fibres through the actin contractile fibre/dystrophin/DAG/ECM link (Petrof *et al*, 1993).

6.7 DMD- future prospects and directions.

In contrast to the continuing ambiguity over dystrophin's true function, considerable progress has been made recently towards a possible therapeutic strategy for DMD. Satellite cell transplantation into mdx muscle (e.g. Beauchamp *et al*, 1999) results in the order of 500 new myonuclei generated from each transplanted stem cell nucleus. Transplantation of single myofibres containing around 7 myonuclei can potentially give rise to around 3,000 new fibres. These dystrophin positive fibres remain in the transplanted tissue over several months (T. Partridge, 1999). These results are encouraging, though for now the physical logistics of transplanting myoblasts into every skeletal muscle in the body limits the capabilities of the technique.

A more promising therapeutic area is upregulation of the dystrophin related protein utrophin. Upregulation of utrophin expression in transgenic mdx mice has been demonstrated to ameliorate the dystrophic phenotype (Tinsley *et al*, 1996). DMD/BMD patients possess a fully functional utrophin gene. If this gene can be induced to overexpress utrophin protein, it could compensate for dystrophin deficiency- though the technology needed to do this is still some way off. Similarly, the discovery of naturally occurring revertant dystrophin positive fibres in DMD patients and mdx mice could be a starting point for future therapies. Hopefully during the coming years the puzzle of dystrophin's function and with it the problem of how to effectively compensate for its absence will be solved.

6.8 Summary.

The aim of this study was to investigate the ability of dystrophin to stabilise the muscle fibre membrane and set up subcellular membrane domains by regulating the distribution and diffusion of membrane components.

The pathology of DMD indicates that muscle fibre membrane integrity is compromised by a lack of dystrophin protein. Membrane prostaglandin metabolism, for example, is dramatically influenced by perturbations in the membrane, and is found to be impaired in DMD (reviewed in Jackson, 1993). Dystrophin, with structural and spatial similarities to spectrin, could stabilise the membrane by acting non specifically as a cytoskeletal 'molecular fence'- a steric barrier to membrane protein diffusion- or alternatively by binding specifically to membrane proteins and restricting them to specialised membrane domains.

Whilst direct linkages between dystrophin and its associated glycoprotein complex had been identified; and co-localisation of dystrophin and voltage gated muscle NaChs had been observed, no study had tested whether dystrophin regulates the distribution of these proteins on the cell surface. This study therefore set out to quantify the restraints on lateral mobility of non-specific membrane glycoproteins and specific DAG/NMJ proteins imposed by dystrophin.

During the course of the mobility experiments it was shown that the presence of dystrophin was not the main influence upon mobility of glycoproteins and lipids within the membranes. Unfortunately, due to the many technical problems encountered during the work, the precise nature of dystrophin's interactions with membrane proteins could not be quantified. Difficulties with tissue labelling, FPR data acquisition and/or tissue viability prevented measurement of the molecular fence contribution of dystrophin. Similarly, traditional methods to produce fluorescent markers to specific membrane protein proved unsuitable in this instance. The role of dystrophin in restricting mobility of DAG complex proteins and sodium channels therefore remains open to question.

The unfortunate technical problems encountered during this work should not spell the end of investigations into dystrophin's contribution to the regulation of membrane protein diffusion. Regulation of membrane structure is a universal feature of eukaryotic cells. It is worthy of note that dystrophin protein expression is not restricted to muscle tissue. Isoforms of dystrophin are expressed throughout the body, particularly in excitable cells. Additionally, dystrophin is highly conserved across species. The universality of dystrophin expression may lend support to a general role for the dystrophin isoforms as organisers of cell membranes.

Three polyclonal antibodies to dystrophin peptides were produced in this study. These are effective dystrophin markers in a range of species. They have been distributed to other Muscular Dystrophy

Group funded projects so that research into the role of dystrophin and its associated proteins may continue.

In conclusion, whilst dystrophin has been shown to be essential for stabilising the muscle cell membrane and imparting mechanical strength, the influence of dystrophin upon membrane fluidity and protein diffusion remains speculative. Further experimentation to produce a viable muscle fibre system is necessary before FPR experiments can properly address the issues of dystrophin, molecular fences and protein tethering.

Appendix.

FPR recovery data.

Appendix

FPR recovery data.

Pooled sets of data from individual FPR recovery curves.

'Removed' refers to the time passed between removal of the tissue from the animal and acquisition of the photobleach recovery curve was obtained. 'Pre cps' is the level of photon counts in counts per second from the tissue prior to photobleaching. '% bleach' gives the extent of fluorescence bleaching each time, relative to normalised pre-bleach levels. '% recovery' (f), 't1/2' (T_D), the half time for diffusion and 'Diff. Coeff', the diffusion coefficient were all determined from the diffusion equation, $D_L = w^2 / 4T_D$.

Data from individual experiments was pooled for analysis according to fluorescent label and tissue type. Sets of curves were analysed to determine the mean, standard deviation and standard error of the mean using Microsoft Excel for Windows 95, version 7. Individual curves were preselected for quality of fit to the diffusion equation, before inclusion in the analysis tables (curve $\chi 2 < 10^{-4}$). The date of each experiment is given.

mdx male Treatment: Lens Culinaris	**Removed**	**pre cps**	**% bleach**	**%recovery**	**t 1/2 (sec)**	**Diff. Coeff.- E-10 cm2/sec**
5.8,97 low X2.	50 min	2566	52	5	1.9	8.64E-10
n=36.	55 min	2743	53	9	1.1	1.40E-09
	1hr 5	8260	48	9	2.6	6.20E-10
	1hr 5	4366	62	1	4.8	3.53E-10
	1hr 10	3975	58	4	2.4	6.80E-10
	1hr 15	4640	58	9	5.7	2.80E-10
	1hr 15	4827	58	12	0.4	3.90E-09
22.7.97	50 min	2630	68	6	2	8.10E-10
	1hr	3139	58	10	2.6	6.10E-10
	1hr	4147	74	8	1.2	1.29E-09
	1hr 5	4087	56	8	0.9	1.78E-09
	1hr 5	4344	59	6	2	8.04E-10
	1hr 10	4553	58	6	1.7	9.30E-10
	1hr 20	4564	65	7	2.8	5.70E-10
	1hr 20	4635	61	6	3.6	4.40E-10
21.7.97	50 min	2789	60	12	2.7	6.00E-10
	50 min	3101	66	8	2.7	5.90E-10
	55 min	4226	67	9	2.3	6.90E-10
	55 min	4366	67	8	4.1	3.90E-10
	55 min	4881	62	10	4.2	3.80E-10
	55 min	3567	60	9	4.9	3.30E-10
	1hr 5	4163	77	6	1	1.60E-10
	1hr 10	4691	65	10	6.2	2.60E-10
	1hr 10	3903	69	9	3.3	4.80E-10
	1hr 15	2039	59	11	3.5	4.50E-10
29.7.97	1hr	6218	60	7	1.7	9.30E-10
	1hr 5	4010	65	3	2	7.96E-10
7.8.97	55 min	2008	63	10	2.9	5.60E-10
	1hr 5	4446	53	2	5.2	3.10E-10
	1hr 40	2730	65	7	3.2	4.96E-10
19.1.99 am	1hr	2483	72	6	0.9	1.80E-09
	1hr 5	2763	72	5	0.8	1.90E-09
	1hr 5	2684	82	8	3.2	5.10E-10
	1hr 15	4020	66	11	4.3	3.80E-10
	1hr 10	2004	73	8	0.5	3.30E-09
	1hr 10	1973	67	12	1.7	9.30E-10
Mean		3792.806	63.27778	7.694444	2.694444	8.77E-10
Standard Deviation.		1280.601	7.300141	2.702585	1.504079	8.01E-10
Standard error of mean.		981.838	5.79321	2.134259	1.194136	5.22E-10

C57Bl 6 months old. Treatment: Lens Culinaris	Removed	pre cps	% bleach	%recovery	t 1/2 (sec)	Diff. Coeff.- E-10 cm2/sec
19.1.98 (pm)	45min	9560	64	10	4.4	3.67E-10
n=28	50 min	6701	73	8	4.9	3.25E-10
	50 min	16744	71	7	2.3	6.84E-10
	55 min	3769	70	11	3.8	4.17E-10
	55 min	6219	80	7	7.4	2.17E-10
	1hr	5520	78	8	6.5	2.47E-10
	1hr	6395	77	7	5.4	2.96E-10
	1hr	12097	87	5	2.9	5.50E-10
	1hr 5	10595	84	6	3	5.35E-10
	1hr 5	4626	78	9	5.9	2.69E-10
	1hr 10	4515	76	9	5.5	2.92E-10
	1hr 10	6357	81	8	5.1	3.17E-10
	1hr 15	4977	79	10	4.9	3.29E-10
	1hr 15	5380	80	8	4.6	3.50E-10
	1hr 15	6259	77	11	6.2	2.60E-10
	1hr 20	8008	82	7	4.5	3.53E-10
	1hr 20	8572	80	8	3.2	5.07E-10
19.1.99pm	40 min	962	58	10	1.1	1.44E-09
	45 min	2052	79	8	4.1	3.90E-10
	45 min	2229	78	6	1.2	1.40E-09
	50 min	2865	76	5	0.4	4.00E-09
	50 min	3251	73	10	2	7.90E-10
	1hr	6369	60	9	0.3	5.90E-09
	1hr 5	1421	69	13	7.2	2.20E-10
	1hr 5	1317	74	10	2.2	7.10E-10
	1hr 10	4096	82	4	0.2	6.77E-09
	1hr 15	1648	75	5	1.2	1.35E-09
	1hr 20	859	60	8	5.9	2.70E-10
Mean.		5477.25	75.03571	8.107143	3.796429	1.06E-09
Standard Deviation.		3679.849	7.325663	2.114137	2.151396	1.67E-09
Standard error of mean.		2727.982	5.59949	1.630102	1.82551	1.04E-09

mdx male 8 months old. Treatment: Scon A	Removed	pre cps	% bleach	%recovery	t 1/2 (sec)	Diff. Coeff.- E-10 cm2/sec
14.7.97	50 min	7971	79	8	3.4	4.69E-10
	55 min	8761	73	11	11	1.40E-10
n= 38	1hr	5592	77	10	11	1.39E-10
	1hr	11261	76	7	6.3	2.54E-10
	1hr 5	9546	77	8	8.7	1.84E-10
	1hr 10	5627	76	11	6.5	2.45E-10
	1hr 15	8037	73	9	5.2	3.08E-10
	1hr 15	9835	70	9	7	2.30E-10
	1hr 20	3432	64	11	3.8	4.26E-10
	1hr 20	5376	70	10	4.3	3.74E-10
	1hr 25	14522	61	12	4.5	3.50E-10
	1hr 30	4218	73	9	2.1	7.70E-10
	1hr 30	6347	70	8	1.9	8.61E-10
	1hr 35	9707	72	8	2.7	5.90E-10
	1hr 35	9621	73	6	1.1	1.47E-09
12.06.98	55 min	2804	65	14	4.8	3.30E-10
	55 min	3177	71	9	2.2	7.20E-10
	1hr	2696	65	6	1.9	8.60E-10
	1hr 5	6358	77	7	2.7	5.90E-10
	1hr 10	4069	77	8	2.9	5.50E-10
	1hr 10	2725	72	11	3	5.30E-10
	1hr 15	3494	61	15	5.6	2.90E-10
	1hr 20	4880	60	13	4.1	3.90E-10
	1hr 20	4207	76	8	1	1.50E-09
	1hr 25	3255	73	10	4.1	3.90E-10
	1hr 25	2898	66	11	6.3	2.60E-10
	1hr 25	3261	71	8	1.3	1.20E-09
	1hr 30	2380	57	13	2.3	7.10E-10
	1hr 30	4659	79	8	2.2	7.20E-10
	1hr 40	3769	77	10	3.8	4.20E-10
	1hr 40	4064	70	8	3.2	5.00E-10
7.1.98	40 min	1561	63	7	1.9	8.20E-10
	55 min	5082	72	5	3.8	4.20E-10
	1hr	3796	66	9	7.3	2.20E-10
	1hr 5	2184	64	8	6.2	2.60E-10
	1hr 5	1640	66	8	6.4	2.50E-10
	1hr 10	2176	71	7	1	1.57E-09
	1hr 15	2697	70	3	1.3	1.28E-09
Mean.		5202.237	70.34211	9.026316	4.178947	5.68E-10
Standard Deviation.		3047.928	5.74351	2.454856	2.573793	3.89E-10
Standard error of mean.		2406.825	4.621884	1.875346	2.021884	3E-10

C57Bl 6 months old. Treatment: Scon A	Removed	pre cps	% bleach	%recovery	t 1/2 (sec)	Diff. Coeff.- E-10 cm2/sec
12.1.97 (pm)/(am)	45min	3750	82	6	2.6	6.22E-10
n=28	45min	2250	80	10	7.3	2.18E-10
	50 min	3413	82	7	5.7	2.83E-10
	50 min	2538	72	10	6.1	2.61E-10
	55 min	4155	81	8	4.6	3.45E-10
	55 min	2351	74	12	4.3	3.73E-10
	1hr	2639	71	12	6.7	2.40E-10
	1hr 5	3779	78	8	4.3	3.69E-10
	1hr 10	3130	76	8	2.8	5.73E-10
	1hr 15	2747	77	11	5.3	3.02E-10
	1hr 25	3662	70	8	6.1	2.61E-10
	1hr 30	3399	72	9	2.7	5.91E-10
	1hr 35	2702	83	12	3.3	4.89E-10
	40 min	3644	87	9	2.8	5.60E-10
	40 min	3467	82	15	4.7	3.43E-10
	45 min	2255	84	14	7.7	2.07E-10
	50 min	2489	84	13	7.1	2.25E-10
	50 min	6520	91	6	2.1	7.70E-10
	50 min	3306	87	8	5.8	2.75E-10
	1hr	2711	85	11	3.5	4.56E-10
	1hr 10	2653	81	12	3.1	5.10E-10
	1hr 10	5307	88	7	4	4.05E-10
	1hr 15	1880	81	14	4.1	3.94E-10
	1hr 15	2452	84	13	3.2	4.95E-10
	1hr 20	2452	84	13	3.2	4.95E-10
	1hr 20	3109	84	11	3.6	4.48E-10
	1hr 25	2864	78	13	3.8	4.20E-10
	1hr 30	3002	73	14	2.5	6.30E-10
Mean.		3165.214	80.39286	10.5	4.392857	4.13E-10
Standard Deviation.		968.9409	5.560038	2.673602	1.613124	1.47E-10
Standard error of mean.		684.6173	4.522959	2.321429	1.341327	1.21E-10

C57Bl 6 months old. Treatment: RCA 120	Removed	pre cps	% bleach	%recovery	t 1/2 (sec)	Diff. Coeff.- E-10 cm2/sec
19.1.98 (am)	50 min	6001	82	13	6.1	2.62E-10
n=31	50 min	5161	76	12	3.3	4.88E-10
	1hr	5470	88	6	3.4	4.67E-10
	1hr	4055	93	9	4.2	3.85E-10
	1hr 5	4122	86	8	2.5	6.34E-10
	1hr 5	5235	81	8	3.1	5.10E-10
	1hr 10	4863	83	9	6	2.65E-10
	1hr 10	4068	80	11	3.9	4.13E-10
	1hr 15	5039	83	9	4.7	3.43E-10
	1hr 15	9879	82	6	4.9	3.28E-10
	1hr 15	4537	79	10	3.2	5.06E-10
	1hr 20	7479	82	9	2.2	7.45E-10
	1hr 20	7570	87	8	2.1	7.45E-10
	1hr 20	4534	82	9	4.5	3.53E-10
	1hr 25	7664	87	6	3.7	4.36E-10
	1hr 25	4247	84	9	3.3	4.82E-10
	1hr 25	6199	84	7	2.6	6.16E-10
20.1.99 am	40 min	922	75	14	2.4	6.60E-10
	45min	1337	73	10	3.6	4.40E-10
	50 min	538	65	19	8.2	1.96E-10
	55 min	604	68	12	1.7	9.64E-10
	1hr	794	79	11	3.2	5.00E-10
	1hr 10	719	74	14	3	5.40E-10
	1hr 10	681	75	13	2.5	6.46E-10
	1hr 15	2302	78	7	1.1	1.50E-09
	1hr 15	1874	69	12	1.3	1.20E-09
	1hr 20	1390	73	11	2	7.80E-10
	1hr 20	1506	74	11	1.7	9.10E-10
20.1.99pm		2015	87	7	1.6	1.00E-09
	45 min	772	70	14	1.4	1.10E-09
X2<1.5	55 min	477	80	16	2.7	6.00E-10
	1hr	1319	77	12	5.5	2.90E-10
Mean.		3542.91	79.2500	10.3750	3.3000	6.03E-10
Standard Deviation.		2596.789	6.4907	3.0665	1.5990	3.00E-10
Standard error of mean.		2243.35	5.234375	2.460938	1.19375	2.29E-10

mdx male Treatment: RCA 120	**Removed**	**pre cps**	**% bleach**	**%recovery**	**t 1/2 (sec)**	**Diff. Coeff.- E-10 cm2/sec**
9.6.98	55 min	1504	68	12	6.5	2.40E-10
n=21	55 min	1589	70	14	5.5	2.90E-10
	1hr	1168	58	16	4.2	3.80E-10
	1hr 5	1047	61	16	4.8	3.40E-10
	1hr10	1718	72	12	3	5.20E-10
	1hr 10	1450	71	14	7.9	2.00E-10
	1hr 15	2023	73	11	2.7	5.90E-10
	1hr 15	2479	74	10	3.2	5.10E-10
	1hr 20	1552	68	9	2	8.20E-10
	1hr 20	1698	68	11	3.9	4.10E-10
	1hr 20	2253	73	10	2.9	5.50E-10
	1hr 30	2156	74	13	1.5	1.10E-10
	1hr 30	2876	71	13	4.3	3.80E-10
	1hr 35	4899	69	9	3.9	4.10E-10
	1hr 40	2463	75	14	0.8	2.10E-10
17.6.98	55 min	3810	69	5	1.1	1.47E-09
	1hr	3846	70	11	6.7	2.37E-10
	1hr 10	3649	66	12	7.2	2.21E-10
	1hr 20	2598	59	12	6.4	2.48E-10
	1hr 30	19496	68	11	5.5	2.91E-10
	1hr 35	8474	70	11	6.5	2.40E-10
Mean.		3464.19	68.90476	11.71429	4.309524	4.13E-10
Standard Deviation.		4032.096	4.668027	2.492847	2.094255	2.94E-10
Standard error of mean.		2227.51	3.356009	1.823129	1.734694	1.89E-10

All samples pooled
X2<E-4

C57Bl 12 months old. Treatment: Scon A. 29+/- 1oC	Removed	pre cps	% bleach	%recovery	t 1/2 (sec)	Diff. Coeff.- E-9 cm2/sec
22.6.99pm	55 min	3360	77	61	0.9	1.79E-09
	55 min	1096	59	67	1.1	1.46E-09
	1hr	2749	77	66	1.1	1.41E-09
	1hr 5	1525	70	69	1	1.60E-09
	1hr 5	907	69	81	0.3	4.94E-09
	1hr 5	622	67	70	0.4	4.30E-09
	1hr 10	1323	76	60	0.4	3.94E-09
	1hr 10	1850	77	59	0.8	1.90E-09
	1hr 15	1271	73	51	1.2	1.35E-09
mobile 25.6.99pm	45 min	1961	76	67	1.9	8.24E-10
	1hr 5	703	77	77	2.5	6.35E-10
9.6.99 am						
	30min	552	56	59	1.1	1.45E-09
	35 min	1300	74	68	0.3	6.21E-09
	40 min	1118	72	78	1.5	1.06E-09
	45 min	623	61	74	0.8	1.90E-09
	45 min	545	68	73	0.3	5.57E-09
	50 min	910	69	83	0.9	1.87E-09
n=17						
Mean.- mobile		1318.529	70.47059	68.41176	0.970588	2.48E-09
Standard Deviation.		787.1634	6.643772	8.689497	0.594522	1.77E-09
Standard error of mean.		571.391	5.266436	6.788927	0.427682	1.48E-09
Immobile.						
22.6.99 pm	35 min	2457	84	7	2.4	6.60E-10
25.6.99 pm	25 min	5120	84	16	18	8.70E-11
	25 min	1801	63	14	14	1.11E-10
*	40 min	461	60	12		
*	55 min	339	75	4		
*	55 min	504	71	6		
	1hr	236	74	12	5	3.23E-10
n=7						
Mean.- immobile		1559.714	73	10.14286	9.85	2.95E-10
Standard Deviation.		1784.332	9.309493	4.488079	7.363649	2.65E-10
Standard error of mean.		1342.531	7.142857	3.836735	6.15	1.96E-10

mdx 9 months old. Treatment: SconA. 29+/- 1oC	**Removed**	**pre cps**	**% bleach**	**%recovery**	**t 1/2 (sec)**	**Diff. Coeff.- E-10 cm2/sec**
24.6.99 pm	35 min	256	60	16		
n=24	35 min	1084	70	9	3.4	4.75E-10
	35 min	806	71	17	14	1.11E-10
	40 min	2261	88	4	7.1	2.26E-10
	45 min	4036	90	5	3.7	4.30E-10
25.6.99am	25 min	997	81	15	5.4	3.00E-10
	25 min	1603	79	15	6.3	2.53E-10
	30 min	1638	77	9	3.1	5.24E-10
*	30 min	1241	78	13	2.9	5.50E-10
	30 min	611	63	19	4.8	3.35E-10
4.5.99	30min	5416	87	8	8.2	1.96E-10
	35 min	2373	83	14	31.7	5.00E-11
	40 min	1019	81	15	7.2	2.28E-10
	40 min	1624	81	16	10	1.59E-10
	45 min	1328	84	12	5.6	2.88E-10
	45 min	2686	88	9	6	2.67E-10
	50 min	2651	84	6	11	1.49E-10
	50 min	3585	87	6	4.8	3.34E-10
	1hr	2049	80	9	4.1	3.92E-10
	1hr	1989	88	7	3.8	4.21E-10
	1hr 5	1803	86	8	6.7	2.39E-10
	1hr 10	3463	80	10	8.3	1.90E-10
	1hr 15	4121	86	4	2.6	6.22E-10
	1hr 15	3055	82	8	10	1.57E-10
Mean.		2153.958	80.58333	10.58333	7.421739	3E-10
Standard Deviation.		1273.72	7.762321	4.43226	6.037154	1.49E-10
Standard error of mean.		1008.951	5.604167	3.847222	3.586767	1.2E-10

* analysed by eye
No recovery. Difficult to fit to curves.

C57 BL 9 months old. Treatment: ODAF. 22+/- 1oC	**Removed**	**pre cps**	**% bleach**	**%recovery**	**t 1/2 (sec)**	**Diff. Coeff.- E-10 cm2/sec**
18.6.99 am	25 min	327	89	4	25	6.40E-11
	30 min	376	90	2	1.1	1.39E-09
n=21	35min	1053	90	8	11	1.47E-10
*	35 min	519	71	25		
	40min	508	85	2	7	2.28E-10
*	55 min	232	78	19		
*	1hr 10	259	77	3		
*	1hr 10	377	78	9		
*	1hr 15	419	82	5		
*	1hr 15	192	65	8		
21.6.99 *	30 min	187	81	11		
	30 min	290	79	12	0.7	2.41E-09
*	35 min	175	74	6		
*	35 min	194	65	4		
*	35 min	291	75	11		
*	40 min	263	73	8		
	40 min	343	82	8	9.4	1.70E-10
	40 min	200	67	5	1.9	8.45E-10
*	55 min	124	63	12		
*	55 min	141	61	6		
*	1hr	256	81	9		
Mean.		320.2857	76.47619	8.428571	8.014286	7.51E-10
Standard Deviation.		200.6712	8.755678	5.536889	8.55442	8.77E-10
Standard error of mean.		129.4966	7.07483	3.863946	6.102041	6.84E-10

* analysed by eye
No recovery. Difficult to fit to curves.

C57 2 months old. Treatment: ODAF. 29+/- 1oC	Removed	pre cps	% bleach	%recovery	t 1/2 (sec)	Diff. Coeff.- E-10 cm2/sec
Pooled *	30 min	486	84	14	0.5	3.49E-10
22.6.99 am *	35 min	3707	94	5	6	2.68E-10
n=20	35 min	1479	95	11	10.3	1.60E-10
	40 min	753	91	5	5.3	3.00E-10
	45 min	779	81	6	2.4	6.69E-10
	50 min	1696	94	10	17	9.28E-10
	1hr	1382	93	7	11	1.43E-10
*	1hr	240	78	11		
	1hr 5	1472	88	14	11	1.45E-10
	1hr 10	791	79	20	6.2	2.57E-10
23.6.99 am *	30 min	486	84	14	0.5	3.49E-10
*	35 min	3707	94	5	6	2.68E-10
	35 min	1479	95	11	10.3	1.60E-10
	40 min	753	91	5	5.3	3.00E-10
	45 min	779	81	6	2.4	6.69E-10
	50 min	1696	94	10	17	9.28E-10
	1hr	1382	93	7	11	1.43E-10
*	1hr	240	78	11		
	1hr 5	1472	88	14	11	1.45E-10
	1hr 10	791	79	20	6.2	2.57E-10
Mean.		1278.5	87.7	10.3	7.744444	3.58E-10
Standard Deviation.		953.1178	6.489668	4.680306	4.92105	2.6E-10
Standard error of mean.		668.7	5.76	3.7	4.071605	1.96E-10

* analysed by eye
No recovery. Difficult to fit to curves.

mdx 9 months old. Treatment: ODAF. 23+/- 1oC	**Removed**	**pre cps**	**% bleach**	**%recovery**	**t 1/2 (sec)**	**Diff. Coeff.- E-10 cm2/sec**
16.6.99 am	30min	722	87	16	31	5.15E-11
n=25	35 min	577	78	22	30	5.42E-11
	35 min	526	75	5	5.7	2.83E-10
	40 min	576	80	15	10	1.57E-10
recovered	50 min	241	70	48	2	7.85E-10
	50 min	346	70	34	7.7	2.07E-10
	55 min	1116	90	10	12	1.38E-10
	55 min	1069	87	12	14	1.17E-10
	55 min	516	80	23	13	1.24E-10
	1hr	761	89	19	29	5.48E-11
	1hr 5	377	81	16	7.4	2.17E-10
	1hr 10	479	85	16	20	7.91E-11
*	1hr 15	295	55	2		
*	1hr 15	219	52	4		
16.6.99 pm	30min	419	90	24	38	4.22E-11
	40 min	327	87	27	22	7.38E-11
	40 min	528	86	22	29	5.47E-11
	45 min	593	87	20	18	8.75E-11
	50 min	316	82	23	27	5.87E-11
	1hr	517	86	14	25	6.53E-11
	1hr 5	719	87	14	6.5	2.45E-10
	1hr 5	797	85	15	20	7.83E-11
	1hr 10	346	75	40	9.6	1.67E-10
	1hr 15	405	84	17	22	7.23E-11
	1hr 15	323	71	22	15	1.04E-10
Mean.		524.4	79.96	19.2	17.99565	1.44E-10
Standard Deviation.		235.0564	10.02696	10.42433	9.778338	1.55E-10
Standard error of mean.		177.248	7.4944	7.504	8.265406	9.14E-11

* analysed by eye
No recovery. Difficult to fit to curves.

mdx 9 months old. Treatment: ODAF. 29+/- 1oC	Removed	pre cps	% bleach	%recovery	t 1/2 (sec)	Diff. Coeff.- E-10 cm2/sec
17.6.99 pm+am *	30min	390	90	11		
* n=22	35 min	540	60	7		
	40 min	1628	90	10	26	6.05E-11
	45 min	670	86	9	3.8	4.20E-10
	50 min	524	85	16	14	1.13E-10
	55 min	3321	94	11	28	5.70E-10
*	1hr	202	74	12		
	1hr	281	78	16	7.5	2.13E-10
	1hr 5	358	81	9	4.5	3.56E-10
*	1hr 10	218		6		
*	1hr 10	244	74	5		
*	1hr 15	382	75	4		
am	35 min	204		4		
	40 min	186	48	2	12	1.30E-10
	45 min	375	84	11	0.3	5.19E-09
	45 min	218	68	25	14	1.17E-10
	50 min	239	51	2		
	55 min	585	88	8	1	1.60E-09
	55 min	217		7		
	1hr 5	1049	90	19	8.9	8.21E-11
	1hr 10	397	82	25	15	1.05E-10
	1hr 15	1004	93	7	7.3	2.19E-10
Mean.		601.4545	78.47368	10.27273	10.94615	7.06E-10
Standard Deviation.		702.5765	13.49225	6.482077	8.601804	1.41E-09
Standard error of mean		424.0661	10.50416	4.867769	6.665089	8.27E-10

* analysed by eye
No recovery. Difficult to fit to curves.

References.

References

Ahn A.H and Kunkel, L.M, The structural and functional diversity of dystrophin. Nature Genetics 3, 283-291. (1993).

Amalfitano, A, Rafael, J.A and Chamberlain, J.S. Sucture and mutation of the dystrophin gene. Dystrophin; Gene, Protein and Cell Biology. Ch 1 pp 1-26 Brown and Lucy eds. Cambridge University press. (1997).

Anderson, M.J. and Cohen, M.W. Nerve-induced and spontaneous redistribution of acetylcholine receptors on cultured muscle cells. Journal of Physiology, 268, 757-773, (1977).

Angelides K.J. Fluorescently labelled sodium channels are localised and immobilised to synapses of innervated muscle fibres. Nature 321, 63-66, (1986).

Angelides, K.J. Fluorescent Analogues of Toxins. In Methods in Cell Biology, Academic Press, 29, 29-58, (1989).

Angelides, K.J, Elmer, L.W, Loftus, D, and Elson, E. Distribution and lateral mobility of Voltage-dependant sodium channels in neurons. J. Cell Biology 106, 1911-1925, (1988).

Apel, E.D. and Merlie, J.P. Assembly of the postsynaptic apparatus, Current Opinion in Neurobiology, 5, 62-67, (1995).

Arahata, K, Ishiura, S., Ishguro, T., Tsukahara, T., Suhara, Y., Eguchi, C., Ishihra, T., Nonaka, I., Ozawa, E., and Sugita, H. Immunostaining of skeletal and cardiac muscle surface membrane with antibody against Duchenne muscular dystrophy peptide. Nature, 333, 861-863, (1988).

Axelrod, D. Lateral motion of membrane proteins and biological function. Journal of Membrane Biology, 75, 1-10, (1983).

Axelrod, D., Ravdin, P., Koppel, D.E., Schlessinger, J., Webb, W.W., Elson, E.L. and Podleski, T.R. Lateral motion of fluorescently labelled acetylcholine receptors in membranes of developing muscle fibres. P.N.A.S. 73, 4594-4598, (1976).

Barany, M. and Venkatasubramanian, P.N. Estimation of tissue phospholipids by natural abundance ^{13}C-NMR. Biochemica et Biophysica Acta, 923, 339-346, (1988).

Beauchamp, J.R., Morgan, J.E., Pagel, C.N. and Partridge, T.A. Dynamics of myoblast transplantation reveal a discreet minority of precursors with stem cell-like properties as the myogenic source. Journal of Cell Biology, 144, 1113-1121, (1999).

Benke, T.A., Jones, O.T., Collingridge, G.L and Angelides, K.J. N-Methyl-D-Aspartate receptors are clustered and immobilised on dendrites of living cortical neurons. Neurobiology, 90, 7819-7823, (1993).

Bennett, V. The membrane skeleton of erythrocytes and its implications for more complex cells. Annual Review of Biochemistry, 54, 273-304, (1985).

Bewick, G.S., Nicholson, L.V.B., Young, C., O'Donnel, E. and Slater, C.R., Different distributions of dystrophin and related proteins at nerve-muscle junctions. Neuroreport, 3, 857-860, (1992).

Bewick G.S, Young C and Slater C.R. Spatial relatioships of utrophin, dystrophin, β-dystroglycan and β-spectrin to acetylcholine receptor clusters during postnatal maturation of the rat neuromuscular junction. Journal of Neurocytology 25, 367-379 (1996).

Bianchi, A.B, Hara, T, Ramesh, V, Gao, J, Klein-Szanto, A-J, MÖ, F, Menon, A.G, Trofatter, J.A, Gusella, J.F, Seizinger, B.R. Mutations in transcript isoforms of the neurofibromatosis 2 gene in multiple human tumor types. Nature Genetics 6, 185-192, (1994).

Bloch, R.J. and Pumplin, D.W. Molecular events in synaptogenesis: nerve-muscle adhesion and postsynaptic differention. American Journal of Physiology, 254, C345-C364, (1988).

Boullier, J.A, Peacock, J.S., Roess, D.A and Barisas, B.G. Protein and lipid lateral diffusion in normal and Rous sarcoma virus transformed chick embryo fibroblasts. Biochemica *et* Biophysica Acta, 1107, 193-199, (1992).

Brown, S.C and Lucy J.A. Functions of dystrophin. Dystrophin; Gene, Protein and Cell Biology. Ch 7, pp 163-200. Brown and Lucy eds. Cambridge University press. (1997).

Bulfield, G, Siller, W.G, Wight, P.A.L and Moore, K.J. X-chromosome linked muscular dystrophy (*mdx*) in the mouse. Proceedings of the National Academy of Sciences USA 81, 1189-1192, (1984).
Butz, S., Rawer, S., Rapp, W. and Birsner, U. Immunization and affinity purification of antibodies using resin-immobilized lysine-branched synthetic peptides. Peptide Research, 7, 20-22, (1994).

Byers, T.J., Kunkel, L.M. and Watkins, S.C. The subcellular distribution of dystrophin in mouse skeletal, cardiac and smooth muscle. Journal of Cell Biology, 115, 411-421, (1991).

Campbell, K.P. Three muscular dystrophies: Loss of cytoskeleton-extracellular matrix linkage. Cell, 80, 675-679, (1995).

Campbell K.P and Kahl S.D. Association of dystrophin and an integral membrane glycoprotein. Nature 321, 259-262 (1989).

Cohen, M.W., Lacobson, C., Godfrey, E.W., Campbell, K.P. and Carbonetto, S. Distribution of α-dystroglycan during embryonic nerve-muscle synaptogenesis. Journal of Cell Biology, 129, 1093-1101, (1995).

Cullen, M.J., Walsh, J., Roberds, S.L. and Campbell, K.P. Ultrastructural localization of adhalin, α-dystroglycan and merosin in normal and dystrophic muscle. Neuropathology and Applied Neurobiology, 22, 30-37, (1996).

Deconinck, A.E., Potter, A.C., Tinsley, J.M., Wood, S.J., Vater, R., Young, C., Metzinger, L., Vincent, A., Slater, C.R. and Davies, K.E. Postsynaptic abnormalities at the neuromuscular junctions of utrophin-deficient mice. Journal of Cell Biology, 136, 883-894, (1997).

Dubowitz, V. Muscle Biopsy: A practical approach. (Balliere Tindall ,East Sussex, England), (1985).

Dubreuil, R.R *et al.* Structure, calmodulin binding and calcium binding properties of recombinant alpha spectrin polypeptides. J.Biol. Chem. 266, 7189-93. (1991).

Duggan, D.J. and Hoffman, E.P. Autosomal recessive muscular dystrophy and mutations of the sarcoglycan complex. Neuromuscular Disorders, 6, 475-482, (1996).

Edidin, M. Patches and fences: probing for plasma membrane domains. Journal of Cell Science, Supplement 17, 165-169, (1993).

Edidin, M., Kuo, S.C. and Sheetz, M.P. Lateral movements of membrane glycoproteins restricted by dynamic cytoplasmic barriers. Science, 254, 1379-1382, (1991).

Edidin, M and Stroynowski, I. Differences between the lateral organisation of conventional and inositol phospholipid-anchored membrane proteins. A further definition of micrometer scale membrane domains. Journal of Cell Biology 112, 1143-1150, (1991).

Ervatsi, J.M. and Campbell, K.P. Membrane organisation of the dystrophin-glycoprotein complex. Cell, 66, 1121-1131, (1991).

Ervatsi, J.M. and Campbell, K.P. A role for the dystrophin glycoprotein complex as a transmembrane linker between laminin and actin. Journal of Cell Biology, 122, 809-823, (1993) a).

Ervasti J.M. and Campbell K.P. Dystrophin and the membrane skeleton. Current Opinion in Cell Biology 5, 82-87, (1993 b).

Ervasti, J.M., Ohlendieck, K., Kahl, S.D., Gaver, M.G. and Campbell, K.P. Deficiency of a glycoprotein component of the dystrophin complex in dystrophic muscle. Nature, 345, 315-319, (1990).

Fanin, M., Daniele, G.A., Vitiello, L., Senter, L. and C. Angelini. Prevalence of dystrophin positive fibres in 85 Duchenne muscular dystrophy patients. Neuromuscular Disorders, 2, 41-45, (1992).

Fertuck H.C. and Salpeter, M.M. Quantiation of junctional and extrajunctional acetylcholine receptors by electron microscope autoradiography after ^{125}I-α-bungarotoxin binding at mouse neuromuscular junctions. Journal of Cell Biology, 69, 144-158, (1976).

Flucher B and Daniels M.P. Distribution of Na^+ channels and ankyrin In neuromuscular junctions is complememtary to that of acetylcholine receptors and the 43 kd protein. Neuron 3, 163-169, (1989).

Franco, A and Lansman, J.B. Calcium entry through stretch inactivated ion channels in mdx myotubes. Nature 344, 670-673, (1990).

Friedrichson, T. and Kurzchalia, T.V. Microdomains of GPI anchored proteins in living cells revealed by crosslinking. Nature, 394, 802-805, (1998).

Froehner, S.C. The submembrane machinery for nicotinic acetylcholine receptor clustering, Journal of Cell Biology, 114, 1-7, (1991).

Froehner, S.C., Luetje, C.W., Scotland, P.B. and Patrick, J. The postsynaptic 43K protein clusters muscle nicotinic acetylcholine receptors in Xenopus oocytes. Neuron, 5, 403-410, (1990).

Gautam, M., Noakes, P.G., Mudd, J, Nichol, M., Chu, G.C., Sanes, J.R. and Merlie, J.P. Failure of post-synaptic specialisations to develop at neuromuscular junctions of rapsyn-deficient mice. Nature, 377, 232-236, (1995).

Gee, S.H., Montanaro, F., Lindenbaum, M.H. and Carbonetto, S. Dystroglycan-alpha, a dystrophin-associated glycoprotein, is a functional agrin receptor. Cell, 77, 675-686, (1994).

Harlow and Lane a). Serum preparation. In: Antibodies, A laboratory manual. Cold Spring Harbor Press. p119, (1988).

Harlow and Lane b). Coupling peptides to carrier proteins using glutaraldehyde. In: Antibodies, A laboratory manual. Cold Spring Harbor Press. pp78-79, (1988).

Hoffman, E.P, Brown, R.H. and Kunkel, L.M. Dystrophin: the protein product of the Duchenne Muscular Dystrophy locus. Cell 51, 919-928. (1987).

Hoffman, E.P. and Gorospe, J.R.M. The animal models of Duchenne muscular dystrophy: windows on the pathophysiological consequences of dystrophin deficiency. In, Current Topics in Membrane Research, 38, (Mooseker and Morrow, eds), Academic Press, New York, pp 113-154, (1992).

Hoffman, E.P., Morgan, J.E., Watkins, S.C. and Partridge, T.A. Somatic reversion/supression of the mouse mdx phenotype in vivo. Journal of Neurological Sciences, 99, 9-25, (1990).

Jackson, M.J. Molecular mechanisms of muscle damage. In Molecular and Cell Biology of Muscular Dystrophy (T. Partridge, ed), Chapman and Hall, London, pp 257-282, (1993).

Jacobson, K., Derzko, H.Z., Wojcieszyn, J. and Organisciak, D. Lipid lateral diffusion in the surface membrane of cells and in multibilayers formed from the plasma membrane lipids. Biochemistry, 20, 5269-5275, (1981).

Jacobson, K., Ishihara, A. and Inman, R. Lateral diffusion of proteins in membranes. Annual Review of Physiology, 49, 163-175, (1987).

James, P.S., Wolfe, C.A., Ladha, S. and Jones, R., Lipid diffusion in the plasma membrane of ram and boar spermatozoa during maturation in the epididymis measured by fluorescence recovery after photobleaching. Molecular Reproduction and Development, 52, 207-215, (1999).

Joe, E-H. and Angelides, K.J. Clustring of voltage dependent sodium channels on axons depends on Schwann cell contact. Nature, 356, 333-335, (1992).

Joe, E.H., and Angelides, K.J. Clustering and mobility of voltage -dependent sodium channels during myelination. Journal of Neuroscience, 13, 2993-3005, (1993).

Kaplan, M.R., Meyer-Franke, A., Lambert, S., Bennet, V., Duncan, I.D., Levinson, S.R. and Barres, B.A. Induction of sodium channel clustering by oligodendrocytes. Nature, 386, 724-728, (1997).

Karpati, G. and Carpenter, S.C. The deficiency of a sarcolemmal cytoskeleton (dystrophin) leads to necrosis of skeletal muscle fibres in Duchenne-Becker dystrophy, in: Neuromuscular Junction, (Sellin, L.S., Libelius, R. and Thesloff, S. eds) Elsevier, Amsterdam, pp429-436, (1988).

Khurana, T.S., Watkins, S.C., Chafey, P., Chelley, J., Tomé, F., Fardeau, M., Kaplan, J. and Kunkel, L.M. Immunolocalisation and developmental expression of dystrophin related protein in skeletal muscle. Neuromuscular Disorders, 1, 185-194, (1991).

Klein, C.J., Coovert, D.D., Bulman, D.E., Ray, P.n., Mendell, J.R., and Burghes, A.H.M. Somatic reversion/suppression in Duchenne muscular dystrophy (DMD): evidence supporting a frame-restoring mechanism in rare dystrophin-positive fibers. American Journal of Human Genetics, 50, 950-959, (1992).

Kloster, K.L., Tengbe, M.A., Furtula, V. and Nothnagel, E.A. Effects of low temperature on lateral diffusion in plasma membranes on maize (*Zea mays* L.) root cortex protoplasts: relevance to chilling sensitivity. Plant, Cell and Environment, 17, 1285-1294, (1994).

Knowles, D.W., Chasis, J.A., Evans, E.A. and Mohandas, N. Cooperative action between band 3 and glycophorin A in human erythrocytes: immobilisation of band 3 induced by antibodies to glycophorin A. Biophysical Journal, 66, 1726-1732, (1994).

Koenig, M. and Kunkel, L.M. Detailed analysis of the repeat domain of dystrophin reveals four potential hinge segments that may confer flexibility. Journal of Biological Chemistry, 265, 4560-4566, (1990).

Koenig, M, Monaco, A.P. and Kunkel, L.M. The complete sequence of dystrophin predicts a rod-shaped cytoskeletal protein. Cell, 53, 219-228, (1988).

Kordeli, E., Lambert, S., and Bennet, V. Ankyrin G. A new ankyrin gene with neural-specific isoforms localized at the axonal initial segment and node of Ranvier. Journal of Biological Chemistry, 270, 2352-2359, (1995).

Kusumi, A. and Sako, Y. Cell surface organisation by the membrane skeleton. Current Opinion in Cell Biology, 8, 566-574, (1996).

Kusumi, A., Sako, Y. and Yamamoto, M. Confined lateral diffusion of membrane receptors as studied by single particle tracking (nanovid microscopy). Effects of calcium-induced differentiation in cultured epithelial cells. Biophysical Journal, 65, 2021-2040, (1993).

Ladha, S., James, P.S., Clark, D.C., Howes, E.A. and Jones, R. Lateral mobility of plasma membranes in bull spermatozoa: heterogeneity between surface domains and rigidification following cell death. Journal of Cell Science, 110, 1041-1050, (1997).

Levine, B.A, Moir, A.J.G, Patchell, V.B and Perry, S.V. Binding sites involved in the interaction of actin with the N-terminal region of dystrophin. FEBS Letters 298, 44-48. (1992).

Lidov, H.G., Byers, T.J. and Kunkel, L.M. The distribution of dystrophin in the murine central nervous system: an immunocytochemical study. Neuroscience 54, 167-187, (1993).

Lidov, H.G., Byers, T.J., Watkins, S.C. and Kunkel, L.M. Localisation of dystrophin to postsynaptic regions of central nervous system cortical neurons. Nature 348, 725-728, (1990).

Love, D.R., Hill, D.F., Dickson, G., Spurr, N.K., Byth, B.C., Marsden, R.F., Walsh, F.S., Edwards, Y.H. and Davies, K.E. An autosomal high molecular weight transcript in skeletal muscle with homology to dystrophin. Nature, 339, 55-58, (1989).

Love, D.R, Morris, G.E, Ellis, J.M, Fairbrother, L, Marsden, R.F, Bloomfield, J.F, Edwards, Y.H, Slater, C.P, Parry, D.J. and Davies, K.E. Tissue distribution of the dystrophin-related gene product and expression in the *mdx* and *dy mouse*. PNAS 88, 3243-3247. (1991).

Lyons, P.R. and Slater, C.R. Structure and function of the neuromuscular junction in young adult *mdx* mice. Journal of Neurocytology, 20, 969-981, (1991).

Matsumara, K., Tomé, F.M.S., Collin, H., Azibi, K., Chaouch, M., Kaplan, J-C., Fardeau, M. and Campbell, K.P. Deficiency of the 50K dystrophin-associated glycoprotein in severe childhood autosomal recessive muscular dystrophy. Nature, 359, 320-322, (1992).

Menke, A. and Jockusch, H. Decreased osmotic stability of dystrophin-less muscle cells from the mdx mouse. Nature 349, 69-71, (1991).

Metcalf, T.N., Wang, J.L. and Schindler, M. Lateral diffusion of phospholipids in the plasma membrane of soybean protoplasts: Evidence for membrane lipid domains. P.N.A.S. U.S.A., 83, 95-99, (1986),

Michalak, M. and Opas, M. Functions of dystrophin and dystrophin associated proteins. Current Opinion in Neurology, 10, 436-442, (1997).

Myles, D., Primakoff, P. and Koppel, D. A localised surface protein of guinea pig sperm exhibits free diffusion in its domain. Journal of Cell Biology, 98, 1095-1099, (1984).

Nicholson, L.V.B., Davidson, K., Johnson, M.A., Slater, C.R., Young, C., Bhattacharya, S, Gardner-Medwin, D, et al . Dystrophin in skeletal muscle. II. Immunoreactivity in patients with Xp21 muscular dystrophy. Journal of Neurological Sciences, 94, 137-146, (1989).

Nicholson, L.V.B., Johnson, M.A., Bushby, K.M.D. and Gardner-Medwin, D. Functional significance of dystrophin-positive fibres in Duchenne Muscular Dystrophy. Arch Dis Child 68, 632-636, (1993).

Nitkin, R.M., Smith, M.A., Magill, C., Fallon, J.R., Yao, Y.M.M., Wallace, B.G. and McMahan, U.J. Identification of agrin, a synaptic organizing protein from Torpedo electric organ. Journal of Cell Biology, 105, 2471-2478, (1987).

Ohlendieck, K, and Campbell, K.P. Dystrophin-associated proteins are greatly reduced in skeletal muscle from mdx mice. J. Cell Biology 115, 1685-1694. (1991 a).

Ohlendieck, K. and Campbell, K.P. Dystrophin constitutes 5% of membrane cytoskeleton in skeletal muscle. FEBS Letters, 283, 230-234, (1991 b).

Ohlendieck, K., Matsumara, K., Ionasescu, V.V., Towbin, J.A., Bosch, E.P., Weinstein, S.L., Sernett, S.W. and Campbell, K.P., Duchenne muscular dystrophy: deficiency of dystrophin-associated proteins in the sarcolemma. Neurology, 43, 795-800, (1993).

Olivera B.M, Gray W.R, Zeikus R, McIntosh J.M, Varga J, River J, De Santos V and Cruz L.J. Peptide neurotoxins from fish-hunting cone snails. Science 230, 1338-1343, (1985).

Partridge, T.A. Dystrophinopathy models, mechanisms and therapies. Dystrophin; Gene, Protein and Cell Biology. Ch 11. Pp310-331. Brown and Lucy eds. Cambridge University press (1997).

Partridge, T.A. The quest for the muscle stem cell- is it worthwhile? European Congress of Cell Biology seminar, (1999).

Pasternak, C., Wong, S. and Elson, E.L. Mechanical function of dystrophin in muscle cells. Journal of Cell Biology, 128, 355-361, (1995).

Peran, M, Salas, R. and Hooper, H.T. Lateral mobility and anchoring of recombinant GABA receptors. Journal of Molecular Neuroscience, (1999) Submitted.

Peters, L.L., Birkenmeir, C.S., Bronson, R.T., White, R.A., Otto, S.E.E., Bennet, V., Higgins, A., and Barker, J.E. Purkinjie cell degeneration associated with erythroid ankyrin deficiency in *nb/nb* mice. Journal of Cell Biology 114, 1243-1259, (1991).

Peters, R. and Cherry, R.J. Lateral and rotational diffusion of bacteriorhodopsin in lipid bilayers: Experimantal test of the Saffman-Delbruck equations. P.N.A.S., 79, 4317-4321, (1982)

Petrof, B.J., Schrager, J.B., Stedman, H.H., Kelly, A.M. and Sweeny, H.L. Dystrophin protects the sarcolemma from stresses developed during muscle contraction. P.N.A.S. U.S.A., 90, 3710-3714, (1993).

Porter, G.A, Dmytrenko, G.M, Winkelmann, J.C and Bloch, R.J. Dystrophin colocalises with β-spectrin in distinct subsarcolemmal domains in mammalian skeletal muscle. Journal of Cell Biology 117, 997-1005, (1992).

Rafael, J.A, Cox, G.A, Corrado, K, Jung, D, Campbell, K.P and Chamberlain J.S. Forced expression of dystrophin deletion constructs reveals structure-function correlations. J. Cell Biology 134, 93-102, (1996).

Roberds, S.L., Anderson, R.D., Ibraghimov-Beskronovaya, O. and Campbell, K.P. Primary structure and muscle-specific expression of the 50kDa dystrophin associated glycoprotein (Adhalin). Journal of Biological Chemistry, 268, 23739-23742, (1993).

Roberts, R.G., Coffey, A.J., Bobrow, M. and Bentley, D.R. Exon structure of the human dystrophin gene. Genomics, 16, 536-538, (1993).

Rodriguez-Boulan, E. and Nelson, J.W. Morphogenesis of the epithelial cell phenotype. Science, 245, 718-725, (1989).

Saffman, P.G. and Delbruck, M. Brownian motion in biological membranes. P.N.A.S., U.S.A., 72, 3111-3113, (1975).

Sako, Y and Kusumi, A. Compartmentalised structure of the plasma membrane as revealed by nanometer-level motion analysis. Journal of Cell Biology, 125, 1251-1264, (1994).

Sako, Y. and Kusumi, A. Barriers for lateral diffusion of transferrin receptor in the plasma membrane as characterised by receptor dragging by laser tweezers: fence versus tether. Journal of Cell Biology, 129, 1559-1574, (1995).

Sambrook, J., Fritsch, E.F. and Maniatis, T. Molecular Cloning: A laboratory manual (2nd edition). Cold Spring Harbor Laboratory Press, New York, (1989).

Sato, K., Ihsida, Y., Wakamatsu, K., Kato, R., Honda, H., Ohizumi, Y., Nakamura, H. Ohya, M., Lancelin, J-M, Kohda, D. and Inagaki, F. Active site of μ-conotoxin GIIIA, a peptide blocker of muscle sodium channels. Journal of Biological Chemistry, 266, 16989-16991 (1991).

Schlessinger, J., Koppel, D.E., Axelrod, D., Jacobson, K., Webb, W.W. and Elson, E.L. Lateral transport on cell membranes: Mobility of concanavalin A receptors on myoblasts. P.N.A.S. 73, 2409-2413, (1976).

Schroeder, R., London, E. and Brown, D. Interactions between saturated acyl chains confer detergent resistance on lipids and glycoslyphosphatidylinositol (GPI) -anchored proteins: GPI-anchored proteins in liposomes and cells show similar bahaviour. P.N.A.S USA, 91, 12130-12134, (1994).

Sealock, R., Butler, M.H., Kramarcy, N.R., Gao, K.-X, Murnane, A.A., Douville, K. and Froehner, S.C. Localisation of dystrophin relative to acetylcholone receptor domains in electric tissue and adult and cultured skeletal muscle. Journal of Cell Biology, 113, 1133-1144, (1991).

Sealock, R and Froehner, S. Dystrophin and construction of the neuromuscular junction. In Dystrophin; Gene, Protein and Cell Biology. Ch 6. pp139-162. Brown and Lucy eds. Cambridge University press (1997).

Sheets, E.D., Simson, R. and Jacobson, K. New insights into membrane dynamics from the analysis of cell surface interactions by physical methods. Current Opinion in Cell Biology, 7, 707-714, (1995).

Sheetz, M.P, Schindler M, and Koppel D.E. Lateral mobility of integral membrane proteins is increased in spherocytic erythrocytes. Nature 285, 510-512, (1980).

Sicinski, P, Geng, Y., Ryder-Cook, A.S., Barnard, E.A., Darlison, M.G. and Barnard, P.J. The molecular basis of muscular dystrophy in the mdx mouse: a point mutation. Science, 244, 1578-1588, (1989)

Simson, R., Yang, B., Moore, S.E., Doherty, P., Walsh, F.S. and Jacobson, K.A. Structural mosaicism on the submicron scale in the plasma membrane. Biophysical Journal, 74, 297-308, (1998).

Singer, S.J. and Nicholson, G.L. The fluid mosaic model of the structure of cell membranes. Science, 175, 720-731, (1972).

Smith,F.J.D., Eady, R.A.J., Leigh, I.M., McMillan, J.R., Rugg, E.L., Kelsell, D.P., Bryant, S.P., Spurr, N.K., Geddes, J.F., Kirtschig, G., Milana, G., de Bono, A.G., Owaribe, K., Wiche, G., Pulkkinen, L., Uitto, J., McLean, W.H.I., and Lane, E.B. Plectrin deficiency results in muscular dystrophy with epidermolysis bullosa. Nature Genetics, 13, 450-457, (1996).

Srinivasan, Y., Elmer, L., Davis, J., Bennett, V. and Angelides, K.J. Ankyrin and spectrin associate with voltage dependent sodium channels in brain. Nature, 333, 177-180, (1988).

Stya, M. and Axelrod, D.A. Diffusely distributed acetylcholine receptors can participate in cluster formation on cultured rat myotubes. PNAS 80, 449-453, (1983).

Tank, D.W., Wu, E.-S. and Webb, W.W. Enhanced molecular diffusibility in muscle membrane blebs: Release of lateral constraints. Journal of Cell Biology, 92, 207-212, (1982).

Thi Man, N., Ginjaar, I.B., Van Ommen, G.J.B. and G.E. Morris. Monoclonal antibodies for dystrophin analysis. Epitope mapping and improved binding to SDS-treated muscle sections. Biochemical Journal 288, 663-668, (1992).

Thi Man, N. and Morris, G.E. Use of epitope libraries to identify exon-specific monoclonal antibodies for characterisation of altered dystrophins in muscular dystrophy. American Journal of Human Genetics, 52, 1057-1066, (1993).

Thiet Thanh, L., Thi Man, N., Helliwell, T.R. and Morris, G.E. Characterisation of revertant muscle fibres in Duchenne muscular dystrophy, using exon-specific monoclonal antibodies against dystrophin. American Journal of Human Genetics, 56, 725-731, (1995 a).

Thiet Thanh, L., Thi Man, N., Hori, S., Sewrey, C.A., Dubowitz, V. and Morris, G.E. Characterisation of genetic deletions in Becker muscular dystrophy using monoclonal antibodies against a deletion prone region of dystrophin. American Journal of Medical Genetics, 58, 177-186, (1995 b).

Thompson, N,L. and Axelrod, D. Reduced lateral mobility of a fluorescent lipid probe in cholesterol-depleted erythrocyte membrane. Biochemica et Biophysica Acta, 597, 155-165, (1980).

Tinsley, J.M, Blake, D.J, Zuellig, R.A and Davies, K.E. Increasing complexity of the dystrophin-associated protein complex. Proceedings of the National Academy of Sciences USA 91, 8307-8313, (1994).

Tinsley, J.M., Blake, D.J. and Davies, K.E. Dystrophin, utrophin and their associated proteins. In Dystrophin; Gene, Protein and Cell Biology. Ch 3. Pp56-78. Brown and Lucy eds. Cambridge University press (1997).

Tinsley, J.M., Potter, A.C., Phelps, S.R., Fisher, R., Trickett, J.I. and Davies, K.E. Amelioration of the dystrophic phenotype of *mdx* mice using a truncated utrophin transgene. Nature, 384, 349-353, (1996).

Turner, G, Dunckley, M.G. and Dickson G. Gene therapy of Duchenne Muscular Dystrophy. Dystrophin; Gene, Protein and Cell Biology. Ch 10. pp274-309. Brown and Lucy eds. Cambridge University press (1997).

Tsuji, A., Kawasaki, K., Ohnishi, S, Merlke, H. and Kusumi, A. Regulation of band 3 mobilities in erthrocyte ghost membranes bu protein association and cytoskeletal meshwork. Biochemistry, 27, 7447-7452, (1988).

Tsuji, A. and Ohnishi, S. Restriction of the lateral motion of band 3 in the erythrocyte membrane by the cytoskeletal network: dependence on spectrin association state. Biochemistry, 25, 6133-6139, (1986).

Varma, R. and Mayor, S. GPI-anchored proteins are organized in submicron domains at the cell surface. Nature, 394, 798-801, (1998).

Vaz, W.L.C., Criado, M., Madiera, V.M.C, Schoellmann, G. and Jovin, T.M. Size dependence of the translational diffusion of large integral membrane proteins in lipid-crystalline phase lipid bilayers. A study using fluorescence recovery after photobleaching. Biochemistry, 21, 5608-5612, (1982).

Velasquez, J.L., Thompson, C.L., Barnes, E.M. and Angelides, K.J. Distribution and lateral mobility of GABA/ benzodiazapine receptors on nerve cells. Journal of Neuroscience, 9, 2163-2169, (1989).

Vybiral, T., Winkelmann, J.C., Roberts, R., Joe, E-H., Casey, D.L., Williams, J.K. and Epstein, H.F. Human cardiac and skeletal muscle spectrins: Differential expression and localization. Cell Motility and the Cytoskeleton, 21, 293-304, (1992).

Watkins, S.C., Hoffman, E.P., Slayter, H.S. and Kunkel, L.M. Immunoelectron microscopic localization of dystrophin in myofibres. Nature, 333, 863-866, (1988).

Winckler, B. and Poo, M.M. No diffusion barrier at the axon hillock. Nature, 379, 213. (1996).

Winckler, B., Forscher, P. and Mellman, I. A diffusion barrier maintains distribution of membrane proteins in polarized neurons. Nature, 397, 698-701, (1999).

Winder, S.J, Knight, A.E and Kendrick-Jones, J. Protein Structure. Dystrophin; Gene, Protein and Cell Biology. Ch 2. pp27-55. Brown and Lucy eds. Cambridge University press (1997).

Wolf, D.E., Maynard, V.M., McKinnon, C.A. and Melchior, D.L. Lipid domains in the ram sperm plasma membrane demonstrated by differential scanning calorimetry. P.N.A.S., 87, 6893-6896, (1990).

Wolfe, C.A., James, P.S., Mackie, A.R., Ladha, S. and Jones, R. Regionalised lipid diffusion in the plasma membrane of mammalian spermatozoa. Biology of Reproduction, 59, 1506-1514, (1998).

Worton, R.G. and M.W. Thompson. Genetics of Duchenne Muscular Dystrophy. Annual Review of Genetics, 22, 601-629, (1988).

Yechiel, E. and Edidin, M. Micrometer scale domains in fibroblast plasma membranes. Journal of Cell Biology, 105, 755-760, (1987).

Zs.-Nagy, Zhang, X., Kitani, K. and Nonomura, Y. The influence of dystrophin on lateral diffusion of proteins in sarcolemma of L-185 and C2 myoblasts and mature striated muscle cells of rats and mice, as measured by FRAP technique. Biochemical and Biophysical research communications, 215, 67-74, (1995).

Acknowledgements.

I wish to thank all members of Lab 8 in the University of Durham, Dept. of Biological Sciences for their encouragement, assistance and friendship during the course of this PhD- especially the other surviving PhD students in the KJA group, Sue Harris, Macarena Peran, and Angela Wright. Thank you also to Judith Chambers and Peter Hunter for technical assistance.

Thanks are due to Dr R.W. Banks for gallantly taking over the supervision of this project under difficult circumstances, and to Dr Colin Jahoda for adopting an informal second supervisor role.

I am particularly indebted to Dr Helen Hooper, without whose encouragement, moral support and verbal abuse this project would have floundered. Sharing a bench for three years has been great fun, thank you.

Finally I must acknowledge The Muscular Dystrophy Group of Great Britain and Northern Ireland for their financial support. This project was funded by a 'Muscular Dystrophy Group Prize PhD Studentship'.